

THE UNIVERSITY OF HULL

**MYOCARDIAL INSULIN RESISTANCE IN
EXPERIMENTAL URAEMIA**

Being a Thesis submitted for the Degree of Doctor of Philosophy
in the University of Hull

by

Dunja Aksentijević, BSc (Hons)

February 2008

To my parents.

ABSTRACT

Cardiac complications are a major cause of death in patients with chronic kidney disease (CKD). Left ventricular hypertrophy (LVH) is a significant contributing factor to uraemic cardiomyopathy and results in significant molecular, cellular and metabolic remodelling. Progression of LVH leads to the development of insulin resistance, a feature common to CKD and heart failure, further jeopardising survival of the uraemic heart.

The aim of this thesis was to investigate the effect of uraemia on cardiac physiology, function and metabolism. Specifically, the aim of the study was to examine the cellular mechanisms underlying the development of myocardial insulin resistance in uraemia.

The experimental model was induced surgically *via* a two-stage 5/6 nephrectomy in adult male Sprague-Dawley rats over three, six weeks or nine weeks. An integrated experimental approach combining *in vivo* and *ex vivo* methods was used to characterize the morphology and physiology of the experimental model, examine myocardial function and energy provision; assess alterations in myocardial protein expression and determine potential mechanism involved in the development of insulin resistance.

Uraemic animals exhibited impaired renal function (creatinine 69 ± 2 vs. 40 ± 2 μM $n=41$; $p < 0.05$), cardiac hypertrophy (dry heart weight: tibia length 0.5 ± 0.01 vs. 0.4 ± 0.01 g/cm; $n=30$; $p < 0.05$), impaired glucose tolerance, hyperinsulinaemia, anaemia and hypertension.

In perfused hearts, uraemia caused a limited response of the uraemic heart to an increase in workload, demonstrated by cardiac dysfunction and metabolic adaptation. This profile was exacerbated in the presence of insulin. *In vivo* studies highlighted that insulin sensitivity was reduced in uraemic animals (HOMA-IR 1.27 ± 0.3 vs. 0.58 ± 0.1 ; $n=8$ $p < 0.02$) and declined progressively with renal dysfunction. LV tissue from the uraemic model showed an increase in myocardial GLUT4 and normal insulin mediated translocation mechanism.

In conclusion, uraemic animals exhibited a reduction in insulin sensitivity, glucose intolerance and hyperinsulinaemia, indicating onset of insulin resistance after 6 weeks of uraemia. Profile of myocardial GLUT4 expression and response to insulin stimulation suggested that insulin resistance is not a consequence of impaired translocation. The lack of overt metabolic remodelling suggests a compensatory phase of left ventricular hypertrophy.

ACKNOWLEDGEMENTS

I would like to express the deepest gratitude to my supervisors Dr Anne-Marie L. Seymour and Dr Sunil Bhandari. Thank you Dr Seymour for your unreserved support, guidance, enthusiasm and for your faith in me and my work. Thank you Dr Bhandari for your supervision and clinical expertise. I would also like to thank the NHS East Yorkshire Renal Fund for financial support and the University of Hull Clinical Biosciences Institute for awarding me the Frederick Atkinson fees scholarship.

I am grateful to Jenny Foster and Kath Bulmer for the technical support; Leigh Madden and Anne Lowry for the microscopy assistance; Ian Hanning at the Clinical Chemistry Department, Hull Royal Infirmary, for the urea and electrolyte serum analysis; Dr Simon Richardson, Katie Smith, Victoria Foster for the assistance with the biochemical assays, Dr David Semple for IT help and K.Y. Lee for developmental work on SERCA and PLB. I would like to thank Amanda, Alkistis, David, Katie and Ashwin for being fantastic friends and colleagues and for sharing with me memorable conference trips! I am very grateful to my partner Keith for his patience, love and understanding and all my friends and family for their relentless moral support.

I am forever indebted to my parents for their selfless dedication to me and my ambitions. Thank you for all the love, strength, encouragement, criticism and financial support you have given me. Zauvijek sam vam zahvalna!

CONTENTS

ABSTRACT	3
ACKNOWLEDGEMENTS	5
CONTENTS	6
FIGURES	10
TABLES	11
ABBREVIATIONS	11
1. INTRODUCTION.....	15
1.1 Background	16
1.2 Myocyte Structure	18
1.2.1 Cardiac Excitation –Contraction Coupling	21
1.3 Energy Metabolism in the Healthy Heart.....	
1.3.1 Fatty Acids	25
1.4 NMR and Cardiac Metabolism.....	33
1.5 Chronic Kidney Disease.....	35
1.5.1 Vascular Disease	38
1.5.2 Pathophysiological Effects of Uraemic Retention Solutes.....	40
1.5.3 Hypertension	41
1.5.4 Anaemia.....	42
1.6 Left Ventricular Hypertrophy	44
1.6.1 Contractile dysfunction	48
1.6.2 Metabolic alterations	50
1.7 Insulin Resistance in Uraemia.....	53
1.7.1 Insulin Signalling	55
1.7.2 Cardiac Dysfunction & Substrate Metabolism in Insulin Resistance	56
1.7.3 Post –Translation Protein Modification.....	59
1.8 Objectives	61
2. MATERIALS & METHODS.....	62
2.1 Materials.....	63
2.2 Experimental model	69
2.3 Non-invasive Blood Pressure Measurement	70
2.4 Glucose Tolerance Test	72
2.5 Heart Perfusion Studies	72
2.5.1 Krebs Henseleit Buffer	72
2.5.2 Bovine Serum Albumin Preparation	73
2.5.3 Preparation of BSA/Palmitate Krebs-Henseleit Buffer.....	74
2.5.4 Langendorff Isovolumic Heart Perfusion.....	74
2.5.5 Physiological Measurements.....	77
2.6 Left Ventricular Tissue Dissection.....	79
2.7 Morphometric Measurements.....	79

2.8	Blood Analysis	79
2.9	Protein Expression Analysis.....	80
2.9.1	Vertical Polyacrylamide Gel Preparation.....	80
2.9.2	Sample Preparation and Protein Separation	82
2.9.3	Western Blotting.....	84
2.9.4	Technical Developments	88
2.10	Subcellular Membrane Fractionation	89
2.11	¹³ C Magnetic Resonance Spectroscopy	91
2.11.1	Tissue Extraction.....	91
2.11.2	Deuterated Phosphate Buffer and NMR Sample Preparation	91
2.11.3	NMR Spectroscopy	91
2.11.4	¹³ C- Glutamate Labelling Pattern & the Analysis of ¹³ C Spectra	92
2.11.5	Isotopomer Analysis.....	95
2.12	Ventricular Myocyte Isolation.....	100
2.12.1	Preparation of Buffers	100
2.12.2	Cell Isolation	101
2.12.3	Cardiomyocyte Morphology	101
2.13	Biochemical Assays	102
2.13.1	Glucose assay	102
2.13.2	Lactate assay.....	103
2.13.3	Free Fatty Acids Assay.....	104
2.13.4	Measurement of Pyruvate Dehydrogenase Activity.....	106
2.13.4.1	Tissue Extraction.....	106
2.13.4.2	PDH Activity Measurement	106
2.13.5	Citrate Synthase Activity.....	107
2.13.5.1	Tissue Extraction.....	107
2.13.5.2	Citrate Synthase Assay	108
2.13.6	Tissue Triglyceride Assay	108
2.13.7	Glycogen Assay.....	109
2.14	Statistical Analysis	110
3.	CHARACTERISATION OF THE EXPERIMENTAL URAEMIA MODEL .	111
3.1	Introduction	112
3.2	Aims and Objectives	113
3.3	Methods.....	113
3.4	Results	113
3.4.1	Morphological Features.....	114
3.4.2	Blood Pressure.....	115
3.4.3	Hypertrophy.....	116
3.4.4	Serum Electrolyte Analysis	119
3.4.5	Anaemia.....	121
3.4.6	Insulin and Proinsulin Measurements	122
3.4.7	Serum Metabolite Profile	123
3.5	Discussion	124
3.5.1	Morphology	124
3.5.2	Hypertrophy and Haemodynamic Alterations.....	125
3.6	Summary	128

4. CARDIAC FUNCTION & METABOLISM IN URAEMIA	129
4.1 Introduction	130
4.2 Aims and Objectives	131
4.3. Materials and Methods	132
4.3.1 Heart Perfusions	132
4.4 Results	134
4.4.1 Cardiac Function	134
4.4.2 Metabolic Profile	137
4.4.3 Triglyceride and Glycogen Content Analysis	139
4.5 Discussion	142
4.5.1 Cardiac Function and Metabolism in Uraemia.....	142
4.6 Summary	149
5. MYOCARDIAL PROTEIN EXPRESSION IN EXPERIMENTAL URAEMIA	150
5.1 Introduction	151
5.1.2 Metabolic Transporters.....	151
5.1.3 Fatty Acid Transporters.....	159
5.2 Aims and Objectives	160
5.3 Methods	160
5.4 Results	161
5.4.1 Contractile Function Regulatory Proteins	164
5.4.2 Subcellular Membrane Fractionation	167
5.5 Discussion	169
5.5.1 Metabolic Protein Expression.....	170
5.5.2 Contractile Protein Expression.....	174
5.6 Summary	178
6. INSULIN RESISTANCE IN URAEMIA	179
6.1. Introduction	180
6.2. Aims and Objectives	181
6.3. Materials and Methods	182
6.3.1 GLUT4 Expression and Translocation in Isolated Cardiomyocytes.....	182
6.4. Results	184
6.4.1. Oral Glucose Tolerance Test.....	184
6.4.2. Skeletal Muscle GLUT 4 Expression.....	191
6.4.3. GLUT4 Expression and Translocation in Isolated Cardiomyocytes.....	192
6.5. Discussion	196
6.5.1. Oral Glucose Tolerance.....	196
6.5.2. Cardiomyocyte GLUT4 expression.....	198
6.6. Summary	201

7. DISCUSSION.....	202
7.1 Future Work	206
7.1.1 Experimental Uraemia.....	206
7.1.2 Cardiac Function and Metabolism	207
7.1.3 Insulin Resistance.....	208
7.1.4 Study Limitations	209
Full Papers.....	211
Abstracts.....	211
REFERENCES	213

FIGURES

Figure 1.1 Cardiovascular Disease Mortality in General Population & in CKD Patients.....	16
Figure 1.2 Ultrastructure of the Cardiomyocytes & Schematic Representation of Contractile Filaments.....	19
Figure 1.3 Ca ²⁺ Transport in Ventricular Myocytes.....	22
Figure 1.4 Three Stages of Fuel Metabolism in the Heart.....	24
Figure 1.5 Long Chain Fatty Acid Uptake & Oxidation in Cardiomyocyte.....	27
Figure 1.6 PPAR α Mediated Transcriptional Control.....	29
Figure 1.7 Myocardial Glucose Uptake & Metabolism.....	32
Figure 1.8 Confounding Factors in Uraemia.....	38
Figure 1.9 Haemodynamic Changes Induced by Anaemia.....	43
Figure 1.10 Wall Stress and Patterns of Hypertrophy.....	48
Figure 1.11 Metabolic Adaptation & Maladaptation of the Heart.....	52
Figure 2.1 Fitting Occlusion Cuff & Pulse.....	70
Figure 2.2 Blood Pressure/ Pulse Illustration.....	71
Figure 2.3 Cannulated Heart.....	75
Figure 2.4 Langendorff Perfusion Apparatus.....	76
Figure 2.5 Heart Function Trace During Perfusion.....	78
Figure 2.6 Protein Standard Curve.....	83
Figure 2.7 Brilliant Blue Polyacrylamide Gel Staining.....	84
Figure 2.8 Subcellular Membrane Fractionation Protocol.....	90
Figure 2.9 Distribution of ¹³ C isotope from [1- ¹³ C] glucose.....	93
Figure 2.10 Multiplate Peak Patterns of ¹³ C Glutamate.....	94
Figure 2.11 Measurement of C4 Glutamate Peak Heights.....	97
Figure 2.12 Example of the tcaCALC Output.....	99
Figure 2.13 Photomicrograph of Control Cardiomyocyte 40x Magnification.....	102
Figure 2.14 Glucose Assay Standard Curve.....	103
Figure 2.15 Lactate Concentration.....	104
Figure 3.1 The effect of LVH on isolated cardiomyocyte size.....	118
Figure 3.2 Serum Creatinine & Urea Concentration.....	120
Figure 3.3 Development of Anaemia.....	121
Figure 3.4 Serum Insulin & Proinsulin Concentrations.....	122
Figure 4.1 Experimental Protocol for Perfusion Studies.....	133
Figure 4.2 Cardiac Efficiency (A) & Oxygen Consumption (B).....	136
Figure 4.3 Profile of Substrate Oxidation in the Presence of 1mU/ml Insulin.....	137
Figure 4.4 Profile of Substrate Oxidation in the Absence of 1mU/ml Insulin.....	138
Figure 4.5 Six week Tissue Triglyceride & Glycogen Content.....	140
Figure 4.6 Citrate Synthase Activity.....	141
Figure 4.7 PDH Activity.....	141

Figure 5.1 Structure of GLUT Family of Proteins Displaying Homology Between GLUT 1 & 4 (residues unique to GLUT4 shown in red).....	152
Figure 5.2 GLUT 4 Translocation Pathways: PI3K and PI3K Independent.....	155
Figure 5.3 The Effect of Uraemia Development on LV ANF Expression	161
Figure 5.4 Glucose Transporters Expression in Uraemia	163
Figure 5.5 CD36 Expression in Uraemia.....	164
Figure 5.6 Ca ²⁺ Handling Protein Expression in Uraemia.....	165
Figure 5.7 Na ⁺ K ⁺ ATPase α_1 Expression in Uraemia.....	166
Figure 5.8 LV Membrane Fraction Analysis in 6week Uraemia.....	168
Figure 6.1 Glucose (A) & Insulin (B) Responses to an Oral Glucose Challenge	185
Figure 6.2 HOMA-IR Index for Control and 6 Week Uraemia.....	186
Figure 6.3 Glucose (A) & Insulin (B) Responses to an Oral Glucose Challenge.....	188
Figure 6.4 HOMA-IR index for control and 9 week uraemia.....	189
Figure 6.5 Correlation Between Serum Creatinine and HOMA-IR & Insulin	190
Figure 6.6 GLUT4 Expression in Skeletal Muscle (gastrocnemius)	191
Figure 6.7 GLUT4 Immunofluorescence (arrows) in Isolated Cardiomyocytes	193
Figure 6.8 GLUT4 Immunofluorescence (arrows) in Isolated Cardiomyocytes	194
Figure 6.9 GLUT4 Immunofluorescence Intensity in Isolated Cardiomyocytes.....	195

TABLES

Table 1.1 Comparison of Complete Oxidation of Glucose and Palmitate.....	25
Table 1.2 Metabolic and Biochemical Consequences of Chronic Kidney Failure	35
Table 1.3 Structural & Functional Changes of the Heart in Renal Failure.....	36
Table 1.4 Cardiac Risk Factors in Uraemia	37
Table 1.5 Transcriptional Responses of the Heart in Hypertrophy & Diabetes	46
Table 2.1 Materials & Suppliers (Miscellaneous)	63
Table 2.2. Antibody Suppliers	67
Table 2.3 Assay Kits.....	68
Table 2.4 Veterinary Drugs & Agents	68
Table 2.5 Resolving Polyacrylamide Gel Composition.....	81
Table 2.6 Tissue Lysis Buffers	82
Table 2.7 SDS PAGE & Western Blotting Protocol Details	86
Table 2.8 SDS PAGE & Western Blotting Protocol Details	87
Table 2.9 The Chemical Shifts of Glutamate.....	95
Table 2.10 Cardiomyocyte Isolation Buffer Composition.....	100
Table 3.1 Animal Morphology at 3, 6 and 9 weeks.....	114
Table 3.2 Blood Pressure Measurements.....	115
Table 3.3 Hypertrophy Indices	117
Table 3.4 Cardiomyocyte Morphology of Uraemic & Control Experimental Groups	118
Table 3.5 Serum Electrolytes.....	119
Table 3.6 Serum Metabolite Concentrations	123
Table 4.1 Myocardial Function in the Presence and Absence of Insulin.....	135

ABBREVIATIONS

ADP	Adenosine diphosphate
ACE	Angiotensin converting enzyme
Akt/PKB	Serine/threonine kinase or Protein kinase B
AMP	Adenosine monophosphate
ATP	Adenosine triphosphate
AV	Atrioventricular
ANF	Atrial natriuretic factor
BSA	Bovine serum albumin
BWt	Body weight
Ca ²⁺	Calcium
cAMP	Cyclic adenosine monophosphate
CAT	Carnitine acylcarnitine translocase
CH	Cardiac hypertrophy
CKD	Chronic kidney disease
CK	Creatine kinase
CO	Cardiac output
CO ₂	Carbon Dioxide
CPT1	Carnitine palmitoyl transferase 1
CPT 2	Carnitine palmitoyl transferase 2
D ₂ O	Deuterated water
DP	Diastolic pressure
ET	Endothelin
ETC	Electron transport chain
EDTA	Ethylene diamine tetraacetic acid
Erk	Extracellular signal-regulated kinase
FABP	Fatty acid-binding protein
FAO	Fatty acid oxidation
FAT/CD36	Fatty acid translocase
FADH ₂	Flavin adenine dinucleotide (reduced)
FID	Free induction decay
FFA	Free fatty acid
GAPDH	Glyceraldehyde-3-phosphate dehydrogenase
GATA	Transcription factor
GLUT1/4	Glucose transporter 1/4
GP	Glycogen phosphorylase
GSK-3	Glycogen synthase kinase-3
GPCR	G-protein coupled receptors
GAB	Grb-2 associated binder scaffolding adapter molecules
G-6-P	Glucose-6-phosphate
HK	Hexokinase
HR	Heart rate
Hcy	Homocysteine
Hb	Haemoglobin

HDL	High-density lipoprotein
HPLC	High performance liquid chromatography
HOMA-IR	Insulin resistance homeostasis assessment model
HRP	Horse radish peroxidase
IGF	Insulin-like growth factor
I _R	Insulin receptor
Jak	Janus Kinase
K-H	Krebs-Henseleit
kDa	Kilo Dalton
LCFA	Long-chain fatty acids
LVH	Left ventricular hypertrophy
LVDP	Left ventricular developed pressure
LV	Left ventricle
LDH	Lactate dehydrogenase
LPL	Lipoprotein lipase
MAPKs	Mitogen-activated protein kinases
MCAD	Medium chain acyl CoA dehydrogenase
mCPT1	Muscle type carnitine palmitoyl transferase 1
MCT-1	Monocarboxylate transporter
MEK/MEKK	Mitogen-activated protein kinase/extracellular signal-regulated kinase kinase
MHC	Myosin heavy chain
mM	Milimolar
MI	Myocardial Infarction
MVO ₂	Myocardial oxygen consumption
NAD ⁺	Nicotinamide adenine dinucleotide (oxidised)
NADH	Nicotinamide adenine dinucleotide (reduced)
NCX	Sodium calcium exchanger
NFAT	Nuclear factor of activated T cells
nM	Nanomolar
NMR	Nuclear magnetic resonance
NO	Nitric oxide
p38	Type of MAPK
PAGE	Polyacrylamide gel electrophoresis
PCA	Perchloric acid
PCNA	Proliferative cell nuclear antigen
PCr	Phosphocreatine
PDC	Pyruvate dehydrogenase complex
PDH	Pyruvate dehydrogenase
PDK	Pyruvate dehydrogenase kinase
PDGF	Platelet derived growth factor
PDP	Pyruvate dehydrogenase phosphate
PFK	Phosphofructokinase
PGC-1	PPAR γ co-activator-1
P _i	Inorganic phosphate
PI3-K	Phosphatidylinositol 3-kinase
PIP3	Phosphatidylinositol(3,4,5) triphosphatase
PPAR α	Peroxisome proliferators activated receptor α -isoform

PT	Pyruvate transferase
PTH	Parathyroid hormone
RNA	Ribonucleic acid
ROS	Reactive oxygen species
RPP	Rate pressure product
RyR	Ryanodine receptor
SA	Sinoatrial
SERCA	Sarcoendoplasmic reticulum Ca ²⁺ -ATPase
SDS	Sodium dodecyl sulphate
SHR	Spontaneously hypertensive rat
SNARE	N-ethylmaleimide-sensitive fusion protein attachment receptors
SP	Systolic pressure
SR	Sarcoplasmic reticulum
Stat	Signal transducers and activators of transcription
TCA	Tricarboxylic acid cycle
TGN	Trans-Golgi network
TG	Triglyceride
TMS	Tetramethylsilane
VEGF	Vascular endothelial growth factor
VAMP	Vesicle associated membrane protein
Wt	Weight
Y	Anaplerotic flux

1. INTRODUCTION

1.1 Background

Chronic kidney disease (CKD) currently affects 6 million patients in the United Kingdom, and over 12 million in the United States, with thousands of new cases diagnosed every year (www.kidneyresearchuk.org, 2008). The mortality from cardiovascular disease in uraemia is substantially higher (1000 fold) than in an age, sex and race matched general population (*Fig. 1.1*), accounting for more than 50% mortality.

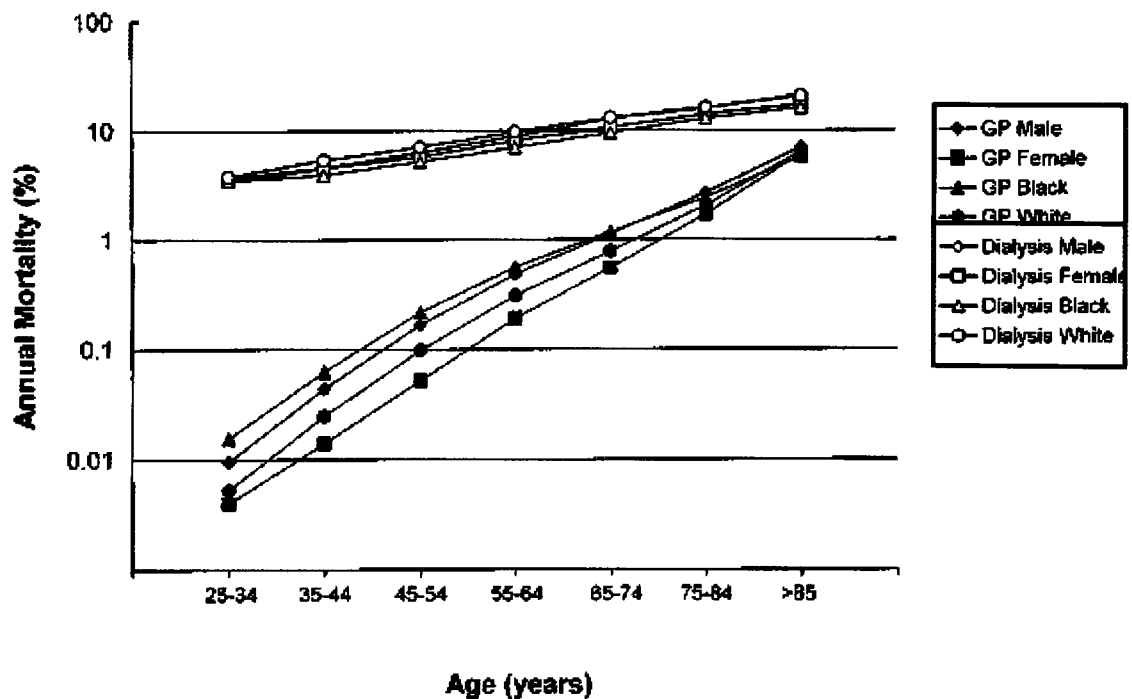


Figure 1.1 Cardiovascular Disease Mortality in General Population & in CKD Patients

(Parfrey and Foley, 1999)

Historically this cardiovascular mortality rate was attributed exclusively to coronary heart disease resulting from accelerated atherogenesis (Amann and Ritz, 1997). However, studies have shown that myocardial infarction accounts only for 30-50% of cardiac deaths in uraemia (Wing et al., 1984, Rostand et al., 1986), but left ventricular hypertrophy (LVH) is present in more than 75% of uraemia (Levey et al., 2007) and may play an important role in patient mortality.

Metabolic syndrome and insulin resistance are common features in patients with CKD (Lastra et al., 2006). Insulin resistance has been identified as an independent predictor of cardiovascular mortality in uraemia (Shinohara et al., 2002). However, no study to date has examined the cellular and metabolic mechanisms of myocardial insulin resistance in uraemia. An understanding of this may allow the future development of potential treatments for cardiac dysfunction in uraemia.

1.2 Myocyte Structure

Cardiomyocytes, smooth muscle cells, endothelial cells and fibroblasts are essential components of heart tissue and function. The majority of myocardial tissue volume *in vivo* is made up of cardiomyocytes, (25% cardiac cell population), whilst fibroblasts dominate in numbers (Camelliti et al., 2005). All cardiomyocytes retain properties of conductance with some properties of pacemaker.

Contractile cardiomyocytes are similar in structure but differ to other functional somatic cell types. They are arranged longitudinally, forming fibers and are rich in myofibrils. Despite the presence of numerous lateral and end-to-end connections between cardiac muscle fibres, the contractile cells do not form a true anatomical syncytium (Waller and Schlant, 1998). Intercalated disks at the terminal cell margins and junctions form permeable communicating gap junctions, permitting diffusion of ions and spreading of the action potential between cardiomyocytes (Brooks et al., 1998). Contractile cells consist of sarcomeres together with numerous centrally located mitochondria (40% cell volume) and nucleus (Waller and Schlant 1998). Contractile filaments are arranged in a regular array of thick (A-bands) and thin filament (I-bands)(*Fig.1.2*) (Vozzi et al., 1999). The sarcomere is the functional unit of the contractile apparatus and is the region between two Z-lines (*Fig. 1.2*). Calcium (Ca^{2+}) is a direct activator of the myofilaments causing the contraction (Schlant et al., 1998, Bers, 2002).

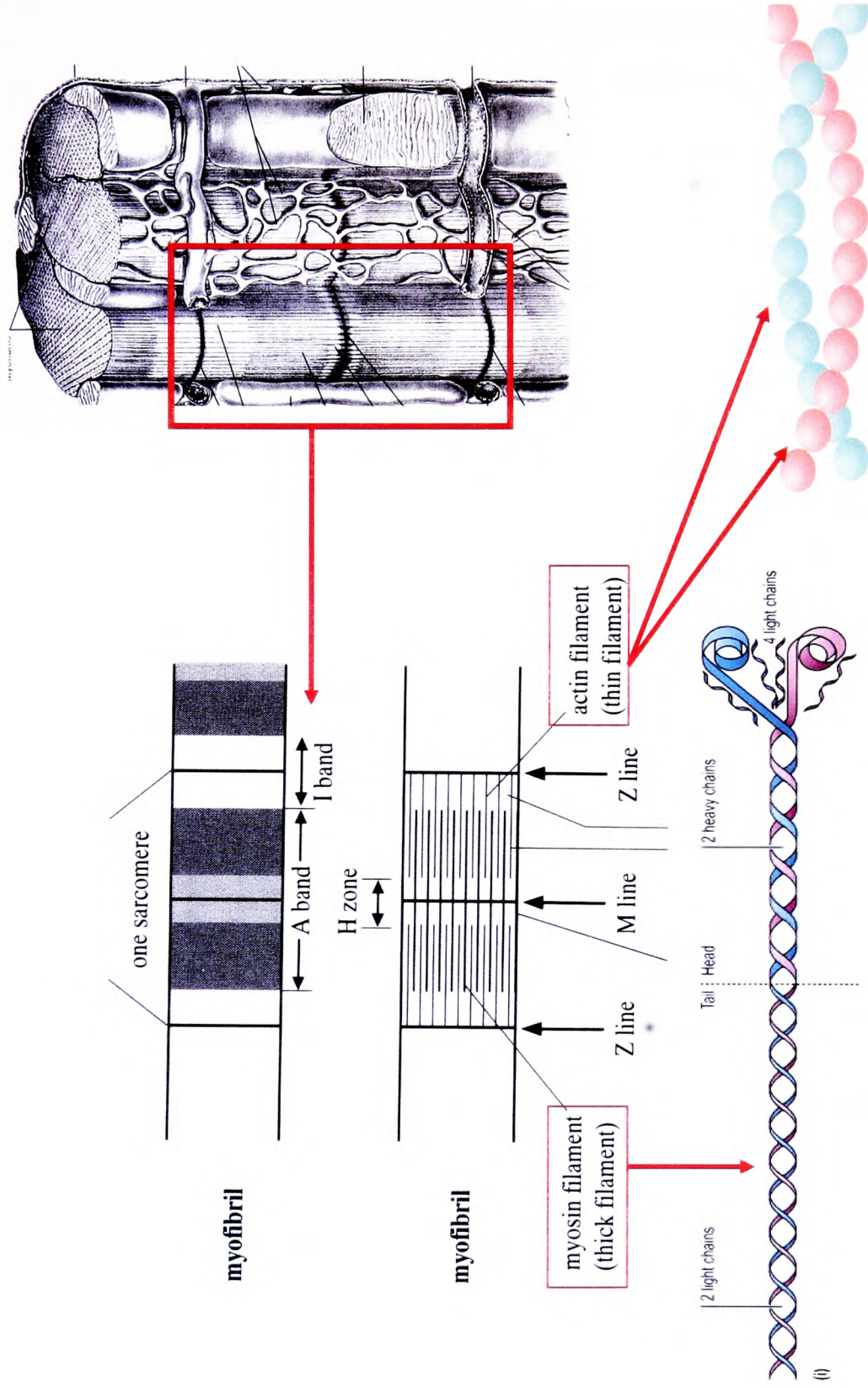


Figure 1.2 Ultrastructure of the Cardiomyocytes & Schematic Representation of Contractile Filaments

Figures adapted from: Taylor, D.J. et al. (1998); Waller and Sclanti, R.C.(1998); Figures courtesy of www.fleshandbones.com

The thick filaments are composed of myosin, a large hexameric structure consisting of two heavy chains, two essential light chains and two regulatory light chain subunits (*Fig. 1.2*) (Katz, 1992). Myosin molecules are set in the filament with their tails toward the centre of the filament so that the heads are concentrated towards two ends leaving the centre portion bare. The ATPase activity is contained within the myosin head, generating energy for force developing in the contracting cardiac muscle (Davies, 2001). There are two isoforms of myosin heavy chains (MHC): α -MHC with greater ATPase activity and β chain with lower ATPase activity (Boheler et al., 1992, Katz, 2001).

Thin filaments are composed of the protein complexes, actin, tropomyosin and troponin (*Fig. 1.2*) (Martini, 2001). The actin “thin filament” consists of a 1 μm long double-stranded helix of polymer of actin with strands of tropomyosin stretched between troponin complexes (Davies 2001). The troponin complex consists of three proteins, troponin C (Ca^{2+} binding), troponin I (inhibitory protein), and troponin T (tropomyosin binding protein) (Schlant et al., 1998). In the resting state, troponin I lies on top of the actin active sites, stabilising the tropomyosin-actin complex. This prevents the interaction between actin and myosin. Myosin interacts with actin hydrolysing ATP to generate energy supply for the muscle contraction. Ca^{2+} interacts with the troponin complex to alter the configuration of tropomyosin, hence allowing the bridging of actin and myosin, causing sarcomere to contract (Schlant et al., 1998). Actin filaments slide along adjacent myosin filaments by cycling of the actinomyosin cross bridges thus bringing the Z lines closer together (*Fig. 1.2*) (Berne et al., 2004).

1.2.1 Cardiac Excitation –Contraction Coupling

Cardiac excitation-contraction coupling is the process linking the electrical excitation of the myocyte to contraction of the heart (Hein et al., 2000). The sarcotubular system is central to the electrical impulse conduction and electromechanical coupling and therefore crucial for myocardial contraction. The structure is the T system, comprised of transversely orientated tubules periodically invaginating sarcolemma. T tubules are observed close to the area of Z band forming intermediary vesicles (*Fig 1.2*) (Waller and Schlant, 1998).

The cardiac contraction cycle is initiated by the sino-atrial node (pacemaker) which triggers heart beat (Berne et al. 2004). The electrical impulse is propagated to the bundle of His via the AV node, and subsequently the bundle branches, the Purkinje network and finally to ventricular myocytes causing depolarisation and subsequent contraction (Martini, 2001). Ca^{2+} plays a critical role in linking excitation and contraction. During the plateau phase of the action potential there is a slow, inward flux of Ca^{2+} from extensive transverse tubule through I_{CaL} channels in sarcolemma into cytosol (*Fig. 1.3*) (Schlant et al., 1998).

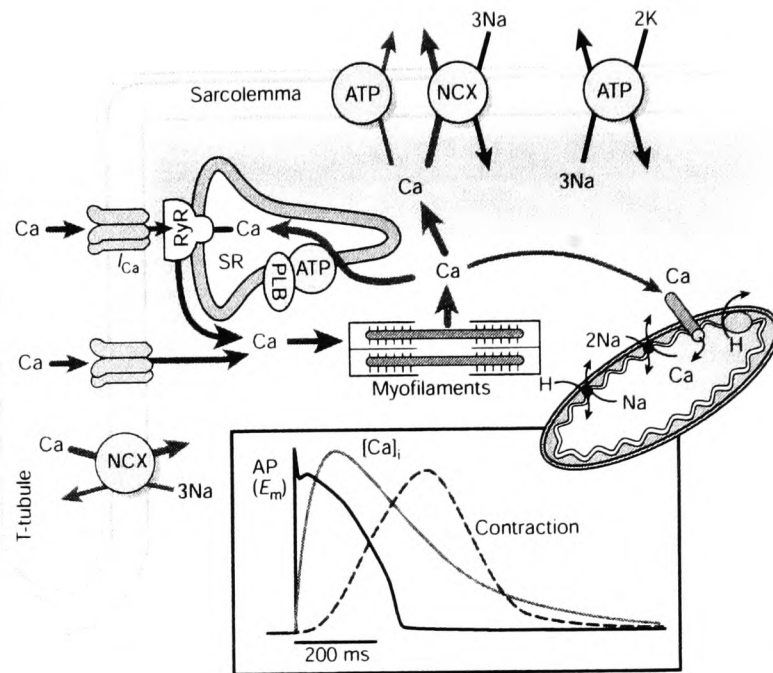


Figure 1.3 Ca^{2+} Transport in Ventricular Myocytes

Figure taken from Bers DM (2002)

T tubules are in close proximity to terminal cisternae of SR containing the ryanodine receptor (RyR), the Ca^{2+} -release channel involved in E-C coupling (Fozzard and Hauck, 1991). RyR are opened by the Ca^{2+} influx into the cell, triggering Ca^{2+} release from the SR for activation of contraction via binding of troponin C (Fig. 1.3i) (Fabiato and Fabiato, 1978). Relaxation occurs when the increase in cytosolic $[Ca^{2+}]$ leads to $[Ca^{2+}]$ uptake into SR, causing Ca^{2+} dissociation from the troponin C (Bers and Perez-Reyes, 1999).

1.2.1.1 Ca^{2+} Handling Proteins

The sarcoplasmic reticulum (SR) Ca^{2+} -ATPase 2a is one of the key proteins involved in Ca^{2+} cycling. It transports 2 mol of Ca^{2+} into the SR lumen by utilizing 1 mol ATP as an energy source (Sharma et al., 2001). Its activity is regulated by phospholamban (PLB), a 52-residue cardiac SR-associated protein. Phosphorylation of phospholamban enhances SERCA2a activity and allows relaxation to occur (Koss and Kranias, 1996). PLB interacts with SERCA2a to reduce its affinity for Ca^{2+} , therefore altering the rate and amount of calcium sequestered by SR during myocardial relaxation (Simmerman and Jones, 1998, Zhai et al., 2000). Phosphorylation of PLB at Ser-¹⁶ or Thr-¹⁷ via β -adrenergic pathway or via calcium/calmodulin kinase II results in increased rate of pumping by the Ca^{2+} ATPase (Sharma et al. 2001). SR calcium re-uptake is determined by the SERCA 2a pump capacity (Sande et al., 2002).

1.3 Energy Metabolism in the Healthy Heart

The heart requires a continuous supply of energy to maintain its function of a pump. Due to the omnivorous nature of the heart, glucose, lactate, fatty acids, ketone bodies and, under some circumstances, amino acids, compete as the substrates for respiration (*Fig. 1.4*).

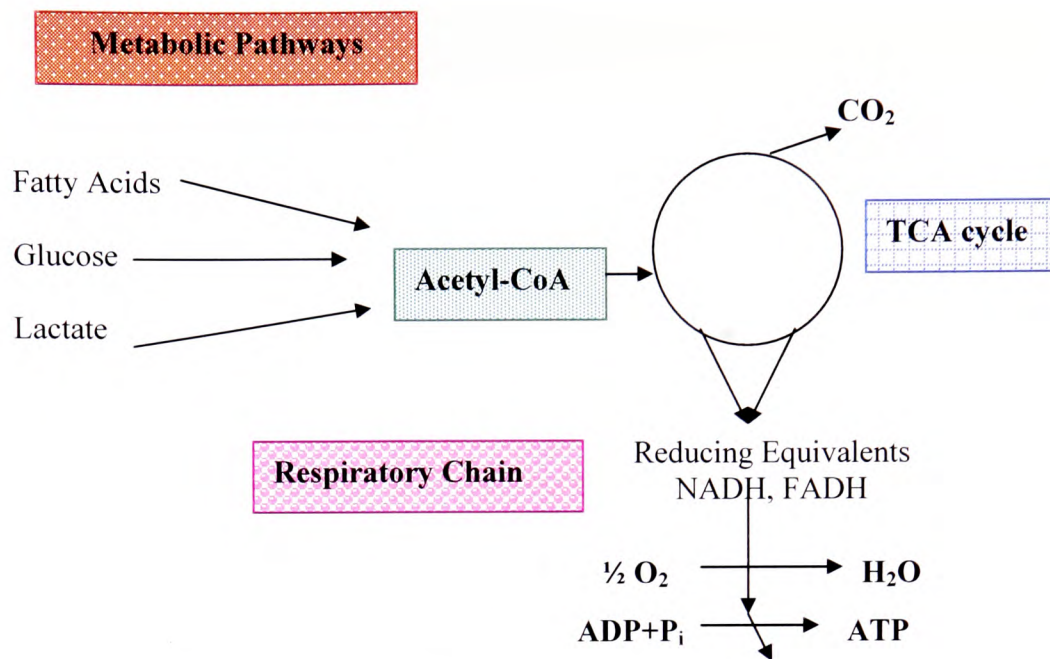


Figure 1.4 Three Stages of Fuel Metabolism in the Heart

Adapted from Taegtmeyer. (1999)

Oxidative phosphorylation is fuelled by the reducing equivalents NADH and FADH₂, products of β-oxidation of fatty acids, the pyruvate oxidation and the TCA cycle (*Fig. 1.4*). 2/3 of energy yielded in ATP hydrolysis fuels contractile work and 1/3 is used for ion pumps and gradient (Na⁺,K⁺) maintenance (Suga, 1990). The primary ion pump that consumes ATP-derived energy is SERCA. Long chain fatty acids are more reduced than glucose and lactate (*Table 1.1*), generating more ATP/g substrate. However, glucose and lactate have 11% higher ratio of ATP synthesis to oxygen consumption ratio making them more oxygen efficient (*Table 1.1*).

	Glucose	Palmitate
ATP Yield	32 ATP	106 ATP
Energy Efficiency	5.3 ATP/CO ₂ produced	6.6 ATP/ CO ₂ produced
Oxygen Efficiency	5.3 ATP/O ₂ consumed	4.6 ATP/ O ₂ consumed

Table 1.1 Comparison of Complete Oxidation of Glucose and Palmitate

Adapted from Opie (1984)

However, ATP synthesis/O₂ consumption ratio is dependant on the coupling of proton influx into mitochondrial matrix with oxidative phosphorylation, and can be reduced compared to theoretical value (*Table 1.1*) (Stanley and Chandler, 2002).

1.3.1 Fatty Acids

Fatty acids are readily extracted from the plasma and can be either rapidly oxidized or converted into triglyceride stores (Taegtmeyer, 1999). Studies in humans have demonstrated that 80% of myocardial free fatty acids (FFA) are oxidized rapidly to CO₂ in the mitochondria and 20% remain stored in the form of triglyceride (Lopaschuk et al., 1994). Plasma availability of FFA and the concentration of FFA transport protein in sarcolemma membrane determine the rate of FFA uptake (Wisneski et al., 1987).

Plasmalemmal fatty acid binding protein (FABP_{pm}); fatty acid translocase (FAT/CD36) with intracellular fatty acid transport protein (heart type FABP) maintain sufficient flux of FA through the sarcolemma into the cell (*Fig. 1.5*) (van der Vusse et al., 2000). FFA are bound to albumin in the plasma and to small fatty acid binding proteins in the cardiomyocyte cytosol (*Fig. 1.5*) (van der Vusse et al., 2000). Intracellular transport of long chain FA is catalysed by three carnitine dependant enzymes 1) carnitine palmitoyltransferase 1 (CPT-1) catalyzes formation of the long-chain acyl CoA between inner and outer mitochondrial membranes 2) carnitine acylcarnitine translocase transports the long-chain product across the inner mitochondrial membrane 3) CPT-II regenerates long chain acyl CoA in the mitochondrial matrix (*Fig. 1.5*) (Glatz and van der Vusse, 1996, van der Vusse et al., 2000). CPT I plays major regulatory role in transport and is inhibited by malonyl CoA.

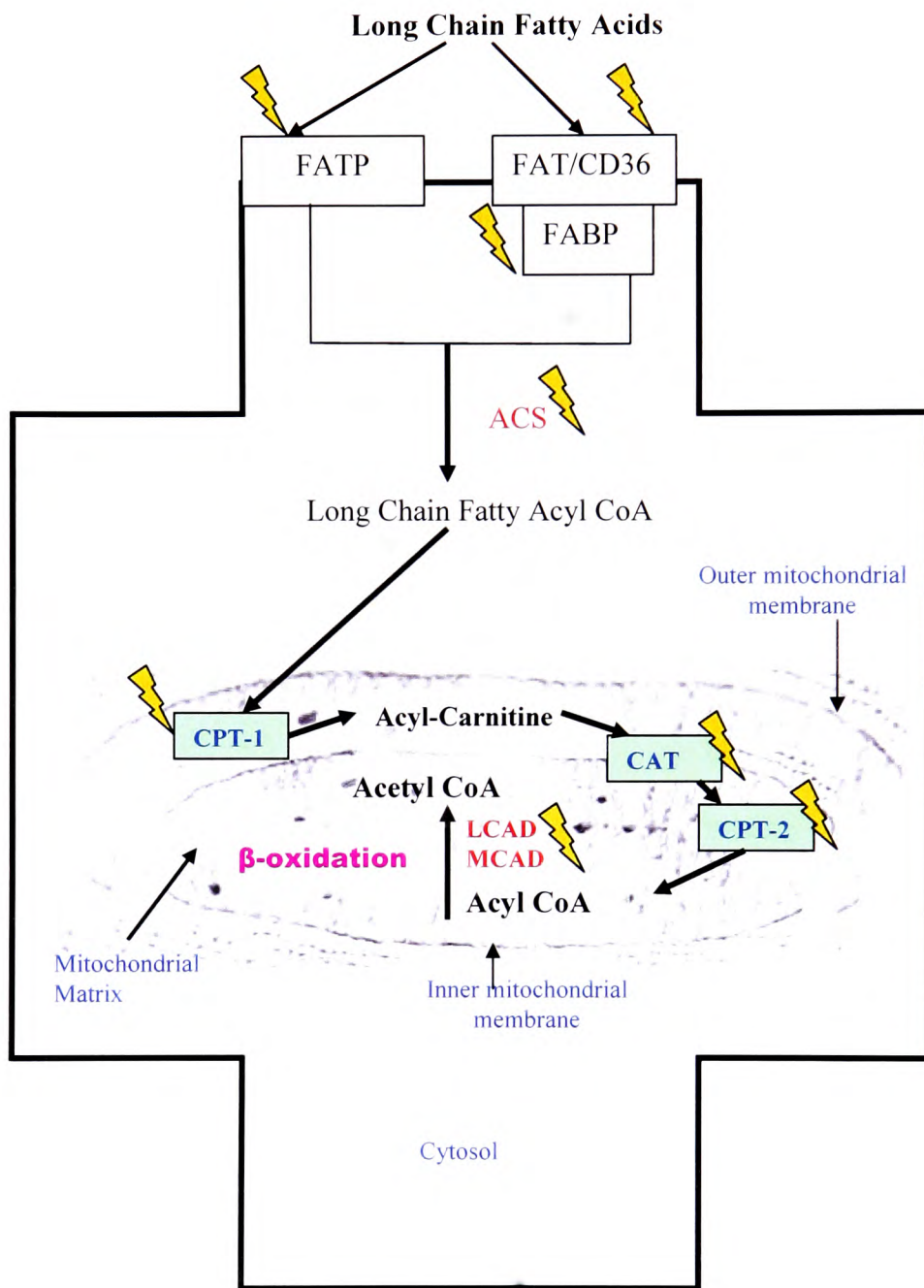


Figure 1.5 Long Chain Fatty Acid Uptake & Oxidation in Cardiomyocyte

ACS- AcylCoA synthase; LCAD-long chain acylCoA dehydrogenase, MCAD-Medium-chain acylCoA dehydrogenase. ⚡ indicates enzymes and proteins whose gene expression is regulated by PPAR α

Diagram adapted from Stanley and Chandler (2002)

1.3.1.1 PPAR α Regulation of Fatty Acid Utilization

The regulation of myocardial substrate utilization is linked to the arterial substrate concentration, hormone levels, inotropic state and the nutritional status of the tissue (Stanley and Chandler, 2002). FA utilization is regulated by peroxisome proliferator-activated receptors (PPARs), via transcriptional activation of genes encoding key enzymes of FA utilisation (Finck and Kelly, 2004). PPARs are a family of ligand activated transcription factors regulating different aspects of cellular lipid metabolism (Finck and Kelly, 2002). Three PPAR isoforms have been described to date- PPAR α , PPAR β and PPAR γ and are all activated by fatty acids. PPAR α is considered the primary transcriptional regulator of cardiac lipid metabolism (Huss and Kelly, 2004). In PPAR α knockout mice, the expression of cardiac genes involved in FA uptake (CD36, FATP), transport (CPT1, CPT2) and oxidation (MCAD, VLCAD and SCAD) is reduced (*Fig. 1.5*) (Huss and Kelly, 2004). Studies by Luptak et al. (2005) suggested that metabolic remodelling in the hearts from PPAR α knockout mice can increase the myocardial susceptibility to functional deterioration during haemodynamic overload.

In vitro assessment has identified LCFA and related metabolites as the most relevant ligands for myocardial PPAR α (Djouadi et al., 1998, Watanabe et al., 2000). Upon activation, PPAR α recruits transcriptional activators essential for target gene transcription initiation (*Fig. 1.6*), namely the retinoid X receptor (RXR) and PPAR promoter response element (PPRE) located upstream of the PPAR α target genes (*Fig. 1.6*).

The cardiac-enriched PPAR γ co-activator-1 (PGC-1) subsequently interacts with the PPAR α complex recruiting other cofactors (SRC-1 and CBP/p300) required for target gene transcription promotion. In the absence of lipid ligand, PPAR-RXR hetero-dimers recruit co-repressors (chicken ovalbumin upstream promoter transcription factor- COUP-TF, Sp1 and Sp3), histone deacetylases (HDACs) and chromatin modifying enzymes, causing transcription silencing by active repression (Fig. 1.6) (Finck et al., 2002).

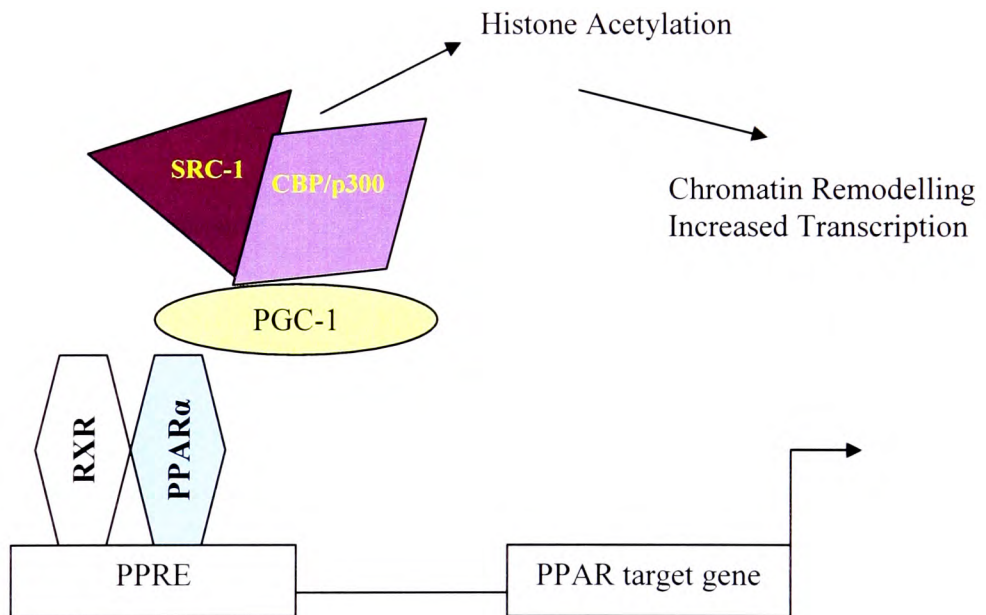


Figure 1.6 PPAR α Mediated Transcriptional Control

Adapted from Kelly (2003)

1.3.1.2 Carbohydrate Metabolism

Healthy heart utilizes glucose and lactate subsequently converted to pyruvate in the cytosol and oxidized to CO₂ in mitochondria. Transport of the exogenous lactate across the sarcolemma is facilitated by a monocarboxylate transporter (MCT-1) (Stanley and Chandler, 2002). Intracellular lactate is rapidly oxidised by lactate dehydrogenase (LDH) and further oxidised to CO₂ in the TCA cycle (Stanley and Chandler, 2002).

The uptake of extracellular glucose is regulated by transmembrane glucose gradient and the concentration and the activity of glucose transporters in a plasma membrane (Stanley et al., 2005). Transporters regulating glucose uptake are from the family of transporters GLUT1 and GLUT4 (Pessin and Bell, 1992). Details about glucose transport are further discussed in *Chapter 5*. Upon entering the cell, free glucose is rapidly phosphorylated by hexokinase to glucose-6-phosphate rendering the glucose impermeable to cell membrane (*Fig. 1.7*) (Stanley et al., 1997). Insulin activates hexokinase and causes its release from the outer mitochondrial membrane therefore increasing phosphorylation and uptake of glucose (Russell et al., 1992, Taegtmeyer, 1994). Glucose-6-phosphate can be used for glycogen synthesis or can enter glycolysis to form pyruvate (Stanley et al., 1997). The committing step in glucose oxidation is the conversion of pyruvate to acetyl CoA by pyruvate dehydrogenase (PDH) complex (*Fig. 1.7*) (Randle, 1986). PDH is a multi-enzyme complex located in the mitochondrial matrix (*Fig. 1.7*).

PDK (pyruvate dehydrogenase kinase) inactivates the PDH by phosphorylation and PDP (pyruvate dehydrogenase phosphatase) catalyses phosphorylation-dephosphorylation cycle and activates the enzyme complex (Randle et al., 1964, Stanley and Chandler, 2002). PDK has 4 isoforms and type II and IV predominate in the heart (Sugden et al., 2000). Schematic summary of the carbohydrate metabolism is outlined in figure 1.7.

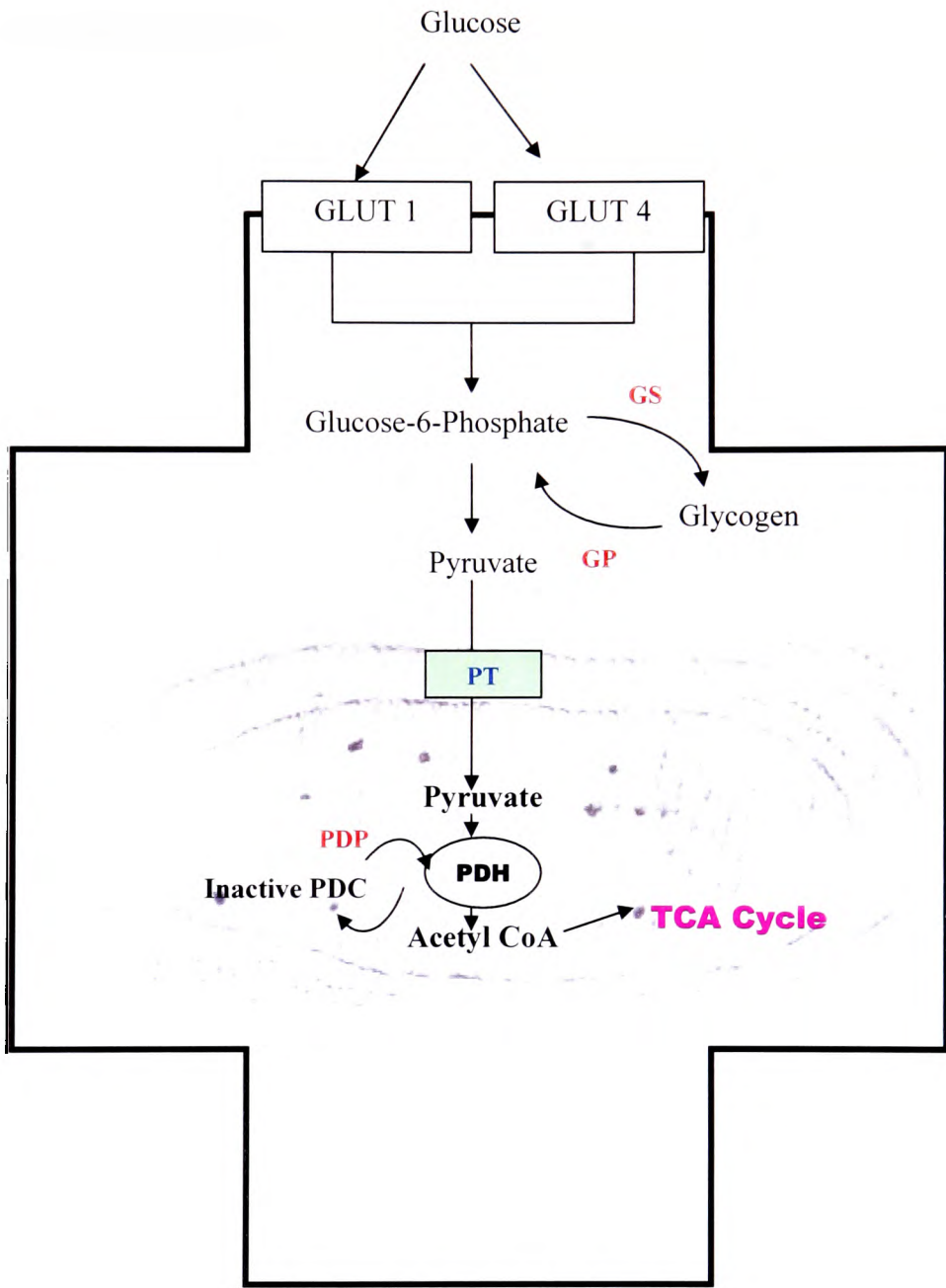


Figure 1.7 Myocardial Glucose Uptake & Metabolism

Adapted from (Kerbey et al., 1976).

1.4 NMR and Cardiac Metabolism

Nuclear magnetic resonance (NMR) spectroscopy is a powerful tool for investigation of various biological processes. A major advantage of the technique is its non-invasive property that enables nuclei detection in their physiological environments (Chatham et al., 2001). NMR spectroscopy enables anatomical, physiological and metabolic information analysis in a single experimental setting (Badar-Goffer and Bachelard, 1991, Seymour, 2003a). It relies on the spin property of nucleus orientating within a magnetic field, exhibited by nuclei with spin 1/2 or 3/2 such as hydrogen (^1H), phosphorus (^{31}P), carbon (^{13}C) and sodium (^{23}Na) (Seymour, 2003a). NMR spectroscopy can be used for metabolic and bioenergetics studies, whilst ^{23}Na , ^{39}K , ^{87}Rb NMR focus is on ion transport and ionic pump regulation (Gadian, 2004, Seymour, 2003a, Ten Hove and Neubauer, 2007).

^{13}C NMR has been an invaluable means of studying myocardial metabolism in health and disease (Gadian, 2004), in particular cardiac hypertrophy (Des Rosiers et al., 2004) and diabetes (Chatham and Seymour, 2002), ageing (Sample et al., 2006) and uraemia (Reddy et al., 2007). ^{13}C NMR spectroscopy has been widely used to investigate a) the relative contribution of substrates to oxidative metabolism (metabolic steady state NMR) and b) fluxes through metabolic pathways (kinetic NMR) (Yu et al., 1995). Kinetic NMR enables continuous measurement of the time course of ^{13}C glutamate enrichment during non-steady state, including the rate limiting steps in glutamate enrichment (Yu et al., 1995).

Metabolic steady-state NMR has been used in this study and examines ^{13}C glutamate enrichment subsequent to steady state establishment (Yu et al., 1995). Detailed mechanism of ^{13}C glutamate analysis is outlined in section 2.11.

There are a number of advantages associated with ^{13}C labelling methods:

- Experiments are simpler to perform and analyse (Malloy et al., 1990a).
- Relative fractional enrichments at each carbon atom can be directly quantified from ^{13}C NMR spectrum, eliminating additional purification steps.
- All labelled metabolites present in sufficient concentrations detected, not solely those for the study (Badar-Goffer and Bachelard, 1991).
- Enrichment patterns in adjacent carbons detected; provides additional information about the activity of pathways and allows simultaneous determination of different labelled substrates.
- ^{13}C NMR is considerably more advanced than radioisotopic techniques which limit the number of pathways investigated as these studies focus only on a measurement of end products (Malloy et al., 1990a).

A major disadvantage of ^{13}C NMR is its relative insensitivity, necessitating the presence of NMR-visible nuclei in sufficient (mM) concentrations to be detectable (Scwartz and Weiner, 1992).

1.5 Chronic Kidney Disease

Chronic kidney disease (CKD) is a syndrome of persistent renal impairment involving loss of glomerular and tubular function, and resulting in a compromised renal homeostatic role (Marshall, 2000). Causes of CKD include renovascular and hypertensive diseases, diabetic end stage renal failure, glomerulonephritis, neoplasm, toxic, infective and congenital CKD as well as systemic diseases (myeloma, systemic lupus erythematosus) (Roderick and Feest, 2005). The major clinical features of CKD are similar, regardless of the underlining cause, due to a decrease in the number of functioning nephrons. The metabolic and biochemical consequences of end-stage renal disease are shown in table 1.2 below.

Chronic Kidney Disease		
Metabolic Features	Biochemical Changes in Plasma	
	Increased	Decreased
<ul style="list-style-type: none"> • Impaired electrolyte homeostasis • Impaired removal of the waste products • Impaired water regulation • Altered acid-base balance • Altered hormone production-vitamin D, Erythropoietin and renin • Impaired blood pressure control 	K ⁺ Urea Creatinine H ⁺ Phosphate, Mg ²⁺	HCO ₃ ⁻ Ca ²⁺

Table 1.2 Metabolic and Biochemical Consequences of Chronic Kidney Failure

Table adapted from Marshall (2000)

Several changes (*Table 1.3*) have been associated with renal failure which may contribute to cardiovascular complications.

Myocardial Changes in Uraemia	
<ul style="list-style-type: none"> • Left ventricular hypertrophy • Alterations in myocyte number • Intermyoctic fibrosis • Coronary heart disease • Microvascular disease • Macrovascular disease 	<ul style="list-style-type: none"> • Reduction of insulin mediated glucose uptake • Altered activity of the insulin dependant glucose transporter GLUT 4 • Reduced stability of energy rich nucleotides • Abnormal control of intracellular Ca in cardiomyocyte • Reduction of inotropic and chronotropic response to α-adrenergic stimulation • Anaemia • Hypertension

Table 1.3 Structural & Functional Changes of the Heart in Renal Failure

Adapted from Amann, and Ritz (2001)

The pathogenesis of uraemic cardiomyopathy is complex resulting from a number of factors including hypertension, hypertrophy, hypervolaemia and anaemia and activation of renin-angiotensin system (RAS) (Amann and Ritz, 2001). Potential cardiac risk factors in CKD population are outlined in table 1.4.

Cardiac Risk Factors in Uraemia	
<ul style="list-style-type: none"> • Anaemia • AV fistula • Volume overload • Hypoalbuminaemia • Hyperhomocysteinaemia • Oxidative stress • LV hypertrophy 	<ul style="list-style-type: none"> • Chronic inflammation • Secondary and tertiary hyperparathyroidism • Uraemic toxins • Insulin Resistance • Diabetes • Hypertension

Table 1.4 Cardiac Risk Factors in Uraemia

Adapted from Rigatto, (2001)

Confounding factors which are associated with uraemic cardiomyopathy are summarized in figure 1.8 below.

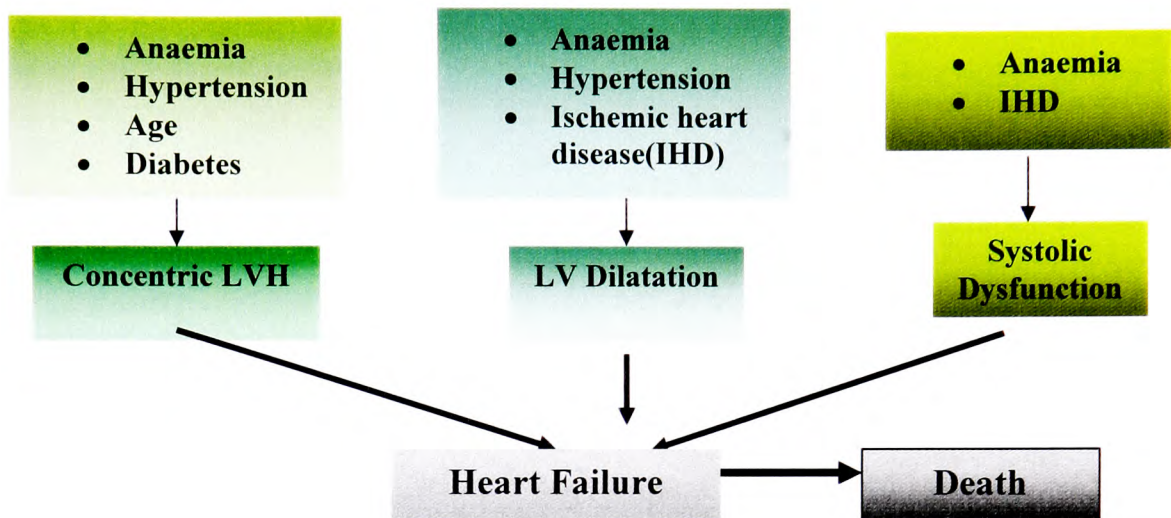


Figure 1.8 Confounding Factors in Uraemia

Adapted from Rigatto, (2001)

1.5.1 Vascular Disease

In uraemia, wall thickening of intramyocardial arteries is a consistent finding (Amann et al., 1995), resulting from enhanced actin content leading to hypertrophy of arteriolar smooth muscle cells (Amann and Ritz 2001). Immunohistochemical investigations have revealed an increase in the expression of vascular endothelial growth factor (VEGF), platelet derived growth factor (PDGF-AB), collagen IV, actin and intergin β -1 in the arteriolar walls of intramyocardial arteries of uraemic heart (Amann et al., 1998a). However, the functional consequences are still not fully defined (Amann and Ritz 2001).

Parathyroid hormone (PTH) plays an important role in the genesis of wall thickening as demonstrated clinically by a correlation between the PTH concentration and cardiac morbidity in dialysis patients (Amann et al., 1995b, Block, 1998). Deposition of collagen fibres between cardiomyocytes and capillaries may increase the risk of ischemia by capillary displacement, in turn causing reduction of heart compliance, altered stress-strain relation and altered electrical stability by re-entrant type of arrhythmias (Tornig et al., 1996, Tornig et al., 1999). Myocardial capillary density is reduced, further interfering with blood and oxygen supply in uraemic heart. This renders myocardium more susceptible to ischaemic injury (Amann et al., 1998a).

Fibrosis is a common occurrence in uraemic myocardium (Amann et al., 1995a). Interstitial cells from subtotally nephrectomized rats stained for proliferating cell nuclear antigen (PCNA) proliferation marker, in addition to 125I-platelet-derived growth factor-AB (PDGF-AB) and integrin- β , detected in cardiac interstitium, unlike the heart in a model of essential hypertension (Amann et al. 1995). *In situ* hybridisation has revealed an increase in cardiac renin and ET-1 mRNA expression in uraemic rats compared to controls (Amann and Ritz 2001). Uraemic patients have high risk of myocardial infarction with a high rate of MI mortality. Reduced ischemia tolerance stems from finding that the greater parts of non perfused uraemic myocardium undergo total necrosis compared to controls resulting in a poor MI tolerance (Dikow et al., 2004).

1.5.2 Pathophysiological Effects of Uraemic Retention Solutes

Disorders of cardiovascular, skeletal, haematological and other systems are thought to result in part from retention of uraemic toxins, namely urea, creatinine, guanidines, inodoxyl sulphate, hippuric acids, parathyroid hormone, β_2 -microglobulin, spermine and putrescine (Vanholder et al., 2001).

Accumulation occurs in plasma and cells and their impaired removal during dialysis may result in inadequate detoxification (Vanholder and De Smet, 1999). Urea itself has several important physiological effects; it inhibits $\text{Na}^+\text{K}^+/\text{Cl}^-$ co-transport in erythrocytes which normally regulates cell volume and extrarenal potassium regulation (Vanholder and De Smet, 1999). In addition it can decrease cAMP production at extremely high concentrations and reduces affinity of haemoglobin for oxygen (Lim et al., 1995). This latter effect is due to excessive 2,3-diphosphoglycerate binding (Monti et al., 1995, Prabhakar et al., 1997). Accumulation of middle weight molecular peptides (MW 300-12000Da) (i.e. β_2 -macroglobulin and parathyroid hormone PTH) have also been considered as potential instigators of uraemic syndrome (Vanholder and de Smet, 1992).

Creatinine is one of the most characteristic uraemic products and is acutely responsible for reduced cardiomyocyte contractility, induction of arrhythmias or asynchronies in a concentration-dependent manner by dysregulating Ca^{2+} availability (Weisensee et al., 1993, Weisensee et al., 1997).

Homocysteine (Hcy) is increased 2-4 fold in CKD and constitutes one of the most prevalent cardiovascular risk factor in CKD (Massy et al., 1994). Hcy was found to stimulate proliferation of vascular smooth muscle cells, one of the most prominent markers of atherosclerosis, altering the balance between pro- and anti- coagulants in vessel walls and predisposing vessels towards thrombogenicity (Tsai et al., 1992, Harpel et al., 1996).

1.5.3 Hypertension

Hypertension results from extracellular fluid expansion, neurohormonal activation (Morgan and Baker, 1991), endothelial dysfunction (Puddu et al., 2007) and artery stiffening (Duprez and Cohn, 2007) and can cause pressure overload hypertrophy in uraemia (London et al., 1999). Hypertension is a major culprit for cardiovascular complications in uraemia and is associated with LVH (Braunwald and Bristow, 2000), cardiac chamber dilation, increased LV wall stress, redistribution of coronary blood flow, reduced coronary artery blood reserve, ischaemia, myocardial fibrosis, heart failure and arrhythmias (Rostand et al., 1991). Concentric hypertrophy arises from the generation of greater pressure during ventricular contraction achieved by arraying of protein contractile units in parallel (*Fig. 1.10*) (Middleton et al., 2001). Concentric hypertrophy development leads to decreased diastolic compliance. Hypertension has shown consistent association with LVH in both early and later stages of the disease (Middleton et al., 2001). Hypervolaemia (salt and water retention) and activation of rennin angiotensin system (RAS) are the major determinants of hypertension in CKD.

1.5.4 Anaemia

In pre-dialysis stage of the CKD, anaemia is the most important factor in volume overload usually occurring in parallel to the pressure overload (London, 2001).

Anaemia is associated with an increase in stroke volume and the heart rate (London, 2001). Anaemia in renal disease results in reduced oxygen delivery and is increasingly dependant on the affinity of Hb for oxygen, blood flow and the adaptation of peripheral tissue.

Primary compensatory mechanisms for the decrease in Hb levels include increase and redistribution in blood flow (London, 2001) and consequently an increase in cardiac output as a consequence of decreased blood viscosity and decreased peripheral vascular resistance (*Fig 1.9*) (London, 1999).

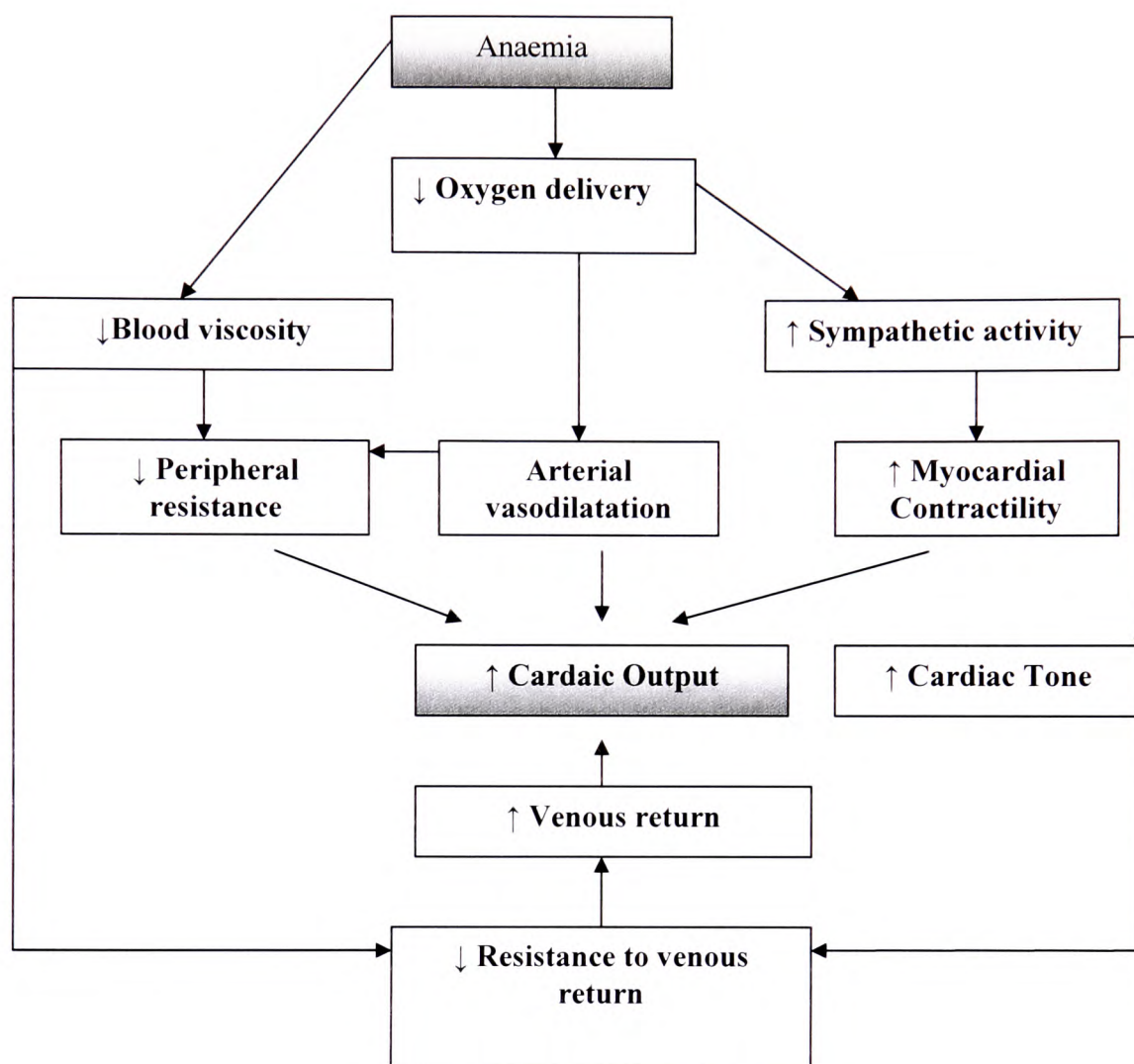


Figure 1.9 Haemodynamic Changes Induced by Anaemia

Adapted from London and Parfey (1997)

Diminished blood viscosity enhances venous return increasing pre-load and LV filling increasing cardiac output. Reduced oxygen delivery causes hypoxic vasodilatation regulated by the production of hypoxia-generated metabolites, increased NO availability and angiogenesis via the opening of new capillaries (Metivier et al., 2000).

Under normal circumstances, an increase in cardiac work and cardiac output by anaemia would result in reversible LV and arterial remodelling (Metivier et al., 2000). However, in uraemia these changes are maladaptive preceding hypertrophy and possibly atherosclerosis. Several treatment studies have demonstrated that partial correction of anaemia in CKD can improve LV dimensions without a full correction of LV hypertrophy and dilation (Middelton et al. 2001).

1.6 Left Ventricular Hypertrophy

LVH is a definitive hallmark of CKD (Amann et al., 2003b, Reddy et al., 2007). LVH is the most potent marker of cardiovascular risk in uraemia due to vascular abnormalities (hypertension, increased arterial stiffness etc.) and a causal risk *per se*, influencing coronary dynamics and myocardial oxygen requirement (De Simone, 2003).

The basis of LVH is the activation of cardiac protein synthesis in cardiomyocytes in response to hyperfunction of the heart (Meerson, 1971). It is an adaptive response of the heart to a chronic haemodynamic overload resulting in molecular, cellular and physiologic adaptations (Stanley et al., 2005). It normalizes myocardial wall stress in response to an increased workload (Grossman et al., 1975). This is in accordance with the Law of La Place stating that the wall stress is proportional to the pressure and the chamber radius and inversely proportional to the wall thickness (Katz, 2001).

$$\text{Wall Stress} = \frac{\text{Pressure} \times \text{Radius}}{\text{Wall Thickness}}$$

Owing to terminal differentiation of adult cardiomyocytes, any adaptation to an increased workload is going to be compensated primarily via cell hypertrophy versus hyperplasia (Beltrami et al., 2001). Pathological hypertrophy progresses through three phases:

- 1) Developing hypertrophy where unpredicted overload exceeds functional reserve causing acute heart failure;
- 2) Compensatory hypertrophy- enlargement of heart to match chronic demands;
- 3) Fulminant heart failure- myocyte incapacitation and loss, accompanied by cardiac function deterioration and subsequent failure (Meerson, 1971, Bugaisky et al., 1991).

Hypertrophic stimuli include mechanical stress/stretch and neuro-humoral factors which initiate hypertrophic response (i.e. RAS) and are sensed by the heart cells via an array of membrane-bound receptors:

- 1) stretch-sensitive receptors,
- 2) G-protein-coupled receptors (GPCRs),
- 3) gp130-linked receptors,
- 4) integrins
- 5) receptors associated with the intracellular tyrosine kinase or serine/threonine domains (Heineke and Molkentin, 2006).

Coordinated myocardial transcriptional responses in hypertrophy and diabetes (model of hypertrophy and insulin resistance) are given in table 1.5 below (Taegtmeyer et al., 2005).

HYPERTROPHY DIABETES		
Contractile proteins		
α-MHC	↓	↓
β-MHC	↑	↑
Cardiac α-actin	↓	↓
Skeletal α-actin	↑	↑
Ion Pumps		
α_2NaKATPase	↓	↓
SERCA2a	↓	↓
Metabolic Proteins		
GLUT4	↓	↓
GLUT1	↔	↓
Muscle CPT-1	↓	↔
Liver CPT-1	↔	↔
mCK	↓	↓
PPARα	↓	↑
PDK4	↓	↑
MCD	↓	↑
UCP2	↓	↔
UCP3	↓	↓

Table 1.5 Transcriptional Responses of the Heart in Hypertrophy & Diabetes

Arrow denotes increase and decrease in expression; ↔ no change

Adapted from Taegtmeyer et al. (2005)

LVH can also be interpreted as natural evolution of cardiac disease in uraemia. Structural changes in LVH can occur as a result of volume and pressure overload (*Fig. 1.10*). Two contrasting models of adaptation can develop depending on the pattern of imposed stress (Middleton et al 2001). Chronic pressure and volume overload in uraemic hearts accelerates cardiomyocyte loss via apoptosis and necrosis (Amann et al. 2003). The number of cardiomyocytes was found to be significantly reduced in chronic renal failure (Amann et al. 2003). The mechanism of cell loss is not fully understood. However, it has been suggested that the local renin-angiotensin system (RAS), activated by increased cardiac workload, plays an important part in cell loss and hypertrophy, as cardiomyocyte loss was prevented by administration of the angiotensin-converting enzyme (ACE) inhibitor ramipril (Mann et al., 2001, Amann et al., 2003a). Certain myocyte ventricular population stained positive for proliferation marker PCNA (proliferating nuclear antigen) indicating possible cell cycle reactivation in myocytes, potentially culminating in apoptosis (Amann et al., 1998b).

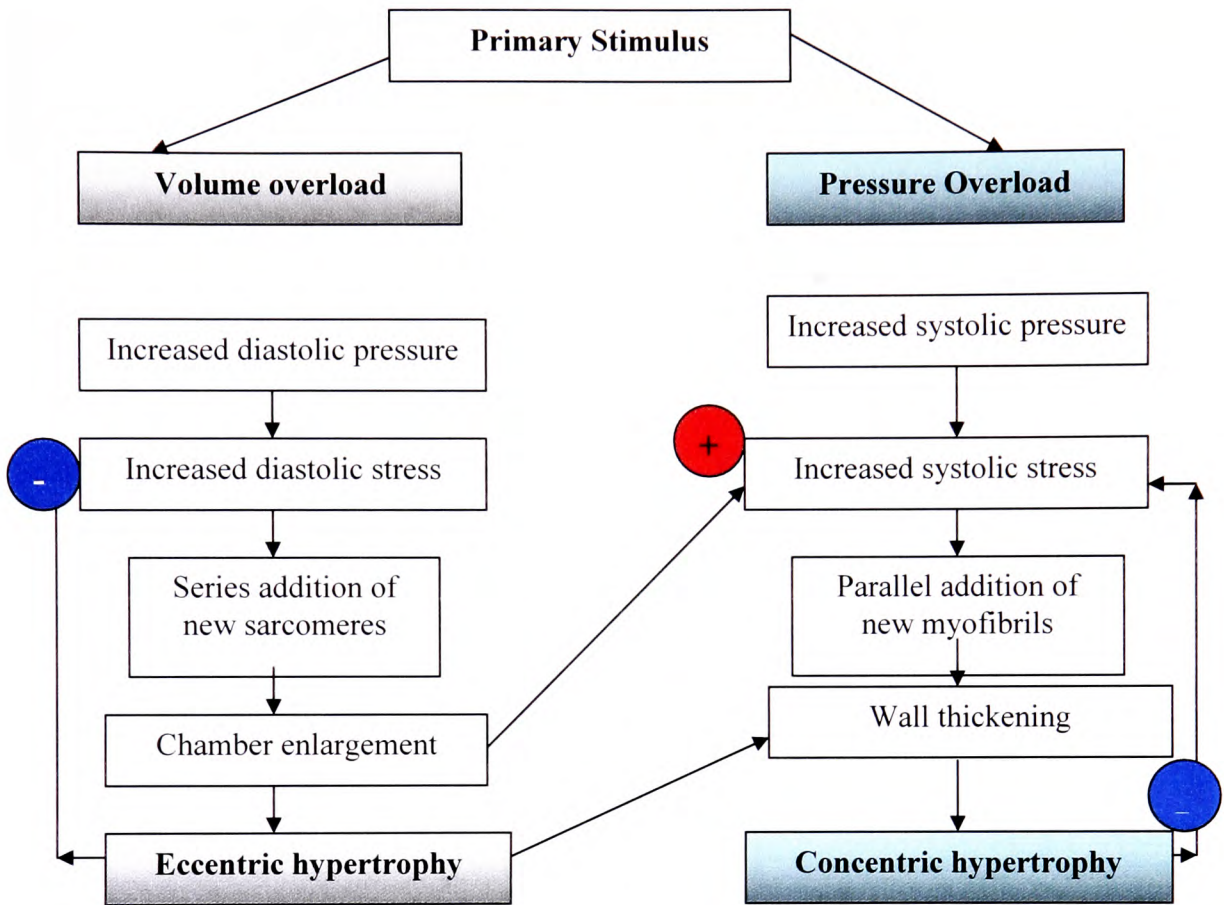


Figure 1.10 Wall Stress and Patterns of Hypertrophy

Adapted from London (2001)

1.6.1 Contractile dysfunction

Hypertrophic growth of the myocardium, in response to pathological stimuli, is thought to preserve cardiac pump function, although prolongation of the hypertrophic state is a leading predictor for the development of arrhythmias, sudden death and heart failure (Ho et al., 1993, Wilkins et al., 2004).

Compensated cardiac hypertrophy and subsequent heart failure are associated with alterations in cellular Ca^{2+} homeostasis, which either underlies or accompanies the alteration in contractile phenotype (Fowler et al., 2007). Contractile dysfunction in uraemia is accompanied by a pro-arrhythmogenic tendency with increased occurrence of ventricular premature beats, couplets, runs of ventricular tachycardia, late ventricular depolarisations and increased QT interval dispersion (Niwa et al., 1985, de Lima et al., 1999, Donohoe et al., 2000b). Myocardial calcium content of the dialysis patient is greater than in control subjects and it has been associated with altered contractile function and cardiac arrhythmias (Rostand et al., 1991). Electrical pacing of a single uraemic ventricular cardiomyocyte shows contractile abnormalities confirming that the cardiomyopathy occurs at the cellular level (McMahon et al., 1996). Cells from uraemic animals showed a reduction in contraction amplitude in addition to impaired contraction and relaxation velocities under maximum Ca^{2+} induced stimulus, suggesting altered Ca^{2+} cytoplasmic handling (McMahon et al., 2002). Therefore uraemia potentially leads to alterations in the cardiac calcium cycling and contractile function.

One of the known causes of intracellular calcium overload is a reduction in energy availability required for the maintenance of normal ionic gradients (Bers, 2006), and the reduction in PCr/ATP ratio is well documented in experimental uraemia (Raine et al., 1993). In addition, reduced $\text{Na}^+/\text{Ca}^{2+}$ exchanger actively interferes with relaxation in uraemia possibly by working in reverse mode (McMahon et al. 2006).

Renal failure is also associated with the rapid inactivation of the ventricular cardiomyocyte L-type Ca^{2+} currents which may reduce calcium influx and contribute to shortening of the action potential duration (Donohoe et al., 2000a). In addition, abnormalities in the cardiac transient repolarizing K^{+} current are a potential cause of altered cardiac action potential in uraemia (Donhoe et al. 2000). Sodium pump functional abnormalities have been known for many years, with circulating pump inhibitors being present in the serum of uraemic patients (Stokes et al., 1990, Sohn et al., 1992, Periyasamy et al., 2001), causing an acute alteration in calcium cycling and cardiomyocyte relaxation through sodium pump inhibition (Periyasamy et al., 2001). The inhibition of the sodium pump initiates a signal cascade that can cause alterations in gene transcription and ultimately result in cardiac hypertrophy in isolated cardiomyocytes (Xie et al., 1999).

1.6.2 Metabolic alterations

It has been postulated that metabolic remodelling is the adaptive response to hypertrophy, maintaining structural and functional remodelling of the heart (De Simone, 2003). Thus, metabolism provides the connection between environmental stimuli and signalling pathways of cardiac growth and function. LVH is characterized by a switch in the preference of metabolic substrates from long chain fatty acids to glucose and was observed in both experimental and clinical LVH (Lopaschuk et al., 1992, Allard et al., 1994, Davila-Roman et al., 2002).

This occurs as an adaptive response to prolonged haemodynamic overload in LVH in order to maintain sufficient cardiac output (Allard et al., 1994, Sambandam et al., 2002, Allard 2004). The pattern of change in substrate utilization that develops in pathologic LVH resembles that in foetal hearts with increased preference for glucose as the major source of energy (Lopaschuk et al., 1992), reflecting the re-expression of foetal metabolic phenotype (Taegtmeyer, 2000, Tian, 2003, Allard, 2004) and downregulation of adult metabolic phenotype in addition to evidence of reduction of FA oxidation (Remondino et al., 2000). Furthermore, progression of LVH from compensated to decompensated stage, as observed in the failing human heart, is also characterized by a decrease in metabolic gene expression from the adult to the foetal heart levels (Razeghi et al., 2001). Figure 1.11 below summarizes the metabolic adaptation versus maladaptation in the hypertrophied heart.

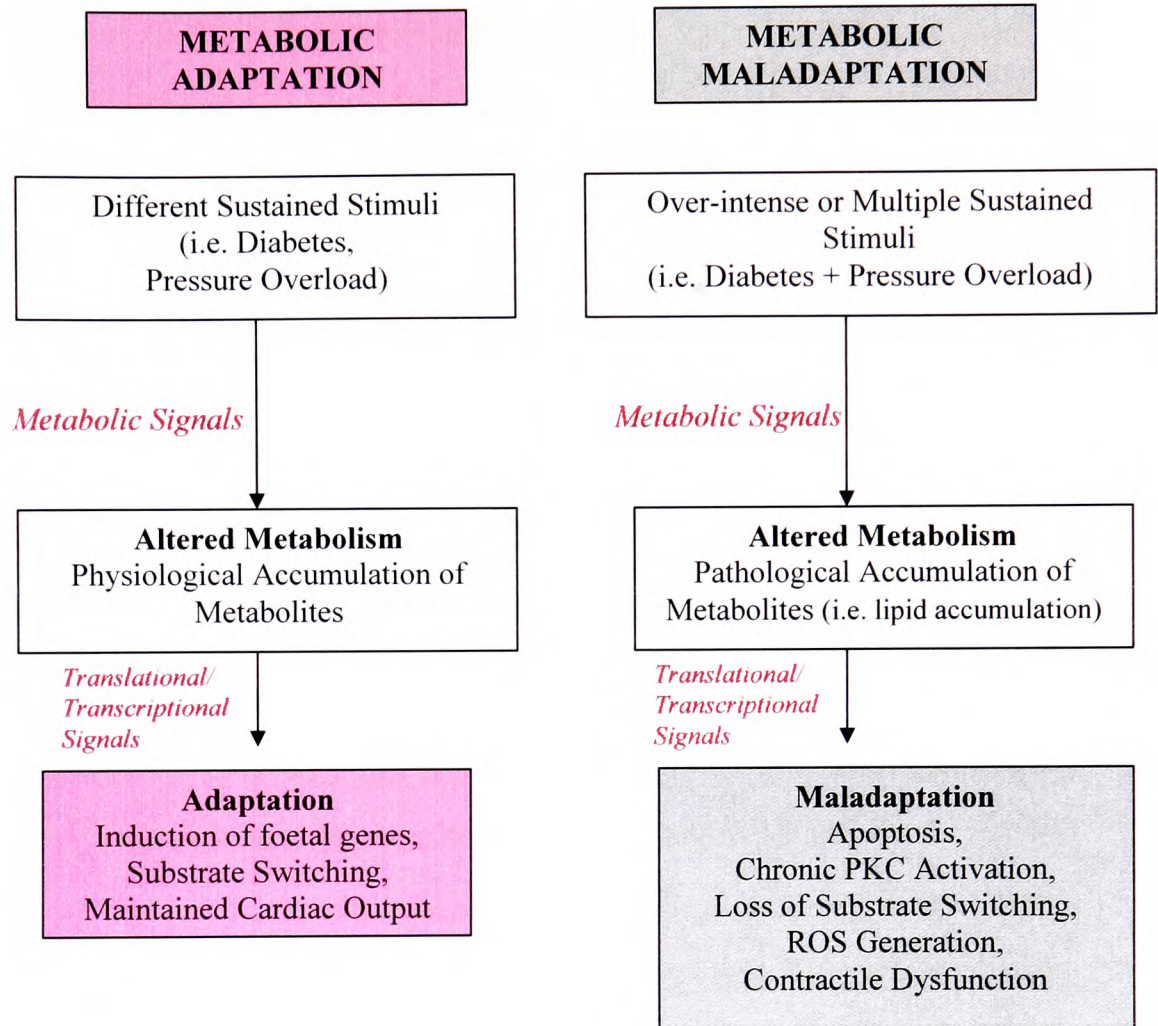


Figure 1.11 Metabolic Adaptation & Maladaptation of the Heart

Adapted from Taegtmeyer et al. (2005), Young et al. (2002)

³¹P NMR assessment of uraemic hearts (Raine et al., 1993) has revealed significant reductions in phosphocreatine content and phosphocreatine/ATP ratio in addition to an increase in free cytosolic ADP concentrations. These findings imply altered myocardial energy supply in uraemia (Raine et al. 1993).

During chronic renal failure, total serum carnitine levels are raised in response to depressed renal clearance of esterified carnitine. By contrast, uraemic patients undergoing dialysis present with secondary carnitine deficiency (Huot et al., 2002). The carnitine serum levels of dialysis patients can be 50-80% lower than normal levels in healthy adults (Schreiber and Lewis, 2001). Carnitine is a cofactor essential for LCFA oxidation as it shuttles LCFA into the mitochondria. Furthermore, mitochondrial uptake of octanoate, a medium chain fatty acid not requiring carnitine shuttle, is unaffected in LVH therefore confirming that the reduction in LCFA uptake is not due to impaired β oxidation *per se* (El Alaoui-Talibi et al., 1997, Allard, 2004). Low plasma carnitine levels in CKD may lead to a reduction in fatty acid oxidation contributing to uraemic cardiomyopathy by decreasing the adaptability and left ventricular ejection fraction in 75% of CKD dialysis patients (Schreiber and Lewis, 2001). Reduced fatty acid oxidation has been observed in CKD patients *in vivo* clinical studies. Trials with dialysis patients administered L-carnitine showed that the ejection fraction and LVH improved in 37% with the recovery of mitochondrial FFA supply and oxidation (Schreiber and Lewis, 2001).

1.7 Insulin Resistance in Uraemia

Insulin resistance is a diminished ability of insulin to exert its biological actions across a broad range of concentrations (Okada et al., 2007). Numerous studies using euglycemic glucose clamp have revealed that the progression from normal to impaired glucose tolerance is associated with the development of insulin resistance (DeFronzo et al., 1978, DeFronzo et al., 1981).

Insulin resistance is usually associated with the metabolic role of insulin and its ability to affect glucose uptake in insulin sensitive tissues (i.e. hyperinsulinaemia and impaired glucose tolerance). Insulin resistance is associated with type 2 diabetes, hypertension, central obesity and dyslipidaemia, all of which are significant risk factors for chronic kidney disease (Chen et al., 2003, Nishimura et al., 2006). The kidneys are an important regulator of glucose homeostasis and any alteration in function will have detrimental impact (Becker et al., 2005). Insulin resistance is widely recognised in uraemic patients even at the earliest stages of renal dysfunction (Kauffman and Caro, 1983, Lim et al., 2003). Moreover, clinical studies have indicated that a greater degree of insulin resistance may predispose to renal injury by worsening renal haemodynamics through glomerular hyperfiltration (Dengel et al., 1996).

The early stage of insulin resistance is characterized by hyperinsulinaemia and euglycaemia as β pancreatic cells have diminished ability to maintain high rates of insulin secretion. Subsequent insulinopenia leads to the impaired glucose tolerance and overt diabetes (Shulman, 1999). DeFronzo et al. (1981) examined insulin sensitivity in patients with uraemia compared to 36 control subjects. They discovered a 47% reduction in insulin-mediated glucose metabolism in patients with renal failure. However, insulin-mediated glucose uptake by liver is normal in uraemia indicating that the peripheral tissue insensitivity is the underlying cause of insulin resistance (DeFronzo et al., 1981, Chen et al., 2003).

1.7.1 Insulin Signalling

In addition to its metabolic effect, insulin has anti-apoptotic effect. Studies on ischaemia-reperfusion have clearly demonstrated protective effect mediated via PI-3K phosphorylation of serine/threonine kinase Akt (PKB) which in turn activates mTOR and p70s6k (Jonassen et al., 2001) and in turn apoptotic regulator BAD was maintained in inactive phosphorylated state. Dephosphorylation of BAD results in translocation to the mitochondria with the subsequent heterodimerization with Bcl-xl or Bcl-2 to promote cell death (Jonassen et al. 2001). Critical downstream element of PI3K/Akt is glycogen synthase kinase-3(GSK-3), key regulator of apoptosis.GSK-3 regulates glycogen synthesis in response to insulin (Pap and Cooper, 1998). Its activity is inhibited by Akt phosphorylation in response to growth factor stimulus. GSK-3 also phosphorylates wide range of substrates including transcription factors and translation initiation factor eIF2B (Welsh et al., 1996). GSK-3 is a central element in PI3K/Akt survival pathway, with phosphorylation of any of its downstream targets serving to activate apoptotic cell death (Pap and Cooper, 1998). Insulin resistance in uraemia may therefore remove all the protective mechanisms against apoptosis, further increasing the vulnerability of the uraemic heart to cell loss and heart failure. However, the exact underlying causes of the insulin resistance observed in uraemia still remain unclear with numerous proposed suspected mechanisms.

Insulin resistance in uraemia may be triggered by the underlying hypertension. There is increasing evidence that the angiotensin II inhibits insulin and IGF-1 signalling through the PI3K/Akt pathway inhibiting vasodilation and glucose transport (Sowers, 2004).

ANG II binding to its receptor AT₁R, increases generation of ROS in the vasculature through activation of membrane bound NAD(P)H oxidase. In addition, binding causes activation of low molecular weight G proteins such as RhoA. Generation of ROS and RhoA inhibits PI3K/Akt signalling mediated actions including endothelial NO synthase activity, Na pump activation and Ca-MLC desensitization. Inhibition of PI3K/Akt signalling results in decreased endothelial cell NO production, increased myosin light chain activation with vasoconstriction and diminished glucose transport (Sowers and Frohlich, 2004).

1.7.2 Cardiac Dysfunction & Substrate Metabolism in Insulin Resistance

Experimental model of hypertension (SHR) and insulin resistance have exhibited decreased GLUT4 and a decreased ratio of GLUT4/GLUT1 mRNA expression (Paternostro et al., 1995a, Paternostro et al., 1999a). However, defective glucose utilization, characteristic of insulin resistance, cannot be account solely by reduced transporter expression, as little or no reduction in heart GLUT4 content was observed in obese insulin resistant *db/db* and *ob/ob* mice (Koranyi et al., 1990, Mazumuder et al., 2004).

Insulin resistance affects myocardial energy metabolism, as heart is exposed to hyperinsulinaemia and hyperglycaemia due to impaired insulin-mediated glucose uptake and glycolysis (Buchanan et al., 2005). Although reduced glucose uptake may contribute to decreased glucose utilization in insulin resistant hearts, in CIRKO (insulin receptor knockout) mice hearts and *ob/ob* severely insulin resistant mice, basal rates of glucose oxidation is reduced, suggesting additional mechanism for reduced glucose utilization than impaired insulin signalling (Boudina and Abel, 2006). One possible mechanism could be via reduction in PDH flux, as observed in the hearts of ZDF (zucker diabetic fatty) and *ob/ob* rats (Boudina et al., 2005). Another possible mechanism is reduced mitochondrial oxidative capacity due to mitochondrial uncoupling defects, which are common in insulin resistant mice hearts (Boudina et al. 2005).

The insulin resistant myocardium adapts to this environment by increasing the reliance on fatty acids as a main metabolic fuel primarily by increasing the expression of PPAR α regulated genes (Young et al., 2002a, Mazumder et al., 2004). However, initial increase in FFA oxidation in insulin resistance is accounted for by an alternative mechanism to PPAR α upregulation as it was found to occur at a later stage of the disease (Boudina et al. 2006). Some studies have found evidence for downregulation of PPAR α in the diabetic heart (Depre et al., 2000, Young et al., 2001), supporting positive involvement of the alternative pathway. However, the precise mechanism is yet to be elucidated. Increased reliance of the insulin resistant heart on fatty acids as a main fuel results in metabolic inefficiency, declined cardiac function and inability to modulate substrate utilization in response to changes in insulin and FFA supply (Mazumder et al. 2004).

Increase in FFA oxidation is associated with an increase in MVO_2 (oxygen consumption) relative to hearts that are predominantly oxidizing glucose (Vik-Mo and Mjos, 1981, How et al., 2006). Thus, the increase in FFA oxidation in diabetes may be energetically detrimental due to high oxygen cost /ATP molecule produced. Increased MVO_2 accompanied by decreased cardiac efficiency have been found in obese IR and diabetic rat models (Mazumuder et al., 2004, Boudina et al., 2005, Buchanan et al., 2005, How et al., 2006). However, a study on ZDF rats has, in contrast, revealed reduced FFA oxidation rates accompanied by decreased MVO_2 (Young et al., 2002a). The mechanism for insulin resistance and diabetes associated increase in MVO_2 and accompanying reduction in cardiac efficiency is not fully elucidated. In addition to increased FFA uptake and oxidation, both accounting for increased MVO_2 , oxygen may also be utilized for: a) FFA esterification (high TG content is a hallmark of insulin resistance and diabetes) b) ROS production; c) futile ATP consuming cycles (mitochondrial thioesterases, long chain acyl CoA synthase reactions in fatty acid cycling etc.). Increased MVO_2 could also reflect increased mitochondrial uncoupling (Boudina and Abel 2006). Despite an increase in mitochondrial mass in *ob/ob* animals (Boudina and Abel 2006), there is a global defect in oxidative phosphorylation and reduced expression of complexes I, II and V of the electron transport chain, hence further raising possibility of increased mitochondrial uncoupling (Boudina et al., 2005; Boudina and Abel 2006).

There is strong evidence from perfusion studies in diabetic hearts utilizing FFA, that the increased MVO_2 accompanied by reduced cardiac efficiency is due to FFA-induced activation of the mitochondrial uncoupling proteins (UCPs) and adenine nucleotide translocator (ANT) in addition to a superoxide generation (Boudina and Abel 2006). Mitochondrial uncoupling could therefore potentially play a major role in the development of cardiac dysfunction in IR states such as obesity, type 2 diabetes and potentially uraemia. However, uraemic cardiomyopathy is a specific model, as it is typically characterized by diminished oxidation of fatty acids (Nishimura et al., 2006), possibly due to insulin resistance. However, the exact mechanism remains to be fully elucidated.

1.7.3 Post-Translation Protein Modification

Uraemia is characterized by *in vivo* irreversible carbamylation of the α -amino and ϵ -amino acid group of proteins by cyanite, resulting in the formation of carbamoyl amino acids (C-AA). This would alter protein activity by modifying structure and charge (Kraus et al., 2001, Kragelund et al., 2004). For example, *in vitro* insulin carbamylation by cyanite results in reduction of insulin activity to 50% of original molecule. Binding capacity of carbamoylated insulin, as studied in rat hepatocyte, was 1/5 of unaltered insulin molecule, hence indicating significant protein structure and function deterioration (Oimomi et al., 1987, Kragelund et al., 2004). Urea and urea-derived cyanate may lead to carbamylation of proteins involved in signal transduction and translocation of GLUT4 by structural and functional modification (Kraus et al. 2004).

α -amino-carbonyl-L-asparagine (N-C-Asn) affects the insulin-sensitive glucose transporter system and *in vivo* concentration of N-C-Asn is high in patients with ESRD. The amino acid N57 is the potential N-glycosylation site in GLUT4 (Kraus et al., 2004). The -COOH terminus domain of 30 amino acids is a unique feature of GLUT4, containing double leucine (489, 490), acting as a signal for rapid endocytosis and intracellular retention in the absence of insulin (Verhey et al., 1995). N-C-Asn inhibiting effect on glucose transport in IR in uraemia could thus be due to:

- a) Competition with glycosylation site GLUT4 N57, hence causing decrease in GLUT4 glycosylation.
- b) Enhanced activity of domain responsible for rapid GLUT4 endocytosis resulting in rapid endocytosis and retention of GLUT4.
- c) N-C-Asn in the presence of insulin resulting in restricted GLUT 4 redistribution to the cell surface.
- d) N-C-Asn altering insulin induced signal transduction thus interfering with GLUT4 activity.

1.8 Objectives

One of the causes of myocardial insulin resistance in uraemia may arise from glucose uptake and metabolism. Insulin resistance is also potentially a result of cumulative confounding factors associated with the uraemic cardiomyopathy, many of which themselves occur as a result of left ventricular remodelling. However, the precise underlying mechanism still remains unclear.

Consequently, the focus of this project was to use an integrated approach combining physiological and cellular techniques to:

- a)** Evaluate alterations in myocardial structure and function in uraemia;
- b)** Investigate oxidative metabolism of the uraemic heart under conditions of increased work;
- c)** Examine potential mechanisms underlying insulin resistance in uraemia at the level of the myocardial expression of the proteins responsible for the energy provision (metabolic transporters);
- d)** Investigate the cellular basis of myocardial insulin resistance.

2. MATERIALS & METHODS

2.1 Materials

Materials and respective suppliers are listed in tables 2.1-2.4. All chemicals, unless otherwise stated, were of AnalaR grade from BDH (Poole, UK).

Table 2.1 Materials & Suppliers (Miscellaneous)

SUPPLIERS	MATERIALS
ADInstruments, Hastings, UK	Mac Lab/2e System Chart v 5.0 software
Animalcare Ltd. York, UK	Sterile isotonic saline NaCl
Apollo Scientific Ltd. Bradbury, UK	Deuterated water (D ₂ O) (DE50K)
Bio-Rad Laboratories, Hemel Hempstead, UK	Bio-Rad protein assay (500 0006) Bio-Rad mini protean system
Bio-Rad Microscience Ltd , Hemel Hempstead, UK	LaserPix Software
British Oxygen Corporation, Manchester, UK	Oxygen PL 07350-5000 (D fitting)
Bruker BioSpin Ltd, Coventry, UK	Bruker TopSpin 1.3 software
Carbiochem, La Jolla, CA, USA	Mira cloth 25 µm nylon gauze
Cambridge Isotope Laboratories Inc, Andover, USA	(1- ¹³ C) D-glucose (CLM-420) (3- ¹³ C 98%) L-lactate (CLM-1578) (¹³ C 98%) Sodium palmitate (CLM-6059)
ChemLab Instruments, London, UK	Freeze Dryer Modulyo
Charles-River, Margate, UK	Sprague-Dawley Rats
Cole Parmer Ltd, London, UK	Sialistic Tubing (508-007)
Fisher Scientific, Loughborough, UK	L-Glutamine (BP 379)

GE Healthcare UK Ltd, Little Chalfont, UK	Amersham ECL Western Blotting detection reagents (1059243)
Gilmont Instruments, Barrington, RI, USA	Micrometer glass syringe
Harvard Apparatus, Edenbridge, UK	Gaseous anaesthetic apparatus: Fluovac(vacuum pump), Veterinary Fluosorber;
	Ohmeda Fluotec 3 (vaporizer) Haemostatic Clip (micro aneurism/ micro vascular) Non-invasive blood pressure monitor
Invitrogen Life Technologies, Carlsbad, CA,USA	Prestained Benchmark Protein Molecular Marker (10748-010)
Johnson & Johnson, UK	Surgicel Absorbable Haemostatic; oxidised regenerated cellulose(190x7.5cm)
	Ethilon 3-0 polyamide 6 violet braided absorbable
	Ethicon 3-0, vicryl polyglactin910 blue monofilament, non-absorbable
	Ethicon-Mersilk black braided non-absorbable
Kodak, Steinheim, Germany	Kodak BioMax Light Film (819 4540) Kodak GBX developer & replenisher (1900943) Kodak GBX fixer & replenisher (1901875)
Linton Instrumentation.co.uk	Animal restraining cages
MatTek Corporation, Ashland, OR, USA	Microwell Dishes
Media Cybernetics, Silver Spring, CO, USA	Image Pro-Plus v. 5.1.2
Medicell International Ltd, London, UK	Visking dialysis tubing

Merck, Hohenbrunn, Germany	Taurine (8.08616)
Millipore, Watford, UK	0.45µm filter (HA type; HAWP-04700) 5.0 µm filter (SVPP type; SVLP-04700) 0.22 µm syringe filter
Nestle, UK	Marvel Semi-skimmed powder milk
Pierce, Cramlington, UK	Restore™ Western Blot Stripping Buffer (21059)
Radiometer Ltd, Crawley, UK	ABL 77 Blood Gas Analyser
Roche Diagnostics Ltd, Lewes, UK	ACCU-CHECK® Advantage Plus Test Strips (04735102001) Mini-protease cocktail (11836153001)
Sarstedt, Numbrecht, Germany	Microvette 200 µl capillary tubes
SensoNor, Horten, Norway	SensoNor 840 pressure transducer
Serologicals, Norcross, GA, USA	Bovine serum albumin-fatty acid free (BSA; 3320)
Sepatech GmbH, Osterode/Harz, Germany	Megafuge 1.0 Hereans
Sigma Chemical Company Ltd Poole, UK	Acrylamide/Bis 30:0.8 (%w/v)(A3699
	Adenine diphosphate (A-2754)
	Amyloglucosidase (A-7420)
	Ammonium persulfate (A 3678)
	2,2-Azino-di-(3-ethylbenzthiazoline)-6 sulphonate (ABTS; A-1888)
	Bovine serum albumin (A7030 & A6003) (BDM; B-0753)
	Bromophenol Blue (B-8026)

Sigma Chemical Company Ltd Poole, UK	Brilliant blue G solution (B8522-1EA)
	Chelex chelating resin (C-7901)
	CoA (C-3019)
	Citrate synthase (C-3260)
	Dichloroacetic acid (D-5470)
	Glucose oxidase (G-7141)
	Glycine (electrophoresis min99%) (G8898)
	HEPES (H-0527)
	Insulin (I-5500)
	Lactate dehydrogenase (L-2625)
	Lactate-sodium salt (L-7022)
	Lauryl sulphate (L-377)
	2- Mercaptoethanol (M-6250)
	Palmitic Acid-sodium salt (P-9767)
	Peroxidase (P-8125)
	Phenyl methyl sulfonyl fluoride (PMSF) (P-9767)
	Potassium fluoride (P-2569)
	Ponceau S solution 0.1% (w/v) in acetic acid (P7170)
	Pyruvate-sodium salt (P-2256)
	Sodium dodecyl sulphate approx 99% for electrophoresis (L3771)
Trizma Base (T-6066)	
Tween 20 (P-5927)	
TEMED (T-9281)	

Vickers Laboratories, Pudsey, UK	Acetic Acid
Worthington Biochemical Corporation, Lakeland, NJ, USA	Collagenase Type II (394 U/mg ; 4176)

Table 2.2 Antibody Suppliers

SUPPLIERS	ANTIBODIES
Abcam, Cambridge, UK	Rabbit pAb to CD36 (ab 36977-100)
	Mouse mAb Sodium Potassium ATPase α_1 464.6 (ab 7671-50)
AbD Serotec, Oxford, UK	Mouse anti-Rat GLUT4 (4670-1725)
	Rabbit Anti Mouse IgG:HRP()
Autogen Bioclear (Santa Cruz), Calne, UK	Donkey anti-goat IgG-HRP (sc-2033)
	Goat polyclonal GLUT4 (c-20) (sc-1608)
	Goat polyclonal GLUT1 (c-20) (sc-1605)
	Goat polyclonal Phospholamban (L-15) (sc-21923)
	Goat polyclonal SERCA 2a (c-20) (sc-8094)
	Goat polyclonal anti-rabbit HRP (sc-2004)
	Rabbit polyclonal IgG ANP (FL-153) (sc-20158)
Molecular Probes, Leiden, Netherlands	Alexa Fluor 568 goat anti mouse IgG antibody (A11004)

Table 2.3 Assay Kits

SUPPLIERS	KITS
Mercodia, Uppsala, Sweden	Ultrasensitive Rat Insulin ELISA (10-1137-01) Rat Proinsulin ELISA (10-1118-01)
Roche Diagnostics GmbH, Mannheim, Germany	Free fatty acids, half micro kit (1-383-175)
Sigma Chemical Company Ltd. Pool, UK	Triglyceride assay kit (336)

Table 2.4 Veterinary Drugs & Agents

SUPPLIERS	DRUGS/AGENTS
Animal Health Ltd, Southampton, UK	Duphacillin (Ampicillin Microfine Formulation)
Leo Laboratories Ltd, Dublin, Ireland	Heparin sodium 100 IU/ml
Merial Animal Health Ltd, Harlow, UK	Isoflurane-Vet
Novartis Animal Health Ltd, Royston, UK	Thiovet (0.025 g/ml thiopentone sodium) Thiopentol 25% (w/v)
Pfizer, Tadworth, UK	Rimadyl

2.2 Experimental model

All procedures were performed in accordance with the Home Office Guidance on the Operation of Animals (Scientific Procedures) Act 1986.

Uraemia was induced surgically, using aseptic techniques, in male Sprague-Dawley rats (200-240 g Bwt) via 5/6 nephrectomy as described previously (Reddy et al., 2007). Rimadyl, an analgesic agent, (4 mg/kg Bwt) was administered sub-cutaneously and anaesthesia induced using 3% isoflurane /3L/min O₂ and maintained using 2.5% isoflurane/L/min O₂. A laparotomy was performed, the left kidney isolated and the renal artery temporarily occluded using a microvascular clip. Approximately 2/3 (~ 0.5 g) of kidney cortex was removed. Normal blood flow was restored and blood loss limited using absorbable haemostatic material Surgicel[®].

Sham operated control rats underwent the same procedure except that the left kidney was solely decapsulated. Saline was administered directly into the abdomen to compensate for any fluid loss.

The muscle layer was sutured with absorbable suture (Ethicon, Vicryl) and the epidermal layer with non-absorbable suture (Ethilon). Amfipen (42mg/kg Bwt), an antibiotic, was administered sub-cutaneously. Seven days later, animals were anaesthetised again, the right kidney exposed through a flank incision and removed. Sham operated controls underwent the same procedure, with decapsulation as before. 24 h post surgery, rats were housed individually and pair fed. Animals had unlimited access to water, they were weighed weekly and maintained for 3, 6 and 9 weeks post surgery.

2.3 Non-invasive Blood Pressure Measurement

Blood pressures of uraemic and control animals were measured using a non-invasive blood pressure monitor based on the Korotkoff method (Jamieson et al., 1997, Lee et al., 2002). Animals were placed in restraining cages and a small microprocessor controlled occlusion cuff placed on the base of the tail as shown (*Fig. 2.1*). Animals were acclimatized to the restraining cage and the occlusion cuff. Body temperature was maintained via a heating pad and lamp (*Fig. 2.1*) (Bunag, 1983). Inflation of the tail cuff caused the pulse to decrease and signal to disappear (*Fig. 2.2*). Deflation of the cuff caused reappearance of the pulse (*Fig. 2.2*), reflecting systolic pressure.

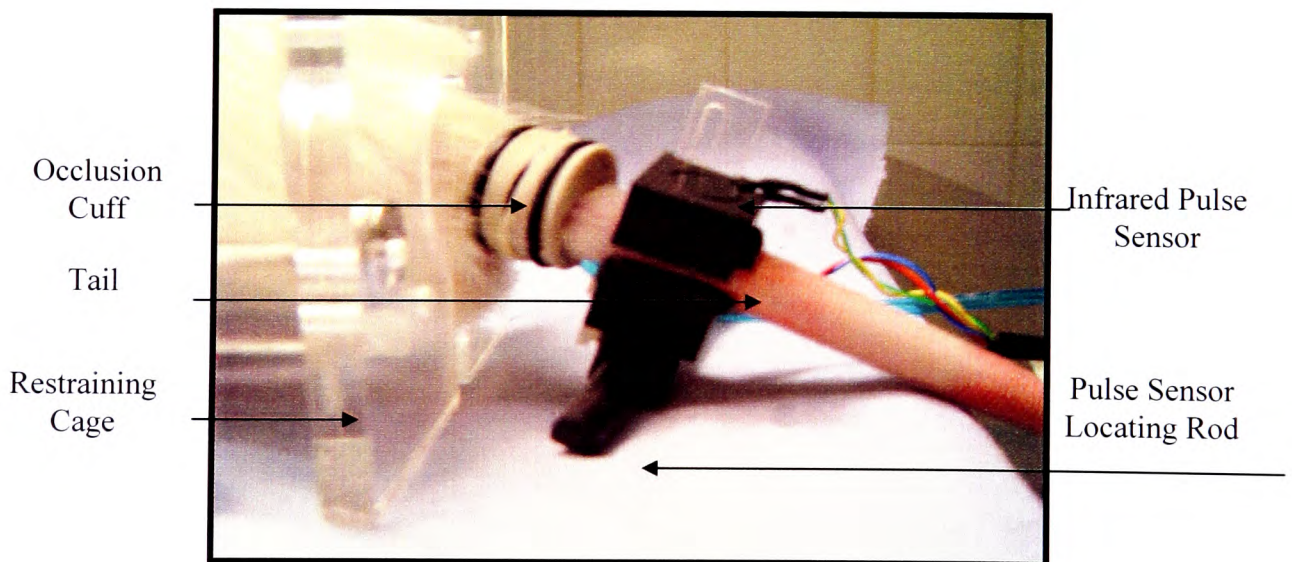


Figure 2.1 Fitting Occlusion Cuff & Pulse Sensor for Non-invasive Blood Pressure Measurement

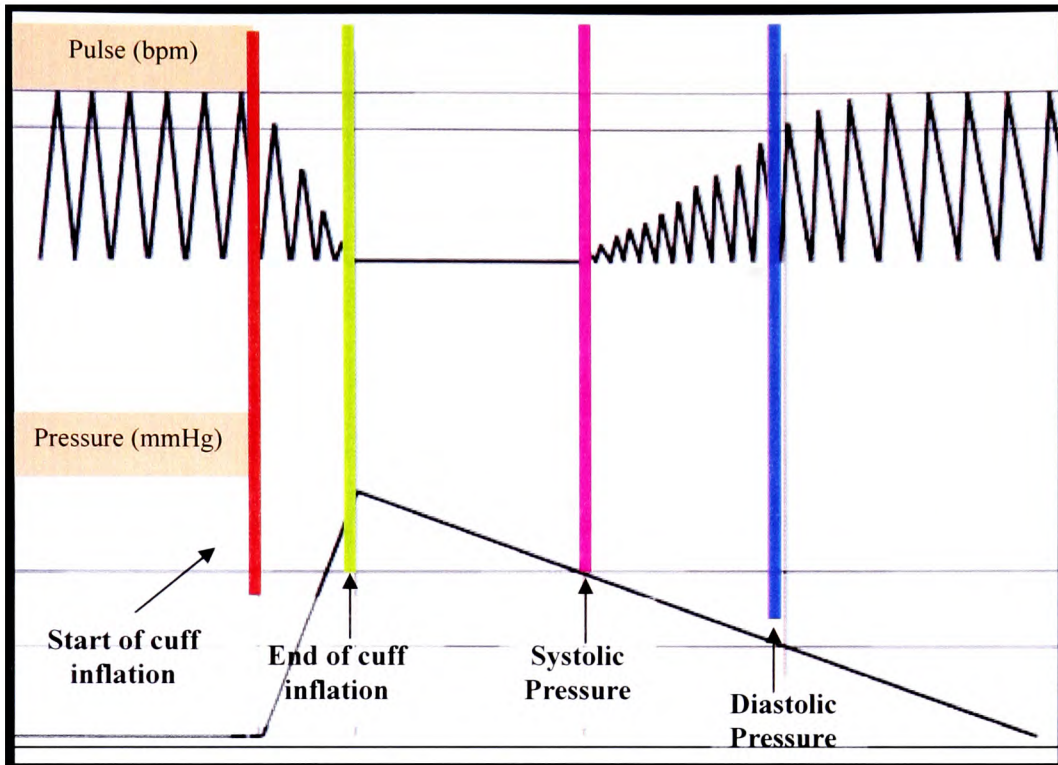


Figure 2.2 Blood Pressure/ Pulse Illustration

Adapted from Harvard Apparatus Advanced Blood Pressure Monitor Instruction Manual

When the pulse strength returned to approximately 75% of its original, diastolic pressure was recorded. The mean arterial pressure was given as:

$$\text{Mean Arterial Pressure} = \frac{\text{Systolic Pressure} - \text{Diastolic Pressure}}{3} + \text{Diastolic Pressure}$$

[mmHg]

7 readings per animal were taken over a 20 min period and their mean calculated.

2.4 Glucose Tolerance Test

The oral glucose tolerance test (OGTT) was based on the method of Veliquette et al (2005). OGTT was performed 6 weeks post-induction of uraemia. Animals were fasted overnight. Local anaesthetic (EMLA) cream was applied to the tail and animals were placed on a heating pad, 15 min prior to blood collection. OGTT was initiated with a single dose of 6g/kg glucose, administered via oral gavage. Blood samples (~5-7µl) were collected via tail venipuncture prior to glucose administration and at 30, 60, 90 and 120 minutes post glucose-load into Sarstedt microvette 200µl capillary tubes. Blood was centrifuged at 3600g, 4°C for 10 min and serum glucose concentration was analysed using ACCU-CHECK® Advantage Plus Test Strips and digital monitor. Serum samples were collected and stored at -20 °C for insulin analysis. Animals were sacrificed and heart tissue harvested as described in section 2.5.4.

2.5 Heart Perfusion Studies

2.5.1 Krebs Henseleit Buffer

Krebs-Henseleit (K-H) bicarbonate buffer was used for all heart perfusions containing 3% (w/v) fatty acid free albumin (BSA), and (in mM): glucose 5; palmitate 0.3 ; lactate 1 ; pyruvate 0.1 ; glutamine 0.5; NaCl 118; NaHCO₃ 25; KCl 4.8; KH₂PO₄ 1.2; MgSO₄.7H₂O 1.2 and CaCl₂.2H₂O 1.25 pH 7.4. Buffer was prepared using ultra-pure water MiliQ 18 megΩ and filtered through 0.45µm HA filters.

2.5.2 Bovine Serum Albumin Preparation

2.5.2.1 Dialysis Tubing Preparation

Visking dialysis tubing (28.6 mm diameter) with a 12-14 kDa molecular size cut-off was cut into 20 cm length pieces. Tubing was thoroughly rinsed with ultra-pure water and subsequently boiled in 500 ml of 2% (w/v) Na₂CO₃ and 1 mM EDTA (pH 8.0) for 10 min, followed by thorough rinsing with ultra pure water and a further 10 min boiling in 500ml 1 mM EDTA (pH 8.0).

2.5.2.2 BSA Dialysis

A 30% (w/v) solution of BSA (fatty acid free) in 118 mM NaCl and 2.5 mM CaCl₂ was dialysed for 48 hours at 4°C against a 20 fold larger volume of 118 mM NaCl and 2.5 mM CaCl₂ solution to remove any small molecular weight impurities. The resultant volume of BSA was recorded, aliquoted and stored at - 20°C until further use. Appropriate corrections were made for NaCl and CaCl₂ in the K-H buffer to account for their presence in K-H stock. Corrections were made using the equation below.

Mass of chemical in 30% BSA /L of buffer (g) = $V_{albumin\ L\ buffer} \times M_{wt\ chemical} \times Molarity$

$$\begin{aligned} CaCl_2 \text{ in } 30\% \text{ BSA (g)} &= \text{volume of BSA/L} \times 147.02 \times 0.0025 \\ \text{i.e.} &= 0.185 \text{ L} \times 147.02 \times 0.0025 = 0.068\text{g} \\ \text{corrected } CaCl_2 \text{ for } 1\text{L K-H buffer} &= 0.184\text{g} - 0.068\text{g} = 0.116\text{g} \end{aligned}$$

$$\begin{aligned} NaCl \text{ in } 30\% \text{ BSA (g)} &= \text{volume of BSA/l} \times 58.44 \times 0.118 \\ \text{i.e.} &= 0.185 \text{ L} \times 58.44 \times 0.118 = 1.275\text{g} \\ \text{corrected NaCl for } 1\text{L K-H buffer} &= 6.89\text{g} - 1.275\text{g} = 5.615\text{g} \end{aligned}$$

2.5.3 Preparation of BSA/Palmitate Krebs-Henseleit Buffer

Unlabelled or uniformly labelled ^{13}C sodium palmitate was dissolved in hot water ($\sim 80^\circ\text{C}$) and added to the 30% (w/v) BSA stock solution, and K-H buffer added to give a final concentration of 3% (w/v) BSA. The resulting K-H buffer was filtered through 5 μm low protein binding filters prior to use.

2.5.4 Langendorff Isovolumic Heart Perfusion

Animals were weighed and anaesthetised with an intra-peritoneal injection of sodium thiopentone (100mg/kg Bwt). Hearts were rapidly excised, rinsed in ice-cold K-H buffer containing heparin (100 IU/ml) and cannulated via the aorta (*Fig. 2.3*) in a modified isovolumic Langendorff mode (*Fig. 2.3*). (Ross, 1972, Ogino et al., 1996). The left ventricular wall apex was pierced to prevent accumulation of fluid in the left ventricle resulting from Thebesian circulation.

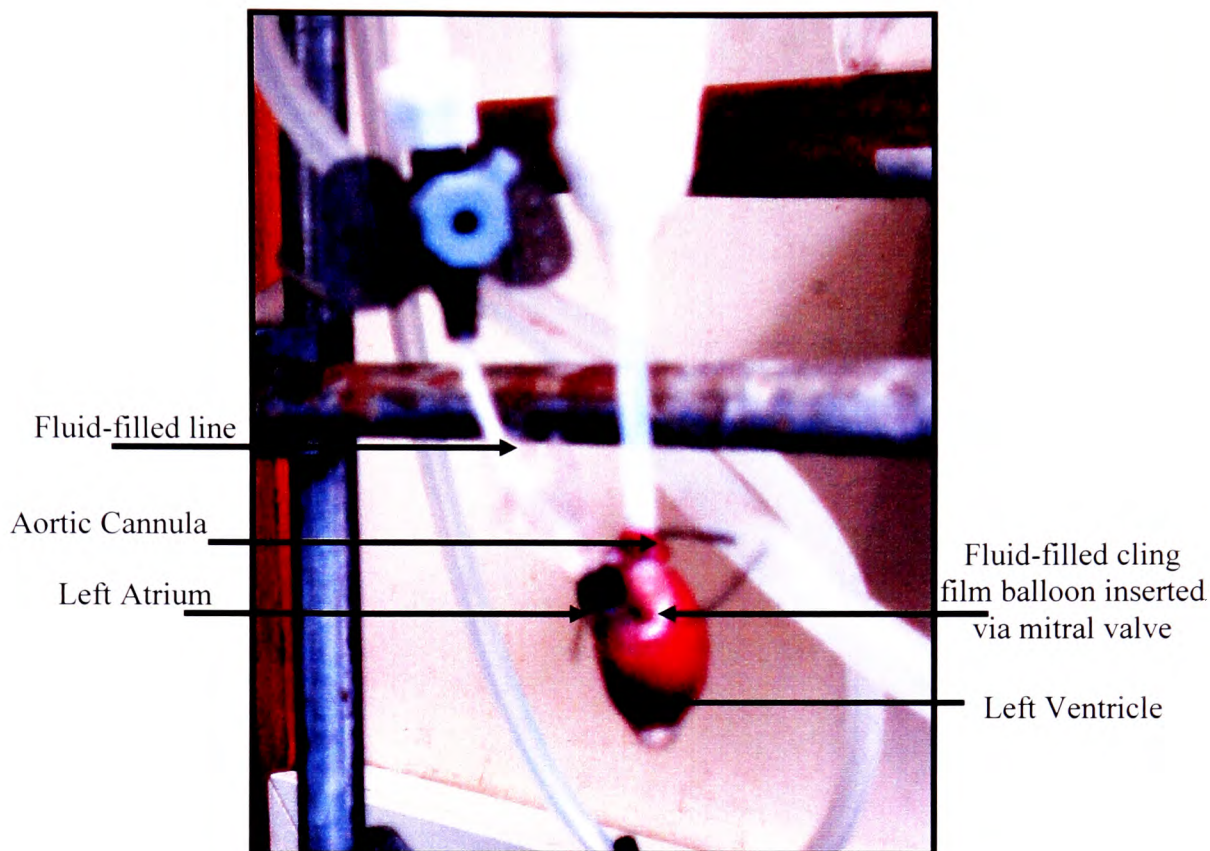


Figure 2.3 Cannulated Heart

A specially constructed oxygenator (*Fig. 2.4*), (Gamcsik et al., 1996) was used for perfusion experiments allowing buffer temperature to be maintained at 37°C and buffer to be equilibrated with 95% O₂ / 5% CO₂ (Gamcsik et al., 1996). Flow rate was maintained at 14 ml/min with a MHRE/22 Mk3 Flow inducer, Watson-Marlow pump, equivalent to a perfusion pressure of 85 cm H₂O (63.5 mmHg). Individual experimental protocols are described in the relevant chapters. At the end of each perfusion, hearts were freeze clamped using Wollenberger tongs, cooled in liquid nitrogen and stored at -196°C until further analysis.

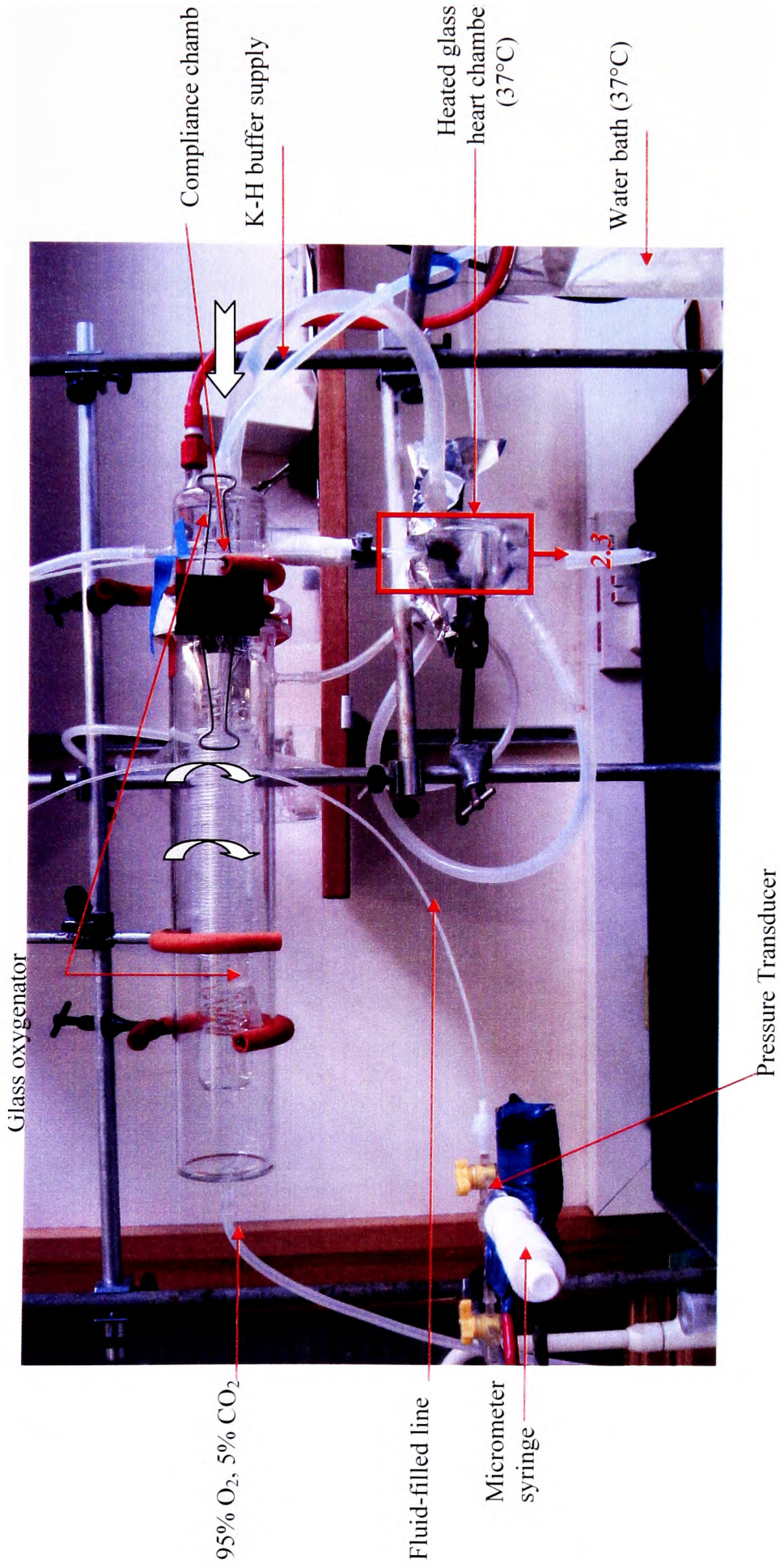


Figure 2.4 Langendorff Perfusion Apparatus

↔ Indicates flow of K-H buffer

2.5.5 Physiological Measurements

Function was monitored using a cling film balloon, inserted into the left ventricle through the left atrium, and connected via a fluid-filled line to a SensoNor 840 pressure transducer and a 2 channel MacLab/2e system (Figure 2.4) (Ogino et al., 1996). The volume in the intra-ventricular balloon was adjusted using a 2.0 ml micrometer syringe to achieve an initial LV diastolic pressure of 4-7 mmHg (Ogino et al., 1996). Left ventricular developed pressure (LVDP) was calculated from the difference between systolic (SP) and diastolic pressures (DP) (Fig. 2.5) for 20 min intervals and averaged for over the duration of the experiment. $+dP/dt_{max}$ and $-dP/dt_{min}$, indicators of cardiac contractile function, were derived from LVDP and averaged over the duration of perfusion experiment. The oxygen content of the perfusate was determined at 15 min intervals using a Radiometer blood gas analyser ABL 77 and oxygen consumption (MVO_2) determined as shown below, normalised for heart weight (Neely et al., 1967).

$$\text{Oxygen consumption} = \left\{ \frac{pO_2 \text{ perfusate} - pO_2 \text{ effluent} \times O_2 \text{ solubility at } 37^\circ\text{C} \times \text{CFR}}{760 \text{ mmHg}} \right\} \left\{ \frac{\quad}{\text{Dry Heart Weight (g)}} \right\}$$

($\mu\text{moles } O_2/\text{min/g dry heart wt}$)

pO_2 measured in mmHg; O_2 solubility at 37°C , $1\text{atm} = 0.199 \mu\text{mol/ml}$;
CFR, coronary flow rate (ml/min).

Rate pressure product (RPP), was determined as the product of the heart rate and LVDP. The ratio RPP/ MVO_2 was used as a measure of myocardial efficiency (Chatham et al., 1999).

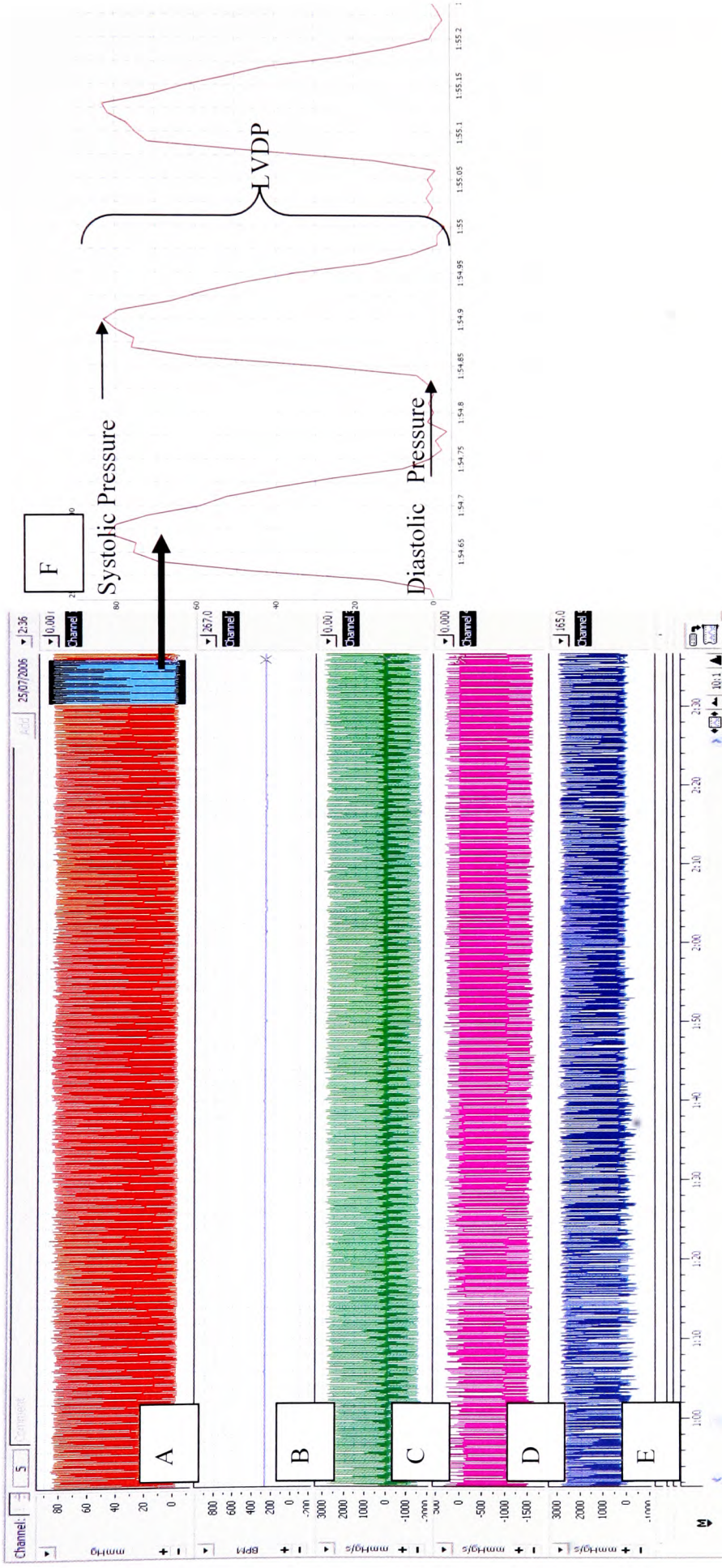


Figure 2.5 Heart Function Trace During Perfusion

A-left ventricular developed pressure LVDP (mmHg) B-heart rate (bpm) C- dP/dt D- $-dP/dt_{min}$

E- $+dP/dt_{max}$ F- Enlargement of highlighted section of LVDP Trace; sampling frequency 200 samples/s

2.6 Left Ventricular Tissue Dissection

Cardiac tissue was briefly perfused with K-H buffer to remove residual blood. Tissue was dissected into different chambers, freeze-clamped with Wollenberger tongs and stored in liquid nitrogen until further use.

2.7 Morphometric Measurements

Tibia length was measured using a pair of callipers. Frozen heart weight was recorded and normalized to tibia length to assess the degree of cardiac hypertrophy (Yin et al., 1982). Approximately 0.3g wet weight of tissue was powdered and dried at 50°C until reaching constant weight to determine wet to dry heart weight ratio. Lung weights were recorded and dried to a constant weight at 50°C to determine wet lung:dry lung weight ratio.

2.8 Blood Analysis

Blood samples, taken from the thoracic cavity at the time of sacrifice (~4ml), were centrifuged at 2700g at 4°C for 10 min. (Megafuge 1.0 Hereans Sepatech GmbH). Serum samples were analysed for urea and electrolyte by the Clinical Biochemistry Laboratory at the Hull Royal Infirmary. At the time of sacrifice, ~1ml of venous blood sample was collected from the *vena cava*, centrifuged at 1400g and aliquoted.

Insulin and proinsulin levels were assessed using ultrasensitive rat specific insulin ELISA kit and rat proinsulin ELISA kits respectively. Haematocrit was measured using an ABL 77 Series blood gas analyser.

2.9 Protein Expression Analysis

Protein expression was analysed by sodium dodecyl sulphate polyacrylamide gel electrophoresis (SDS PAGE) and western blotting for GLUT4 and GLUT1 (Santalucia et al., 1992, Allard et al., 2000), ANF (Latif et al., 1993) and CD36 (Luiken et al., 2002). SERCA2a, phospholamban (PLB) and $\alpha_1\text{Na}^+\text{K}^+\text{ATPase}$ expression methods were developed using guidelines from manufacturer technical instructions.

2.9.1 Vertical Polyacrylamide Gel Preparation

BioRad Mini Protean[®] II was used for electrophoretic protein separation. The glass plate sandwiches used for gel preparation were cleaned with ethanol and air dried. The gel mould was assembled in the casting stand by aligning the glass plates with each other and tightening the assembly screws. The resolving polyacrylamide gel was prepared and its composition (*Table 2.5*) determined by the investigated protein (*Table 2.7* and *2.8*). Components were mixed as per order in a *table 2.5* with TEMED added last to prevent premature gel polymerisation.

Component	7.5% Gel Volume(ml)	10% Gel Volume (ml)	12% Gel Volume (ml)
H ₂ O	4.85	4.0	3.35
10% (w/v) SDS	0.1	0.1	0.1
1.5M Tris (pH 8.8)	1.5	2.5	2.5
Acrylamide/bis (30% w/v)	2.5	3.33	4.0
Ammonium persulfate(10% w/v)	0.05	0.05	0.05
TEMED	0.01	0.01	0.01

Table 2.5 Resolving Polyacrylamide Gel Composition

The gel mixture was poured using a glass Pasteur pipette between the glass plates forming the gel matrix, leaving approx 2.5 cm from the top of the plates to the top of the resolving gel. Saturated butanol was poured on top of the resolving gel in order to eliminate air bubbles, and left to set for 30 min. A clear interface between gel and butanol was an indicator of completed polymerisation. Butanol was subsequently poured off and a 3% (v/v) polyacrylamide stacking gel prepared [ml: H₂O 7.4; 10% (w/v) SDS 0.1; 1.5 M Tris pH 6.8 1.25; acrylamide/bis 30% (w/v) 1.3; ammonium persulfate 10% (w/v) 0.05; TEMED 0.02]. Role of the stacking gel was to concentrate the samples into narrow bands for separation in the resolving gel. The stacking gel was added to the top of the resolving gel and a comb inserted immediately avoiding air bubbles in resulting sample well areas. Gel was allowed to polymerise for 30 min. Combs were removed from the polymerised gel and the glass plates mounted on the electrode apparatus, placed in the electrophoresis tank and running buffer added (mM: Tris 25 SDS 0.1% (v/v), glycine 192; pH 8.3).

2.9.2 Sample Preparation and Protein Separation

Left ventricular tissue samples from uraemic and control animals were homogenized with Ultra-Turrax T2 homogeniser with appropriate lysis buffers (Table 2.6).

Lysis Buffers	
ANF, SERCA2a, PLB, $\alpha_1\text{Na}^+\text{K}^+\text{ATPase}$	GLUT1, GLUT4, CD36
1% Sodium Dodecyl Sulphate (SDS) 1mM phenylmethylsulphonyl fluoride (PMSF)	50mM Tris buffer pH7.4 1mM PMSF Protease inhibitor cocktail

Table 2.6 Tissue Lysis Buffers

Tissue homogenates were centrifuged at 10200g for 10 min at 4°C and the supernatant removed for ANF, SERCA2a, PLB and $\alpha_1\text{Na}^+\text{K}^+\text{ATPase}$ analyses and the tissue pellet for GLUT1, GLUT4 and FAT/CD36 analyses. Protein concentration was determined using a BioRad spectrophotometric assay, with a 1 mg/ml Bovine Serum Albumin (BSA) solution as standard (Fig. 2.6) (Bradford, 1976). 2 ml of the dye reagent (25% solution filtered using Whatman #1 filter paper) was added to 60 μl of the diluted protein extract (1 in 20 dilution for supernatant; 1 in 50 dilution for pellet), incubated at room temperature for 10 min and absorbance was measured at 595 nm.

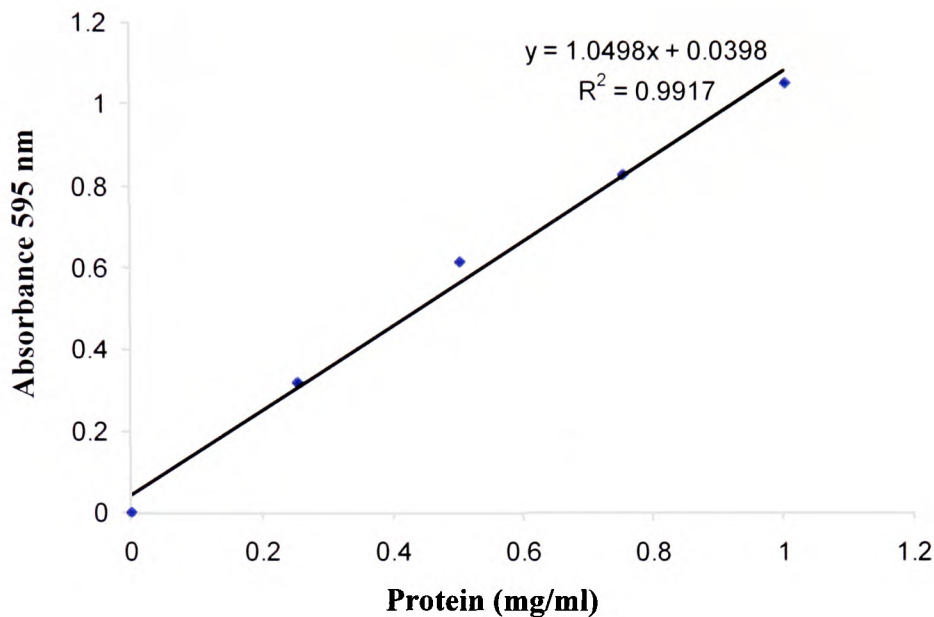


Figure 2.6 Protein Standard Curve

Protein samples were diluted with Laemmli buffer [Tris pH 6.8 125 mM; SDS 2% (w/v), glycerol 10% (v/v); bromophenol blue 0.001% (w/v); 2-mercaptoethanol 5% (v/v); pH 7.6] (Laemmli, 1970) to give a concentration of 25 $\mu\text{g}/100 \mu\text{l}$ (GLUT1, ANF, CD36, SERCA2a, PLB, $\alpha_1\text{Na}^+\text{K}^+\text{ATPase}$) and 40 μg (GLUT4). Samples were boiled at 100°C for 3 min before loading (25 μg or 40 μg for GLUT4) onto polyacrylamide gels. For $\alpha_1\text{Na}^+\text{K}^+\text{ATPase}$ samples were heated in a water bath at 60°C to prevent aggregation. Samples were separated on polyacrylamide gel (10 $\mu\text{l}/\text{lane}$) as detailed in table 2.6 and 2.7. Brilliant blue polyacrylamide gel staining revealed the protein separation (*Fig. 2.7*).

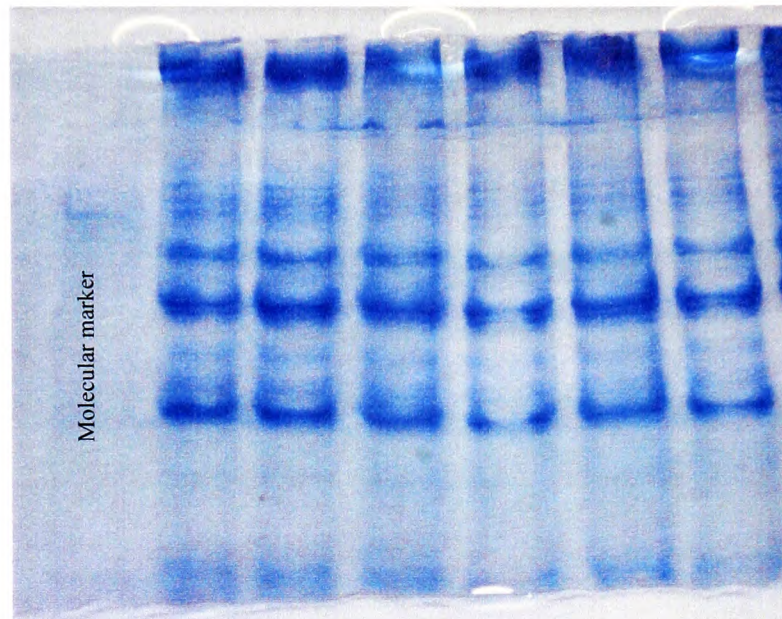


Figure 2.7. Brilliant Blue Polyacrylamide Gel Staining
2.5 μg protein/lane

2.9.3 Western Blotting

Proteins were transferred to nitrocellulose or PVDF membranes, pre-incubated in transfer buffer for 30 min (transfer buffer tris 25 mM; glycine 192mM; pH 8.3) and protein transfer monitored using the pre-stained benchmark protein ladder (10-190 kDa) (Gersten, 1996). PVDF membranes were prepared by equilibration for 15 min in methanol prior to 30 min incubation with the transfer buffer. Blots were incubated with blocking buffer [7.5% or 5% (w/v) Marvel in PBS or TBS and 0.02% (v/v) Tween 20] (*Table 2.7* and *2.8*). Membranes were probed with the respective antibodies as described in tables 2.7 and 2.8. Buffers containing PBS pH 7.6, 1% Marvel, 0.2 % TWEEN were used for antibody dilution and excess removed by washing in PBS or TBS buffer containing 0.2% TWEEN pH 7.4 (*Table 2.7* and *2.8*).

Membranes were exposed for 1h at room temperature to the appropriate secondary antibodies complexed to goat-anti rabbit polyclonal horseradish peroxidase (HRP) and were visualized using an enhanced chemiluminescence technique (ECL) kit. Liver tissue was used as a negative control for ANF, GLUT4, SERCA2a, and phospholamban; adipose tissue as a positive control for CD36 protein expression, and kidney as positive control for Na⁺K⁺ATPase expression. Atrial tissue and ventricular tissue from SHR animals (experimental model of hypertrophy) were used as a positive ANF expression control. In order to estimate the level of expression of the proteins, the optical density of the resulting protein bands was determined semi-quantitatively and compared.

PROTEIN	PAGE	PROTEIN TRANSFER CONDITIONS	BLOCKING BUFFER	PRIMARY ANTIBODY	SECONDARY ANTIBODY	MEMBRANE WASH
ANF	12%	12 h 4°C	7.5% MARVEL PBS pH 7.4 0.02% Tween-20 1h, room temp.	Rabbit polyclonal IgG ANP 1:1000 1 h, room temp.	Goat-anti rabbit HRP 1:2000 1 h, room temp.	5 min x 3
GLUT1	10%	1h 4°C + methanol	7.5% MARVEL PBS pH 7.4 0.02% Tween-20 2h, 32°	Goat polyclonal GLUT1 1:2000 12 h, 4°C	Donkey anti-goat IgG-HRP 1:4000 1h, room temp.	45 min x 4
GLUT4	10%	1h 4°C + methanol	5% MARVEL PBS pH 7.4 0.02% Tween-20 1h, room temp.	Mouse anti-Rat monoclonal GLUT4 1:3000 12h, room temp.	Rabbit Anti Mouse IgG-HRP 1:2000 1h, room temp.	15 min x 3
Polyclonal GLUT4	10%	1h 4°C + methanol	7.5% MARVEL PBS pH 7.4 0.02% Tween-20 1.5h 32°C	Goat polyclonal GLUT4 1:5000 12h, 4°C	Donkey anti-goat IgG-HRP 1:8000 1h, room temp.	5 min x 5

Table 2.7 SDS PAGE & Western Blotting Protocol Details for Individual Proteins

Antibodies diluted with PBS pH 7.4 buffer containing 1% Marvel+ 0.02% Tween

PROTEIN	PAGE	PROTEIN TRANSFER CONDITIONS	BLOCKING BUFFER	PRIMARY ANTIBODY	SECONDARY ANTIBODY	MEMBRANE WASH
CD36	10%	1h 4°C + methanol	5% MARVEL TBS pH 7.4 0.02% Tween-20 1 h, room temp.	Rabbit pAb to CD36 1:6000 12h, 4°C	Goat-anti rabbit HRP 1:8000 1h, room temp	5 min x 5 [Ⓜ]
SERCA2a	7.5%	12h 4°C PVDF membrane	5% MARVEL PBS pH 7.4 0.02% Tween-20 1h, room temp.	Goat polyclonal SERCA 2a 1:2000 1 h, room temp.	Donkey anti-goat IgG- HRP 1:3000 1h, room temp.	3 x 10 min x 3
Phospholamban	12%	12h 4°C PVDF membrane	5% MARVEL PBS pH 7.4 0.02% Tween-20 1h, room temp.	Goat polyclonal Phospholamban 1:300 1 h, room temp.	Donkey anti-goat IgG- HRP 1:3000 1h, room temp.	10 min x 2
$\alpha_1\text{Na}^+\text{K}^+$ ATPase	7.5%	12h 4°C	5% MARVEL TBS pH 7.4 0.02% Tween-20 1h, room temp.	Mouse mAb $\alpha_1\text{Na}^+\text{K}^+$ ATPase 1:5000 1 h, room temp.	Rabbit Anti Mouse IgG-HRP 1:7000 1h, room temp.	15 min x 1 [Ⓜ] 15 min x 3

Table 2.8 SDS PAGE & Western Blotting Protocol Details for Individual Proteins

Antibodies diluted with PBS pH 7.4 buffer containing 1% Marvel+ 0.02% Tween except for [Ⓜ] diluted with TBS

2.9.4 Technical Developments

Methods for protein detection were optimized for blocking buffer composition, incubation time, incubation temperature, number of membrane washes and antibody dilution in order to overcome problems of substantial background staining and to improve resolution. Polyclonal GLUT4 antibody was replaced by a monoclonal antibody which improved resolution, but its detection required further optimisation. Protein concentration, blocking buffer composition and incubation temperature were initially based on the method of Allard et al. (2000). CD36 detection based on the method of Luiken et al. (2002), and optimised in this study. Methods for SERCA2a, PLB and $\alpha_1\text{Na}^+\text{K}^+\text{ATPase}$ protein expression detection were based on the manufacturers' (SantaCruz, AbCam) instructions. Finalised protocols are outlined in tables 2.7 and 2.8.

2.10 Subcellular Membrane Fractionation

Subcellular membrane fractionation was achieved by differential sucrose gradient centrifugation based on the method of Young *et al.* (1997). The method is summarized schematically in figure 2.8.

Membrane fractions were harvested, diluted five fold in NaHCO₃ (10mM)/NaN₃ (5mM) solution and centrifuged at 190000g for 1h at 4°C. The resulting pellets were re-suspended in sucrose (250mM)/Tris (50mM), pH 7.4, and frozen at -80°C for subsequent use. Isolated plasma membrane fractions were characterized by detection of $\alpha_1\text{Na}^+\text{K}^+\text{ATPase}$ as described in section 2.9. GLUT4 detection in the subcellular membranes utilised the polyclonal antibody for membrane probing as protein levels were low in the different fractions (section 2.9, Table 2.7).

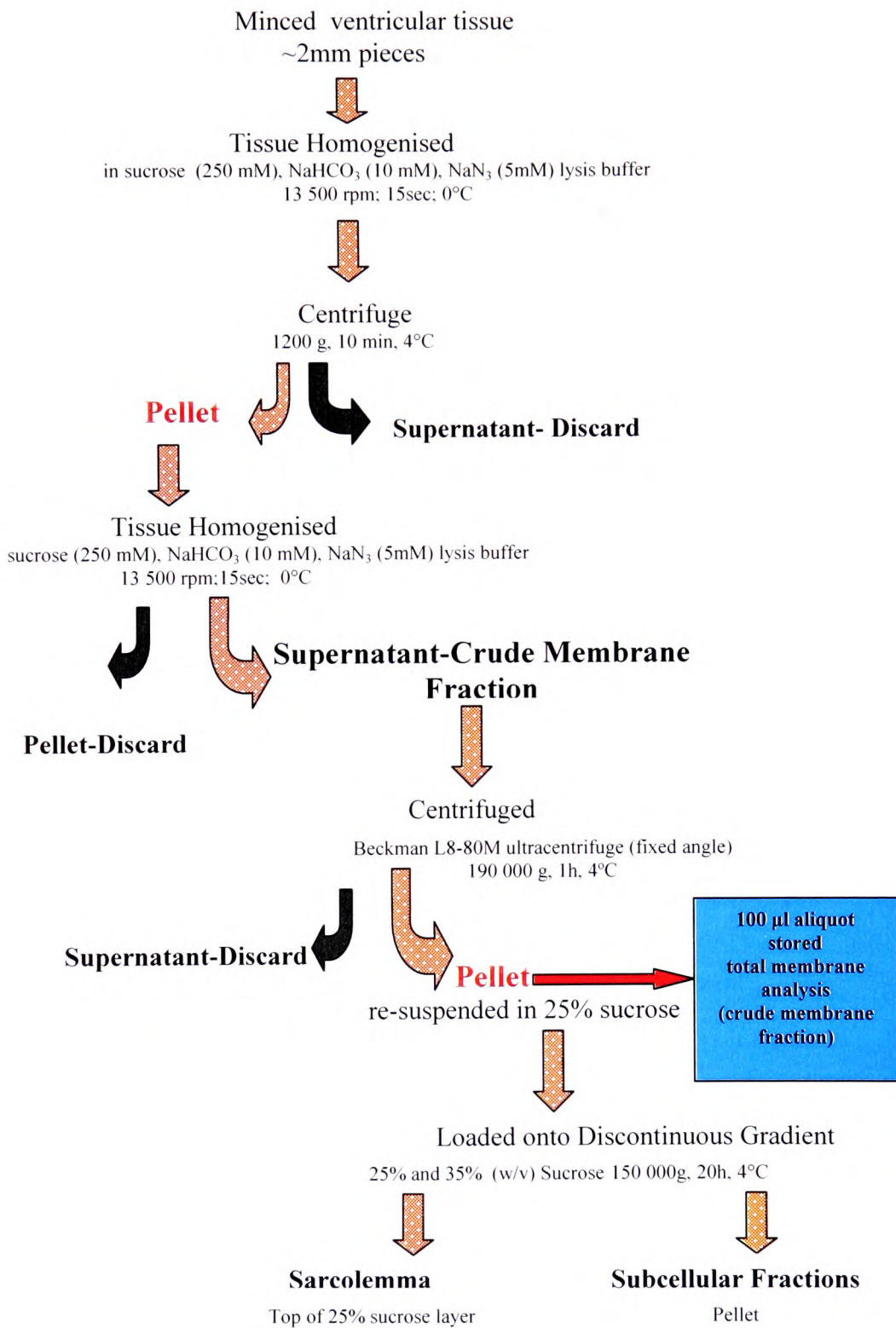


Figure 2.8 Subcellular Membrane Fractionation Protocol

2.11 ¹³C Magnetic Resonance Spectroscopy

2.11.1 Tissue Extraction

Frozen hearts were weighed and ground to a fine powder under liquid nitrogen and extracted at 4°C with 6% perchloric acid (PCA) (v/w) in a ratio of 5:1 as described previously (Seymour et al., 1990). The suspension was centrifuged at 1500g, 4°C for 10 min (Megafuge 1.0 Hereans Sepatech GmbH) and a known volume of supernatant decanted and neutralised with 6M KOH to pH6.8 at 4°C. The mixture was centrifuged and the supernatant lyophilised at -40°C in a freeze drier (Freeze Drier Modulyo). Samples were stored at -80°C until further use.

2.11.2 Deuterated Phosphate Buffer and NMR Sample Preparation

Lyophilised tissue extracts were reconstituted in 0.95ml of 50mM deuterated phosphate (KH₂PO₄) buffer pH 7.0 lyophilised and resuspended in D₂O. A small amount of chelating resin (chelex) was added to samples to remove any paramagnetic ions and filtered through a 0.22 µm syringe filter into a 5 mm NMR tube.

2.11.3 NMR Spectroscopy

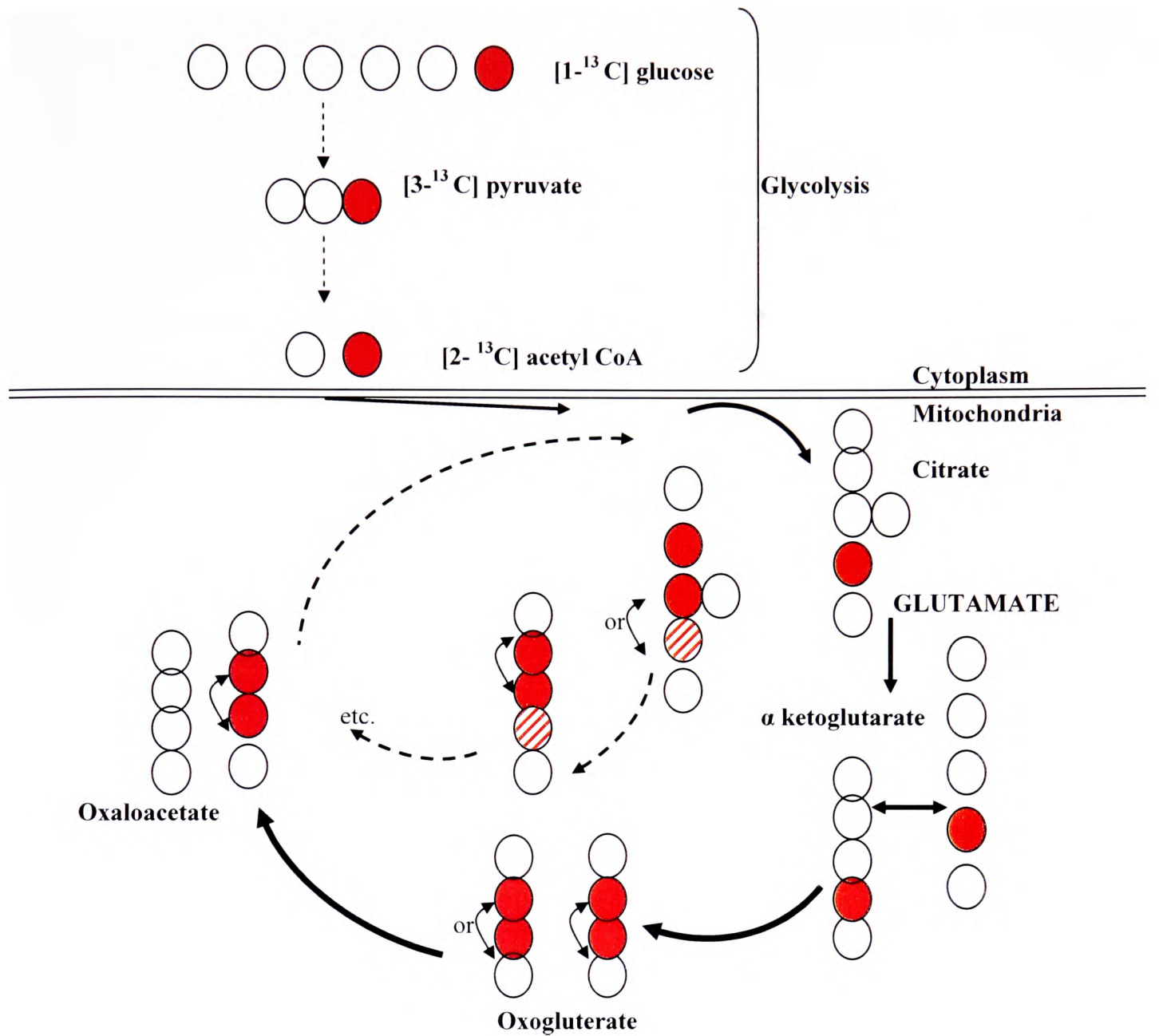
High-resolution ¹H decoupled (WALTZ 16 decoupling) ¹³C NMR spectra were acquired at 126 MHz using a vertical-bore, ultra-shielded Bruker wide bore magnet (11.5 Tesla) interfaced with a Bruker spectrometer using a 5 mm broadband probe.

Free induction decays (FID) were collected with 18 000 scans using a 90° pulse (9.95 μ sec pulse duration) and 1sec interpulse delay. ^{13}C spectra were analysed using Bruker Topspin 1.3 software.

2.11.4 ^{13}C - Glutamate Labelling Pattern & the Analysis of ^{13}C Spectra

The analysis of ^{13}C glutamate isotopomers reflects the oxidative metabolism of exogenous ^{13}C labelled substrates as glutamate is present in sufficient concentration for detection by NMR and is in exchange with the TCA cycle intermediates (Malloy et al., 1990a, Seymour, 2003a). If 1- ^{13}C glucose is metabolised by the heart, the ^{13}C label is transferred to the C3 position of pyruvate and subsequently to the C2 position in acetyl-CoA (Fig. 2.9). In the first turn of TCA cycle, ^{13}C , label is transferred initially to the C4 of α -ketoglutarate (Fig. 2.10a) and subsequently the label is randomly transferred into C2 and C3 of succinate and subsequent TCA cycle intermediates.

In the second turn of TCA cycle, ^{13}C label enters both as the 2- ^{13}C acetyl CoA and the C2/C3 positions of oxaloacetate. Subsequently, the label appears in the C₂, C₃ and C₄ atoms of glutamate (Fig 2.10). As neighbouring atoms are labelled, there is “cross-talk” between ^{13}C - ^{13}C giving rise to the splitting of the multiplets within individual carbon resonances (Table 2.9).





-  ^{13}C from $[2-^{13}\text{C}]$ acetyl CoA entering the TCA cycle on 1st turn of the cycle
-  ^{13}C from $[2-^{13}\text{C}]$ acetyl CoA entering cycle on 2nd turn of the cycle

Figure 2.9 Distribution of ^{13}C isotope from $[1-^{13}\text{C}]$ glucose during the first 1½ turns of the TCA cycle

Adapted from Seymour2003

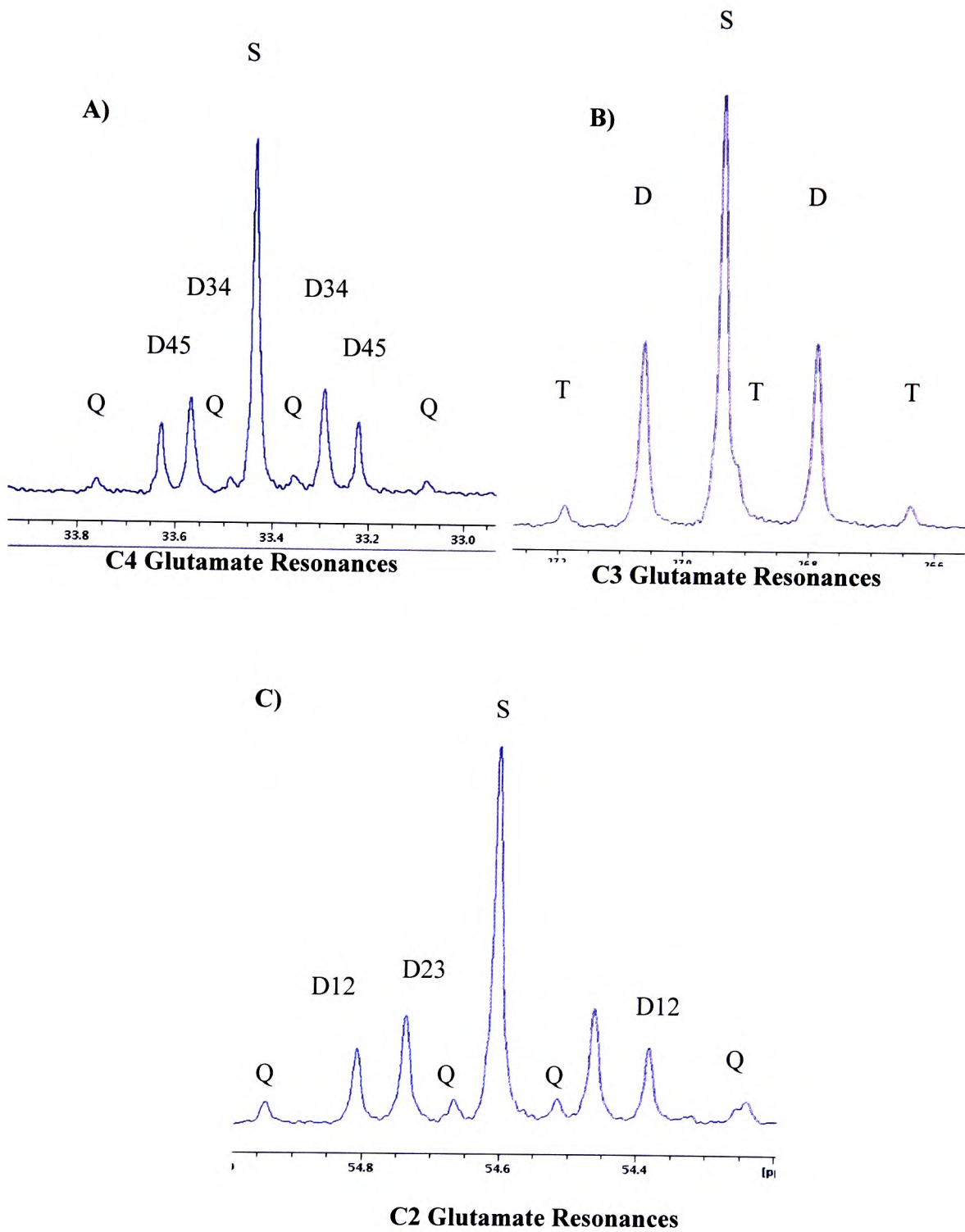


Figure 2.10 Multiplate Peak Patterns of ^{13}C Glutamate

A) C4 Glutamate Resonances, B) C3 Glutamate Resonances, C) C2 Glutamate Resonances. S-singlet; D-doublet; T-triplet; Q-quartet

Glutamate C Atom	Chemical Shift (ppm)	Number of Peaks	Multiplet	
C2	55.2	9	C2S C2D12 C2D23 C2Q	Singlet Doublet Doublet Quartet
C3	27.6	5	C3S C3D C3T	Singlet Doublet Triplet
C4	34.2	9	C4S C4D34 C4D45 C4Q	Singlet Doublet Doublet Quartet

Table 2.9 The Chemical Shifts of Glutamate

2.11.5 Isotopomer Analysis

tcaCALC™ software v.2.07 (www.utsouthwestern.edu/rogersnmr) was kindly provided by Dr M.H. Jeffrey, Southwestern Medical Centre, Texas (Jeffrey, 1990, Malloy et al., 1990a). It was used to determine the relative contributions of exogenous substrates (U-¹³C palmitate, 1-¹³C glucose and 3-¹³ lactate) to substrate oxidation from analysis of the glutamate isotopomer patterns.

This tcaCALC™ model is based on the following assumptions (Malloy et al., 1990b):

- Carbon only enters the TCA cycle via acetyl CoA or the anaplerotic pathways
- The concentration or the fractional enrichment of TCA intermediates and the exchanging pools is constant (i.e. metabolic steady state)
- All ^{13}C entering oxaloacetate has been randomized between C2 and C3 carbon positions
- Anaplerotic reaction flux equals disposal reaction flux
- There is minimal $^{13}\text{CO}_2$ entry
- Contribution of natural abundance ^{13}C to TCA cycle is negligible
- All metabolic reactions are at steady state

The peak heights for each of the multiplets were measured using the Bruker software peak picking route and expressed as a percentage of the sum of peak heights for each corresponding carbon of glutamate to give fractional intensity value of the multiplet (*Fig. 2.11*)

$$\text{C4S} = \frac{\text{Peak height of 1}}{\sum \text{peak heights (1} \rightarrow \text{4d)}}$$

$$\text{C4D45} = \frac{\text{Peak Height of 3a+3b}}{\sum \text{peak heights (1} \rightarrow \text{4d)}}$$

$$\text{C4D34} = \frac{\text{Peak heights of 2a+2b}}{\sum \text{peak heights (1} \rightarrow \text{4d)}}$$

$$\text{C4Q} = \frac{\text{Peak heights of 4a+4b+4c+4d}}{\sum \text{peak heights (1} \rightarrow \text{4d)}}$$

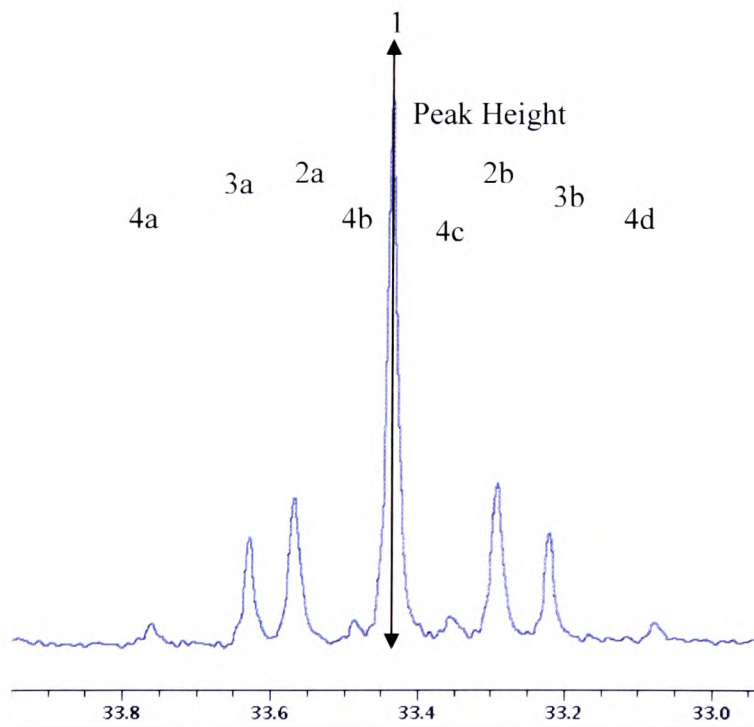


Figure 2.11 Measurement of C4 Glutamate Peak Heights

The ratio of the integrated total area under the C3 and C4 resonances gave the ratio of carbon atom fractional enrichment. Data was entered into tcaCALC programme along with the estimated fractional enrichment of acetyl CoA from different ¹³C labelled substrates (*Fig. 2.12*). tcaCALC generates relative fractional enrichments (FAT) of acetyl CoA (*Fig. 2.12*)

Fc0- Fraction unlabelled at both C atoms

Fc1-Fraction labelled at carbonyl C atom in acetyl CoA

Fc2- fraction labelled at methyl C atom in acetyl CoA

Fc3-Fraction labelled at C atoms C1 and C2 in acetyl CoA

$$Fc0+Fc1+Fc2+Fc3=1$$

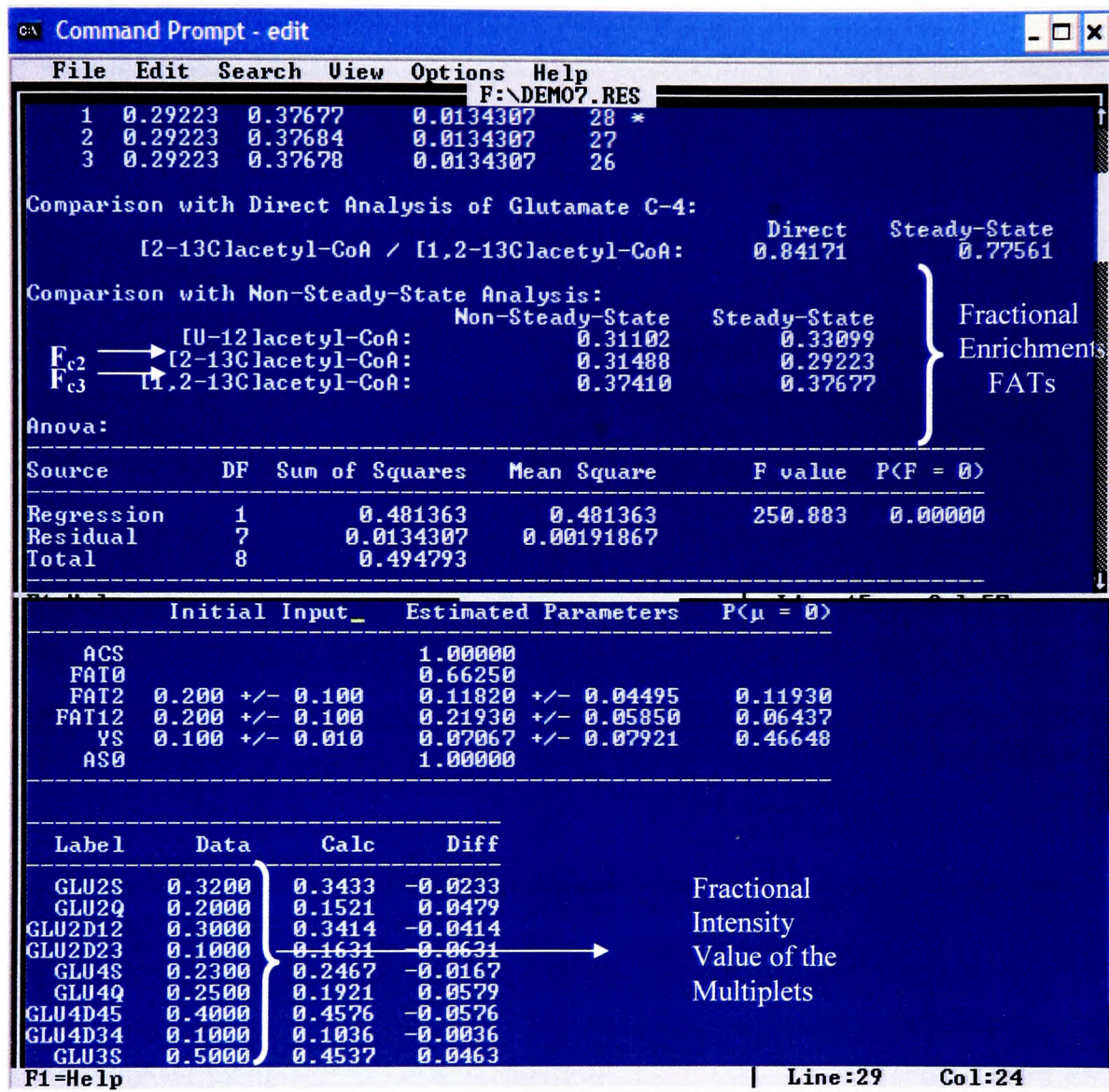


Figure 2.12 Example of the tcaCALC Output

2.12 Ventricular Myocyte Isolation

Cardiomyocytes were isolated 6 weeks post surgery by collagenase digestion using the method of Smolenski *et al.*,(1992).

2.12.1 Preparation of Buffers

All buffers were prepared using Milli Q ultra pure water, filtered through 0.45 μm filter and stored at 4°C (Table 2.10). 2,3-butanedione monoxime (BDM) was added to prevent cell hypercontraction during the early phase of calcium restoration (Zhou *et al.*, 2000, Sambrano *et al.*, 2002).

Buffer 1: Non-circulating buffer (mM); pH 7.3	
NaCl	60
KCl	16
MgSO ₄ .7H ₂ O	3.2
KH ₂ PO ₄	1.2
HEPES	10
Mannitol	80
BDM	10
Taurine	20
Glucose	11
Pyruvate	5

Buffer 2: Modified Krebs-Ringer-HEPES (mM); pH 7.3	
NaCl	120
KCl	2.6
MgSO ₄ .7H ₂ O	1.2
HEPES	10
CaCl ₂	1
KH ₂ PO ₄	1.2
Glucose	11
Pyruvate	2

Table 2.10 Cardiomyocyte Isolation Buffer Composition

2.12.2 Cell Isolation

Rats were anaesthetized as described in section 2.5.4 and hearts rapidly excised, cannulated via the aorta and perfused with Buffer 1, gassed with 100% O₂ at 37°C, for 10 min at a flow rate of 11.5 ml/min. The left atrium was perforated and a small piece of tubing inserted into the mitral valve to prevent closure. The perfusion medium was switched to a re-circulating system with 30 ml of Buffer 1 containing 0.1% (w/v) collagenase (394 U/mg) and 0.5% (w/v) BSA. CaCl₂ (1M stock) was added in 5µl increments to give a final Ca²⁺ concentration of 1mM and hearts perfused for a further 30-45 min. Ventricular tissue was dissected, gently agitated in 15 ml of Buffer 2, filtered through 25µm nylon gauze and centrifuged at 15g for 10 min at room temperature. The pelleted cardiomyocytes were resuspended in Buffer 2, gassed with 100% O₂ with additional components as indicated in the individual experimental protocols.

2.12.3 Cardiomyocyte Morphology

Photomicroscopic analysis of cardiomyocyte dimensions (length and width) was performed using a Leitz LaborLux® S light microscope, 40x objective magnification lens connected to a Cool SNAP-PRO digital camera to Image Pro-Plus® v 5.1.2 software (*Fig. 2.13*). Cells were selected for measurements based on their appearance –only rod shaped myocytes with intact sarcomere striations were analysed. 60 cells per heart were measured in order to marginalise sampling error to less than 3% (Gerdes et al., 1996).

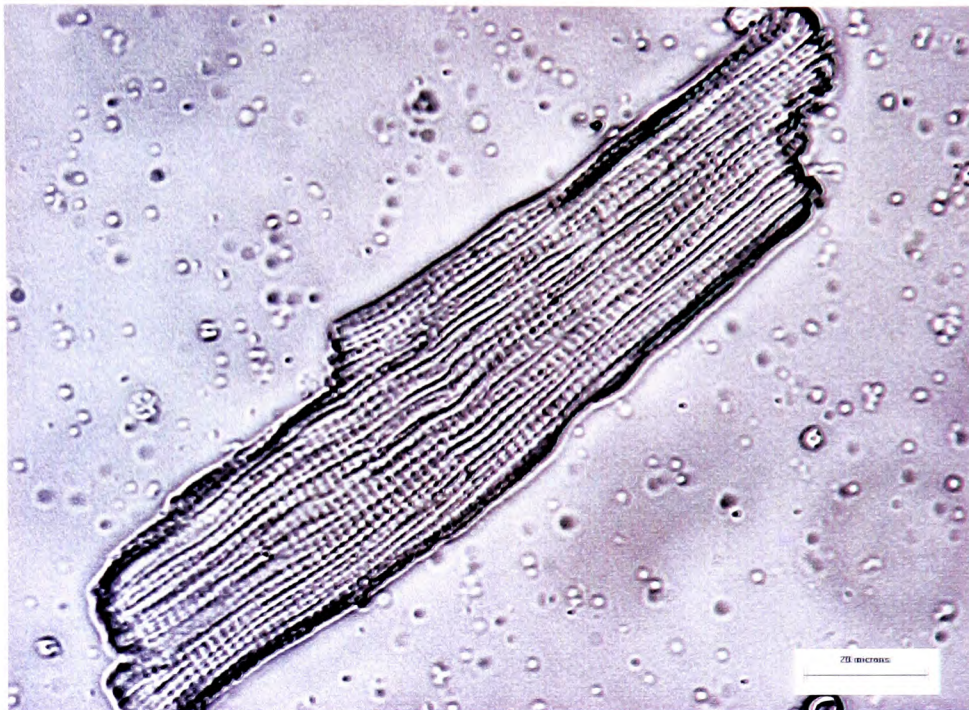
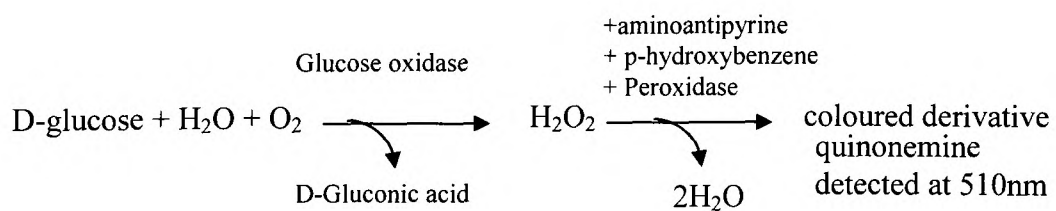


Figure 2.13 Photomicrograph of Control Cardiomyocyte 40x Magnification

2.13 Biochemical Assays

2.13.1 Glucose assay

Serum glucose was assessed using a colorimetric assay glucose oxidase and peroxidase.



10 μ l sample was incubated with 3.5 ml glucose assay reagent (0.1 M NaH_2PO_4 buffer, pH 7.0, 0.8U peroxidase/ml, 10U glucose oxidase/ml, 0.4mM 4-aminoantipyrine, 10mM 4-hydroxybenzene sulphonic acid) for 30 min at 30°C. Absorbance was recorded at 510 nm. A standard curve covering 1-5mM was used for the unknown concentrations is shown in Figure 2.14.

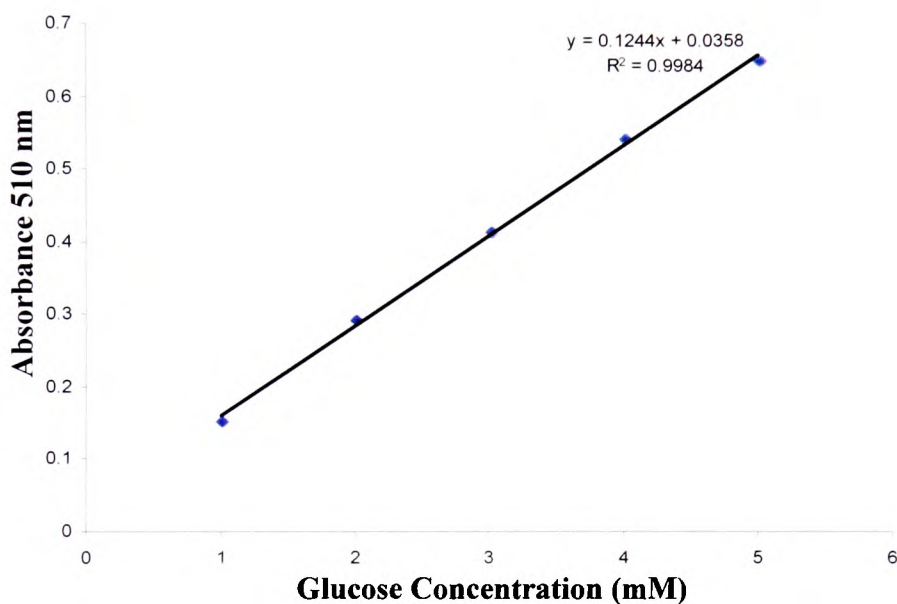


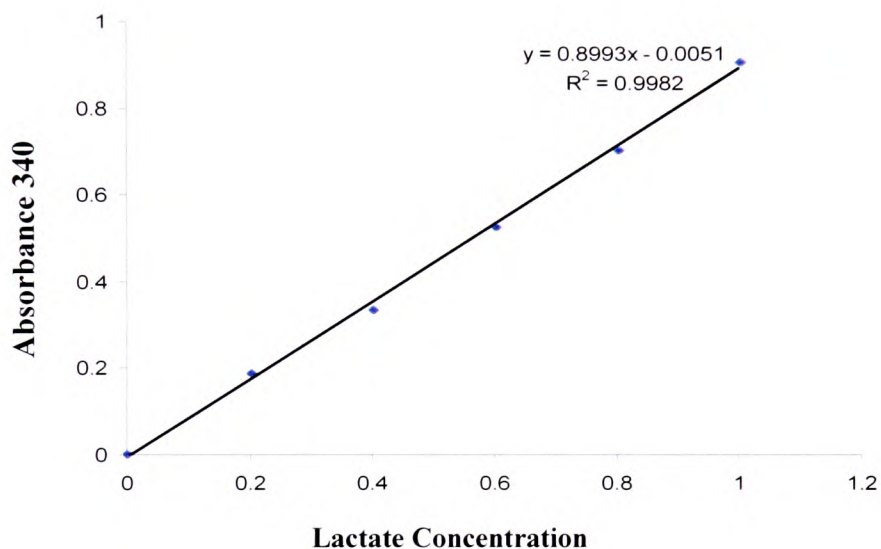
Figure 2.14 Glucose Assay Standard Curve

2.13.2 Lactate assay

Serum lactate was determined using a colorimetric assay based on the following reaction (Bergmeyer and Bernt, 1974).



Deproteinised serum samples were analysed using a 10 μ l sample with 0.1 ml 40mM NAD^+ and 1.25 ml (0.4mM) hydrazine/glycine buffer, pH 9.0 at 340 nm (A_1). 20 μ l lactate dehydrogenase (LDH, 20 U/ml) was added and incubated for 30 min at 37°C and the absorbance read again (A_2). A standard curve for the assay is shown in *Figure 2.15*. Lactate concentration was calculated as shown below.

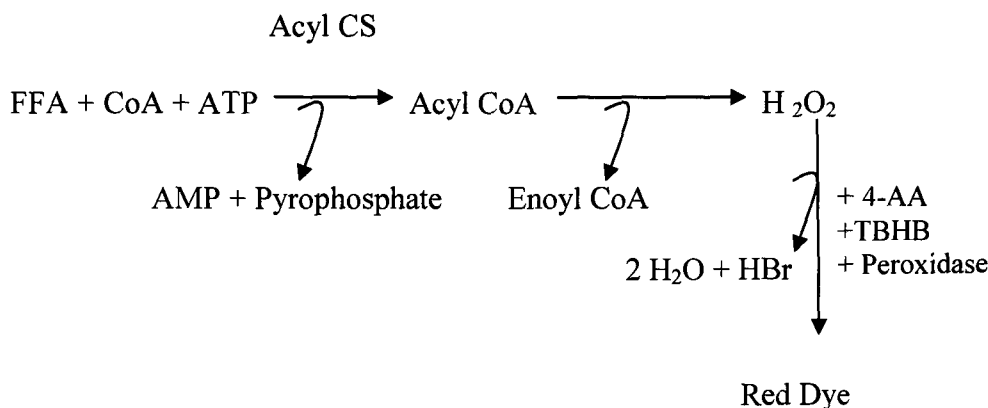


$$\Delta A_{\text{sample}} = \{ (A_2 \text{ Sample} - A_1 \text{ Sample}) - (A_2 \text{ Blank} - A_1 \text{ Blank}) \}$$

Figure 2.15 Lactate Concentration

2.13.3 Free Fatty Acids Assay

Serum free fatty acids were studied using Roche FFA kit (No. 1383175) following Manufacturers instructions. The assay is based on the following reaction:



FFA-free fatty acids; CoA- coenzyme A, Acyl CS- acyl-CoA synthase, ACOD- acyl- CoA oxidase 4-AA-4-aminoantipyrine, HBr- hydrogen bromide, TBHB- 2,4,6-tribromo-3-hydroxy-benzoic acid.

50 µl serum or water (blank) was incubated with 1 ml reaction mixture A (containing ACS, ATP, peroxidase, 4-AA and CoA) for 10 min at 25°C. Subsequently, 50µl N-ethyl-maleinimide was added and absorbance (A₁) read at 546 nm. 50 µl of reaction mixture B (containing acyl CoA oxidase) was added and the mixture incubated for 15 min at 25°C and absorbance (A₂) read at 546 nm. The difference in absorbance (A₂-A₁) for both blank and sample was calculated. Absorbance difference of the blank (ΔA_b) was subtracted from that of the sample (ΔA_s) to obtain ΔA. Serum FFA concentration was calculated using equation below.

$$C = \frac{V}{\epsilon x d x v} \times \Delta A$$

V- final volume (1.15 ml); v-sample volume (0.05ml), d-light path (1cm), ε-extinction coefficient of the dye at 546 nm (19.3 L/mmol/m)

2.13.4 Measurement of Pyruvate Dehydrogenase Activity

2.13.4.1 Tissue Extraction

Approximately 200mg powdered myocardial tissue was homogenised using an Ultra-Turrax T2 homogeniser at maximum speed for 20 sec in 1 ml ice-cold extraction buffer (1:5 tissue:buffer ratio)(mM: HEPES 25; KH₂PO₄ 25; KF 25; Dichloroacetate 1; EDTA 3; ADP 1; Dithiothreitol 1; leupeptin 0.05; Triton X-100 1% v/v; pH 7.0).

The active fraction of PDH (PDH_a) was extracted using buffer containing (mM) HEPES 25, ADP 1, EDTA 1, dichloroacetate 3, KH₂PO₄ 25, Dithiothreitol (DTT) 1, leupeptin 0.05, KF 25 and 1%(v/v) Triton X-100 (pH 7.0) to inhibit PDH phosphatase and PDH kinase as described previously (Seymour and Chatham, 1997).

Total PDH activity (PDH_t) was extracted using buffer containing (mM): HEPES 75; dichloroacetate 5; MgCl₂ 5; ADP 1; dithiothreitol (DTT) 1; leupeptin 0.05; and 1% Triton X-100, pH 7.0. Samples were freeze-thawed 3 x 30 sec. and resulting mixture was centrifuged at 15 600g at 4°C for 10 min.

2.13.4.2 PDH Activity Measurement

PDH activity was measured spectrophotometrically at 340 nm as described by Seymour and Chatham 1997.

0.95ml reaction mixture containing (mM: HEPES 50; MgCl₂ 1; EGTA 0.08; DTT 1; NAD 1.67; Co-enzyme A 0.2; thiamine pyrophosphate 0.2; lactate 16.7; rotenone 4μM; lactate dehydrogenase 2U-added separately) without the sample was incubated at 30°C for 5 minutes prior to the addition of tissue sample. 50-200 μl of tissue extract (PDH_a) or 25-50 μl of tissue extract (PDH_t) were added and the rate of NADH production followed over 2 min.

$$PDH \text{ activity} = \left(\frac{\Delta A}{\epsilon NADH} \right) \times \left(\frac{\text{Total assay } V \text{ (ml)}}{\text{Sample } V \text{ (ml)}} \right) \times \left(\frac{\text{Extraction buffer } V \text{ (ml)}}{\text{Tissue weight (mg)}} \right)$$

(μmol/min/g wet heart weight)

ΔA change in absorbance over 30 sec, $\epsilon NADH=6.22 \text{ mMcm}^{-1}$

2.13.5 Citrate Synthase Activity

2.13.5.1 Tissue Extraction

Powdered cardiac tissue was homogenised using an Ultra –Turrax T2 homogenizer 24 000 rpm for 20 sec in ice-cold extraction buffer (100mM imidazole, 1mM EGTA, 10mM MgCl₂, pH7.2). 10μl Triton X-100 was added to the tissue homogenate, incubated for 1h, at 4°C and centrifuged (800g, 4°C) (Seymour and Chatham 1997). The supernatant was used for the measurement of citrate synthase activity.

2.13.5.2 Citrate Synthase Assay

Citrate synthase activity was measured using 50mM Tris, 0.05% v/v Triton X-100 buffer (pH 8.1) containing (mM) 5,5 dithio-bis-2 nitobenzoic acid (DTNB) 0.2; acetyl CoA 0.1 and oxaloacetate 0.5. 1.98 ml of the assay stock was equilibrated at 30°C prior to 20 µl sample was added. The enzyme activity was measured at 412 nm by following reaction of the released CoA with DTNB (Morgan-Hughes et al., 1977).

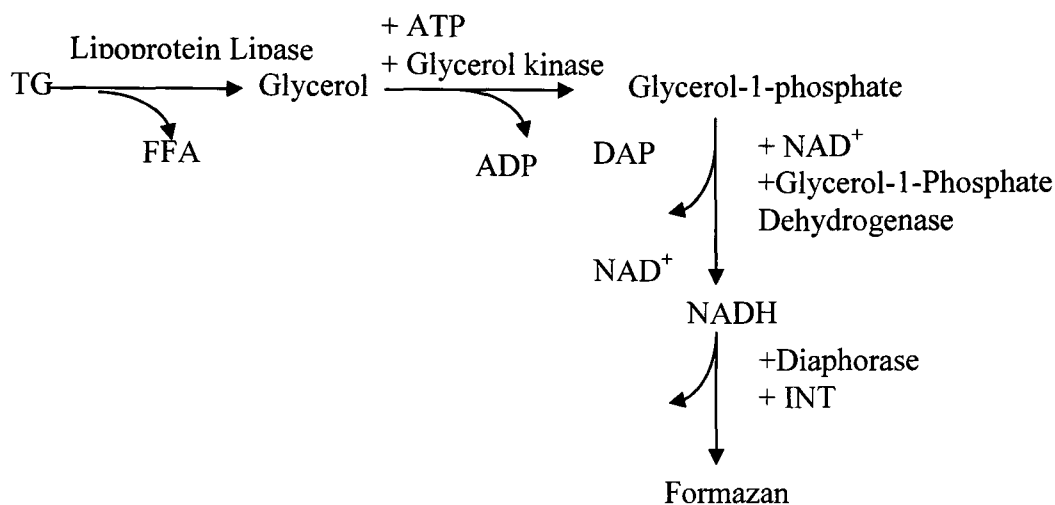
$$\text{Citrate Synthase Activity}(\mu\text{mol}/\text{min}/\text{g}) = \frac{\frac{\Delta A}{13.6} \times \frac{2}{0.02}}{\text{g tissue} / \text{ml}}$$

ΔA change in absorbance over 30 sec; Milimolar absorbtivity DTNB=13.6 mM⁻¹cm⁻¹
Volume in assay =2ml; Volume of extract = 0.02 ml

2.13.6 Tissue Triglyceride Assay

Myocardial TG content was extracted with chloroform methanol mixture based on the method of (Bligh and Dyer, 1959). Powdered cardiac tissue (100mg/ml) was homogenised by Ultra-Turrax T2 homogeniser at 24 000 rpm for 2 min in ice-cold chloroform-methanol-water mixture (2:1:0.8) and centrifuged for 15 min (800g, 4°C). The upper aqueous layer was decanted and the lower chloroform layer dried under 100% gaseous N₂ and re-suspended in 0.5 ml 2-propanol.

TG content was assayed using Sigma TG kit (No. 336) based on the reaction:



TG-triglycerides; FFA-free fatty acids; DAP- dihydroxyacetone phosphate, INT-2-(p-iodophenyl)-3-p-nitrophenyl-5-phenyl tetrazolium chloride

2.13.7 Glycogen Assay

Glycogen extraction was based on the method of Walaas and Walaas (1950). In brief, myocardial glycogen was extracted by alkali digestion by dissolving approximately 0.1-0.4 g tissue in 0.5 ml 30% (w/v) potassium hydroxide and at 100°C for 30 min. Subsequently, 0.2 ml of 2% (w/v) anhydrous sodium sulphate and sufficient 100% (v/v) ethanol, to give a final concentration of 75%, were added. Samples were centrifuged at 27 000g for 10 min at 4°C and the pellet was rinsed with 80% ethanol. The resultant glycogen pellet was dried at 37°C for 30 min and digested in 0.1ml 0.5M amylo- α -1,4- α -1,6-glucosidase, 0.5 ml 1M sodium acetate buffer pH 5.0 and 1.4 ml water for 1 hour at 37°C.

Glucose concentration of resulting solution was determined spectrophotometrically as described in section 2.13.1

$$\text{Glucose equivalents } (\mu\text{mol}) = \frac{\text{Mean Absorbance } (\Delta A) \text{ of sample}}{\text{Absorbance of standard}} \times \text{Concentration of standard}$$

$$\text{Glycosyl Units/} \left. \begin{array}{l} \text{g wet weight} \\ \text{= } \end{array} \right\} \frac{\text{Glucose equivalents } (\mu\text{mol}) \times \frac{\text{Total volume of extract (ml)}}{\text{Volume of sample in the cuvette (ml)}}}{\text{Weight of tissue used (g)}}$$

2.14 Statistical Analysis

All data are presented as mean \pm standard error mean (S.E.M). Unpaired two-tailed Student t-test was used for comparison of means. Descriptive statistics (Pearson correlation coefficient) was used to assess the relationship between the variables. Statistical analysis was carried out using SPSS statistics software v.15.0. A value of $p < 0.05$ was considered significant.

3. CHARACTERISATION OF THE EXPERIMENTAL URAEMIA MODEL

3.1 Introduction

Chronic kidney disease (CKD) is a syndrome of persistent renal dysfunction (Marshall 1995). The spectrum of CKD aetiologies includes glomerulonephritis, pyelonephritis, interstitial nephritis, diabetes mellitus, hypertension, polycystic disease, nephrotoxic drugs and multisystem disease (Gaw, 2004). Experimental models using a 5/6 sub-total nephrectomy result in the development of uraemia, proteinuria, hypertension and progressive renal failure with significant renal sclerosis in any remnant renal tissue (Marshall, 1995).

Left ventricular hypertrophy (LVH) development is a hallmark of uraemia and a potent predictor of patient mortality (Amann et al., 2003b, Reddy et al., 2007). In addition to LVH, transthoracic echo studies in CKD patients have shown a prevalence of systolic and diastolic dysfunction, ventricular dilatation, increase in QT dispersal and arrhythmias (Stewart et al., 2005). Hypertension *per se* has been shown to reduce the number of cardiomyocytes in uraemia predisposing the heart to failure (Amann et al., 2003b). At a cellular level, LVH in uraemia has been characterized by significant alterations in cell morphology and increase in cell volume (Fowler et al., 2007, Reddy et al., 2007). Anaemia in CKD is caused by a reduction in erythropoietin secretion and may be a contributing factor to the chronic volume overload (Lipsic et al., 2004).

Hypertrophy caused by fluid overload is accompanied by alterations in ventricular compliance which further contribute to systolic and diastolic dysfunction before transition to overt congestive heart failure (De Stefano et al., 2006). However, despite a number of studies, the relationship between individual confounding factors and the development of uraemic cardiomyopathy is still subject to debate.

3.2 Aims and Objectives

The aim of this study was to examine the morphology and physiology of the experimental uraemic model at different stages of the disease using *in vivo* and *ex vivo* methods.

3.3 Methods

Protocols used in this chapter are outlined in sections 2.3; 2.7; 2.8; 2.12.3 and 2.13.

3.4 Results

Experimental uraemia was induced surgically with a low mortality rate (6%; uraemic n=3; control n=1; total n=67). The weight gain between surgeries was 17% (initial weight 236.5g±0.7) with a smaller increase in body weight in uraemic animals versus controls (15.8±0.5 % increase versus 18.1±0.5% increase in body weight p<0.05 n=67). Significant uraemia was induced by removing approximately 1.65 g of kidney tissue over a 2 stage procedure: left partial nephrectomy 0.37±0.01 g (n=67) and right total nephrectomy 1.28±0.02 g (n=67). Despite pair feeding, there was evidence of lower body weight in the 6 week uraemia (*Table 3.1*).

3.4.1 Morphological Features

Experimental model		Body Weight (g)	Tibia Length (cm)	Right Kidney (g)	Left Kidney (g)	Lungs; dry weight: wet weight
3 weeks	CONTROL (n=6)	387.5±12.7	4.2±0.1	2.0±0.2	2.0±0.2	—
	URAEMIC (n=6)	371.0±21.2	4.3±0.1	—	1.8±0.3	—
6 weeks	CONTROL (n=30)	445.2±6.3	4.2±0.02	1.7±0.06	1.6±0.04	0.17±0.01
	URAEMIC (n=30)	420.2±8.2*	4.1±0.04	—	1.5±0.06	0.17±0.01
9 weeks	CONTROL (n=8)	452.5±12.2	4.3±0.06	1.7±0.08	1.7±0.01	0.31±0.05
	URAEMIC (n=8)	480.6±13.1	4.2±0.05	—	1.9±0.20	0.38±0.01

Table 3.1 Animal Morphology at 3, 6 & 9 weeks

Data are presented as mean ± S.E.M. *p<0.05 vs. appropriate control

3.4.2 Blood Pressure

Uraemic animals exhibited a significant degree of hypertension at all stages of uraemia (3, 6 and 9 weeks) compared to controls accompanied by an increased heart rate (Table 3.2). Six week uraemia was characterised by the greatest hypertension (Table 3.2). Control animals blood pressures were not altered over the examined period.

Experimental model		Systolic Pressure (mmHg)	Diastolic Pressure (mmHg)	Mean Arterial Pressure (mmHg)	Heart Rate (bpm)
3 weeks	CONTROL (n=11)	132.29±4.2	85.92±2.7	101.26±3.2	—
	URAEMIC (n=11)	145.36±3.4*	94.26±2.2*	112.53±2.7*	—
6 weeks	CONTROL (n=25)	138.23±1.0	90.36±0.8	105.74±0.8	265.40±3
	URAEMIC (n=25)	158.80±1.5 *	103.94±1.0 *	121.60±1.2 *	290.64±3.0*
9 weeks	CONTROL (n=8)	135.62±2.4	89.30±1.8	103.89±1.8	273.05±4.4
	URAEMIC (n=8)	142.16±2.3*	93.72±1.7	108.93±1.8	318.91±6.8*

Table 3.2 Blood Pressure Measurements

Data are presented as mean ± S.E.M. of 7 readings per animal

* p<0.05 vs. appropriate control group

3.4.3 Hypertrophy

Left ventricular hypertrophy was observed at an organ and a cellular level. Hypertrophy indices (dry heart weight, dry heart weight: body weight and dry heart weight: tibia length) were significantly increased in uraemic versus control animals at 6 week uraemia (*Table 3.3*). Hypertrophy was also observed at a cellular level with a significant alteration in cardiomyocyte width (*Table 3.4*).

Experimental model		Dry Heart Weight (g)	Dry Heart Weight : Tibia Length (g/cm)	Dry Heart Weight: Body Weight x 10 ³
3 weeks	CONTROL (n=5)	1.54±0.10	0.37±0.01	4.35±0.20
	URAEMIC (n=5)	1.50±0.07	0.35±0.01	4.38±0.20
6 weeks	CONTROL (n=30)	1.78±0.05	0.42±0.01	4.19±0.10
	URAEMIC (n=30)	1.98±0.05*	0.48±0.01*	4.64±0.10*
9 weeks	CONTROL (n=8)	1.42±0.05	0.32±0.01	2.99±0.10
	URAEMIC (n=8)	1.64±0.07*	0.38±0.02*	3.66±0.20*

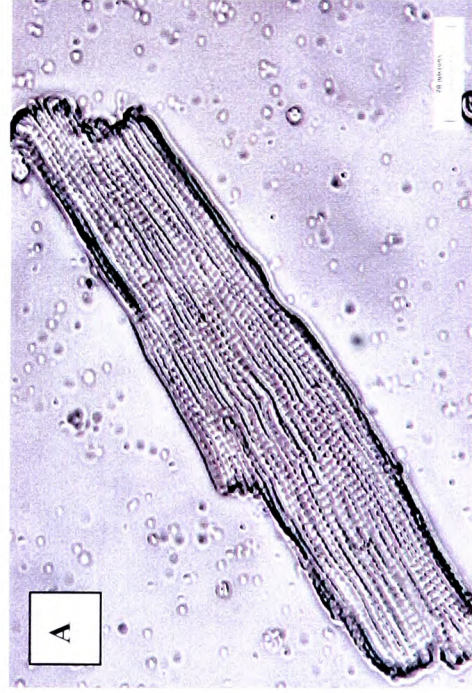
Table 3.3 Hypertrophy Indices

Data are mean ±S.E.M. *p<0.05 vs. controls

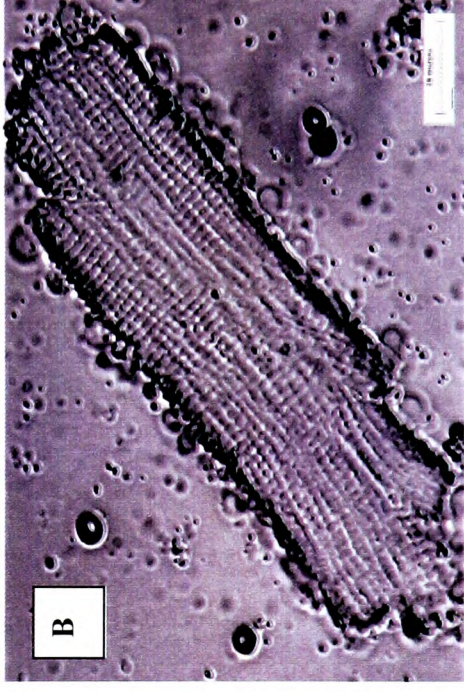
Parameter	CONTROL (n=287)	URAEMIC (n=287)
Cell length (μm)	130 \pm 1.6	131.6 \pm 1.39
Cell width (μm)	32.5 \pm 0.6	35.2 \pm 0.62*
Cell length:width ratio	4.07 \pm 0.08	4.32 \pm 0.093*

Table 3.4 Cardiomyocyte Morphology of Uraemic & Control Experimental Groups

Data presented as mean \pm S.E.M; 5 hearts per group and analysis of 57 cells per heart * $p < 0.05$ vs. control



Control cardiomyocyte



Uraemic cardiomyocyte

Figure 3.1 The effect of LVH on Isolated Cardiomyocyte Size: Photomicrograph of A) Control and B) 6 wk Uraemic Cell

Images taken using a Leitz Laborlux® S microscope with a 40x objective lens connected to a Cool SNAP-PRO camera and analysed using Image-Pro® Plus software

3.4.4 Serum Electrolyte Analysis

Development of uraemia was characterized by a significant decline in renal function as observed from elevated serum concentrations of creatinine and urea (*Fig. 3.2 A,B*)

Electrolyte concentrations were not altered in uraemia (*Table 3.5*).

Experimental model		Sodium (mM)	Potassium (mM)	Chloride (mM)	Bicarbonate (mM)
3 WEEKS	CONTROL (n=6)	138.8±1.7	4.7±0.1	99.5±1.3	26.6±0.7
	URAEMIC (n=5)	140.4±0.7	4.8±0.1	100.8±0.8	25.2±1.4
6 WEEKS	CONTROL (n=34)	141.6±0.3	6.4±0.3	100.9±0.4	24.9±0.5
	URAEMIC (n=37)	140.9±0.3	6.7±0.3	100.4±0.4	25.3±0.5
9 WEEKS	CONTROL (n=2)	139.0±0.00	6.4±0.10	99.0±1.0	30.5±0.1
	URAEMIC (n=2)	140.5±0.5	5.9±0.1	95.0±0.5	29.0±0.0

Table 3.5 Serum Electrolytes

Data are presented as mean ± S.E.M.

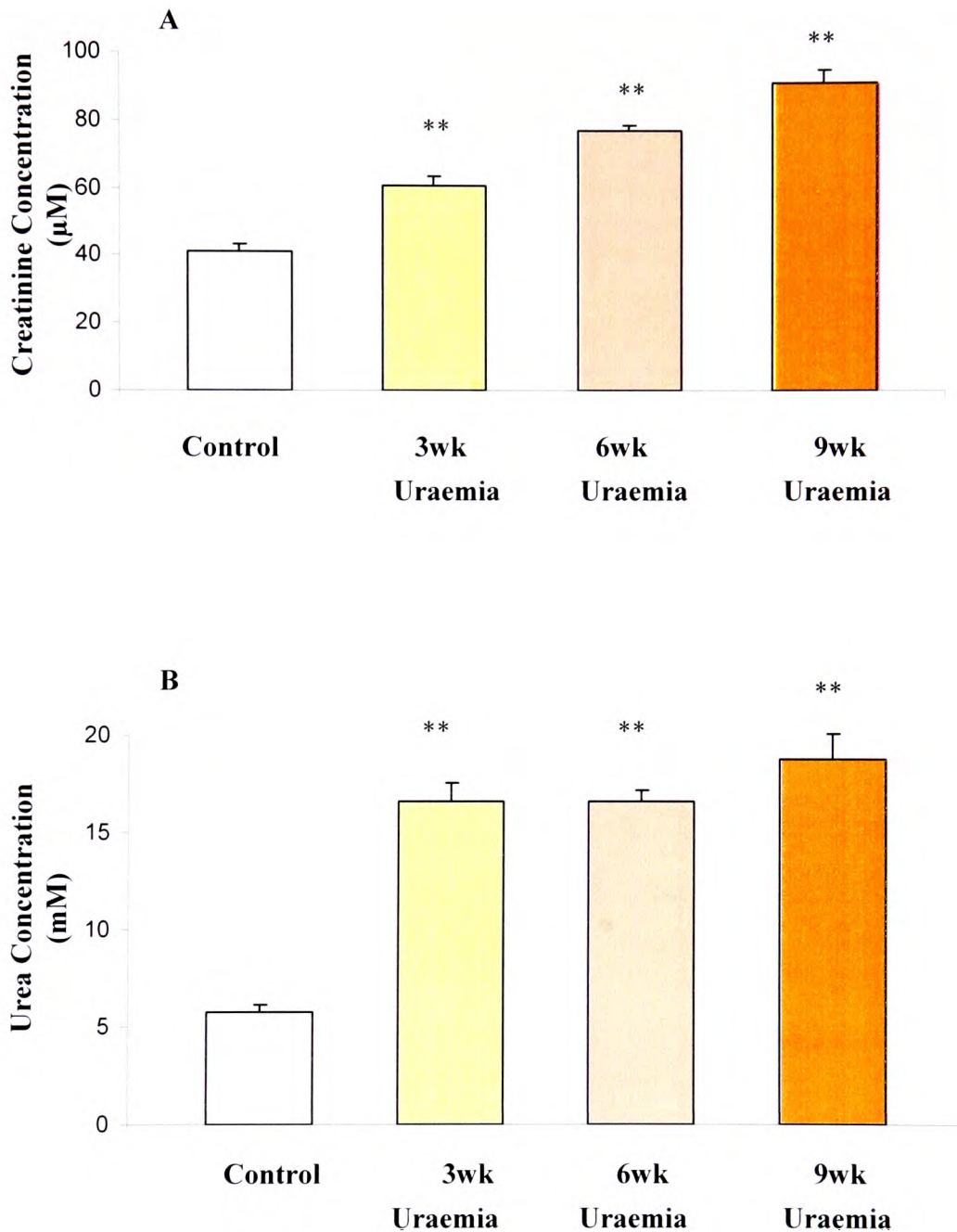


Figure 3.2 Serum Creatinine & Urea Concentration

A) Data are presented as mean \pm S.E.M; n=52 (controls); n=5 (3wk) n=41 (6wk); n=9 (9wk) **p<0.05 vs. control

B) Data are presented as mean \pm S.E.M; n=52 (controls); n=5 (3wk) n=41 (6wk); n=9 (9wk) **p<0.05 vs. control

3.4.5 Anaemia

Uraemic animals were characterized by anaemia at all stages of renal impairment (Fig. 3.3). Anaemia was more severe in the early stages of uraemia (3 week $31.8 \pm 0.8\%$ and 6 week $28.8 \pm 0.8\%$) and recovered over later stages of the experiment (9week $37.8 \pm 1.0\%$).

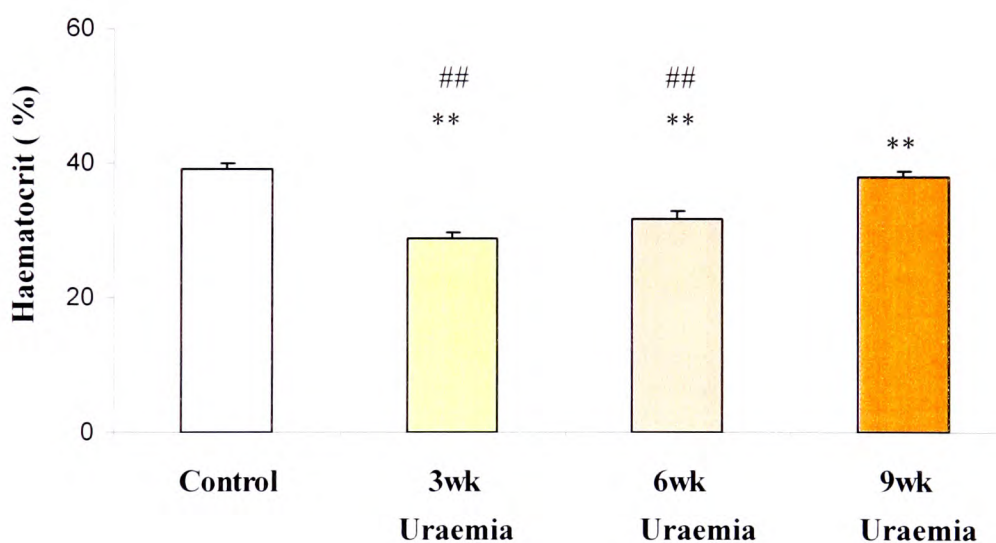


Figure 3.3 Development of Anaemia

Data are presented as mean \pm S.E.M.

n=38 (controls); n=6 (3wk) n=29 (6wk); n= 5 (9wk)

** p< 0.05 vs. control; ## p<0.05 vs. 9 wk uraemia

3.4.6 Insulin and Proinsulin Measurements

Hyperinsulinaemia was observed by 6 week and 9 week uraemia ($p < 0.05$, $n = 22$ and $p < 0.08$, $n = 2$) (Fig. 3.4 A). Proinsulin levels were significantly elevated in 6 week uraemia (Fig. 3.4 B). Proinsulin over insulin ratio was not affected (uraemic 0.41 ± 0.04 vs. control 0.49 ± 0.06 $n = 22$).

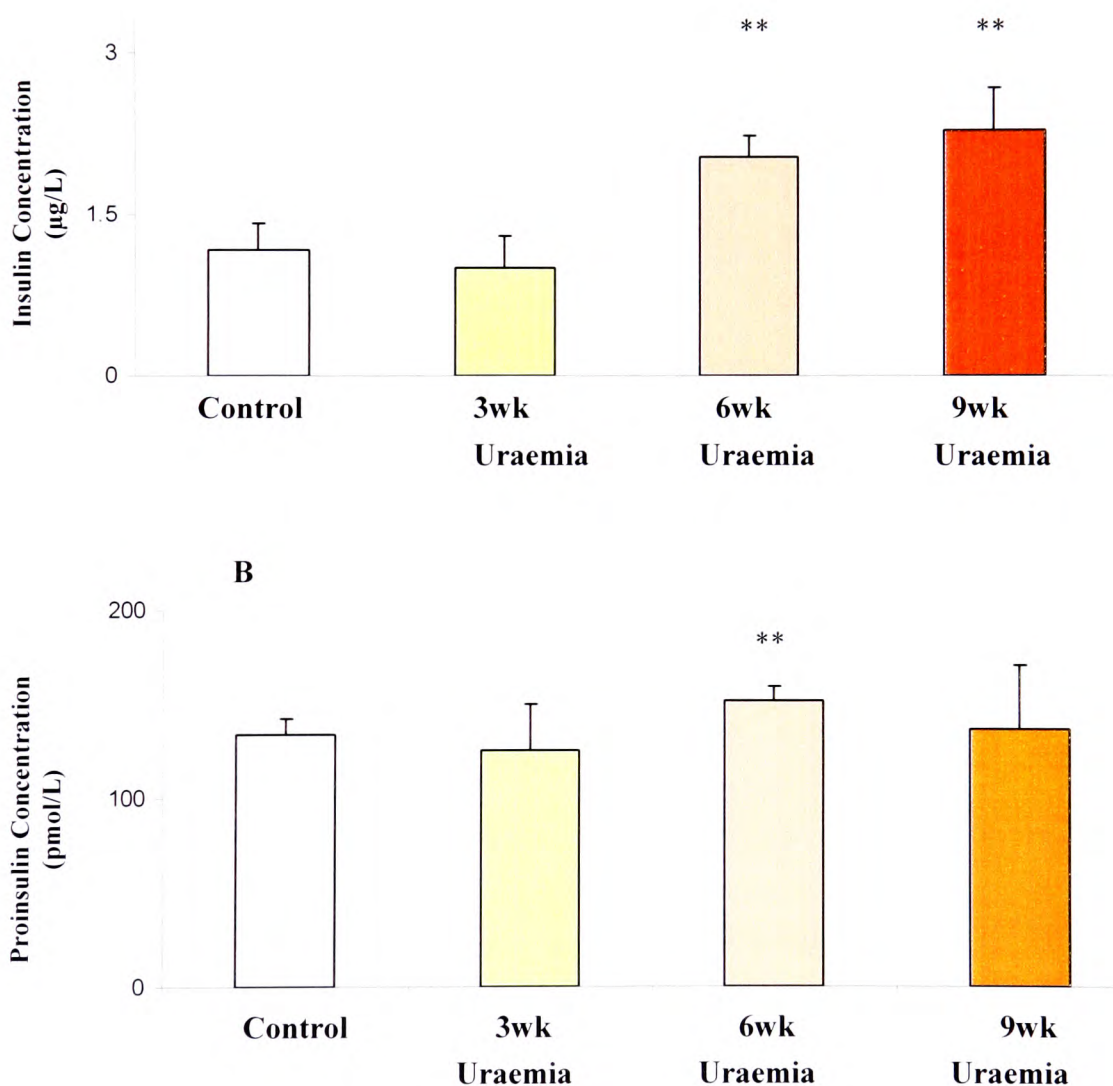


Figure 3.4 Serum Insulin & Proinsulin Concentrations

A) Insulin Concentration. Data are presented as mean \pm S.E.M; $n = 26$ (controls); $n = 2$ (3wk); $n = 22$ (6wk) $n = 8$ (9wk). ** $p < 0.05$ vs. control.

B) Proinsulin Concentration. Data are presented as mean \pm S.E.M; $n = 24$ (controls); $n = 2$ (3wk), $n = 20$ (6wk); $n = 2$ (9wk); ** $p < 0.05$ vs. control

3.4.7 Serum Metabolite Profile

There was minimal alteration in serum glucose, fatty acid and lactate concentrations in uraemic versus control animals in 6 week uraemia (Table 3.6).

Metabolite	CONTROL (n=6)	URAEMIC (n=6)
Glucose (mM)	12.5±0.80	11.4±1.1
Free fatty acids (mM)	0.6±0.01	0.7±0.01
Lactate (mM)	3.6±0.3	4.3±0.4

Table 3.6 Serum Metabolite Concentrations

Data are presented as mean ± S.E.M.

n=6 (glucose); n=8 (free fatty acids);

n=9 (lactate)

3.5 Discussion

This study investigated the development of experimental uraemia on cardiac morphology and physiology. The model is characterized by haemodynamic abnormalities (hypertension and anaemia), cardiac hypertrophy, renal dysfunction and hyperinsulinaemia.

3.5.1 Morphology

Animal body weights were comparable at 3 week and 9 week uraemia. However, at 6 weeks, uraemic animals had significantly lower body weights than controls. This is in contrast to previous observations where no change in body weight in pair fed animals was observed (Reddy et al., 2007). The severity of the uraemic surgical procedure was greater in the present study, as greater amounts of left kidney tissue were removed, which could have resulted in lower body weights. Discrepancy in body weights of partially-nephrectomized animals and control animals inspite of pair feeding has been documented previously (McMahon et al., 2002). Patients with CKD have varying degree of lean body mass and weight loss has been associated with inadequate dietary intake and proteinuria (Cianciaruso et al., 1995, Dwyer et al., 1998).

However, more recent studies have associated insulin resistance with muscle wasting in uraemia (Lee et al., 2007). Insulin resistance diagnosed by HOMA in uraemic patients causes muscle loss by a) suppression of the insulin/IGF-1 pathway b) suppressing PI3K activity and potentially triggering caspase 3 activation, fragmentation of muscle proteins and subsequent activation of the ubiquitin-proteasome system (Lee et al., 2004, Lee et al., 2007, Rommel et al., 2001, Satchek et al., 2004). Impaired insulin signalling may play a central role in the lean body mass loss in uraemia as insulin/insulin-like growth factor-1 (IGF-1) signalling pathway modulate muscle mass, and IGF-1/PI3K/Akt pathway prevents the upregulation of muscle atrophy genes encoding ubiquitin ligases (Glass, 2003, Du and Mitch, 2005).

3.5.2 Hypertrophy and Haemodynamic Alterations

Hypertrophy was apparent in uraemic animals at 6 week and 9 week post-surgery (Table 3.3, 3.4). These changes are in keeping with previous observations (Raine et al., 1993, McMahon et al., 2002, Reddy et al., 2007). Tibial length was used as the normalisation variable for heart weight as it remains constant in animals of same age (Yin et al., 1982). Measurement of cardiomyocyte dimensions confirmed presence of cellular hypertrophy, eliminating effects of fibrosis and cell loss. Cell length and width are considered analogues of the heart chamber diameter and wall thickness respectively (Gerdes et al., 1996).

Therefore, the cellular measurements here indicate an increase in ventricular wall thickness and are consistent with previous observations (Fowler et al., 2007, Reddy et al., 2007). The increase in wall thickness and cell width are characteristic of the developing and compensatory pressure overload (Gerdes et al., 1996). This load leads to addition of the new sarcomeres in parallel, resulting in a disproportionate increase in the LV wall thickness and reduced chamber radius (concentric hypertrophy) (London et al., 1999). Hypertension is evident from the earliest stages of uraemia (*Table 3.2*) which may in turn contribute to the loss of cells in the uraemic heart, hence causing greater workload on the remaining viable cardiomyocytes (Amann et al., 2003b). The progression of concentric hypertrophy and hypertension can lead to decreased diastolic compliance and places the myocardium at a greater risk of ischemia, even in the absence of coronary artery disease (Middleton et al., 2001).

Volume overload leads to lengthening of contractile units causing progression of eccentric hypertrophy resulting in chamber dilation, increase in wall tension, systolic stroke volume, oxygen requirements and myocyte burnout (Middleton et al., 2001). However, this study has not shown lengthening of the uraemic cardiomyocytes, characteristic of volume overload. CKD patients have a higher risk of heart failure and hence greater risk of premature cardiovascular events (Baigent et al., 2000, Mark et al., 2006). However, there is no evidence of heart failure in any stages of uraemia examined in this study as there is a lack of oedematous lungs observed in animal heart failure models (*Table 3.1*) (Afzal and Dhalla, 1992).

The uraemic model is characterized by significant renal dysfunction from the incipient stages of the experiment. Progression of the disease caused further deterioration of renal function as indicated by further increases in creatinine concentration (*Fig. 3.2*). Experimental uraemia was characterized initially by anaemia. However, this recovered with the progression of disease, most probably as a result of recovery of the remnant kidney and kidney hypertrophy (Reddy et al. 2007). Anaemia is an important confounding factor in the uraemic cardiomyopathy and is one of the contributing causes of volume overload (Middleton et al., 2001). Previous work has demonstrated a robust correlation between declines in haemoglobin levels and LVH progression in patients with early stage of uraemia (Levin et al., 1999).

Six and nine week uraemia is characterized by hyperinsulinaemia manifested by an increase in serum insulin and proinsulin levels. The proinsulin: insulin ratio was not altered in uraemia, thus eliminating a defect in proinsulin to insulin processing observed in some animal models of hyperinsulinaemia (Leahy, 1993, Alarcon et al., 1995). Hyperinsulinaemia is associated with underlying insulin resistance which is present from the early stages of uraemia (Stefanovic et al., 2003, Becker et al., 2005). There are no significant alterations in serum metabolites (glucose, FFA, lactate) at 6 weeks consistent with previous findings (Reddy et al., 2007).

3.6 Summary

The experimental model of chronic kidney disease (uraemia) used in this study is characterized by significant renal insufficiency from the onset. Early stages of uraemia (3 weeks) are characterized by haemodynamic disturbances (hypertension and anaemia) in the absence of cardiac hypertrophy. Progression of uraemia to 6 and 9 weeks post surgery further exacerbates the haemodynamic alterations observed and results in the development of compensated concentric LV hypertrophy and hyperinsulinaemia.

4. CARDIAC FUNCTION & METABOLISM IN URAEMIA

4.1 Introduction

Left ventricular hypertrophy is the compensatory response to a chronic increase in cardiac workload through reducing ventricular wall stress (Middleton et al., 2001). Although initially beneficial, the long term outcome of cardiac hypertrophy will lead to functional deterioration and heart failure (Seymour, 2003b). LVH is the definitive hallmark of cardiovascular disease in uraemia and it accelerates the evolution of uraemic cardiomyopathy (Amann et al., 1998b). Left ventricular dysfunction is present in 85% of CKD patients-16% of patients have systolic dysfunction, 41% concentric left ventricular hypertrophy and 28% left ventricular dilatation (Parfrey et al., 1996). Eccentric and concentric hypertrophy arise depending on the stress imposed in uraemia (volume and pressure overload) (Middleton et al., 2001). Despite the enormity of the problem, the cellular mechanisms underlying the LVH development in uraemia are not fully elucidated.

Compensated LVH is characterised by structural, molecular and metabolic adaptations, collectively referred to as “remodelling” (*Chapter 1*). One feature of LVH is a switch in substrate preference from fatty acid oxidation to glycolysis, in order to maintain sufficient cardiac output (Sambandam et al., 2002, Allard, 2004). As energy production is coupled to substrate oxidation, alterations in the profile of myocardial substrate selection may ultimately result in deleterious functional consequences in the hypertrophied heart leading to heart failure (van Bilsen et al., 2004, Stanley et al., 2005).

Little is known about the profile of myocardial substrate utilization in uraemia. Previous work has assessed myocardial metabolism under baseline conditions at an early stage in experimental uraemia and found no evidence of altered substrate oxidation or impaired cardiac function (Reddy et al., 2007). However, studies using ^{31}P NMR have revealed significant reductions in PCr/ATP ratio, implying altered energetics of the uraemic heart (Raine et al., 1993). In addition to LVH, uraemia is characterized by insulin resistance and is further discussed in *Chapter 6*. Previous studies on experimental models of insulin resistance have demonstrated increased myocardial utilization of fatty acids and decreased glucose oxidation, accompanied by a reduction in cardiac efficiency (Belke et al., 2000, Chatham and Seymour, 2002, Mazumder et al., 2004). Thus, in uraemia, insulin resistance may further exacerbate metabolic remodelling in the heart by limiting the uptake and metabolism of glucose and predisposing uraemic heart to progress into energy starvation and failure.

4.2 Aims and Objectives

The aim of this study was to examine the effect of increased workload (increased extracellular $[\text{Ca}^{2+}]$) and insulin on *in situ* myocardial function and profile of substrate oxidation in experimental uraemia using ^{13}C NMR spectroscopy.

4.3. Materials and Methods

Materials used are listed in section 2.1. Perfusion studies were performed 6 week post induction of uraemia. The methods used are outlined in section 2.5, 2.11, 2.13.

4.3.1 Heart Perfusions

Following 20 min equilibration with 1.25 mM Ca^{2+} , the perfusion medium was switched to KHB buffer of identical composition with increased Ca^{2+} concentration (2.5 mM) (*Fig. 4.1*). Hearts were perfused for a further 20 min and switched to buffer containing [$\text{U-}^{13}\text{C}$] palmitate, and either [$3\text{-}^{13}\text{C}$] lactate and unlabelled glucose and pyruvate or unlabelled lactate, pyruvate and [$1\text{-}^{13}\text{C}$] glucose for 45 min (*Fig. 4.1*). Perfusions were carried out in the presence or absence of 1 mU/ml insulin. pO_2 and coronary flow rate measurements were taken at 15 min intervals throughout the perfusion protocol.

AD Instruments Chart 5.5[®] software was used for left ventricular pressure measurements *in situ* and the Blood Pressure Module[®] was used for data analysis. Functional parameters [systolic and diastolic pressures, heart rate, $\text{dP}/\text{dt}_{\text{max}}$ (contraction), $\text{dP}/\text{dt}_{\text{min}}$ (relaxation)] were averaged for 3 cardiac cycles and analysed over the final 45 min of perfusion (average 24 000 data points).

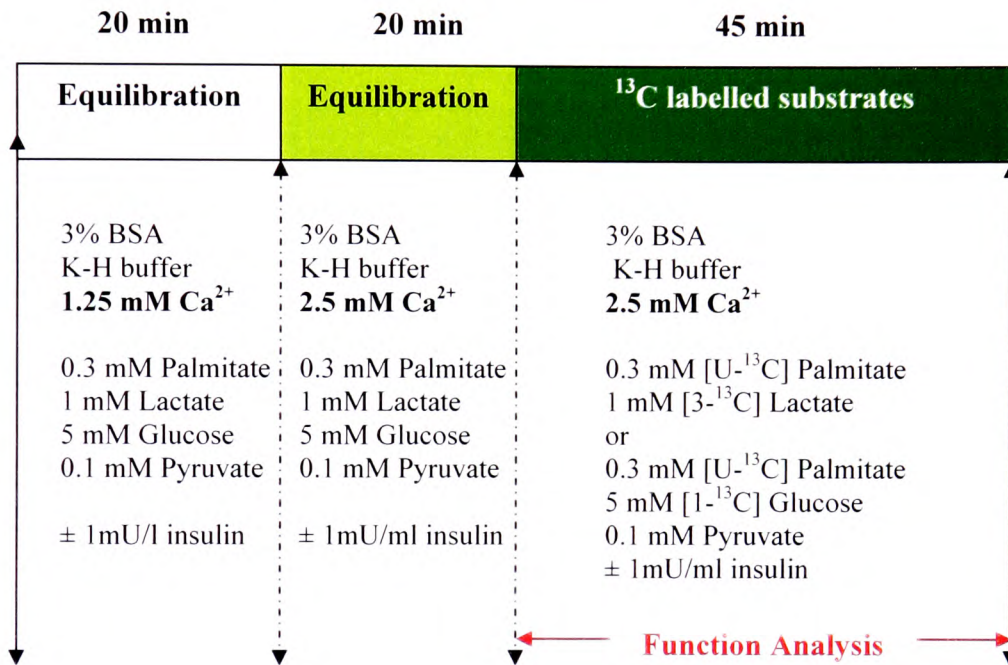


Figure 4.1 Experimental Protocol for Perfusion Studies

4.4 Results

4.4.1 Cardiac Function

Table 4.1 and figure 4.2 show the mean cardiac function, MVO_2 and cardiac efficiency in control and uraemic hearts. In the presence of insulin, uraemic hearts were characterized by increased HR, RPP, and decreased LVDP, $+dP/dt_{max}$ and $-dP/dt_{min}$ vs. controls (Table 4.1). In the absence of insulin, all functional parameters were lower in uraemic hearts vs. control (Table 4.1). Oxygen consumption was markedly reduced in uraemic hearts perfused without insulin in comparison to controls, and showing an apparent increase in cardiac efficiency versus controls uraemic hearts perfused with insulin (Fig. 4.2A).

	+1mU/ml insulin			
	CONTROL (n=8)	URAEMIC (n=8)	CONTROL (n=14)	URAEMIC (n=14)
HR (bpm)	242.1±0.2	240.9±0.3	240.9±0.2	248.5±0.2 [#]
LVDP (mmHg)	154.6±0.2	131.3±0.2 [†]	134.3±0.2	124.7±0.2 [#]
+dP/dt_{max} (mmHg/s)	4788.6±7.2	4184.0±5.2 [†]	4631.8±6.2	4266.1±6.6 [#]
-dP/dt_{min} (mmHg/s)	-2095.5±14.0	-1146.9±15.6 [†]	-2739.6±3.7	-2375.1±3.5 [#]
RPPx10⁻³ (mmHg/min)	37.4±0.1	31.01±0.04 [†]	29.3±0.1	31.8±0.1 [#]

Table 4.1 Myocardial Function in the Presence & Absence of Insulin

Data presented as mean ± S.E.M; [†] p<0.05 vs. control-insulin; [#]p<0.05 vs. control +insulin

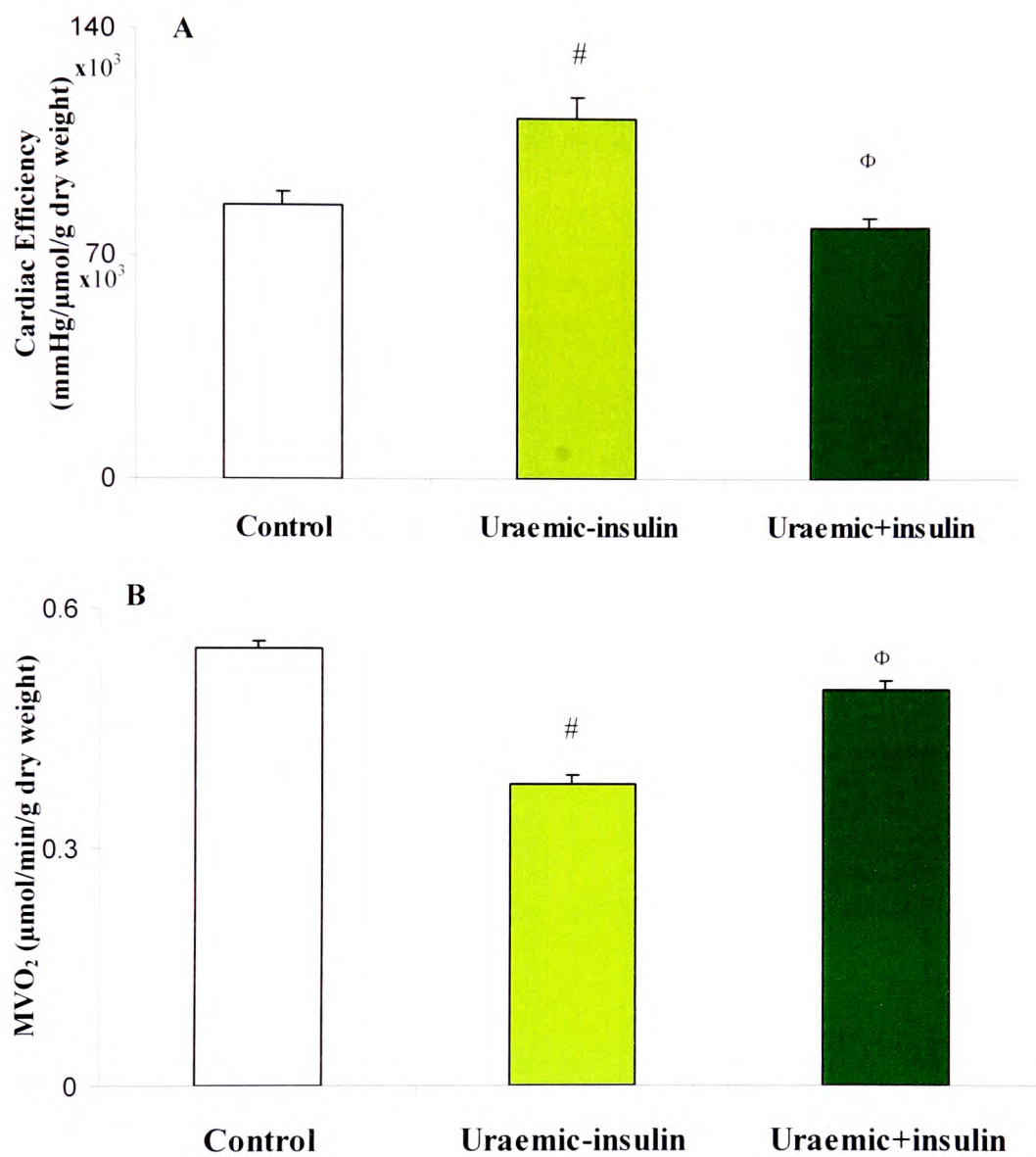


Figure 4.2 Cardiac Efficiency (A) & Oxygen Consumption (B)

Data presented as mean \pm S.E.M.

control n=24, uraemic-insulin n=8; uraemic +insulin n=14

[#]p<0.05 vs. control; ^Φp<0.05 vs. uraemic -insulin

4.4.2 Metabolic Profile

The relative contributions of exogenous ^{13}C labelled glucose, lactate and palmitate to the TCA cycle are shown in figure 4.3. Substrate contribution analysis revealed that the uraemic hearts have a greater reliance on carbohydrates (lactate and glucose) than palmitate (72% vs. 28% $p < 0.05$); however the individual substrate contributions were not significantly altered (*Fig. 4.3*).

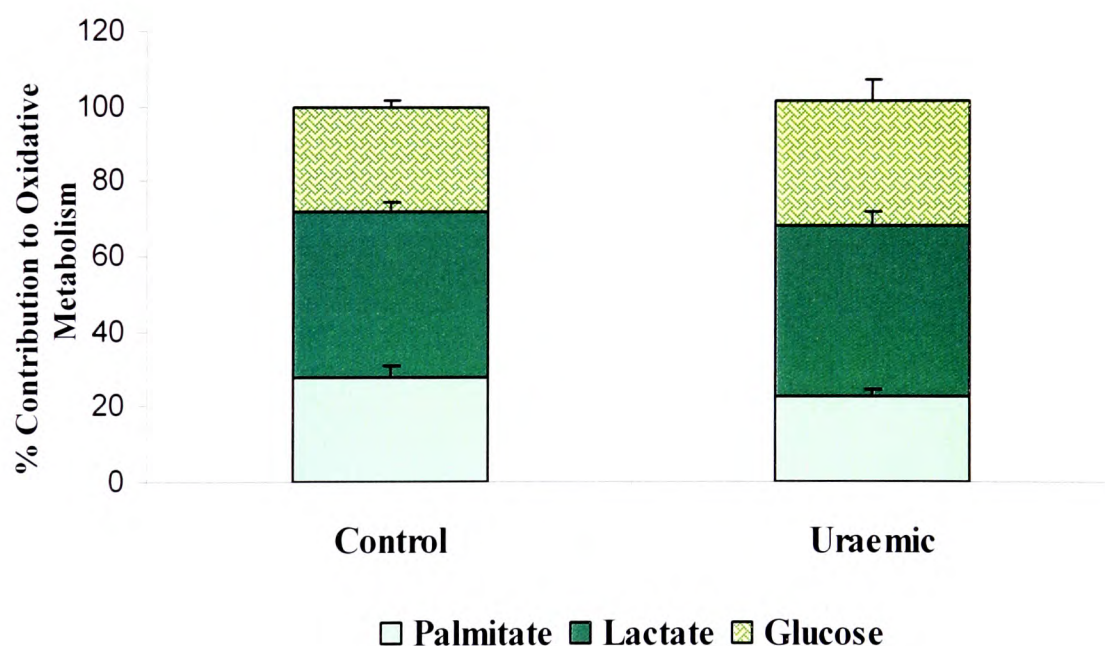


Figure 4.3 Profile of Substrate Oxidation in Presence of 1 mU/ml Insulin

Data are presented as mean \pm S.E.M.

Palmitate (control n=13, uraemic n=15);

Lactate (control n=7, uraemics n=10);

Glucose (control n=6, uraemic=5).

In the absence of insulin, there was little difference in the profile of lactate vs. palmitate use in the uraemic vs. control hearts. However, there was an increase in relative contribution from the unlabelled pool in uraemic vs. control hearts (25.3 ± 3.4 vs. $15.9 \pm 2.3\%$; $p < 0.05$). The unlabelled pool is comprised of exogenous glucose, pyruvate and endogenous glycogen and triglycerides. Lactate and palmitate utilisation were more prevalent than unlabelled substrate contribution within both experimental groups in the absence of insulin (Fig. 4.4).

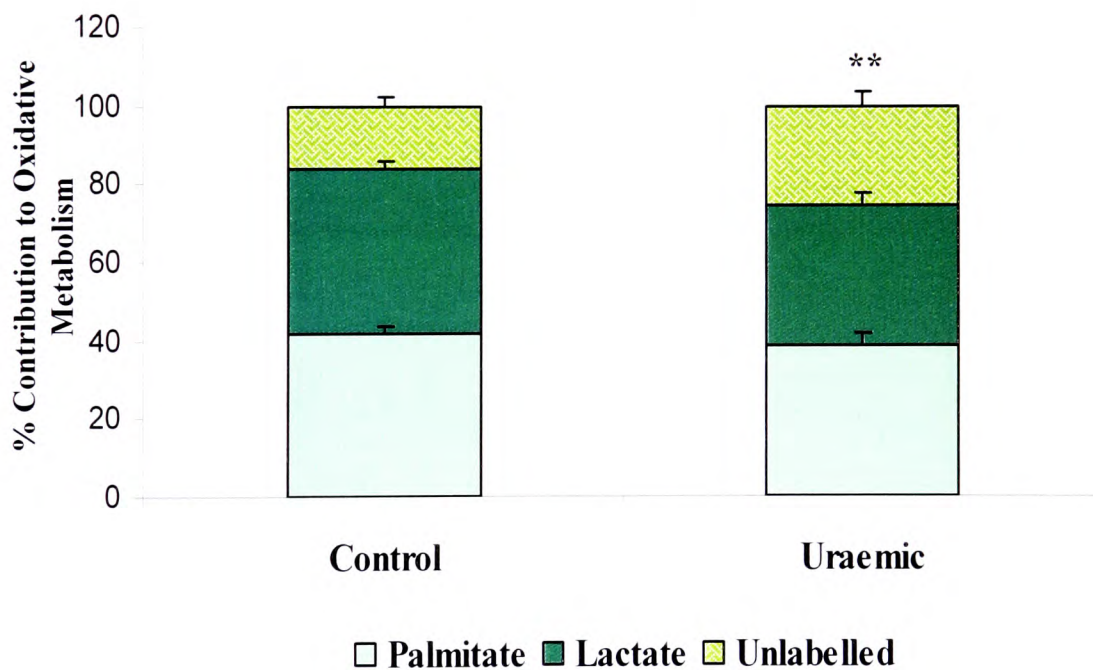


Figure 4.4 Profile of Substrate Oxidation in Absence of Insulin

Unlabelled substrates: glucose, pyruvate, glycogen, tryglycerides

Data are presented as mean \pm S.E.M.

control n=7; uraemic n=8

** $p < 0.05$ vs. control for unlabelled pool

However, the presence of insulin does affect the profile of substrate utilization in uraemic hearts. There is a marked reliance on lactate (44.8 ± 4.3 vs. $36.0 \pm 3.1\%$ $p < 0.05$) with reduced palmitate oxidation ($38.6 \pm 2.1\%$ vs. $22.3 \pm 1.6\%$ $p < 0.05$) relative to perfusions in the absence of insulin. In control hearts perfused with insulin there was less decrease in palmitate oxidation ($41.3 \pm 1.9\%$ vs. $28.8 \pm 3.1\%$ $p < 0.05$) relative to control hearts in the absence of insulin.

4.4.3 Triglyceride and Glycogen Content Analysis

Cardiac tissue triglyceride content was unaltered in 6 week uraemia (*Fig. 4.5 A*), however glycogen content was significantly elevated (*Fig.4.5 B*).

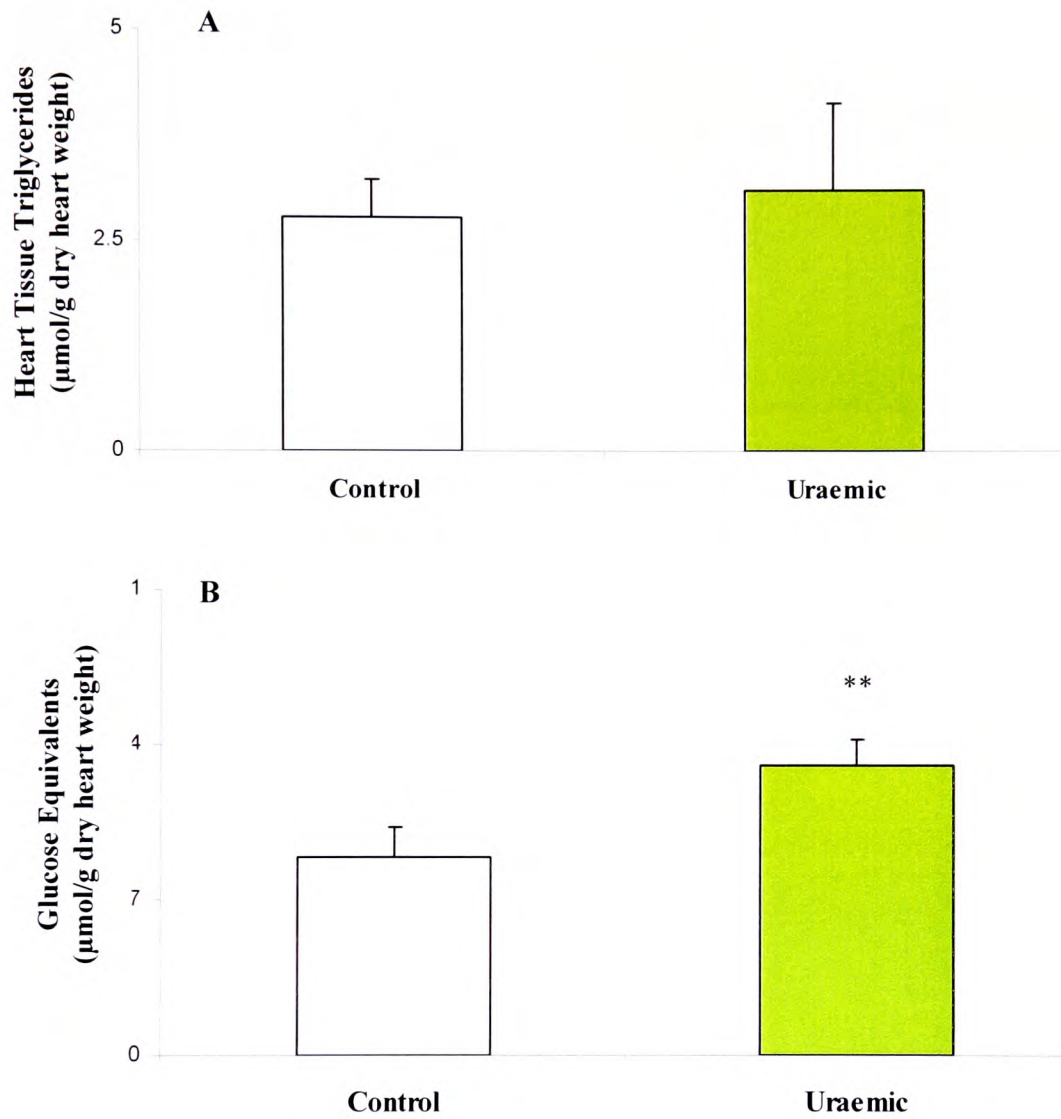


Figure 4.5 Six week Tissue Triglyceride & Glycogen Content

A) Triglycerides. Data are presented as mean \pm S.E.M; n=7 each

B) Glycogen. Data are presented as mean \pm S.E.M; n=8 each **p<0.05 vs. control

PDH activity

Citrate synthase and the PDH activity were not affected in 6 wk uraemia (Fig. 4.6; 4.7).

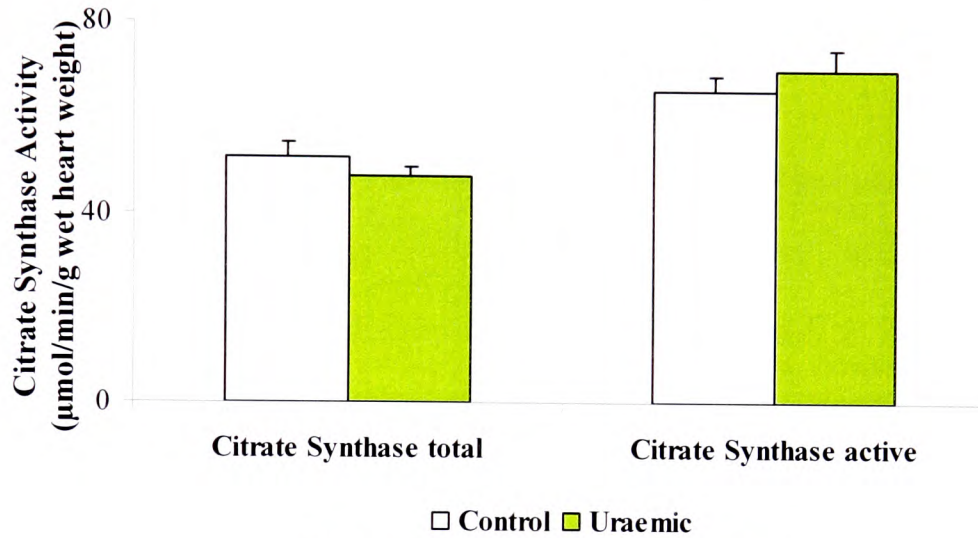


Figure 4.6 Citrate Synthase Activity

Data are presented as mean \pm S.E.M; n=6 (control) n=9 (uraemic)

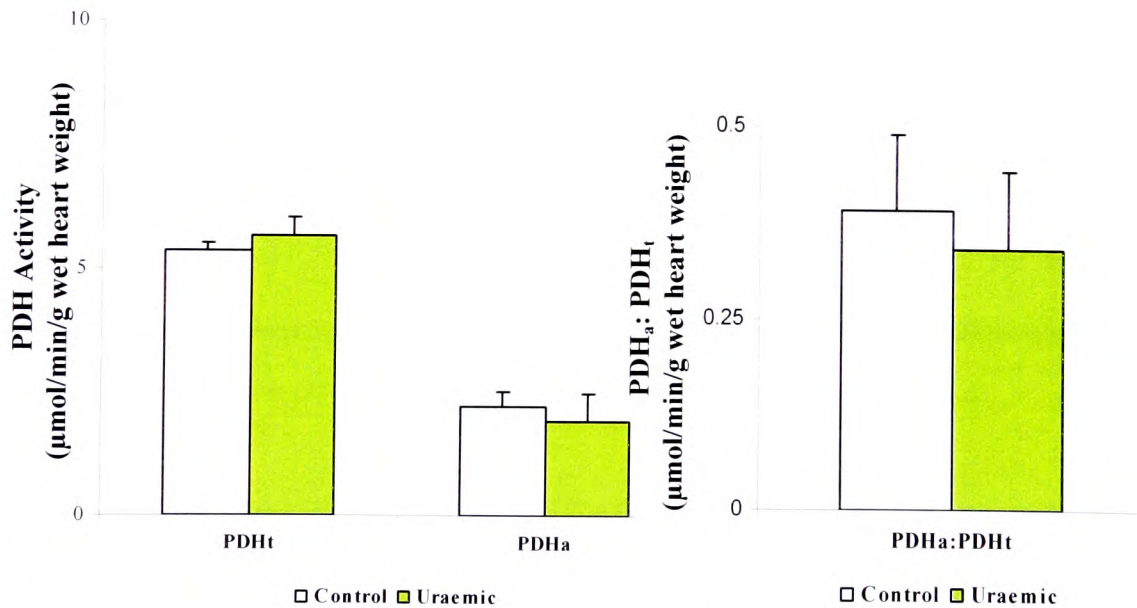


Figure 4.7 PDH Activity

PDH_a-active; PDH_t-total; PDH_a: PDH_t-active: total ratio

Data are presented as mean \pm S.E.M; n=6 (control) n=9 (uraemic)

4.5 Discussion

The aim of this study was to assess cardiac function and energy provision in experimental uraemia under conditions of increased extracellular $[Ca^{2+}]$ (2.5mM) in order to increase both contraction and metabolic demand. Hearts were perfused either in the presence or in the absence of insulin (1mU/ml) to mimic basal metabolic state. Ca^{2+} can be rapidly taken up by mitochondria and activate key enzymes involved in the production of NADH and FADH₂, PDH, OGDH and ICDH (Balaban, 2002). This in turn causes increased delivery of NADH to the respiratory chain, and the maximum rate of oxidative phosphorylation, meeting the enhanced demand for ATP synthesis (Territo et al., 2000, Balaban, 2002).

4.5.1 Cardiac Function and Metabolism in Uraemia

In the absence of insulin and increased workload, uraemic hearts displayed depressed heart rate, LVDP, $+dP/dt_{max}$, $-dP/dt_{min}$, RPP and MVO_2 in comparison to control hearts. These results are consistent with previous observations in the aortic-banded model of cardiac hypertrophy (Allard et al., 2000) and to previous *in situ* cardiac function measurements using the same model of uraemia (Raine et al., 1993).

In the uraemic hearts, enhanced workload in the presence of insulin caused an increase in the heart rate, and concomitantly in the rate pressure product versus controls. This is consistent with the *in vivo* measurements of heart rate (*Chapter 3*) and with clinical observations, where the elevated heart rate together with anaemia are regarded as hallmarks of volume overload (London, 2003).

Cardiac efficiency in uraemic hearts was reduced in the presence of insulin, in parallel with decreases in LVDP, $+dP/dt_{max}$ and $-dP/dt_{min}$. These findings are suggestive of altered ventricular performance at high workloads, consistent with previous reports (Rhodes et al., 1993, Schlant et al., 1998). Reduced LVDP observed in perfused uraemic hearts versus control is in contrast to *in vivo* hypertension (*Table 3.3*). However, it is difficult to draw direct comparison between developed pressure in the *ex vivo* heart perfusion preparation and the *in vivo* observations as the perfused heart is not exposed to the pressure and volume overload present in the uraemic animal and it is not subjected to neurohormonal regulation.

Altered cardiac relaxation in particular, was suggested parallel to this study by an increase in PLB phosphorylation observed in the LV of 6 week uraemic animals (unpublished observations Pavlovic, 2007). An increase in PLB phosphorylation stimulates SERCA2a function and is considered a compensatory response attempting to maintain normal Ca^{2+} handling (Boateng et al., 1997). Previous studies have revealed impaired myocyte relaxation and abnormal Ca^{2+} handling due to altered Na^+/Ca^{2+} pump activity (McMahon et al., 2006).

Altered cardiac relaxation is the main cause of the diastolic dysfunction in uraemia (Facchin et al., 1995), manifested by increased *in vivo* diastolic pressure in this study (*Chapter 3; Table 3.2*). Clinical studies in CKD patients with LVH have shown that diastolic dysfunction is an important mediator of heart failure and death from cardiac causes (Verma et al., 2007). However, at the present stage of uraemia, cardiomyocytes appear to maintain SR function, with unaltered SERCA2a expression. In addition Na⁺K⁺ATPase ion pump expression is increased as a compensatory response and could potentially be maintaining cellular ion gradients to preserve normal contractile function (McMahon et al., 2006). Evidence supporting compensated stage contractile function is the maintenance of cardiac efficiency relative to control hearts. Increasing the severity of uraemia results in the failure of the uraemic heart to respond to an increase in extracellular Ca²⁺ by failing to increase HR and cardiac output (Raine et al., 1993). Equally, additional increase in the extracellular [Ca²⁺] (3.0-5.6mM) may further exacerbate the contractile dysfunction (Raine et al., 1993).

Previous *in vivo* and *in vitro* studies on heart and isolated cardiomyocyte preparations have shown that insulin improves contractile function (Freestone et al., 1996, Allard et al., 2000). However, in uraemia, insulin rendered hearts less efficient with increased oxygen consumption for a reduced amount of work in comparison to the uraemic hearts in the absence of insulin (*Fig. 4.2*). Reduction in cardiac efficiency could be a result of impaired contraction or alternatively, increased oxygen cost for E-C coupling, elevated basal metabolic rate or changes in substrate supply (Burkhoff et al., 1991, How et al., 2005).

The metabolic substrate profile of the uraemic hearts suggests a shift of substrate preference from fatty acids to carbohydrates. In the presence of insulin, there is no alteration in the relative contribution of the individual substrates to oxidative metabolism between uraemic and control animals. This is consistent with the metabolic profile of the uraemic hearts perfused using 1.25 mM extracellular $[Ca^{2+}]$ (Reddy et al. 2007).

Metabolic profile of the uraemic hearts in this study may suggest the development of myocardial insulin resistance and reflect observations from the diabetic *db/db* mice exhibiting decreased cardiac efficiency and increased myocardial oxygen consumption (How et al., 2006). Metabolic profile observed in uraemic hearts could be the direct effect of the developing myocardial insulin resistance further discussed in *Chapters 5* and *6*. Presence of insulin resistance is suggested by unaltered glucose contribution to the TCA cycle in response to an increase in the workload. Moreover, unaltered PDH activity in 6 wk uraemia suggests that there is no enhanced flux of pyruvate to acetyl CoA and hence no net increase in carbohydrate oxidative metabolism compared to controls (Stanley et al., 2005). In the absence of insulin, uraemic hearts display higher contribution from the unlabelled substrates (exogenous glucose and pyruvate; endogenous glycogen and triglyceride) than control.

Overall metabolic substrate profile of the uraemic heart also shows greater reliance on exogenous carbohydrates as the major source of energy (*Fig. 4.4*) with decreased fatty acid oxidation, consistent with remodelling profile in LVH, where decrease in fatty acid oxidation is compensated by increase in carbohydrate utilization. These findings are in keeping with the metabolic profile of the metabolically remodelled hypertrophied heart re-expressing foetal metabolic phenotype (Taegtmeyer et al., 2005). Furthermore, abundance of the relative labelled exogenous glucose, lactate and palmitate utilization (100%) (*Fig. 4.3*) in uraemia in the presence of insulin, suggests that the relative contribution from the unlabelled substrates is negligible under these experimental conditions.

In the presence of insulin, lactate is the dominant energy substrate accompanied by reduction in fatty acid use in the uraemic hearts versus control (*Fig. 4.4*). A greater preference for lactate is characteristic of volume overload hypertrophy, in which maximal lactate transport capacity and increase in MCT1 lactate transporter expression was observed (Evans et al., 2003). In addition, insulin caused an increase in the lactate contribution to the oxidative metabolism in uraemia, accompanied by a decrease in palmitate contribution to the TCA cycle compared to uraemic hearts in the absence of insulin (*Fig. 4.5*). The inhibitory effect of insulin on fatty acid utilization in insulin resistant hearts has been previously documented (Mazumder et al., 2004, Hafstad et al., 2006). The possible mechanisms that may account for this effect include a direct inhibition of AMP kinase by insulin; and indirect insulin effect due to enhanced glucose uptake and utilization resulting in malonyl CoA inhibition of CPT-1, hence reducing the entry of fatty acids into mitochondria for oxidation (Carley and Severson, 2005, Hafstad et al., 2006).

However, uraemic hearts demonstrate some degree of insulin responsiveness in terms of inhibited fatty acid utilization and increased carbohydrate utilization. This observation is in keeping with those of the metabolic insulin responsiveness in *db/db* diabetic hearts (Carley and Severson, 2005, Hafstad et al., 2006). This outcome is also consistent with the single proton emission computed tomography (SPECT) study using an iodinated fatty acid analogue (iodine-123- β -methyl iodophenyl-pentadecanoic acid ^{123}I -BMIPP) to evaluate cardiac metabolism in CKD patients (Nishimura et al., 2006). Thus, clinical study has shown a clear association between severe renal impairment, insulin resistance and impaired fatty acid metabolism.

Uraemic cardiomyopathy may also cause reduction in the expression of the nuclear receptor PPAR α and its co-activator PGC-1, which have been identified as the master switches for the myocardial metabolic remodelling (Barger and Kelly, 2000, Kelly, 2002). Pressure-overload hypertrophy deactivates PPAR α hence dysregulating fatty acid metabolism and leading to downregulation of an adult metabolic phenotype (Barger and Kelly, 2000). Nevertheless, the uraemic heart could be in a state of metabolic adaptation rather than maladaptation as it appears to have retained the metabolic flexibility (the ability to switch the substrate preference) (Taegtmeyer et al., 2005). A lack of change in citrate synthase activity (*Fig.4.7*) suggests no change in mitochondrial density and provides an additional evidence for the maintenance of oxidative capacity and thus absence of metabolic deterioration.

Progression of the renal insufficiency (*Chapter 3*) however will lead to the worsening of the insulin resistant state as shown in *Chapter 6*, and in synergy with the reduced palmitate utilization, will potentially jeopardise myocardial energy supply as a reduction in fatty acid oxidation and insulin resistance would impair glucose metabolism leading to substrate and to energy depletion (Taegtmeyer et al., 2005). This would contribute to the cardiac function deterioration and failure in uraemia (Raine et al., 1993).

Analysis of the endogenous substrates has revealed an increase in the glycogen content of the uraemic hearts. Chronic hyperinsulinaemia observed in the uraemic model (*Chapter 1*) may result in increased glycogen deposition *per se*, by stimulating glycogen synthase activity. In addition, study on muscle biopsies of non-diabetic uraemic patients has shown that the insulin resistance in this patient population is accompanied by elevated level of maximal glycogen synthase enzyme activity (Bak et al., 1989). Despite triglyceride accumulation being highly correlated with the insulin resistance in other experimental hypertrophy models (Atkinson et al., 2003), there was no indication of increased triglyceride content in uraemic hearts. Nonetheless, an increase in the glycogen deposition and unchanged triglyceride content in the uraemic myocardium observed in this study is comparable with the observations in skeletal muscles of chronic haemodialysis patients (Debska-Slizien et al., 2000).

Increased myocardial glycogen content observed in this study is also consistent with the previous studies in which uraemia induced increased myocardial glycogen content (Penpargkul and Scheuer, 1974) and similar results were obtained from myocardial tissue from acutely uraemic, binephrectomized and urethra ligated rats (Horl et al., 1980). An increase in glycogen deposition could be cardioprotective ensuring adequate glucose supply for glycolysis therefore ensuring the adequate energy supply for maintenance of normal cardiomyocyte homeostasis (Fraser et al., 1998).

4.6 Summary

This study demonstrates that the uraemic heart is characterized by developing cardiac dysfunction and metabolic adaptation. Insulin was shown to exacerbate cardiac remodelling in uraemia. Nevertheless, the metabolic and functional adaptations could play a key role in preserving cardiac function at this particular stage of uraemia. The consequences of the myocardial remodelling on long-term survival of the hypertrophied uraemic heart still require further investigation.

5. MYOCARDIAL PROTEIN EXPRESSION IN EXPERIMENTAL URAEMIA

5.1 Introduction

Cardiac hypertrophy causes an adaptive response at the molecular and cellular level. In turn this can lead to altered contractile protein expression and re-expression of the embryonic gene expression in the ventricle, including a stretch induced increase in atrial natriuretic factor (ANF) (Morgan and Baker, 1991, Rockman et al., 1991, Rockman et al., 1994). LVH causes alterations in myocardial energy provision, and furthermore substrate transporter proteins (van Bilsen et al., 2004). Myocardial insulin resistance (IR) and hyperinsulinaemia are clinically established confounding factors in uraemic cardiomyopathy (chapter 6). Alterations in the expression of metabolic transporters and signalling intermediates have been implicated as a potential mechanism for insulin resistance development in skeletal and cardiac muscle (Ferrannini et al., 1993). The development of IR is detrimental for the heart with altered metabolome, as previously discussed in section 1.6.

5.1.2 Metabolic Transporters

5.1.2.1 Glucose Transporters

Glucose transporters assist glucose uptake into cells and are polytopic membrane proteins forming an aqueous pore across the membrane (Bryant and James, 2002). The GLUT family comprises 13 members identified to date. These proteins span the membrane 12 times with amino- and carboxy-termini located in a cytosol (*Fig. 5.1*) (Bryant and James, 2002).

These transporters are conserved over a wide range of organisms implying a common evolutionary origin (Pessin and Bell, 1992, Gould and Holman, 1993). Previous studies have identified that the heart contains two types of glucose transporters, GLUT1 and GLUT4 (Young et al., 1997).

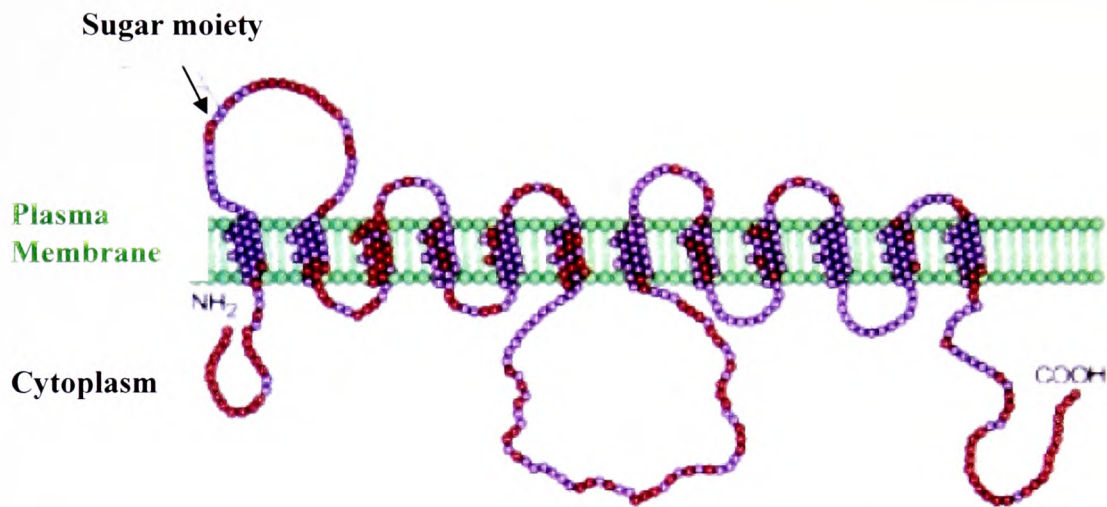


Figure 5.1 Structure of GLUT Family of Proteins Displaying Homology between GLUT 1 & 4 (residues unique to GLUT4 shown in red)

Image adapted from Bryant and Jamesl. (2002)

5.1.2.2 GLUT 1

Basal myocardial glucose uptake is primarily due to the presence of GLUT1 in the sarcolemma (Stanley et al., 1997). During foetal life, GLUT1 is highly expressed however, shortly after birth, there is a progressive decline in mRNA and protein expression, reaching adult levels at day 10 (Santalucia et al., 1992).

In the cardiomyocytes, GLUT1 is compartmentalized to intracellular storage vesicles in contrast to skeletal muscle where GLUT1 is located primarily at the sarcolemma (Becker et al., 2001). In response to metabolic stress, hypoxia and elevated intracellular $[Ca^{2+}]$, there is an increase in myocardial GLUT1 expression, stimulating glucose uptake (Shetty et al., 1993a, Hwang and Ismail-Beigi, 2001). This adaptive response maintains a sufficient supply of ATP by increasing glycolytic activity. GLUT1 expression and activity are increased up to 3-fold under these conditions in a p38 MAPK signalling pathway mediated response (Shetty et al., 1993a, Shetty et al., 1993b, Barros et al., 1997a, Barros et al., 1997b). Hypertrophic induction of GLUT1 expression was also found to be partially sensitive to inhibition of the phosphatidylinositol 3-kinase pathway and was strongly associated with the Ras activation and pathways downstream (Montessuit and Thorburn, 1999). Recent work has shown that GLUT1 and GLUT4 can also readily translocate to sarcolemma in response to lactate, however not via the PI3K-mediated pathway (Medina et al., 2002).

5.1.2.3 GLUT4

The primary target of insulin action in heart cells is glucose transporter 4 (GLUT4) (James et al., 1989, Calderhead et al., 1990, Slot et al., 1991). GLUT4 resides in intracellular storage vesicles and, upon insulin stimulation, translocates to the sarcolemma where it can facilitate uptake of extracellular glucose (Slot et al., 1991, Pessin et al., 1999).

The induction of GLUT4 protein expression occurs on day 20-21 of foetal life with a dissociation of mRNA and protein levels during developmental phase. This suggests that modifications of GLUT4 protein occur at both the translational and posttranslational level (Santalucia et al., 1992).

5.1.2.4 GLUT4 Translocation

Two major signalling pathways have been described in insulin-stimulated GLUT4 translocation: the phosphatidylinositol 3-kinase (PI3K) and the proto-oncoprotein c-Cbl. Insulin-stimulated GLUT4 translocation is triggered at the plasma membrane by binding of the hormone to the insulin receptor (*Fig. 5.2*).

The insulin receptor (I_R), a heterotetramer comprised of two α and β subunits (Bryant et al. 2002), is a tyrosine kinase linked receptor catalyzing the phosphorylation of broad range of intracellular substrates. These include the insulin receptor substrate (IRS) proteins, IRS-1 and IRS-2 (Holgado-Madruga et al., 1996, White, 1998). Insulin binding causes autophosphorylation and activation of the IR tyrosine-kinase domain (*Fig. 5.2*) and subsequent phosphorylation of IRS-1 and IRS-2. As I_R is activated, it, recruits a distinct subset of signalling proteins and interacts specifically with sequences surrounding the phosphotyrosine residue (Saltiel and Pessin, 2002).

The phosphorylation of tyrosine in the IRS family activates the p85 regulatory subunit of the type1A phosphatidylinositol-3 kinase (PI3-K) (Saltiel and Pessin, 2002) which consequently catalyzes the formation of the polyphosphoinositide phosphatidylinositol (3,4,5)-triphosphate (PIP3).

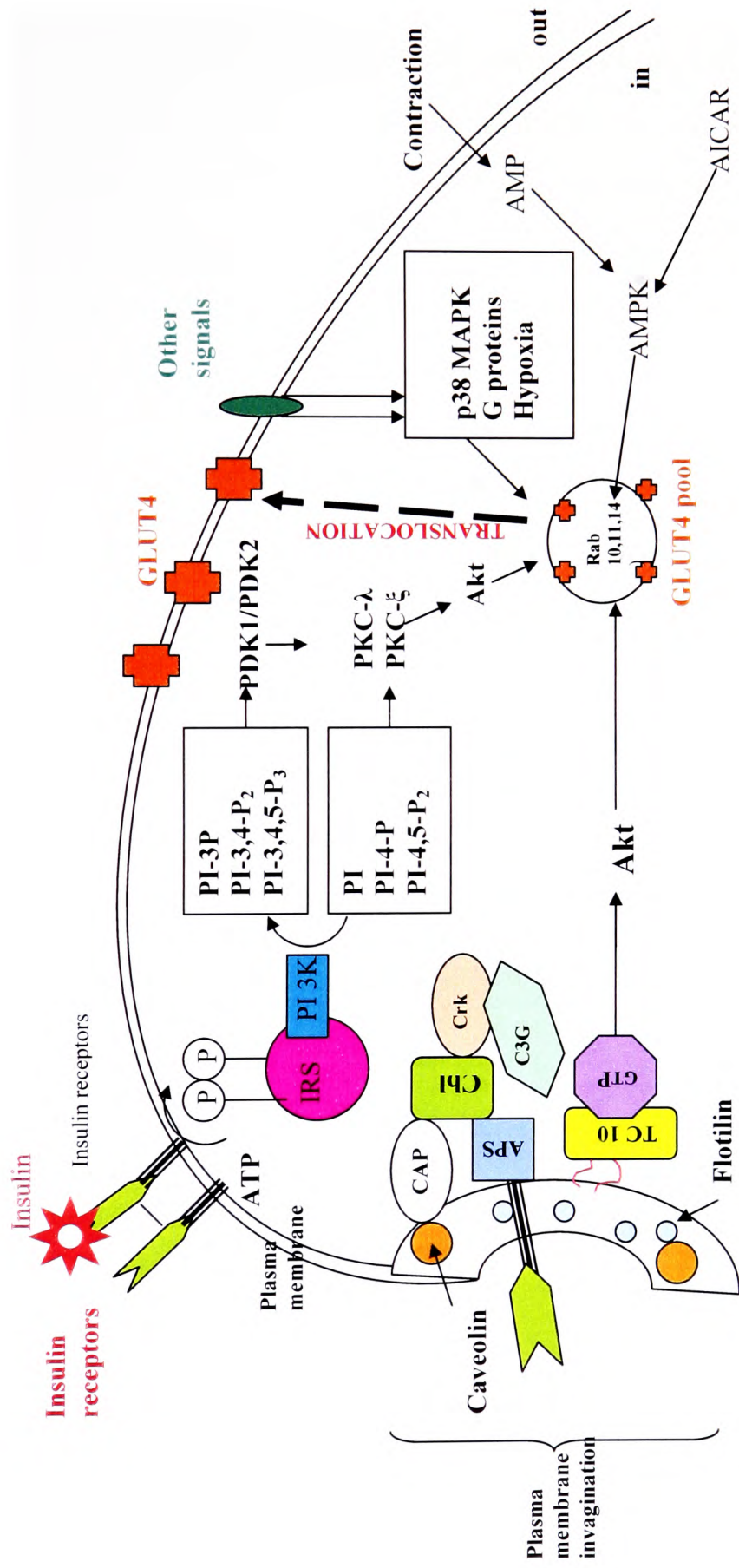


Figure 5.2 GLUT 4 Translocation Pathways: PI3K & PI3K Independent

PIP3 in turn interacts with phosphoinositide-dependant kinase 1(PDK1) (*Fig. 5.2*) which initializes a cascade of phosphorylations leading to activation of the atypical protein kinase C, isoform PKC ζ and Akt/PKB (*Fig. 5.2*) (Corvera and Czech, 1998, Saltiel and Pessin, 2002, Farese et al., 2005, Welsh et al., 2005). PI3K activates Akt by generating PIs (polyphosphoinositides) within the inner leaflet of plasma membrane which in turn act as docking sites for Akt. This brings Akt in close proximity to its upstream regulatory kinase PDK-1 (*Fig. 5.2*) (Bryant and James, 2002).

Upon dissociation of insulin, IR and its substrates undergo rapid dephosphorylation implicating role of protein tyrosine phosphatases (PTPases) involvement in signal termination. PTPase expression upregulation was observed in the insulin-resistant state (Drake and Posner, 1998).

Akt regulates over 35 substrates in the various metabolic processes. The most relevant Akt substrate for GLUT4 translocation is the Rab-GTPase-activating protein (GAP) Akt substrate of 160 kDa (AS160). A prominent feature of AS160 is the presence of the GTPase activating domain for Rab, small G proteins (Rab2, Rab8, Rab10, Rab11 and/or Rab14) each playing a critical role in vesicle formation, movement and fusion of GLUT4 (Zerial and McBride, 2001, Sano et al., 2003, Miinea et al., 2005). Supporting the role of AS160 in GLUT4 translocation is the localization of Rab 10, Rab 11 and Rab 14 on GLUT4 containing vesicles (Larance et al., 2005). Thus, recent immunoisolation of GLUT4 vesicles and mass spectrometry analysis have identified AS160 as a potential connection between PI3K signalling pathway and the GLUT4 trafficking machinery. Further evidence comes from the silencing of the AS160 gene causing enhanced, insulin dependant increase in surface levels of GLUT4 (Larance et al., 2005). Furthermore, Equez et al. (2005) using a knockout of AS160 in adipocytes, demonstrated increased sarcolemmal GLUT4 content and glucose uptake relative to wild type. In conclusion, insulin increases GLUT4 mobilization towards the sarcolemma in a process mediated by the PI3K-Akt-AS160 and PI3K-PKC axes (Imamura et al. 2003, Dugani and Klip, 2005).

GLUT4 positioning in the sarcolemma involves fusion between vesicular VAMP2 and SNARE target membrane proteins (SNAP23 and syntaxin 4) (Widberg et al., 2003, Hodgkinson et al., 2005).

GLUT4 vesicle endocytosis occurs via clathrin-coated pits and caveolae, with the internalized GLUT4 reaching endosomes in 2 min and the endosomal recycling compartment (ERC) in 20 min (Dugani and Klip 2005). Insulin accelerates GLUT4 delivery and exit from the ERC mediated by Akt and PIKfyve (PKB FYVE domain-containing PtdIns3P 5-kinase) (Berwick et al., 2004). Additionally, GLUT4 translocation can be regulated through a PI3K- independent pathway involving c-Cbl associated protein (CAP), Cbl and GTPase TC10 (*Fig. 5.2*). Preventing phosphorylation of Cbl completely inhibited the stimulation of GLUT4 translocation by insulin (Chiang et al., 2001). Furthermore, downregulation of total and phosphorylated Cbl was observed in insulin resistance in isolated cultured adult cardiomyocytes (Rosenblatt-Velin et al., 2004). The latter study indicated suggested that Cbl/CAP is essential for insulin-mediated GLUT4 translocation. The insulin-activated TC10, rho-like GTPase, has a potential role in cytoskeletal re-arrangement to facilitate exocytosis of GLUT4 to the sarcolemma (Omata et al., 2000). In addition, TC10 could be crucial for regulation of GLUT4 docking and fusion with the plasma membrane and work in combination with the PI3K mediated pathway, with the TC10 activation upstream of this event (*Fig. 5.2*) (Chiang et al. 2001, Saltiel and Pessin, 2002).

5.1.3 Fatty Acid Transporters

Cellular uptake of fatty acids (FA) is governed by metabolic demands of the tissue (van der Vusse et al., 2000). There are three distinct plasma membrane associated proteins: the 62 kDa FA transport protein (FATP); and the 88 kDa FA translocase (FAT) (the rat homologue of the human CD36) and the 43 kDa plasma membrane FA binding protein (FABPm) (Luiken et al., 1997, Luiken et al., 2002).

The majority of FFA uptake in the heart occurs via CD36 transporter (Luiken et al., 1999a, Luiken et al., 1999b). Insulin directly stimulates CD36 translocation in a similar manner to the GLUT4, mediated by a PI3K dependant mechanism (Luiken et al., 2002). However, there are at least two separate intracellular storage pools for CD36, one responsive to insulin and another stimulated by contractile activity mediated by activation of AMPK (Coort et al., 2007). The proportion of CD36 stored in intracellular pools in the basal conditions is much smaller than the size of GLUT4 storage compartments (Coort et al. 2007).

Regulation of FA and glucose uptake in cardiomyocytes share a common mechanism in terms of transporter translocation; induction by similar physiological stimuli and signalling components (Coort et al., 2007). This study using dipyridamole to translocate selectively CD36 to the sarcolemma has proposed that the CD36 and GLUT4 are either stored in distinct intracellular compartments or stored in the same compartment but their translocation induced by different signalling mechanisms (Coort et al., 2007). Dipyridamole induced FAT/CD36 translocation to the sarcolemma but had no effect on the subcellular distribution of GLUT4.

Furthermore, the study reported that the contraction-induced AMPK-mediated signal branches off into separate mobilization of GLUT4 and of FAT/CD36, and that dipyridamole activates a yet unidentified target in the FAT/CD36 mobilizing branch. There may be a sorting mechanism in place to selectively excise either one of the transporter containing transport vesicles from the common storage pool (Luiken et al., 2004). However, further work is required to fully elucidate the underlining mechanisms.

5.2 Aims and Objectives

The aim of this study was to:

- a) Examine the alterations in expression of markers of hypertrophy- atrial natriuretic factor (ANF), sarcoendoplasmic reticulum ATPase isoform 2a (SERCA2a) and its regulatory protein phospholamban (PLB).
- b) Investigate potential mechanisms underlying insulin resistance in uraemia by investigating the myocardial expression of the key metabolic transporters GLUT1, GLUT4 and FAT/CD36.

In addition, the expression of Na⁺K⁺ATPase isoform α_1 , a marker of myocardial membrane fractions, was examined over the course of uraemia development.

5.3 Methods

Materials and methods used for protein expression analysis are outlined in section 2.9 and 2.10. Optical density of the bands was determined semi-quantitatively and compared.

5.4 Results

Development of LVH from 3 to 9 nine week uraemia was characterized by a progressive increase in ANF expression, with higher expression at 6 week and 9 week uraemia versus respective control tissue (OD 6 wk. 0.12 ± 0.01 ; 9wk. 0.2 ± 0.001 vs. control 0.05 ± 0.02 ; Fig. 5.3).

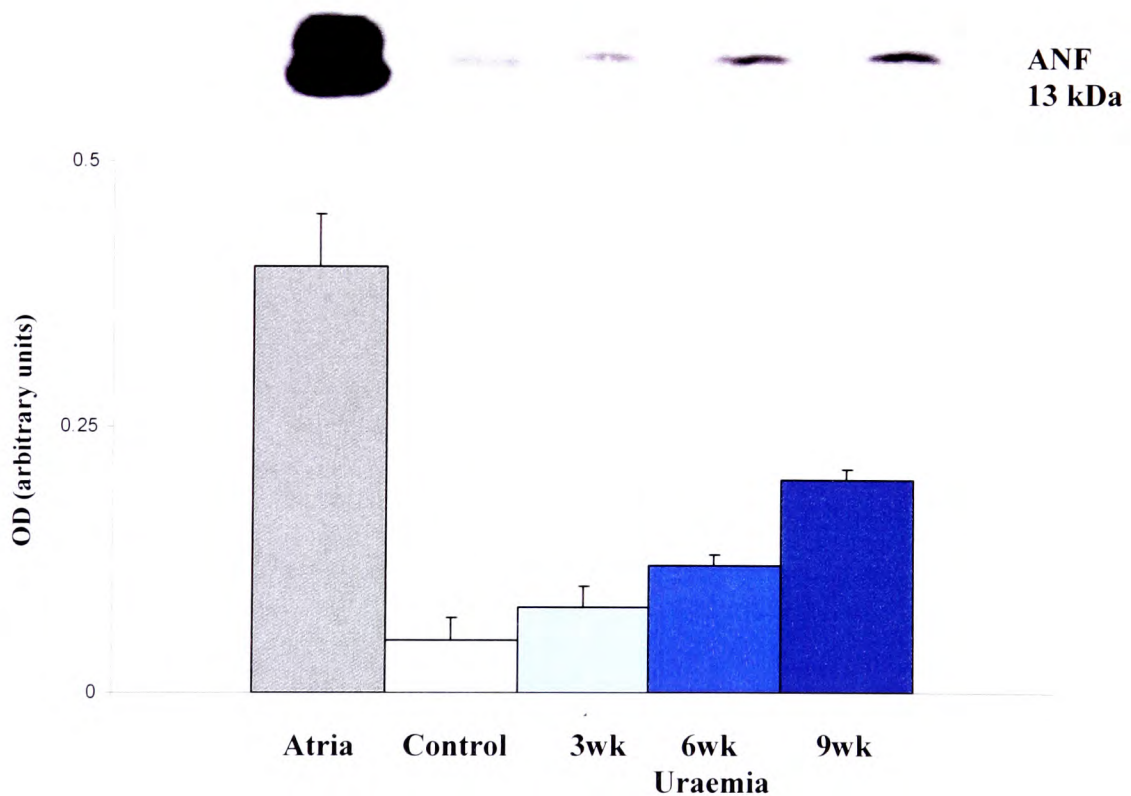


Figure 5.3 The Effect of Uraemia Development on LV ANF Expression

Data are presented as mean \pm S.E.M.

Atria (positive control) n=2; control n=11; 3wk uraemia n=5; 6 wk uraemia n=4;

9 wk uraemia n=2

GLUT1 expression was moderately increased at 3 weeks (uraemic 0.079 ± 0.01 vs. control 0.055 ± 0.01) and 9 weeks post surgery (uraemic 0.09 ± 0.01 vs. control 0.07 ± 0.01) (*Fig. 5.4 A*).

At 3 and 9 weeks, GLUT4 content remained unaltered versus control; however there was a trend for decreased GLUT4 expression at 9 weeks versus control (0.6 ± 0.01 vs. 0.5 ± 0.01 ; *Fig. 5.4B*) and versus 6 week uraemic tissue (0.54 ± 0.01 vs. 0.70 ± 0.01). At 6 weeks, GLUT4 expression in uraemic hearts was significantly increased versus control (0.7 ± 0.01 vs. 0.5 ± 0.01 ; *Fig. 5.4B*).

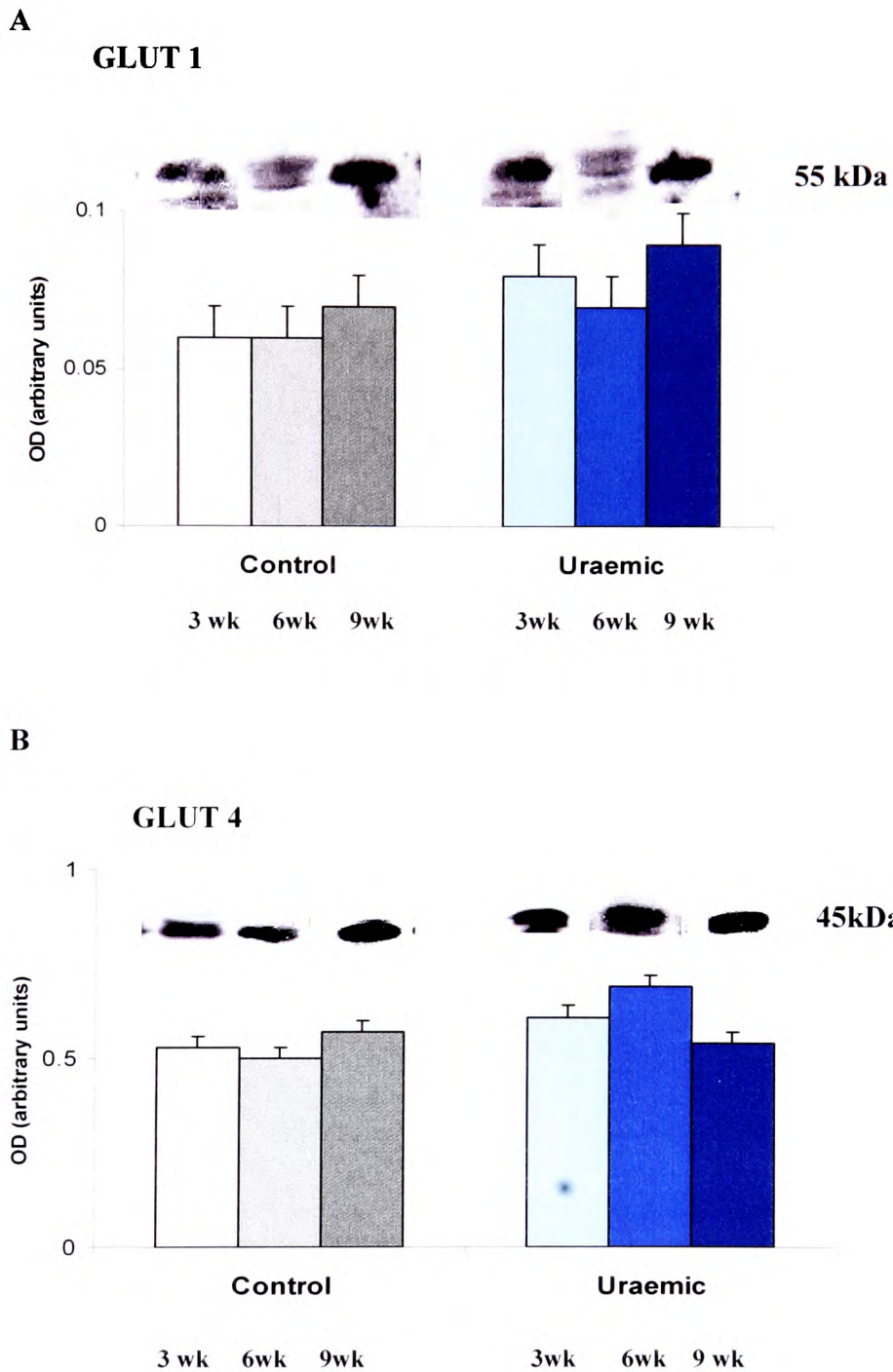


Figure 5.4 Glucose Transporters Expression in Uraemia

Data are presented as mean \pm S.E.M.

A) GLUT1 expression 3wk n=5; 6wk n=5; 9wk n=2

B) GLUT4 expression 3wk n=5; 6wk n=8; 9wk n=2

CD36 expression was elevated with the onset of uraemia but normalised by 9 weeks, consistent with the development of compensated hypertrophy (*Fig. 5.5*).

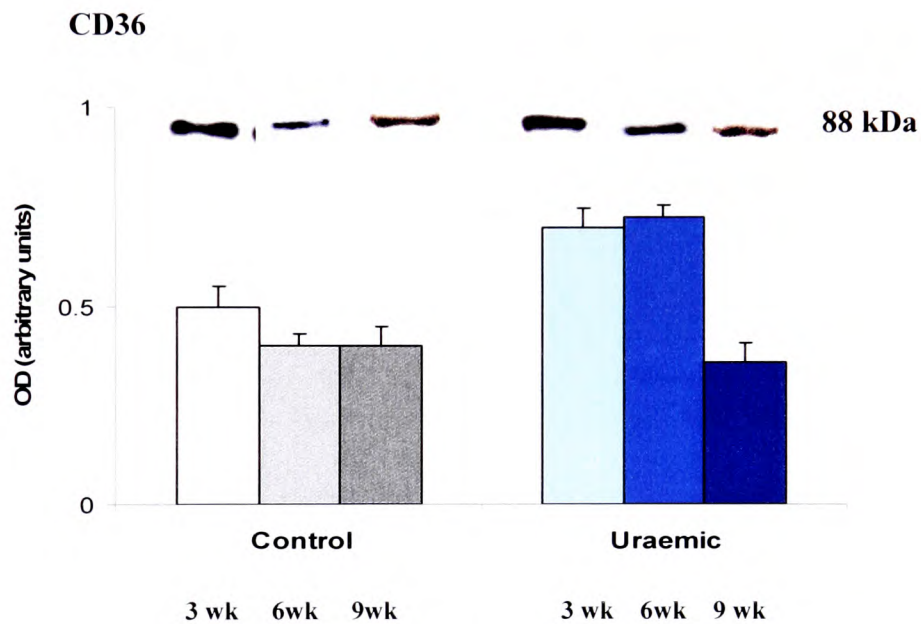


Figure 5.5 CD36 Expression in Uraemia

Data are presented as mean \pm S.E.M.

3wk n=4; 6wk n=4; 9wk n=2

5.4.1 Contractile Function Regulatory Proteins

The expression levels of calcium handling proteins: sarcoendoplasmic reticulum ATPase (SERCA2a) and phospholamban (PLB) were unchanged at any stages of uraemia (*Fig. 5.6 A, B*).

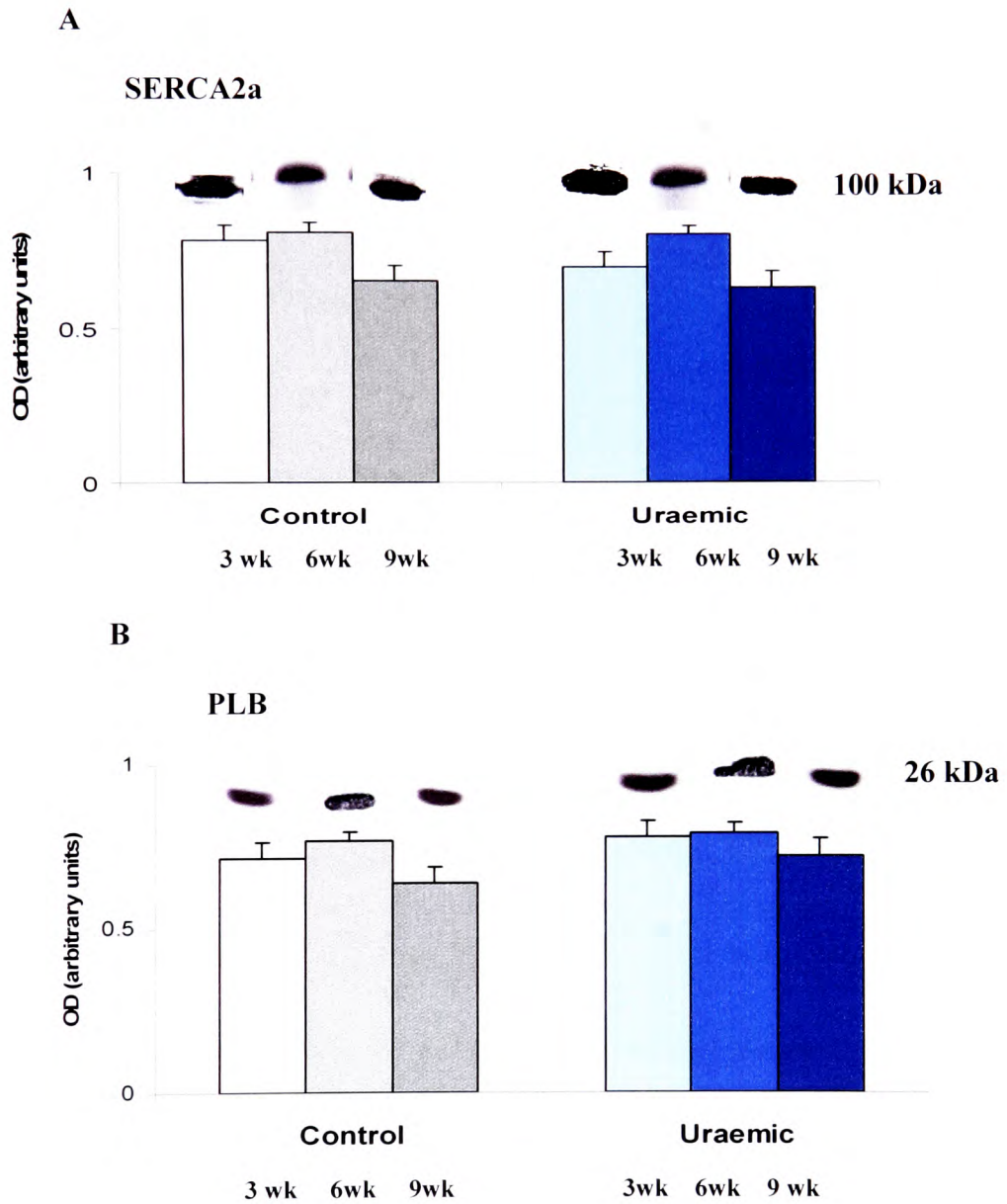


Figure 5.6 Ca^{2+} Handling Protein Expression in Uraemia

Data are presented as mean \pm S.E.M.

A);B) 3wk n=4; 6wk n=2; 9wk n=2

$\alpha_1\text{Na}^+ \text{K}^+\text{ATPase}$ expression was greatest at 6 week uraemia (uraemic 0.50 ± 0.02 vs. control 0.25 ± 0.02) with the level of protein declining with the progression of uraemia (Fig. 5.7).

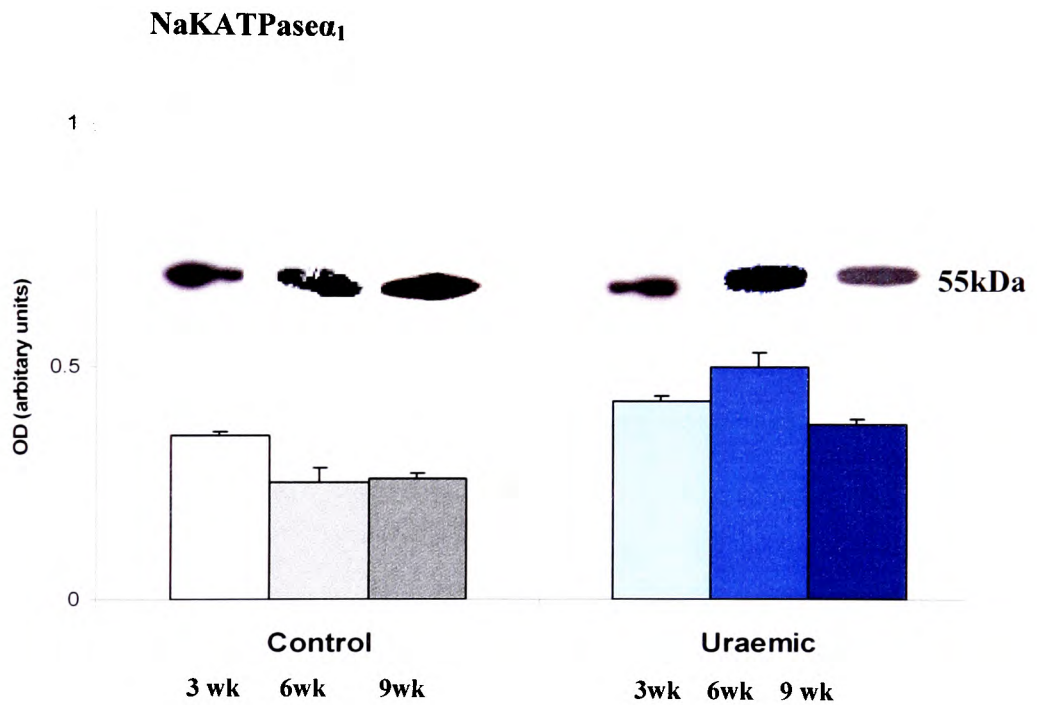


Figure 5.7 $\alpha_1\text{Na}^+ \text{K}^+\text{ATPase}$ Expression in Uraemia

Data are presented as mean \pm S.E.M.

3wk n=2; 6wk n=4; 9wk n=2

5.4.2 Subcellular Membrane Fractionation

Successful membrane fractionation is demonstrated by sarcolemma membrane highly enriched $\alpha_1\text{Na}^+\text{K}^+\text{ATPase}$ protein expression (*Fig. 5.8*). Total membrane yield was similar in both uraemic and control hearts at 6 weeks of uraemia (total membrane $0.24\pm 0.01\text{g}$ vs. $0.27\pm 0.019\text{g}$ $n=7$).

Under basal conditions, GLUT4 was primarily located in the intracellular membrane compartments versus sarcolemma in both groups (*Fig. 5.8*) with approximately 70 fold higher levels in intracellular membranes than sarcolemma under basal conditions (OD 0.64 ± 0.03 vs. 0.0089 ± 0.002). GLUT4 OD measurements in the total membrane fraction were 30% higher in uraemic compared to control myocardium and 20% higher in intracellular fractions (*Fig. 5.8*). GLUT4 content of sarcolemma was reduced by 36% in 6 wk uraemia.

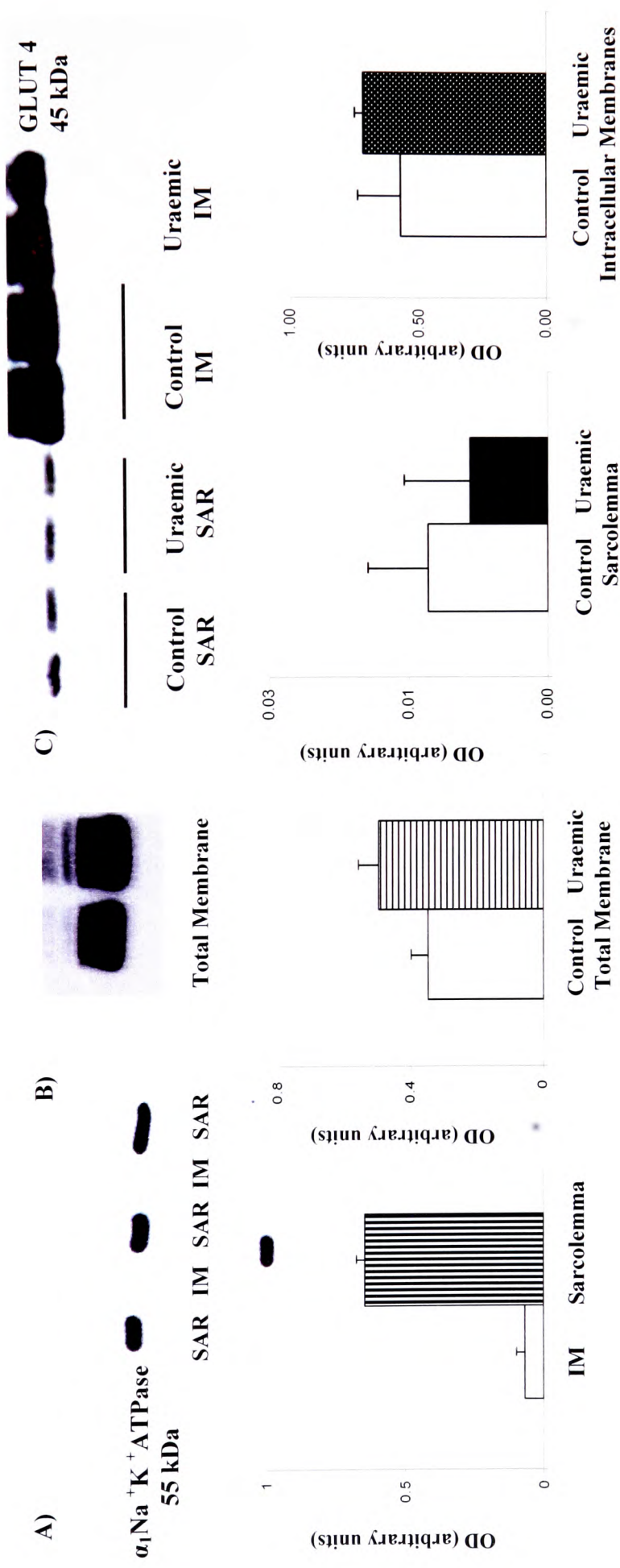


Figure 5.8 LV Membrane Fraction Analysis in 6week Uraemia

Data are presented as mean \pm S.E.M. **A)** Characterisation of membrane fractions via $\alpha_1\text{Na}^+\text{K}^+\text{ATPase}$ n=3; **B)** Total membrane GLUT4 expression n=4; **C)** Subcellular GLUT 4 distribution n=4

5.5 Discussion

ANF Expression in uraemic LV tissue gives a clear indication of the development of the left ventricular hypertrophy. ANF expression increases over the time course of uraemia and provides evidence of the re-expression of foetal metabolic phenotype (Rockman et al., 1994, Baxter, 2004). This is consistent with observations in other experimental models of LV hypertrophy and uraemia (Zoccali et al., 2001, Rosenblatt-Velin et al., 2004, Mak et al., 2004). The decline in haemodynamic homeostasis in the uraemic animal, manifested as hypertension (*Table 3.2*), will cause an increase in chamber stretch and trigger immediate re-expression of ANF in ventricles (Volpe et al., 1991). This may explain the increase of ANF at 9 weeks uraemia. These observations suggest that the severity of LVH progresses with renal function deterioration, and are in keeping with clinical observations (Levin and Foley, 2000). Consistent with the re-expression of ANF are the morphological indices of hypertrophy presented in *Table 3.3* and the increase in cardiomyocyte width in uraemia (*Table 3.4*).

Upregulation of ANF expression can also be interpreted as a protective mechanism against ventricular overload. *In vitro* studies have shown that the increase in ANF expression in LVH as it prevents development of decompensated cardiomyocyte hypertrophy (Richards, 1996, Baxter, 2004).

Disruption of the ANF gene expression caused significant cardiac hypertrophy in mice even with modest hypertension. In addition, transgenic mice overexpressing ANP had lower heart weights (Horio et al., 2000). Therefore the upregulation of ANF expression in LVH in uraemia may be aiding the maintenance of compensated hypertrophy, as no evidence of the heart failure is seen at any examined stage despite progressive uraemia development.

5.5.1 Metabolic Protein Expression

Myocardial GLUT1 expression is not significantly affected by uraemia. This might imply that the basal glucose uptake is not affected. Consistent with this interpretation, Allard et al. (1994) showed in the hypertrophied heart in response to high workload, there was an inability to enhance basal glucose uptake sufficiently to increase glucose utilization. In addition, studies in rat hepatocytes have shown that metabolic stress through hypoxia or inhibition of oxidative phosphorylation does not alter total membrane content of GLUT1, but increases the number of functionally active GLUT1 transporters. This would suggest that the mechanism of unmasking of the previously inactive transport sites by increased energy demand (Liao et al., 2002).

Modulation of GLUT4 is potentially a primary candidate in the development of myocardial insulin resistance. This has been confirmed in studies using GLUT4 knockout mice (Zisman et al., 2000).

A decrease in myocardial GLUT4 expression has been observed both in GLUT4 K/O mice and in aged SHR animals, together with a reduced response to insulin stimulation (Paternostro et al., 1995b, Paternostro et al., 1996, Garvey et al., 1998). In the uraemic heart, GLUT4 expression at 6 week left ventricular tissue was increased and this was further confirmed by the enhanced GLUT4 protein expression in total membrane fraction. Subcellular fractionation of the left ventricle (*Fig. 5.8*) however showed that there was little difference in GLUT4 distribution in uraemic versus control hearts. This implies that there was no alteration in translocation of the GLUT4 to the sarcolemma under basal conditions, in contrast to observations in a transgenic model of GLUT4 overexpression (Brozinick et al., 1996). GLUT1 expression is unaltered in both experimental groups which indicates normal insulin-independent glucose uptake. Studies presented in *Chapter 6* will further demonstrate that GLUT4 can be readily translocated in uraemia. Thus insulin resistance in uraemia does not appear to be a result of abnormal GLUT4 translocation.

A reduction in transporter activity may account for the impaired insulin-mediated myocardial glucose uptake in uraemia, as is observed in soleus muscle (Alkhateeb et al., 2007). The increase in myocardial GLUT4 expression in uraemia may suggest an adaptive response to a possible limitation in GLUT4 transport capacity and is typical of the reversion from the adult to the foetal metabolic phenotype, (*Chapter 1*; section 1.5). Increased myocardial GLUT4 expression in uraemia is more indicative of LVH rather than insulin resistance (Paternostro et al., 1995b, Paternostro et al., 1996, Garvey et al., 1998).

There is clear evidence of hypertension in uraemia suggestive of pressure overload and a consequence of activated programme of embryonic gene expression (Rockman et al., 1994, Baxter, 2004). However, increased total GLUT4 expression does not necessarily translate to functioning transporter activity. There appears to be link between maximal capacity and saturation of GLUT4 translocation mechanism, hence the extent of translocation may not occur in proportion to the increase in expression (Wallberg-Henriksson and Zierath, 2001). Post-translational protein modification may also modulate activity of GLUT4 rendering it less active (*Chapter 1*; section 1.6) including post-translational protein alteration such as increased *O*-linked *N*-acetylglucosamine modification (Buse, 2006). Myocardial proteins in uraemia are susceptible to post-translational protein modification as uraemia is associated with *in vivo* urea-derived cyanate carbamoylation (*Chapter 1*; section 1.6) (Kraus and Kraus, 1991, Kraus and Kraus, 1998, Kraus and Kraus, 2001). In support of this hypothesis are studies which have demonstrated that the incubation of normal rat tissue with the serum of uraemic patients resulted in an *in vitro* insulin resistant state and vice versa (Maloff et al., 1983, McCaleb et al., 1984a, McCaleb et al., 1984b). Therefore, there are compounds present in the uraemic serum that may be a cause of the insulin resistant state. This putative altered GLUT4 function by post-translational modifications needs further study.

By 9 weeks of uraemia, GLUT4 myocardial content is decreased compared to controls and 6 week uraemic tissue. This is in keeping with the onset of more severe insulin resistance, observed from increased HOMA-IR, severe glucose intolerance and hyperinsulinaemia in 9 week uraemia as shown in *Chapter 6*.

Expression of GLUT4 versus GLUT1 appears to be inversely related. The trend for an increase in GLUT4 expression is accompanied by a decrease in GLUT1 expression and *vice versa* (Fig. 5.4). In the setting of LV and insulin resistance, the capacity to increase GLUT1 expression could be cardioprotective. The increase in GLUT1 expression was demonstrated as a compensatory mechanism in the haemodynamically overloaded hearts (Liao et al., 2002). It had cardioprotective role in preventing heart failure development and improving the survival rate of mice with the chronic pressure overload (Liao et al., 2002). Therefore, inability to increase GLUT1 expression in a setting of metabolic remodelling will contribute to the overall poor energy provision in the uraemic cardiomyopathy.

Possible indication of the altered glucose uptake and metabolism, despite increased GLUT4 expression, is the elevation of CD36 expression in 3 week and 6 week uraemia. An increase in CD36 expression at the sarcolemma is a hallmark of insulin resistant state, as observed from obese Zucker rats (Coort et al., 2007). This study goes on to demonstrate systemic insulin resistance in uraemia further discussed in *Chapter 6*. Increased serum insulin has been shown to increase the rate of protein synthesis and decreases the rate of protein degradation (Jefferson et al., 1977). Hence, hyperinsulinaemic stimuli could further contribute to alterations in GLUT4 and CD36 expression. In addition, CD36 may also be subject to a post-translational protein modification as described previously. Supporting this argument is the lack of change both in the contribution of fatty acids to oxidative metabolism and myocardial triglyceride content, despite an increase in CD36 expression (*Chapter 4*).

5.5.2 Contractile Protein Expression

Results have demonstrated that the expression of SERCA2a and PLB were not altered in any stage of uraemia examined (*Fig. 5.6*). Consistent with the developing hypertrophy, there is a trend for a reduction in SERCA2a expression at 9 weeks versus 3 and 6 week uraemic tissue (*Fig. 5.6*). This observation is in keeping with work of de la Bastie et al. (1990) and Boateng et al. (1997, Boateng et al., 1998) who have shown that in a compensated cardiac hypertrophy, as observed in this study, the activity of CaATPase was reduced even though protein level was unchanged. The lack of statistically significant difference may in part be due to low n numbers and analysing greater number of samples may clarify this issue.

In the normal myocardium SERCA2a to PLB stoichiometry is 1:1 (Currie and Smith, 1999). However, studies in the failing human myocardium and in animal models of heart failure have shown altered PLB: SERCA2a ratio (Currie and Smith, 1999) consistent with the development of dysfunction. The trend for altered PLB: SERCA2a ratio in 3 week and 9 week uraemia (11% and 14% reduction) might suggest the onset of developing contractile dysfunction in uraemia. In addition, previous work from this laboratory has demonstrated significantly depressed Ca²⁺ transport by SERCA2a in the uraemic heart despite high Ca²⁺ serum levels, suggesting Ca²⁺ handling is impaired in uraemic heart (Snaith et al., 1990).

Development of insulin resistance, a hallmark of uraemia, has been linked to cardiomyocyte dysfunction involving depressed SERCA2a activity and impaired relaxation, however without alterations in protein expression of SERCA2a, NCX and PLB (Wold et al., 2005). Ongoing studies on 6 week uraemic ventricular tissue have shown increase in phospholamban (PLB) threonine¹⁷ phosphorylation (personal communication Dr D. Pavlovic and Prof M. Shattock, Raine's Institute, Kings College, London).

PLB threonine¹⁷ is phosphorylated by a Ca²⁺-calmodulin-dependent protein kinase and is associated with stimulation of cardiac SR Ca²⁺ uptake rates. Phosphorylation is triggered at low [Ca²⁺], resulting in an overall increase in the affinity of SERCA for calcium uptake (Simmernan et al., 1986, Koss and Kranias, 1996). Therefore increase in phosphorylation of PLB stimulates SERCA2a function. In a setting of an increase in PLB phosphorylation and reduced SERCA2a function, can be viewed as a compensatory mechanism attempting to maintain normal cardiac Ca²⁺ handling. Sucrose-fed-induced insulin resistance studies revealed that the subtle E-C coupling dysfunction in insulin resistance may arise as a result of only certain number of cardiomyocytes being affected by insulin resistance induced remodelling (Wold et al., 2005). Thus the heart may have the capacity to compensate for mild functional impairments in early stages of the insulin resistance development (Depre et al., 2000, Wold et al., 2005). McMahon et al. (2006) have demonstrated that uraemic cardiomyocytes differ from other heart failure experimental models, particularly as SR function was found to be compensated in hypertrophy.

This study demonstrated that, despite well established contractile dysfunction, SR function is not impaired in uraemia as highlighted by identical relaxation times of control and uraemic cells during inhibition of $\text{Na}^+/\text{Ca}^{2+}$ exchanger (McMahon et al., 2002, McMahon et al., 2006). Study by Kennedy et al. (2003) in rats subject to partial nephrectomy for 4 weeks has, in contrast to our work, shown decreased SERCA2a RNA and protein expression, alongside reduced $\text{Na}^+ \text{K}^+ \text{ATPase}$ activity in addition to an increase in NCX-1 exchanger as compensatory mechanism. All the changes underlined a potential diastolic dysfunction observed in uraemia. However in contrast to findings here, Kennedy's study indicated more severe hypertrophy with 77% significant increase in ANF expression in uraemic LV tissue versus control. In the present study, at 3 weeks there was 40% increase in ANF expression without statistical significance (*Fig. 5.3*). However, the extent of renal impairment was not detected in their study, making comparison of data difficult.

$\alpha_1\text{Na}^+\text{K}^+\text{ATPase}$ expression is significantly increased at 6 week uraemia versus control. However, with the progression of uraemia there is a trend for a decline in its expression. Analysis of the expression of phospholemman (FXYP1), a regulatory protein for $\alpha_1\text{Na}^+ \text{K}^+ \text{ATPase}$, in 6 week ventricular tissue has revealed significant alterations in FXYP1 phosphorylation patterns (Personal communication, Dr Pavlović, the Raine Institute, St Thomas's Hospital London). There was no change in total FXYP1 expression but serine phosphorylation was increased which is indicative of increased PKA activity, and resulting in increased $\alpha_1\text{Na}^+\text{K}^+\text{ATPase}$ activity (Pavlovic et al., 2007).

Furthermore, this study gave no evidence of the lack of $\alpha_1\text{Na}^+\text{K}^+\text{ATPase}$ inhibition but it has shown increased protein expression and by association increased activity. Circulating inhibitors of $\alpha_1\text{Na}^+\text{K}^+\text{ATPase}$ have been demonstrated in the uraemic serum (Stokes et al., 1990). Increased $\alpha_1\text{Na}^+\text{K}^+\text{ATPase}$ expression and activity may be adaptive responses overcoming the effect of circulating inhibitors, in the attempt to maintain normal transmembrane ionic gradients or possibly linked to LVH. The background of $\alpha_1\text{Na}^+\text{K}^+\text{ATPase}$ expression in uraemia is inconsistent. Greiber et al. (1994) have shown no difference in mRNA expression of α_1 and α_2 isoforms in their experimental model of chronic renal failure. Bonilla et al. (1991) reported decreases in both mRNA levels and pump activity in skeletal muscle and Kennedy et al. (2003) have demonstrated decreased mRNA expression in left ventricular tissue in 4 week uraemia. At present, there is no consensus on the changes in expression. Difference between our results and published data can be explained by a difference in the surgical procedure, possibly affecting the severity of the disease or stage at which uraemia is studied. The present data would suggest that $\alpha_1\text{Na}^+\text{K}^+\text{ATPase}$ expression is reduced with the progression of uraemia. Furthermore, $\alpha_1\text{Na}^+\text{K}^+\text{ATPase}$ protein expression in the remnant kidney from uraemic animal is reduced in keeping with the literature (data not shown). Further examination of the Ca^{2+} SERCA2a uptake and the expression of NCX-1 pump, as well as the assessment of the intracellular ion concentrations and currents may provide better insight into alteration of the contractile function at an early stage of experimental uraemia.

Possible cause of the altered protein expression observed in this study could be potentially caused by a) cardiomyocyte proliferation or fibroblast infiltration causing a decrease of the amount of protein per cell causing the value overestimation versus controls b) deposition of extracellular matrix (fibrosis), cardiomyocyte hypertrophy or apoptosis resulting in an increase in amount of protein per cell, further augmenting the difference in protein expression between two experimental models. Use of the cardiomyocyte reference protein (i.e. actin) or isolating cardiomyocytes prior to protein estimation might have addressed these concerns and produced more quantitative data.

5.6 Summary

Uraemia is characterized by alterations in the expression of proteins responsible for energy provision and utilisation. Uraemia is associated with the development of LVH and alterations in expression of myocardial insulin-mediated metabolic transporters, GLUT4 and CD36. Uraemia is also characterized by developing contractile dysfunction, with altered $\alpha_1\text{Na}^+\text{K}^+\text{ATPase}$ expression in addition to moderate alterations in SERCA2a: PLB ratio. These observations are characteristic of LV hypertrophy and consistent with the *ex-vivo* cardiac function alterations in uraemia (Chapter 4).

6. INSULIN RESISTANCE IN URAEMIA

6.1. Introduction

Insulin resistance and hyperinsulinaemia are present at the incipient stages of renal disease (Stefanovic et al., 2003, Kaysen, 2007). They precede development of diabetes and it is itself an independent predictor of cardiovascular mortality in uraemia (Shinohara et al., 2002, Chen et al., 2003, de Vinuesa et al., 2006). Alterations in carbohydrate metabolism in CKD patients were first reported in the early 20th century (Neubauer, 1910, Myers and Bailey, 1916, Frohlich, 2001). Presently, insulin resistance in uraemia has been defined in terms of hyperinsulinaemia, impaired glucose tolerance and hyperglycaemia (DeFronzo et al., 1981, Caro and Lanza-Jacoby, 1983, Kauffman and Caro, 1983).

The cellular mechanisms underlying insulin resistance in uraemia remain unclear. In the model of chronic uraemia in rats, binding of insulin to its receptor is unaltered in skeletal muscle, liver and adipocytes (DeFronzo et al., 1978, Caro and Lanza-Jacoby, 1983, Maloff et al., 1983, Jacobs et al., 1989). Furthermore, insulin receptor tyrosine kinase activity in adipocytes, muscle and liver appears unaltered (Cecchin et al., 1988). The consensus is that insulin resistance in uraemia arises as a post-insulin receptor defect, distal to the insulin receptor kinase.

The progression of LVH can also lead to the development of insulin resistance via impaired metabolic substrate transport (Weinberg, 1995, Paternostro et al., 1996, Paternostro et al., 1999b). Furthermore, the development of insulin resistance and the accompanying hyperinsulinaemia may potentially exacerbate cardiac hypertrophy by stimulating insulin-like growth factor receptors (Bornfeldt et al., 1992, Galvan et al., 2000). Insulin resistance can arise if there are alterations in any of the elements involved in insulin action - namely, insulin signalling, glucose transporter expression, or transporter translocation (Paternostro et al., 1995b, Garvey et al., 1998, Cefalu, 2001). Studies in adipose tissue from chronically uraemic rats have revealed a decrease in glucose transporter systems, insulin-stimulated glucose uptake and metabolism (Maloff et al., 1983, Jacobs et al., 1989). However, these observations cannot be extrapolated to the myocardium, and to date no study to date has investigated *in vivo* insulin sensitivity and the cellular basis of myocardial insulin resistance in uraemia.

6.2. Aims and Objectives

The aim of this study was to determine if the model of uraemia used exhibits systemic insulin resistance, and subsequently the cellular basis of myocardial insulin resistance using an integrated approach of *in vivo* and *in vitro* methods.

6.3. Materials and Methods

Oral glucose tolerance test was performed 6 and 9 weeks post surgery as described in section 2.4 (oral glucose tolerance test). Insulin resistance was assessed using the homeostasis model assessment (HOMA-IR). HOMA-IR was calculated using the following formula (Matthews et al., 1985):

$$HOMA-IR (mmol/L \times \mu U/ml) = \frac{\text{fasting glucose (mM)} \times \text{fasting insulin } (\mu U/ml)}{22.5}$$

Skeletal muscle (gastrocnemius) GLUT4 expression analysis was performed as outlined in section 2.9.

6.3.1 GLUT4 Expression and Translocation in Isolated

Cardiomyocytes

Cardiomyocytes were isolated 6 weeks post surgery as described in section 2.12. Isolated cells were incubated in 1 μ M insulin Krebs-Ringer-Henseleit buffer (4% BSA, pH 7.4), for 1 hour at 37°C and gassed with 100% O₂. Cells were fixed with 4% paraformaldehyde in PBS (w/v) for 20 min and permeabilized with 1% Triton X-100 in PBS (v/v) for 45 min.

Confocal microscopy studies were initially based on methods described by Martin et al., (2000, Yang et al., 2002) and conditions, namely antibody concentration, fluorescent probe concentration and confocal microscope settings, were optimized for the cardiomyocyte visualization. All subsequent antibody incubations and cell rinses were performed in PBS containing 0.1% BSA ($\geq 96\%$ fatty acid free). Cells were probed with $2\mu\text{g/ml}$ mouse monoclonal GLUT4 antibody and visualized with $4\mu\text{g/ml}$ secondary FITC-conjugated goat anti-mouse IgG antibody. Cardiomyocytes probed with the FITC-conjugated antibody were transferred on to glass bottom, microwell dishes with 0.17 mm thick coverslip. GLUT4 was visualized using a confocal microscope Nikon Eclipse TE 8000-E and Radiance laser scanning 2100 system with inverted x60 water immersion lens and Zeiss Lasersharp 2000 software.

Photomultiplier settings were maintained for all image acquisitions. In order to minimise photobleaching of the fluorescent probe, cells were randomly selected and identified using low illumination light microscopy followed by confocal image acquisition. Cells were excited at 543nm with green Helium-Neon (HeNe) laser light (Laser 91.1%; Gain 90.9; Offset 1.4, Iris 2.0). GLUT4 fluorescence was visualised using a 100% DET 2/3 dichroic mirror and HQ600/50 BLD emission filter. Fluorescence images of 1024×1024 pixels (pixel size/depth 16 bit/channel) were recorded, using a scan speed of 500 lines per second and Kalman collection filter ($n=3$ scans). Fluorescence was quantified in LaserPix software. Regions were drawn around individual cells and the fluorescence intensity recorded. Readings were corrected for background fluorescence, defined as fluorescence measured external to the cell, using the same area as for cell analysis.

6.4. Results

6.4.1. Oral Glucose Tolerance Test

6 weeks post-induction of uraemia, animals exhibited physiological fasting glucose concentration and hyperinsulinaemia. 90 min post glucose load, they were significantly hyperglycaemic and hyperinsulinaemic in comparison to controls (*Fig. 6.1A*). The glucose challenge also produced a significant increase in serum insulin in control animals at both 60 min and 90 min in comparison to the fasting levels. In contrast, uraemic animals were hyperinsulinaemic in the fasting state and reached peak concentration only at 120 min, without significant rise above the fasting insulin levels ($p < 0.06$ vs. fasting state *Fig. 6.1B*). The HOMA-IR was significantly elevated in uraemic animals vs. controls (1.27 ± 0.3 vs. 0.58 ± 0.1 $p < 0.05$; *Fig. 6.2*).

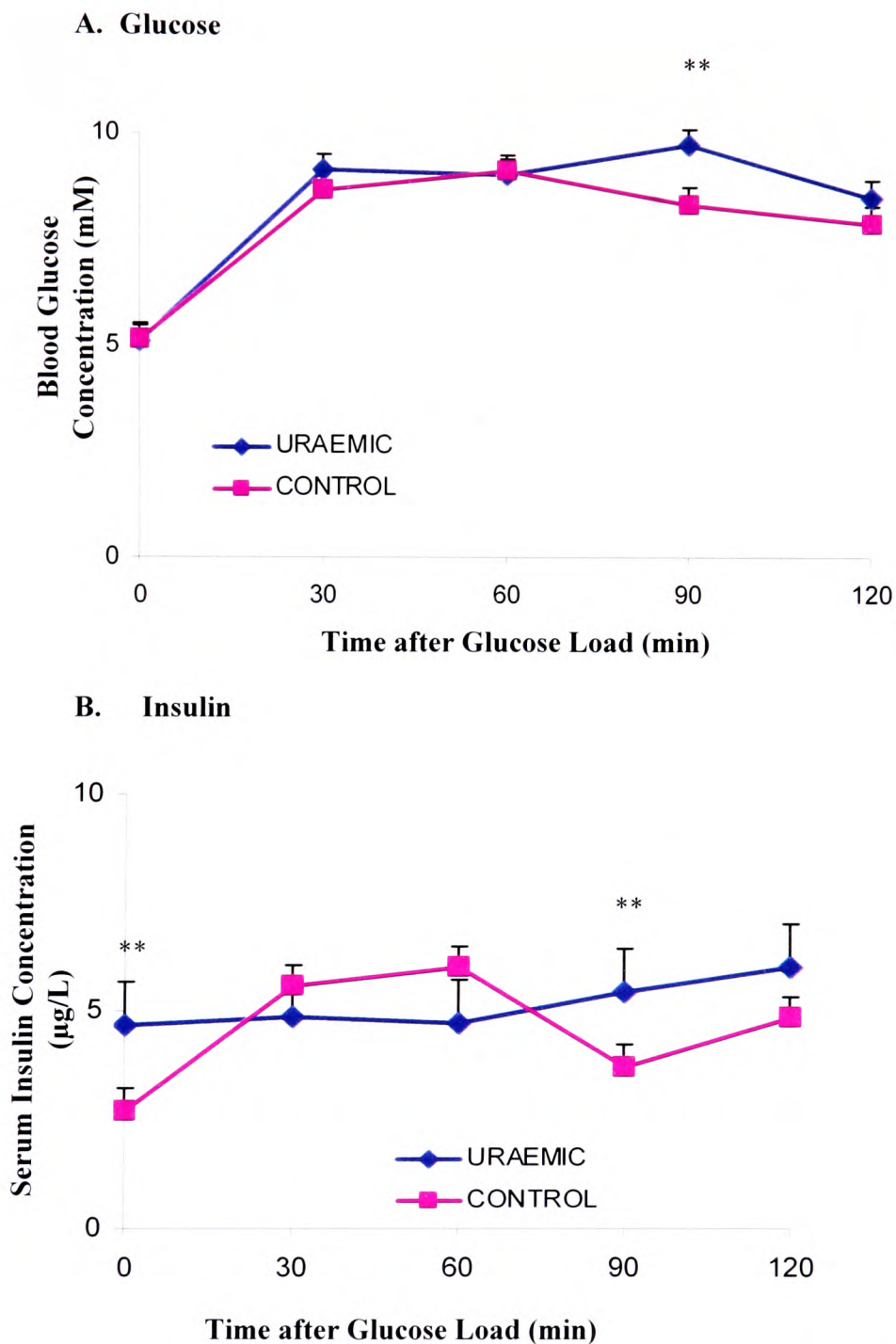


Figure 6.1 Glucose (A) & Insulin (B) Responses to an Oral Glucose Challenge in 6 Week Uraemia

Values are mean \pm S.E.M.

n=8; **p<0.05 vs. control

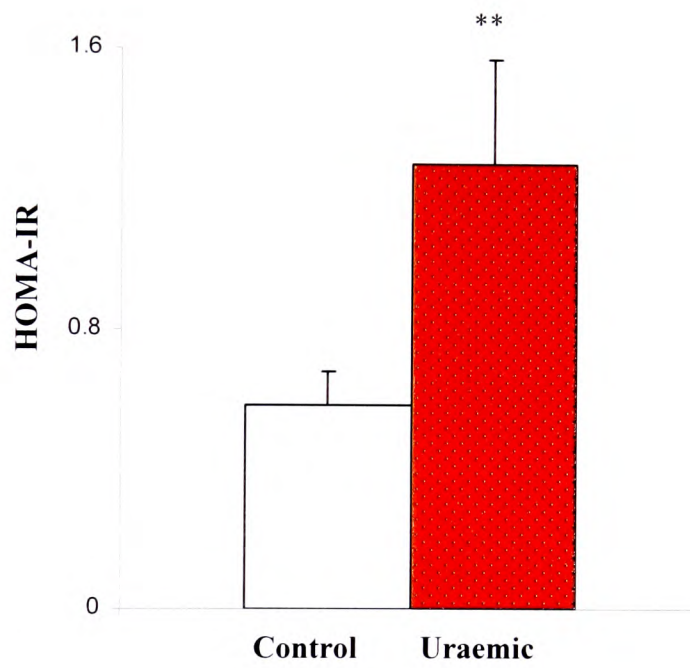


Figure 6.2 HOMA-IR Index for Control & 6 Week Uraemia

Values are mean \pm S.E.M.

n=8; **p<0.05 vs. control

By nine weeks, uraemia was characterized by fasting normoglycaemia and hyperinsulinaemia. Uraemic animals exhibited hyperglycaemia at 30, 60, and 120 min post glucose ingestion and hyperinsulinaemia up to 120 min (30,60 and 90 min) ($p < 0.05$ vs. control serum glucose and serum insulin, *Fig. 6.3*).

HOMA-IR was significantly higher in 9 wk uraemic animals versus controls (7.2 ± 4.0 vs. 1.87 ± 0.7 $p < 0.05$; *Fig. 6.4*) and increased versus 6 wk uraemia (72%).

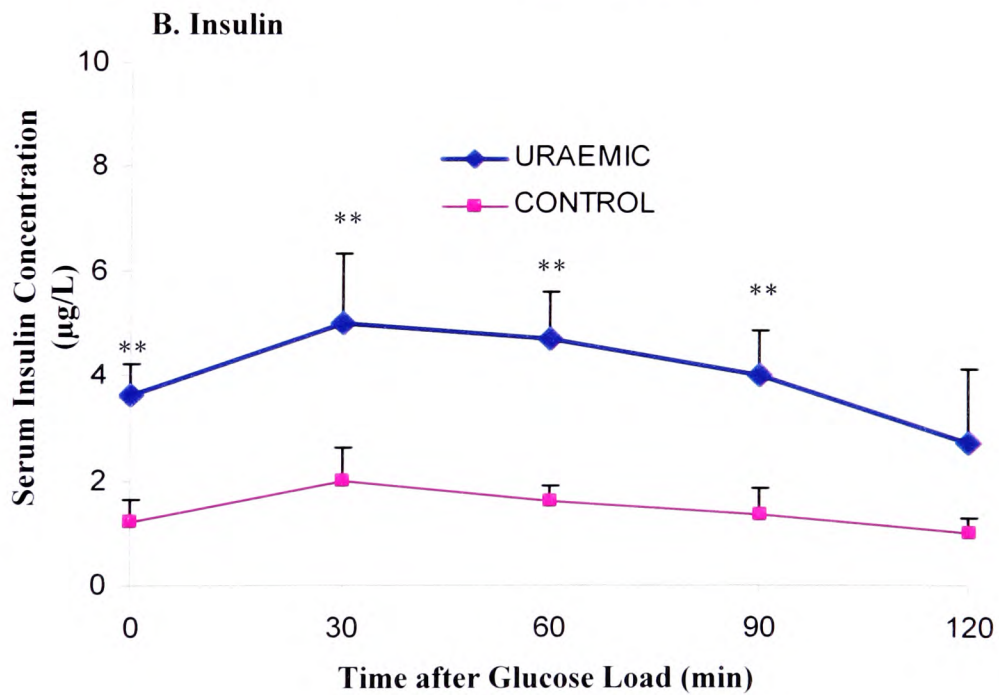
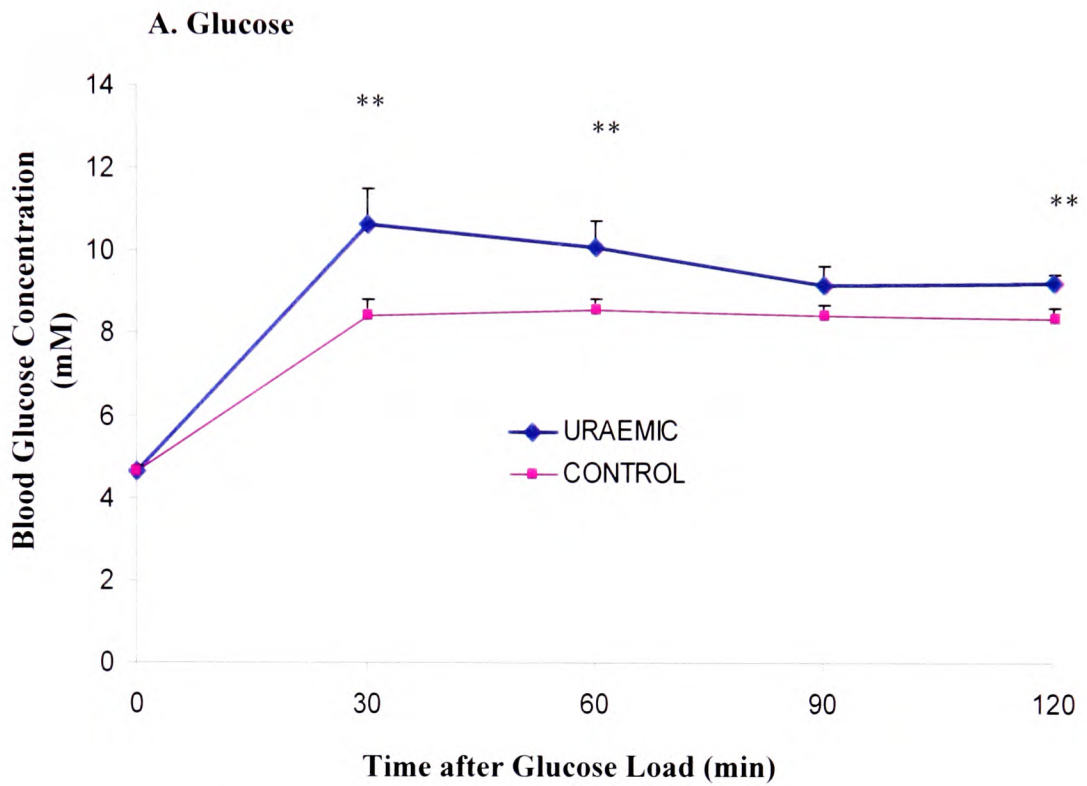


Figure 6. 3 Glucose (A) & Insulin (B) Responses to an Oral Glucose Challenge in 9 Week Uraemia

Values are mean \pm S.E.M; n=6; **p<0.05 vs. control

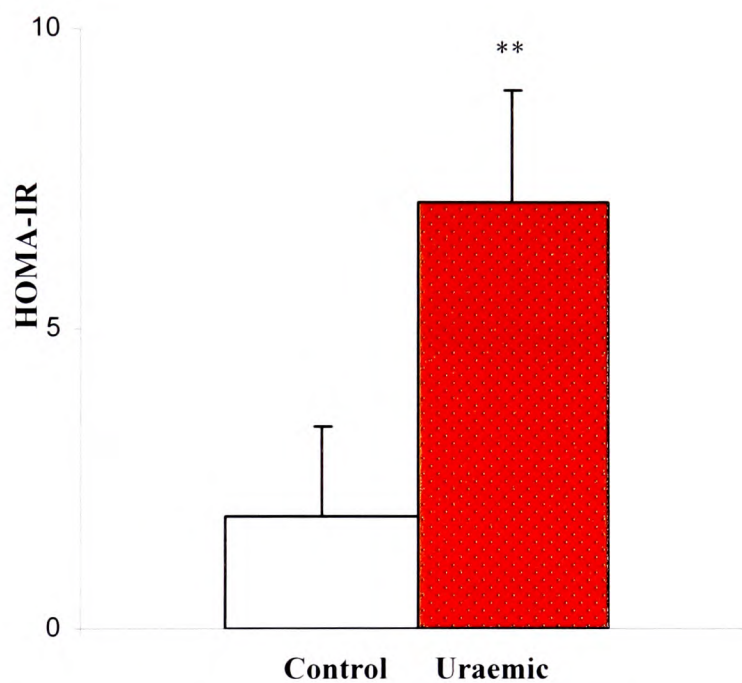


Figure 6.4 HOMA-IR Index for Control & 9 Week Uraemia

Values are mean \pm S.E.M.

n=6; **p<0.05 vs. control

A significant positive correlation was observed between the serum creatinine and serum insulin ($p < 0.02$, Fig. 6.5A) and serum creatinine and HOMA-IR ($p < 0.01$; Fig. 6.5B) indicating greater severity of renal impairment correlated with hyperinsulinaemia.

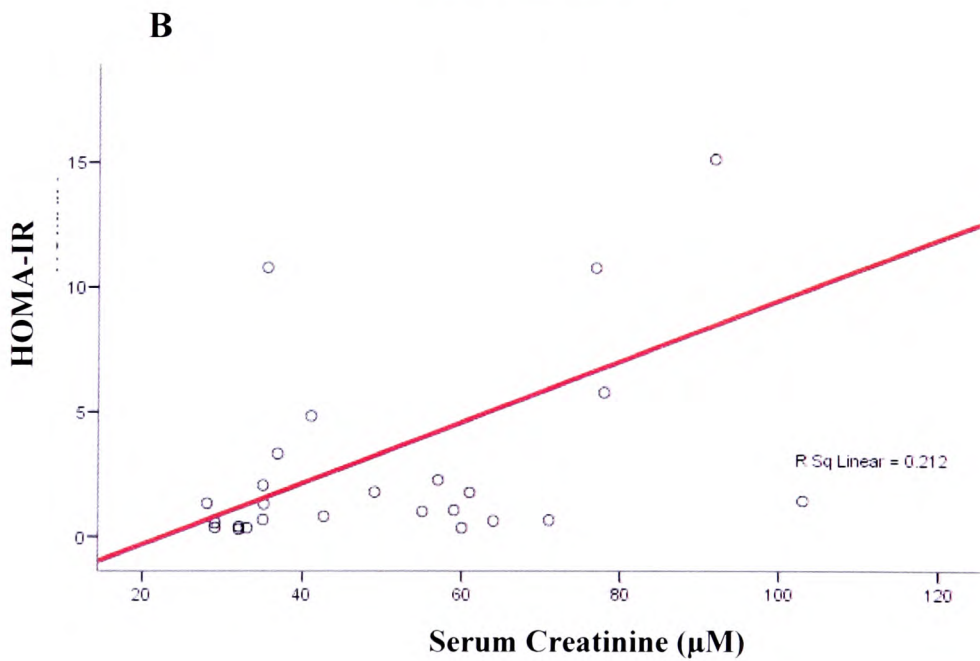
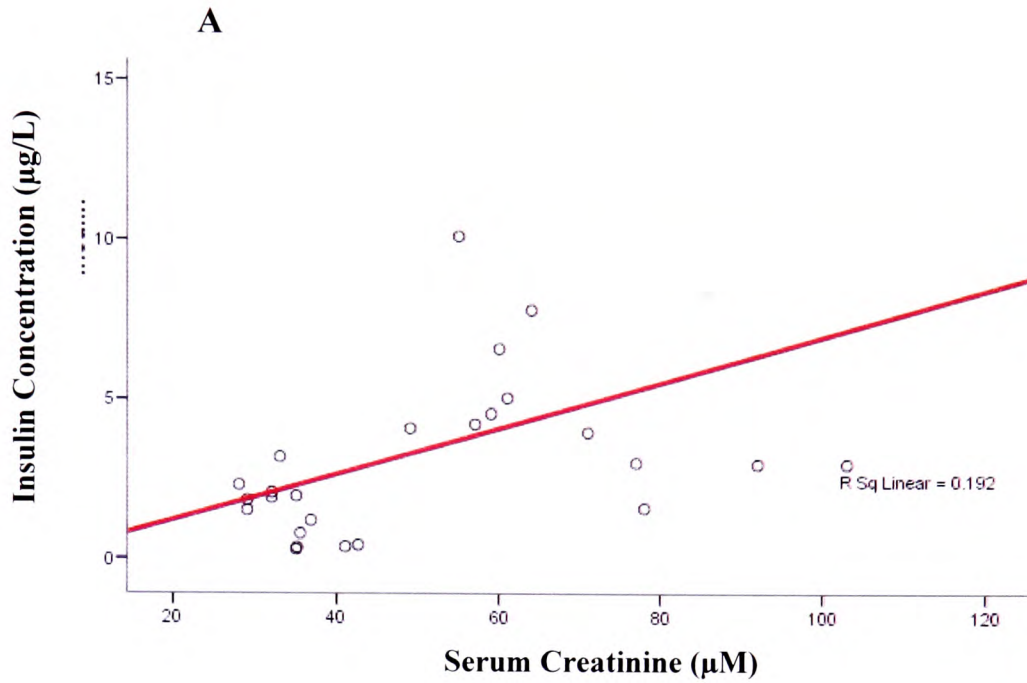


Figure 6.5 Correlation between Serum Creatinine &

A) Post-glucose Load Insulin Concentration B) HOMA-IR

A) Two tailed Pearson correlation coefficient $r=0.438$;
coefficient of determination $r^2= 0.192$; $p<0.05$; $n=26$

B) Two tailed Pearson correlation coefficient $r=0.461$;
coefficient of determination $r^2= 0.212$; $p<0.05$; $n=26$

6.4.2. Skeletal Muscle GLUT 4 Expression

GLUT4 expression in skeletal muscle at 6 weeks uraemia was markedly lower than in controls (OD 0.07 ± 0.02 vs. 0.17 ± 0.01 $p < 0.05$) For comparison, expression in SHR in which insulin resistance is found to be present, skeletal muscle was also reduced (OD SHR 0.0056) (Fig. 6.6).

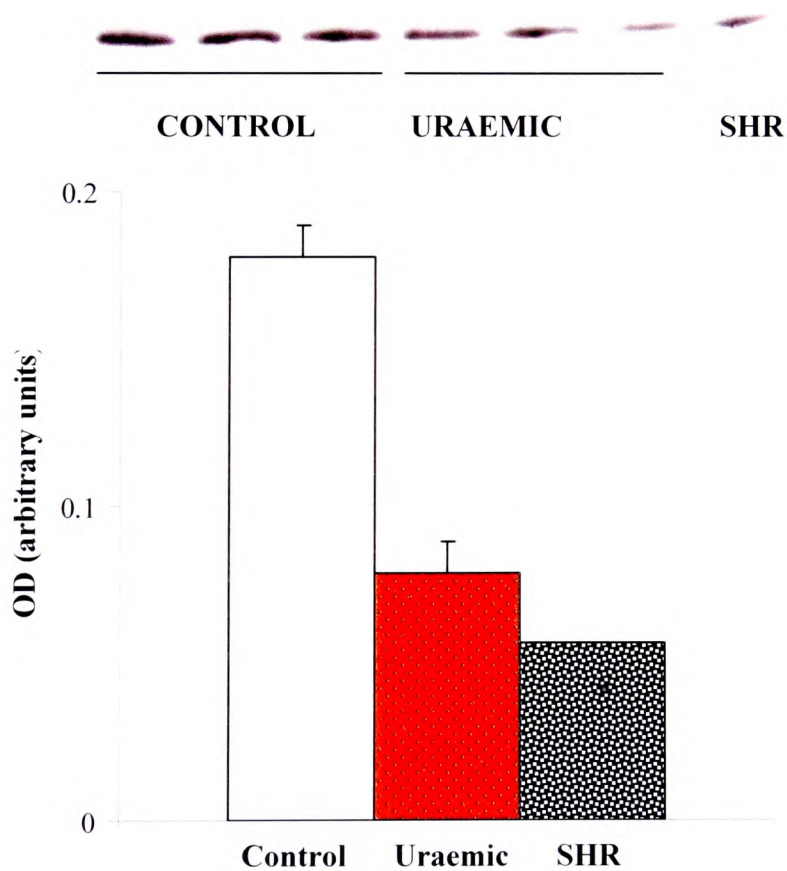


Figure 6.6 GLUT4 Expression in Skeletal Muscle (gastrocnemius)

6 week uraemia and 12 week SHR; Values are mean \pm S.E.M.

control & uraemic n=3; SHR n=1

6.4.3. GLUT4 Expression and Translocation in Isolated Cardiomyocytes

GLUT4 expression in cardiomyocytes in response to insulin stimulation is shown in figures 6.7 and 6.8. Incubation with insulin causes GLUT4 translocation to the cardiomyocyte surface as observed from the prominent GLUT4-specific fluorescence cell surface labelling (*Fig. 6.7 A, B*). In the absence of insulin, GLUT4 is located in the intracellular compartments (*Fig. 6.8 A, B*).

Cardiomyocytes isolated from uraemic animals expressed significantly higher GLUT4 in the presence and absence of insulin versus cells from control animals, as observed from the quantification of fluorescence corresponding to labelled GLUT4 ($p < 0.05$) (*Fig. 6.9*).

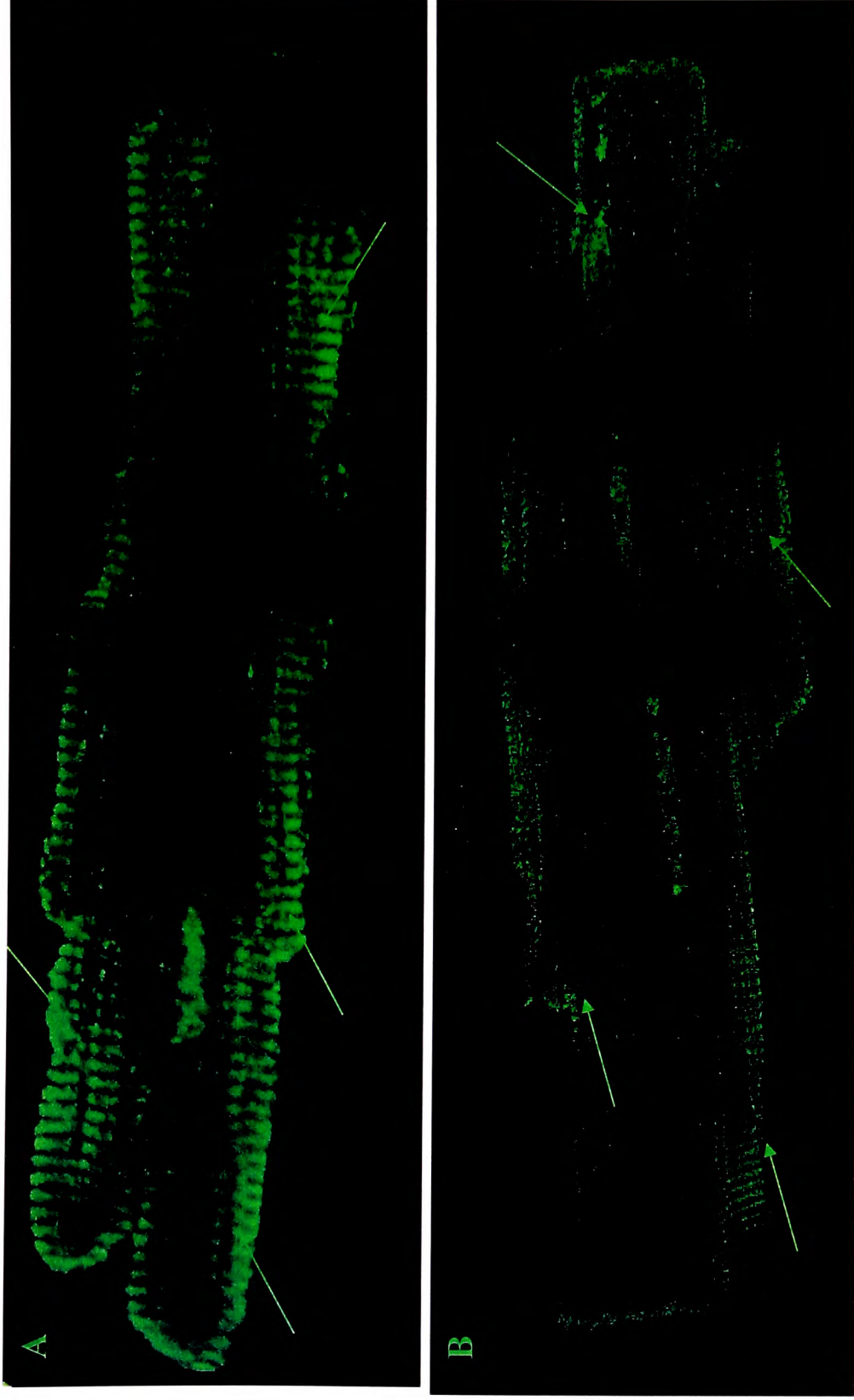


Figure 6.7 GLUT4 Immunofluorescence (arrows) in Isolated Cardiomyocytes

A) GLUT 4 Expression in uraemic cardiomyocyte + 1.0 μ M insulin B) GLUT 4 Expression in control cardiomyocytes + 1.0 μ M insulin

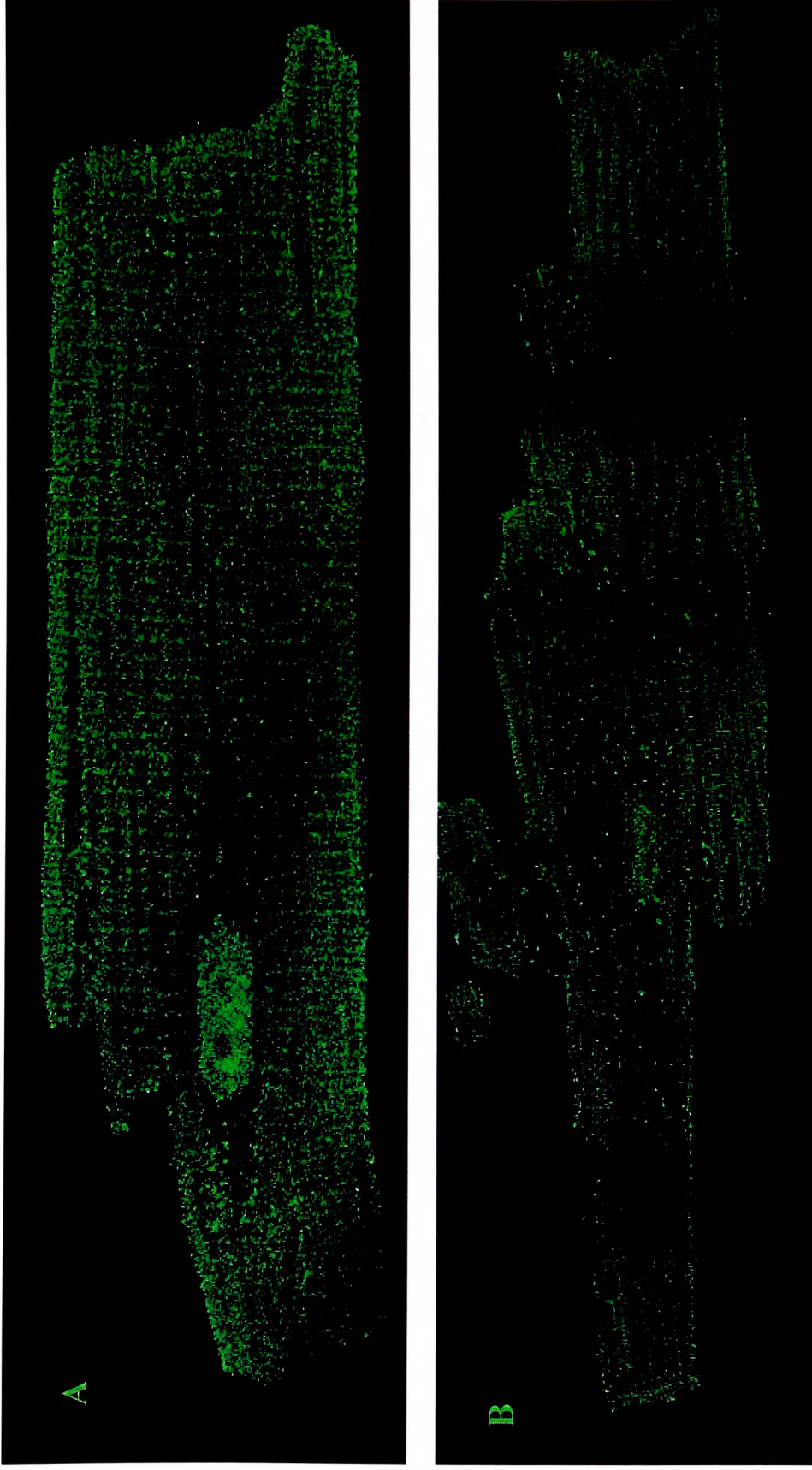


Figure 6.8 GLUT4 Immunofluorescence (arrows) in Isolated Cardiomyocytes

A) GLUT 4 Expression in uraemic cardiomyocytes without 1 μ M insulin; B) GLUT 4 Expression in control cardiomyocytes without 1 μ M insulin

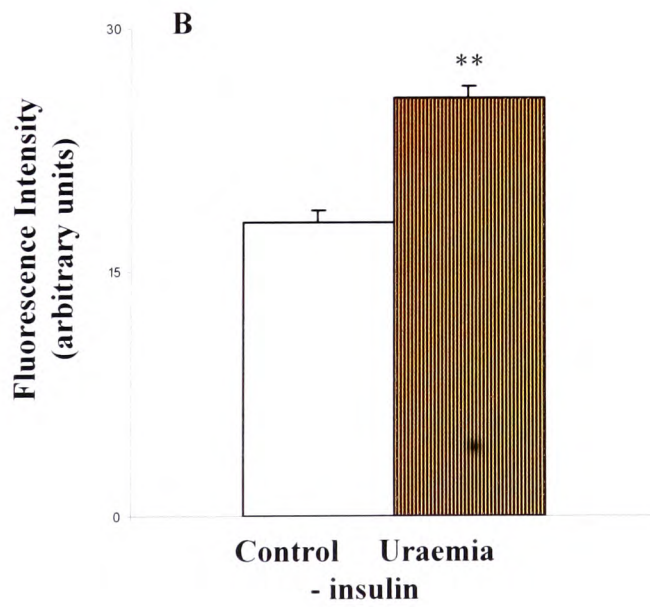
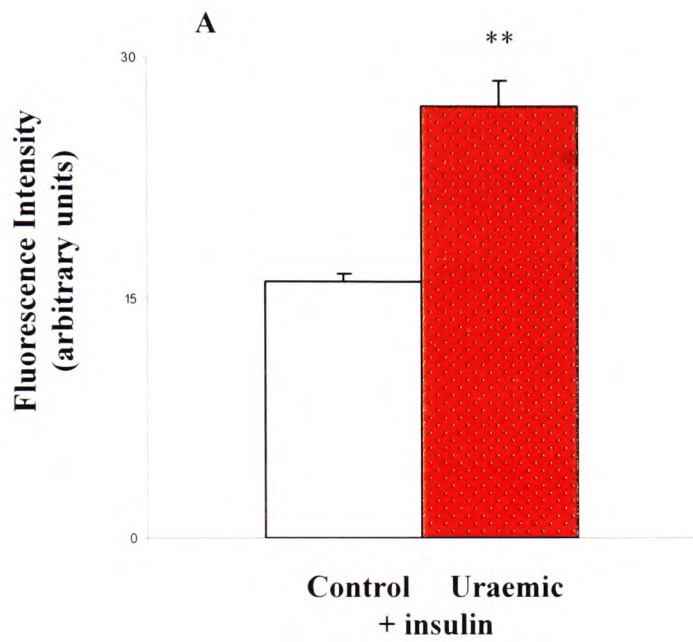


Figure 6.9 GLUT4 Immunofluorescence Intensity in Isolated Cardiomyocytes

Fluorescence intensity presented as mean + S.E.M;

n= 35 (+insulin); n=18 (-insulin);

**p<0.05 vs. control

6.5. Discussion

This study has demonstrated that following 6 and 9 week uraemia, there is insulin resistance *in situ*. These data also indicate that the deterioration in renal function is associated with progressive reduction in insulin sensitivity. Furthermore, it has shown that the mechanism of myocardial insulin resistance at this stage of uraemia is not due to decreased GLUT4 expression or impaired translocation.

6.5.1. Oral Glucose Tolerance

Uraemic animals are characterized by a marked hyperglycaemia 90 min following glucose loading (*Fig. 6.1*). The reduction in insulin sensitivity in uraemic versus control animals has been confirmed by impaired oral glucose tolerance tests and homeostasis model assessment (*Fig. 6.2*) (Matsuda and DeFronzo, 1999). The glucose intolerance and insulin resistance observed in uraemia are consistent with previous observations in experimental models of hypertrophy (Horton et al., 1968, Velliquette et al., 2002). Progression of uraemia shows a further insulin resistance and glucose intolerance (*Fig. 6.4*). There is a positive correlation between serum creatinine (a marker of renal function) and serum insulin and HOMA-IR (*Fig. 6.5*). This correlation implies that the decline in renal function may be associated with a progressive deterioration in insulin sensitivity and increasing hyperinsulinaemia. These findings highlight the detrimental effect of renal dysfunction deterioration on the development of insulin resistance.

Clinical studies have shown that a deterioration in systemic insulin sensitivity and renal dysfunction increases the risk from cardiovascular mortality (Ritz, 2003). It has been suggested that the presence of hyperinsulinaemia may further exert adverse effects on the vasculature as HOMA-IR is independently associated with carotid plaque formation, increased carotid media thickness and subsequently cardiovascular events (Shinohara et al., 2002, Hidvegi et al., 2003, Ishizaka et al., 2003, Yanase et al., 2004). The positive correlation between HOMA-IR and death from cardiac related causes in CKD patients was shown to be independent of age, C-reactive protein, body mass index, hypertension and dyslipidaemia (Shinohara et al., 2002).

Whether kidney dysfunction is a prime cause of hyperinsulinaemia in insulin resistance or vice versa is still the subject of controversy (Shen et al., 2005). Nevertheless, clinical and experimental studies have clearly indicated that renal failure leads to a reduction in systemic insulin removal because the kidneys play a major role in the clearance and degradation of circulating insulin (Rubenstein et al., 1975, Cianciaruso et al., 1987). Therefore the marked hyperinsulinaemia observed in the uraemic group here may have resulted from the combination of impaired renal function and LVH. Fliser *et al.* (1998) in a clinical study at different stages of renal failure found that insulin insensitivity and hyperinsulinaemia were present from the early phase of renal dysfunction and in all CKD patients irrespective of the primary aetiology of the renal failure. The evidence of insulin resistance in the present experimental model of uraemia is consistent with these clinical observations (Becker et al., 2005). Therefore, the model used in this study provides a good model representative of clinical CKD.

6.5.2. Cardiomyocyte GLUT4 expression

To investigate the potential mechanism underlying insulin resistance, myocardial GLUT4 expression was investigated. Total cellular GLUT4 content of the LV was significantly increased, irrespective of the presence of insulin in the media (*Fig. 6.7; 6.8*). This was further confirmed by increased GLUT4 protein expression in left ventricular tissue and total membrane fraction in uraemia (*Chapter 5*). Subcellular fractionation of the left ventricle showed that, in spite of increases in total GLUT4 content, there was no significant difference in the distribution of GLUT4 in uraemic versus control groups (*Chapter 5*). These data indicate that the GLUT4 translocation was unaffected. In contrast, transgenic model of GLUT4 overexpression, characterized by 14 fold increase in GLUT4 levels, is characterized by higher plasma-membrane GLUT4 protein concentration in the basal state and diminished GLUT4 translocation compared to controls (Brozinick et al., 1996). GLUT1 expression was unaltered supporting these findings indicating normal insulin-independent glucose uptake (*Chapter 5*). Observations using confocal microscopy have shown that GLUT4 can be readily translocated with no impairment in transporter recruitment. This suggests that the insulin resistance in uraemia is not a result of abnormal GLUT4 translocation. A reduction in transporter activity may account for the greater impairment in myocardial insulin-mediated glucose uptake in uraemia rather than dysfunctional GLUT 4 translocation, as is observed in soleus and triceps surae muscles (Brozinick et al., 1996, Alkhateeb et al., 2007).

The increase in GLUT4 expression is also a reflection of the re-expression of the foetal metabolic phenotype, consistent with LVH. There is clear evidence of hypertension in uraemia indicative of pressure overload and a consequence of activated programme of embryonic gene expression (Rockman et al., 1994, Baxter, 2004). The increased myocardial GLUT4 expression observed in uraemia may be indicative of LVH remodelling rather than insulin resistance (Paternostro et al., 1995b, Paternostro et al., 1996, Garvey et al., 1998). As mentioned previously, LVH is a hallmark of CKD and its severity progresses with renal function deterioration (Levin et al., 1999). Thus the experimental model features described in his thesis, in addition to the changes observed at the cellular protein level (elevated LV ANF expression), highlight an increase in LV wall thickness characteristic of pressure overload LVH development.

However, increased total GLUT4 protein expression observed in the ventricular cardiomyocytes does not necessarily translate into functioning transporter activity as discussed in chapter 5. Findings in this chapter have presented evidence for systemic insulin resistance in uraemia as demonstrated by HOMA-IR and supported by the reduction in skeletal muscle GLUT4 expression as previously shown in CKD patients (*Fig. 6.2; 6.4*) (DeFronzo et al., 1981, DeFronzo et al., 1985). The hyperinsulinaemia demonstrated *in vitro* (*Chapter 3*) and *in vivo* may result from a reduction in insulin sensitivity in combination with reduced renal insulin clearance and degradation (Kitabachi and Stentz, 1972, Rubenstein et al., 1975).

Increased serum insulin has been shown to increase the rate of protein synthesis and decreases the rate of protein degradation (Jefferson et al., 1977). Furthermore, hyperinsulinaemic stimuli could further contribute to alterations in GLUT4 expression.

Initial attempt to visualize GLUT4 transport using confocal microscopy was performed on viable cardiomyocytes. The aim was to assess *in situ* the dynamic process of GLUT4 translocation in response to insulin stimulus. However the outcome was labelling of GLUT4 of lysed cells with a complete absence of data from the viable cardiomyocytes. Therefore, the method was optimized and cell fixation and permeabilization introduced. Fixation buffer was utilised to cross link, stabilize, and 'fix' the cell membrane, while the permeabilization buffer was used to permeabilize the cell membrane in order for the antibody label to enter the cell effectively (Coons, 1958). Permeabilizing cell membranes allowed the primary antibody access to the target epitope on intracellular GLUT4 and in turn binding of the secondary –FITC conjugated antibody. Specificity of the secondary FITC-conjugated antibody was examined by incubating fixed and permeabilized cells in the absence of the primary antibody. No signal was detected thus eliminating the possibility of non-specific binding of the fluorescent label.

6.6. Summary

This study has demonstrated the presence of systemic insulin resistance and glucose intolerance despite an increase in myocardial GLUT4 expression and intact translocation. The deterioration of renal dysfunction is associated with worsening of the insulin resistant state and glucose intolerance.

These findings suggest that the possible cellular mechanism of myocardial insulin resistance in uraemia is post-translational protein modification resulting in altered transporter functionality. The possibility of altered GLUT4 function by post-translational modifications needs further study.

7. DISCUSSION

Cardiovascular disease is a major cause of mortality in uraemic patients. Death from cardiac causes is a more common endpoint of uraemia than progression to dialysis (Shen et al., 2005). This study successfully generated experimental model of chronic kidney disease (uraemia), characterized by significant renal insufficiency and altered haemodynamic homeostasis from the onset. Progression of uraemia exacerbated the pressure and volume overload observed early in pathology, in addition to the development of compensated LV hypertrophy, hyperinsulinaemia and more profound renal impairment. These characteristics are comparable to the *in vivo* uraemic patients clinical studies data (Shen et al., 2005, Lastra et al., 2006), (Mak and DeFronzo, 1992, Amann et al., 2006).

The present study has demonstrated significant insulin resistance in experimental uraemia, correlating positively with the progression of kidney dysfunction. This key finding is highlighted by impaired glucose tolerance, reduced HOMA-IR, hyperinsulinaemia and altered GLUT4 expression. It has revealed that the mechanism of myocardial insulin resistance in uraemia does not arise from reduced GLUT4 expression and impaired translocation, as described in other models of hypertrophy and insulin resistance (Paternostro et al., 1999a). Despite an increase in ventricular GLUT4 protein levels, traditionally associated with foetal metabolic phenotype than insulin resistance, there is a lack of corresponding increased glucose contribution to the TCA cycle. Furthermore, skeletal muscle GLUT4 content is markedly reduced. Dissociation between skeletal muscle and myocardial GLUT4 content was previously observed in a transgenic mice overexpressing the human GLUT4 (Belke et al., 2001).

These findings are unparalleled as this is the first study to examine the cellular mechanism of myocardial insulin resistance in uraemia. Altered carbohydrate metabolism in terms of systemic disposal and release has been well documented in uraemia (Horl et al., 1980, Mak and DeFronzo, 1992), in addition to recent clinical study findings of reduced myocardial fatty acid utilization (Nishimura et al., 2006). This would, in theory, render uraemic heart non-compliant with the central dogma of myocardial metabolism postulated by Randel (1964), further isolating uraemic cardiomyopathy as a specific pathology. Early stages of uraemia examined in this study appear to be characterized by a degree of metabolic flexibility, without evidence of poor energy provision or pathologic metabolite accumulation (i.e. tryglicerides). In this study, uraemic myocardial metabolic profile suggest overall shift in substrate preference from fatty acids to carbohydrates (mainly lactate), accompanied by poor functional parameters. Hearts from uraemic animals are also characterized by a blunted functional response to increased workload in agreement with a poor cardiac contractility in *db/db* diabetic mice (Belke et al., 2004).

Lack of a definitive substrate switch in uraemic versus control hearts at this particular stage of disease, does not however eliminate the presence of insulin resistance. Uraemic heart displayed a clear functional deterioration in the presence of physiological concentration of insulin under increased workload (mimicking increased workload *in vivo*).

Furthermore, chronic glucose intolerance, hypertension and hypertrophy are traditionally associated with the myocardial insulin resistance and provide milieu of chronically altered haemodynamic and metabolic homeostasis, making uraemic heart susceptible to decompensated remodelling and failure. This notion is supported by poor survival prognosis of uraemic patients (Parfrey and Foley, 1999). Uraemia is also characterized by deleterious effects of uraemic retention solutes (toxins), including urea and creatinine, potentially altering myocardial protein structure via post-translational protein modifications (*Chapter 1*, section 1.6; *Chapter 6*). Increased ventricular glucose and fatty acid transporter expression without concomitant increase in either of the substrate contributions to the TCA cycle support this possibility.

Fasting hyperinsulinaemia accompanied by insulin resistance, has been associated with increased incidence of stroke and death from coronary artery disease and has been traditionally associated with high mortality in uraemia (Yanase et al., 2004). As this study has shown presence of insulin resistance at an early stage of uraemia, accompanied by a cluster of cardiac risk factors (LVH, hypertension), early detection in patients and treatment may reduce risk from cardiovascular death. Current diagnostic practices do not usually include insulin resistance assessment (Shen et al., 2005). However, early insulin resistance identification and methods to intervene after the detection may improve survival of the uraemic patients.

Thiazolidinediones (TZD), PPAR γ agonists (rosiglitazone, ciglitazone, pioglitazone) (Thiemermann, 2004) , are used for the type 2 diabetes treatment (Larsen et al., 2003) and could be potential candidates for treatment of insulin resistance in uraemia. They were shown to improve metabolism in *db/db* mice (Carley et al., 2004). PPAR γ agonist administration could assist by targeting systemic rather than myocardial insulin resistance, due to its small to absent expression of PPAR γ in the heart and high expression in the liver, kidney, heart and muscles (Kelly, 2003, Larsen et al., 2003), or alternatively target LVH reversal (Yamamoto et al., 2001). Correction of systemic insulin resistance and LVH could have beneficial effect on myocardial function and metabolism in uraemia.

7.1 Future Work

7.1.1 Experimental Uraemia

This study has shown that the progression of uraemia corresponds to an increase in insulin resistance. Equally, degree of LVH and kidney dysfunction increase in severity with prolonged uraemia. Therefore, the subsequent stage of this study would be examining the changes in uraemic myocardium at 12 and 16 week uraemia. Preliminary work on one pair of 16 week animals has shown good survival, despite the severity of uraemic procedure, and marked changes in the size of the uraemic cardiomyocytes (6% increase in cell length and 20% increase in cell width). Alternatively, shorter duration of uraemia could be studied in conjunction with the abdominal aortic constriction.

This would provide an additional stress stimulus in uraemia, providing more severe hypertension and LVH from the onset of experimental model in attempt to exacerbate pathological remodelling. This additional step would attempt to eliminate any innate, species specific (rodent) compensatory response to kidney dysfunction.

7.1.2 Cardiac Function and Metabolism

Cardiac function analysis could be performed in a paced heart with the pre-set heart rate reflecting *in vivo* measurements (*Table 3.2*). Equally, external pacing would enable more accurate means to increase cardiac workload by uniformly increasing heart rate throughout the perfusion protocol. Increasing concentration of extracellular calcium in the perfusate [3.0-5.6 mM (Raine et al., 1993)] could further increase perfusion stress and provide better insight into myocardial dysfunction in uraemia.

³¹P NMR *in situ* glucose uptake measurement could be a valuable tool in the assessment of insulin resistance and the functionality of the glucose transporters. It would also allow examination of PCr/ATP ratio from ATP and PCr spectra, reflecting heart energy reserve (Ten Hove and Neubauer, 2007). Previous studies in uraemia have shown alterations in PCr/ATP ratio suggesting varying myocardial energy supply (Del Canale et al., 1986, Raine et al., 1993, Weisensee et al., 1997).

It would also be useful to examine the basal glucose uptake in uraemic hearts, using current perfusion protocol, in order to enable comparison between insulin stimulated and basal metabolic state.

Furthermore, current study design could be applied at later stages of uraemia (9, 12 and 16 wk) in order to monitor the metabolic remodelling accompanying insulin resistance in uraemia.

7.1.3 Insulin Resistance

In order to monitor deterioration in insulin sensitivity in uraemia to the eventual diabetic state, approach used in this project for investigation of insulin resistance could be used at later stages of uraemia. Therefore glucose tolerance, HOMA-IR and GLUT4 expression (cellular and ventricular) should be examined at the subsequent stages of uraemia. This would provide further insight into cellular mechanism of insulin resistance. Equally, examination of the protein glycosylation and metabolic transporter RNA levels would help to expose any post-translational modification as a potential insulin resistance mechanism. Furthermore, protein expression of insulin pathway intermediates (Akt, PI3K, AS160) would eliminate signalling defect as a potential cause of insulin resistance in uraemia (Rosenblatt-Velin et al., 2004). Adiponectin is a recently discovered adipokine playing an important physiological role in impaired glucose homeostasis and is secreted and released by adipose tissue and exhibits potent anti-inflammatory and anti-atherosclerotic properties (Becker et al. 2005). Recent study discovered that the patients with the terminal renal failure had markedly lower adiponectin plasma concentration.

Moreover, significantly lower adiponectin plasma levels were found in patients with the prevalent and incident cardiovascular events. This finding therefore supports the notion that the adiponectin is a vasoprotective factor and that in patients with mild to moderate renal impairment hypoadiponectinemia is a CV risk factor (Becker et al., 2005). Therefore, it would be useful to perform adiponectin serum ELISA to assess the additional insulin resistance associated risk factors in uraemia as potential future therapeutic target.

7.1.4 Study Limitations

Uraemic cardiomyopathy is a specific form of heart disease. This makes comparisons between experimental uraemia and other models of hypertrophy challenging because any findings in uraemia are characteristic of a particular stage of the disease process in the presence of a number of confounding variables (e.g. anaemia, hypertension, uraemic toxins). Therefore, results presented in this study are characteristic of a specified (3, 6, 9 week) stage of uraemia.

Further progression of the disease development may cause additional alterations to the cellular mechanism of myocardial insulin resistance, as renal function would deteriorate further resulting in more severe uraemia. Induction of the experimental model relied on a use of animals under jurisdiction of the UK Home Office legislation (Animals Scientific Procedures Act 1986), and as such, number of animals used in this study had to be kept to a minimum.

This factor, in addition to the time an experimental model took to develop, have affected the number of animals assigned per experiment. Therefore, some findings in this study may be clarified further by increasing the number of experimental animals used. Measurements of blood pressure and glucose tolerance were carried out *in vivo* on restrained animals without anaesthetic. Restraint could have caused a sympathetic response in animals, however if such an effect occurred, it would be consistent between the two groups. Furthermore, use of anaesthetized animals may give depressed, inaccurate readings due to the effect of the anaesthetic (Bunag, 1983, Jamieson et al., 1997). Animals were strictly assigned to one *in vivo* experiment, hence no repeated measurements were made at different stages of uraemia on the same group of animals (i.e. at 6 wk; repeated at 9 wk). As different animal batches were used, this may account for some variation within the data sets.

Contributions of endogenous substrates triglycerides and glycogen and exogenous pyruvate to the oxidative metabolism were not determined. Endogenous substrate pool required ^{13}C enrichment in order for endogenous contribution to be determined. Furthermore, ^{13}C labelled pyruvate would help determine its contribution to the TCA cycle. Both of these aspects could be addressed by additional studies in the future. The metabolic and functional findings cannot be directly extrapolated to the *in vivo* setting. *In vitro* metabolic and functional studies using isovolumic retrograde Langendorff perfusion do not produce adequate conditions including workload, heart rate, neural, humoral stimulation and oxygen delivery (Lydell et al., 2002). The energy demand *in vivo* is greater than that in the experimental settings used in this study, which may alter the substrate utilization (Chatham et al., 1999).

PUBLICATIONS

Full Papers

- Aksentijević D. Bhandari S. Seymour A-M.L. Insulin resistance and altered GLUT4 expression in uraemia (submitted to *Kidney International*)
- Aksentijević D. Bhandari S. Seymour A-M.L. The effect of increased workload on myocardial function and the energy provision in experimental uraemia (in preparation)

Abstracts

- Aksentijević D. Bhandari S. Seymour A-M.L. (2007) Myocardial GLUT4 Expression in experimental uraemia. *J Mol and Cell Cardiol* 42:S55
- Aksentijević D. Lee K.Y. Smith K. Bhandari S. Seymour A-M.L. (2007) Altered expression of myocardial $[Ca^{2+}]$ handling proteins in experimental uraemia. *J Mol Cell Cardiol* 42:S55
- Aksentijević D. Bhandari S. Seymour A-M.L. (2007) The effect of increased $[Ca^{2+}]$ on myocardial function and the energy provision in experimental uraemia. *J Mol Cell Cardiol* 42: S55

- Aksentijević D. Bhandari S. Seymour A-M.L (2007) Uraemic cardiomyopathy is characterized by altered metabolic substrate transport. *Cardiovasc Drugs Ther* (in press)
- Bhandari,S. Seymour A-M.L. Aksentijević D. (2006) Myocardial GLUT 4 expression in experimental uraemia. *J Am Soc Nephrol* SA-PO152
- Aksentijević D. Bhandari S. Seymour A-M.L (2006) The effect of increased calcium on myocardial function in experimental uraemia. *Cardiovasc Drugs Ther* 20: 395
- Aksentijević D. Bhandari S. Seymour A-M.L (2006) Alteration in GLUT4 expression in experimental uraemia. *Cardiovasc Drugs Ther* 20:395
- Aksentijević D. Bhandari S. Seymour A-M.L (2006) The impact of increasing extracellular $[Ca^{2+}]$ on myocardial function in experimental uraemia. *J Mol Cell Cardiol* 40: 932
- Aksentijević D. Bhandari S. Seymour A-M.L (2005) Cardiac remodelling in chronic uraemia. *J Mol Cell Cardiol* 39:191

REFERENCES

<http://www4.utsouthwestern.edu/rogersnmr>].

- AFZAL, N. & DHALLA, N. S. (1992) Differential changes in left and right ventricular SR calcium transport in congestive heart failure. *Am J Physiol Heart Circ Physiol*, 262, H868-H874.
- ALARCON, C., LEAHY, J. L., SCHUPPIN, G. T. & RHODES, C. J. (1995) Increased secretory demand rather than defect in the proinsulin conversion mechanism causes hyperproinsulinaemia in a glucose-infusion rat model of non-insulin-dependant diabetes mellitus. *J Clin Invest*, 95, 1032-1039.
- ALKHATEEB, H., CHABOWSKI, A., GLATZ, J. F., LUIKEN, J. F. & BONEN, A. (2007) Two phases of palmitate-induced insulin resistance in skeletal muscle: impaired GLUT4 translocation is followed by a reduced GLUT4 intrinsic activity. *Am J Physiol Endocrinol Metab*, 293, E783-93.
- ALLARD, M. F. (2004) Energy substrate metabolism in cardiac hypertrophy. *Curr Hypertens Rep*, 6, 430-5.
- ALLARD, M. F., SCHONEKESS, B. O., HENNING, S. L., ENGLISH, D. R. & LOPASCHUK, G. D. (1994) Contribution of oxidative metabolism and glycolysis to ATP production in hypertrophied hearts. *Am J Physiol*, 267, H742-50.
- ALLARD, M. F., WAMBOLT, R. B., LONGNUS, S. L., GRIST, M., LYDELL, C. P., PARSONS, H. L., RODRIGUES, B., HALL, J. L., STANLEY, W. C. & BONDY, G. P. (2000) Hypertrophied rat hearts are less responsive to the metabolic and functional effects of insulin. *Am J Physiol Endocrinol Metab*, 279, E487-93.
- AMANN, K., BREITBACH, M., RITZ, E. & MALL, G. (1998a) Myocyte/capillary mismatch in the heart of uremic patients. *J Am Soc Nephrol*, 9, 1018-22.
- AMANN, K., GHAREHBAGHI, H., STEPHEN, S. & MALL, G. (1995a) Hypertrophy and hyperplasia of smooth muscle cells of small intramyocardial arteries in spontaneously hypertensive rats. *Hypertension*, 25, 124-31.
- AMANN, K., NEUSSUS, R., RITZ, E., IRZYNIEC, T., WIEST, G. & MALL, G. (1995b) Changes of vascular architecture independent of blood pressure in experimental uremia. *Am J Hypertens*, 8, 409-17.
- AMANN, K., RITZ, C., ADAMCZAK, M. & RITZ, E. (2003a) Why is coronary heart disease of uraemic patients so frequent and so devastating? *Nephrol Dial Transplant*, 18, 631-40.

- AMANN, K. & RITZ, E. (1997) Cardiac disease in chronic uremia: pathophysiology. *Adv Ren Replace Ther*, 4, 212-24.
- AMANN, K. & RITZ, E. (2001) The Heart in Renal Failure: Morphological Changes of the Myocardium-New Insights. *Journal of Clinical Basic Cardiology*, 4, 109-113.
- AMANN, K., RYCHLIK, I., MILTENBERGER-MILTENY, G. & RITZ, E. (1998b) Left ventricular hypertrophy in renal failure. *Kidney Int Suppl*, 68, S78-85.
- AMANN, K., TYRALLA, K., GROSS, M. L., SCHWARZ, U., TORNIG, J., HAAS, C. S., RITZ, E. & MALL, G. (2003b) Cardiomyocyte loss in experimental renal failure: prevention by ramipril. *Kidney Int*, 63, 1708-13.
- AMANN, K., WANNER, C. & RITZ, E. (2006) Cross-talk between the kidney and the cardiovascular system. *J Am Soc Nephrol*, 17, 2112-9.
- ATKINSON, L. L., KOZAK, R., KELLY, S. E., ONAY BESIKCI, A., RUSSELL, J. C. & LOPASCHUK, G. D. (2003) Potential mechanisms and consequences of cardiac triacylglycerol accumulation in insulin-resistant rats. *Am J Physiol Endocrinol Metab*, 284, E923-30.
- BADAR-GOFFER, R. & BACHELARD, H. (1991) Metabolic studies using ¹³C nuclear magnetic resonance spectroscopy. *Essays Biochem*, 26, 105-19.
- BAIGENT, C., BURBURY, K. & WHEELER, D. (2000) Premature cardiovascular disease in chronic renal failure. *Lancet*, 356, 147-52.
- BAK, J. F., SCHMITZ, O., SORENSEN, S. S., FROKJAER, J., KJAER, T. & PEDERSEN, O. (1989) Activity of insulin receptor kinase and glycogen synthase in skeletal muscle from patients with chronic renal failure. *Acta Endocrinol (Copenh)*, 121, 744-50.
- BALABAN, R. (2002) Cardiac Energy Metabolism Homeostasis: Role of Cytosolic Calcium. *Journal of Molecular and Cellular Cardiology*, 34, 1259-1271.
- BARGER, P. M. & KELLY, D. P. (2000) PPAR signaling in the control of cardiac energy metabolism. *Trends Cardiovasc Med*, 10, 238-45.
- BARROS, L. F., BALDWIN, S. A. & GRIFFITHS, M. (1997a) Rapid activation of GLUT1 by osmotic stress. *Biochem Soc Trans*, 25, 485S.
- BARROS, L. F., YOUNG, M., SAKLATVALA, J. & BALDWIN, S. A. (1997b) Evidence of two mechanisms for the activation of the glucose transporter GLUT1 by anisomycin: p38(MAP kinase) activation and protein synthesis inhibition in mammalian cells. *J Physiol*, 504 (Pt 3), 517-25.

- BAXTER, G. F. (2004) The natriuretic peptides. *Basic Res Cardiol*, 99, 71-5.
- BECKER, B., KRONENBERG, F., KIELSTEIN, J. T., HALLER, H., MORATH, C., RITZ, E. & FLISER, D. (2005) Renal insulin resistance syndrome, adiponectin and cardiovascular events in patients with kidney disease: the mild and moderate kidney disease study. *J Am Soc Nephrol*, 16, 1091-8.
- BECKER, C., SEVILLA, L., TOMAS, E., PALACIN, M., ZORZANO, A. & FISCHER, Y. (2001) The endosomal compartment is an insulin-sensitive recruitment site for GLUT4 and GLUT1 glucose transporters in cardiac myocytes. *Endocrinology*, 142, 5267-76.
- BELKE, D. D., LARSEN, T. S., GIBBS, E. M. & SEVERSON, D. L. (2000) Altered metabolism causes cardiac dysfunction in perfused hearts from diabetic (db/db) mice. *Am J Physiol Endocrinol Metab*, 279, E1104-13.
- BELKE, D. D., LARSEN, T. S., GIBBS, E. M. & SEVERSON, D. L. (2001) Glucose metabolism in perfused mouse hearts overexpressing human GLUT-4 glucose transporter. *Am J Physiol Endocrinol Metab*, 280, E420-7.
- BELKE, D. D., SWANSON, E. A. & DILLMANN, W. H. (2004) Decreased sarcoplasmic reticulum activity and contractility in diabetic db/db mouse heart. *Diabetes*, 53, 3201-8.
- BELTRAMI, A., KONRAD, U., KAJSTURA, J., YAN, S.-M., FINATO, N., BUSSANI, R., NADAL-GINARD, B., SILVESTRI, F., LERI, A. & ANVERSA, P. (2001) Evidence that human cardiac myocytes divide after myocardial infarction. *The New England Journal of Medicine*, 344, 1750-1757.
- BERGMEYER, H. U. & BERNT, E. (1974) Glucose: Determination with glucose oxidase and preoxidase. IN BERGMEYER, H. U. (Ed.) *Methods of enzymatic analysis*. 2 ed., Verlag Chemie Weinheim.
- BERNE, R. M., LEVY, M. N., KOEPPEN, B. M. & STANTON, B. A. (2004) Chapter 17 Regulation of the Heartbeat. *Physiology*. 5 ed., Mosby.
- BERS, D. M. (2002) Cardiac excitation-contraction coupling. *Nature*, 415, 198-205.
- BERS, D. M. (2006) Altered cardiac myocyte Ca regulation in heart failure. *Physiology (Bethesda)*, 21, 380-7.
- BERS, D. M. & PEREZ-REYES, E. (1999) Ca channels in cardiac myocytes: structure and function in Ca influx and intracellular Ca release. *Cardiovasc Res*, 42, 339-60.

- BERWICK, D. C., DELL, G. C., WELSH, G. I., HEESOM, K. J., HERS, I., FLETCHER, L. M., COOKE, F. T. & TAVARE, J. M. (2004) Protein kinase B phosphorylation of PIKfyve regulates the trafficking of GLUT4 vesicles. *J Cell Sci*, 117, 5985-93.
- BLIGH, E. G. & DYER, W. J. (1959) A rapid method of total lipid extraction and purification. *Can J Biochem Physiol*, 37, 911-7.
- BLOCK, G. H.-S., T LEVIN, NW PORT, FK (1998) Association of serum phosphorus and calcium x phosphate product with mortality risk in chronic hemodialysis patients: a national study. *Am J Kidney Disease*, 31.
- BOATENG, S., SEYMOUR, A. M., DUNN, M., YACOUB, M. & BOHELER, K. (1997) Inhibition of endogenous cardiac phosphatase activity and measurement of sarcoplasmic reticulum calcium uptake: a possible role of phospholamban phosphorylation in the hypertrophied myocardium. *Biochem Biophys Res Commun*, 239, 701-5.
- BOATENG, S. Y., SEYMOUR, A. M., BHUTTA, N. S., DUNN, M. J., YACOUB, M. H. & BOHELER, K. R. (1998) Sub-antihypertensive doses of ramipril normalize sarcoplasmic reticulum calcium ATPase expression and function following cardiac hypertrophy in rats. *J Mol Cell Cardiol*, 30, 2683-94.
- BOHELER, K. R., CHASSAGNE, C., MARTIN, X., WISNEWSKY, C. & SCHWARTZ, K. (1992) Cardiac expressions of alpha- and beta-myosin heavy chains and sarcomeric alpha-actins are regulated through transcriptional mechanisms. Results from nuclear run-on assays in isolated rat cardiac nuclei. *J Biol Chem*, 267, 12979-85.
- BONILLA, S., GOECKE, I. A., BOZZO, S., ALVO, M., MICHEA, L. & MARUSIC, E. T. (1991) Effect of chronic renal failure on Na,K-ATPase alpha 1 and alpha 2 mRNA transcription in rat skeletal muscle. *J Clin Invest*, 88, 2137-41.
- BORNFELDT, K. E., SKOTTNER, A. & ARNQVIST, H. J. (1992) In-vivo regulation of messenger RNA encoding insulin-like growth factor-I (IGF-I) and its receptor by diabetes, insulin and IGF-I in rat muscle. *J Endocrinol*, 135, 203-11.
- BOUDINA, S. & ABEL, E. D. (2006) Mitochondrial uncoupling: a key contributor to reduced cardiac efficiency in diabetes. *Physiology (Bethesda)*, 21, 250-8.
- BOUDINA, S., SENA, S., O'NEILL, B. T., TATHIREDDY, P., YOUNG, M. E. & ABEL, E. D. (2005) Reduced mitochondrial oxidative capacity and increased mitochondrial uncoupling impair myocardial energetics in obesity. *Circulation*, 112, 2686-95.

- BRADFORD, M. M. (1976) A rapid and sensitive method for the quantitation of microgram quantities of protein utilizing the principle of protein-dye binding. *Anal Biochem*, 72, 248-54.
- BRAUNWALD, E. & BRISTOW, M. R. (2000) Congestive heart failure: fifty years of progress. *Circulation*, 102, IV14-23.
- BROOKS, G., POOLMAN, R. A. & LI, J. M. (1998) Arresting developments in the cardiac myocyte cell cycle: role of cyclin-dependent kinase inhibitors. *Cardiovasc Res*, 39, 301-11.
- BROZINICK, J. T., JR., YASPELKIS, B. B., 3RD, WILSON, C. M., GRANT, K. E., GIBBS, E. M., CUSHMAN, S. W. & IVY, J. L. (1996) Glucose transport and GLUT4 protein distribution in skeletal muscle of GLUT4 transgenic mice. *Biochem J*, 313 (Pt 1), 133-40.
- BRYANT, R. G. & JAMES, A. F. (2002) Regulated transport of the glucose transporter GLUT4. *Nature Molecular Cell Biology*, 3, 267-277.
- BUCHANAN, J., MAZUMDER, P. K., HU, P., CHAKRABARTI, G., ROBERTS, M. W., YUN, U. J., COOKSEY, R. C., LITWIN, S. E. & ABEL, E. D. (2005) Reduced cardiac efficiency and altered substrate metabolism precedes the onset of hyperglycemia and contractile dysfunction in two mouse models of insulin resistance and obesity. *Endocrinology*, 146, 5341-9.
- BUGAISKY, L., GUPTA, M. & ZAK, R. (1991) Chapter 63, Cellular and molecular mechanisms of cardiac hypertrophy *The heart and cardiovascular system*. New York, Raven Press pg 1628-1629.
- BUNAG, R. D. (1983) Facts and fallacies about measuring blood pressure in rats. *Clin Exp Hypertens A*, 5, 1659-81.
- BURKHOFF, D., WEISS, R. G., SCHULMAN, S. P., KALIL-FILHO, R., WANNENBURG, T. & GERSTENBLITH, G. (1991) Influence of metabolic substrate on rat heart function and metabolism at different coronary flows. *Am J Physiol*, 261, H741-50.
- BUSE, M. G. (2006) Hexosamines, insulin resistance, and the complications of diabetes: current status. *Am J Physiol Endocrinol Metab*, 290, E1-E8.
- CALDERHEAD, D. M., KITAGAWA, K., LIENHARD, G. E. & GOULD, G. W. (1990) Translocation of the brain-type glucose transporter largely accounts for insulin stimulation of glucose transport in BC3H-1 myocytes. *Biochem J*, 269, 597-601.

- CAMELLITI, P., BORG, T. K. & KOHL, P. (2005) Structural and Functional Characterisation of Cardiac Fibroblasts. *Cardiovascular Research*, 65, 40-51.
- CARLEY, A. N., SEMENIUK, L. M., SHIMONI, Y., AASUM, E., LARSEN, T. S., BERGER, J. P. & SEVERSON, D. L. (2004) Treatment of type 2 diabetic db/db mice with a novel PPARgamma agonist improves cardiac metabolism but not contractile function. *Am J Physiol Endocrinol Metab*, 286, E449-55.
- CARLEY, A. N. & SEVERSON, D. L. (2005) Fatty acid metabolism is enhanced in type 2 diabetic hearts. *Biochim Biophys Acta*, 1734, 112-26.
- CARO, J. F. & LANZA-JACOBY, S. (1983) Insulin resistance in uremia. Characterization of lipid metabolism in freshly isolated and primary cultures of hepatocytes from chronic uremic rats. *J Clin Invest*, 72, 882-92.
- CECCHIN, F., ITTOOP, O., SINHA, M. K. & CARO, J. F. (1988) Insulin resistance in uremia: insulin receptor kinase activity in liver and muscle from chronic uremic rats. *Am J Physiol*, 254, E394-401.
- CEFALU, W. T. (2001) Insulin Resistance: Cellular and Clinical Concepts. *Experimental Biology and Medicine*, 226, 13-26.
- CHATHAM, J. C., DES ROSIERS, C. & FORDER, J. R. (2001) Evidence of separate pathways for lactate uptake and release by the perfused rat heart. *Am J Physiol Endocrinol Metab*, 281, E794-802.
- CHATHAM, J. C., GAO, Z. P. & FORDER, J. R. (1999) Impact of 1 wk of diabetes on the regulation of myocardial carbohydrate and fatty acid oxidation. *Am J Physiol*, 277, E342-51.
- CHATHAM, J. C. & SEYMOUR, A. M. (2002) Cardiac carbohydrate metabolism in Zucker diabetic fatty rats. *Cardiovasc Res*, 55, 104-12.
- CHEN, J., MUNTNER, P., HAMM, L. L., FONSECA, V., BATUMAN, V., WHELTON, P. K. & HE, J. (2003) Insulin resistance and risk of chronic kidney disease in nondiabetic US adults. *J Am Soc Nephrol*, 14, 469-77.
- CHIANG, S. H., BAUMANN, C. A., KANZAKI, M., THURMOND, D. C., WATSON, R. T., NEUDAUER, C. L., MACARA, I. G., PESSIN, J. E. & SALTIEL, A. R. (2001) Insulin-stimulated GLUT4 translocation requires the CAP-dependent activation of TC10. *Nature*, 410, 944-8.
- CIANCIARUSO, B., BRUNORI, G., KOPPLE, J. D., TRAVERSO, G., PANARELLO, G., ENIA, G., STRIPPOLI, P., DE VECCHI, A., QUERQUES, M., VIGLINO, G. & ET AL. (1995) Cross-sectional comparison of malnutrition in continuous ambulatory peritoneal dialysis and hemodialysis patients. *Am J Kidney Dis*, 26, 475-86.

- CIANCIARUSO, B., SACCA, L., TERRACCIANO, V., MARCUCCIO, F., OROFINO, G., PETRONE, A., ANDREUCCI, V. E. & KOPPLE, J. D. (1987) Insulin metabolism in acute renal failure. *Kidney Int Suppl*, 22, S109-12.
- COONS, A. H. (1958) Fluorescent antibody methods. *Gen Cytochem Methods*, 1, 399-422.
- COORT, S. L., BONEN, A., VAN DER VUSSE, G. J., GLATZ, J. F. & LUIKEN, J. J. (2007) Cardiac substrate uptake and metabolism in obesity and type-2 diabetes: role of sarcolemmal substrate transporters. *Mol Cell Biochem*, 299, 5-18.
- CORVERA, S. & CZECH, M. P. (1998) Direct targets of phosphoinositide 3-kinase products in membrane traffic and signal transduction. *Trends Cell Biol*, 8, 442-6.
- CURRIE, S. & SMITH, G. L. (1999) Enhanced phosphorylation of phospholamban and downregulation of sarco/endoplasmic reticulum Ca²⁺ ATPase type 2 (SERCA 2) in cardiac sarcoplasmic reticulum from rabbits with heart failure. *Cardiovasc Res*, 41, 135-46.
- DAVIES, A. (2001) Human Physiology. IN DAVIES, A., BLAKELEY, A. G. H. & KIDD, C. (Eds.), Churchill Livingstone
- DAVILA-ROMAN, V. G., VEDALA, G., HERRERO, P., DE LAS FUENTES, L., ROGERS, J. G., KELLY, D. P. & GROPLER, R. J. (2002) Altered myocardial fatty acid and glucose metabolism in idiopathic dilated cardiomyopathy. *J Am Coll Cardiol*, 40, 271-7.
- DE LA BASTIE, D., LEVITSKY, D., RAPPAPORT, L., MERCADIER, J. J., MAROTTE, F., WISNEWSKY, C., BROVKOVICH, V., SCHWARTZ, K. & LOMPRES, A. M. (1990) Function of the sarcoplasmic reticulum and expression of its Ca²⁺-ATPase gene in pressure overload-induced cardiac hypertrophy in the rat. *Circ Res*, 66, 554-64.
- DE LIMA, J. J., VIEIRA, M. L., LOPES, H. F., GRUPPI, C. J., MEDEIROS, C. J., IANHEZ, L. E. & KRIEGER, E. M. (1999) Blood pressure and the risk of complex arrhythmia in renal insufficiency, hemodialysis, and renal transplant patients. *Am J Hypertens*, 12, 204-8.
- DE SIMONE, G. (2003) Left Ventricular Geometry and Hypotension in End-Stage Renal Disease: a Mechanical Perspective. *Journal of the American Society of Nephrology*, 14, 2421-2427.

- DE STEFANO, L. M., MATSUBARA, L. S. & MATSUBARA, B. B. (2006) Myocardial dysfunction with increased ventricular compliance in volume overload hypertrophy. *Eur J Heart Fail*, 8, 784-9.
- DE VINUESA, S. G., GOICOECHEA, M., KANTER, J., PUERTA, M., CACHOFEIRO, V., LAHERA, V., GOMEZ-CAMPDERA, F. & LUNO, J. (2006) Insulin Resistance, Inflammatory Biomarkers, and Adipokines in Patients with Chronic Kidney Disease: Effects of Angiotensin II Blockade. *J Am Soc Nephrol*, 17, S206-12.
- DEBSKA-SLIZIEN, A., KAWECKA, A., WOJNAROWSKI, K., PRAJS, J., MALGORZEWICZ, S., KUNICKA, D., ZDROJEWSKI, Z., LYSIAK-SZYDŁOWSKA, W., LIPINSKI, J. & RUTKOWSKI, B. (2000) Correlation between plasma carnitine, muscle carnitine and glycogen levels in maintenance haemodialysis patients. *Artificial Kidney and Dialysis*, 23, 90-96.
- DEFRONZO, R. A., ALVESTRAND, A., SMITH, D., HENDLER, R., HENDLER, E. & WAHREN, J. (1981) Insulin resistance in uremia. *J Clin Invest*, 67, 563-8.
- DEFRONZO, R. A., GUNNARSSON, R., BJORKMAN, O., OLSSON, M. & WAHREN, J. (1985) Effects of insulin on peripheral and splanchnic glucose metabolism in noninsulin-dependent (type II) diabetes mellitus. *J Clin Invest*, 76, 149-55.
- DEFRONZO, R. A., TOBIN, J. D., ROWE, J. W. & ANDRES, R. (1978) Glucose intolerance in uremia. Quantification of pancreatic beta cell sensitivity to glucose and tissue sensitivity to insulin. *J Clin Invest*, 62, 425-35.
- DEL CANALE, S., FIACCADORI, E., RONDA, N., SODERLUND, K., ANTONUCCI, C. & GUARIGLIA, A. (1986) Muscle energy metabolism in uremia. *Metabolism*, 35, 981-3.
- DENGEL, D. R., GOLDBERG, A. P., MAYUGA, R. S., KAIRIS, G. M. & WEIR, M. R. (1996) Insulin resistance, elevated glomerular filtration fraction, and renal injury. *Hypertension*, 28, 127-32.
- DEPRE, C., YOUNG, M. E., YING, J., AHUJA, H. S., HAN, Q., GARZA, N., DAVIES, P. J. & TAEGTMEYER, H. (2000) Streptozotocin-induced changes in cardiac gene expression in the absence of severe contractile dysfunction. *J Mol Cell Cardiol*, 32, 985-96.
- DES ROSIERS, C., LLOYD, S., COMTE, B. & CHATHAM, J. C. (2004) A critical perspective of the use of (13)C-isotopomer analysis by GCMS and NMR as applied to cardiac metabolism. *Metab Eng*, 6, 44-58.

- DIKOW, R., KIHM, L. P., ZEIER, M., KAPITZA, J., TORNIG, J., AMANN, K., TIEFENBACHER, C. & RITZ, E. (2004) Increased infarct size in uremic rats: reduced ischemia tolerance? *J Am Soc Nephrol*, 15, 1530-6.
- DJOUADI, F., WEINHEIMER, C. J., SAFFITZ, J. E., PITCHFORD, C., BASTIN, J., GONZALEZ, F. J. & KELLY, D. P. (1998) A gender-related defect in lipid metabolism and glucose homeostasis in peroxisome proliferator-activated receptor alpha- deficient mice. *J Clin Invest*, 102, 1083-91.
- DONOHUE, P., HENDRY, B. M., WALGAMA, O. V., BERTASO, F., HOPSTER, D. J., SHATTOCK, M. J. & JAMES, A. F. (2000a) An altered repolarizing potassium current in rat cardiac myocytes after subtotal nephrectomy. *J Am Soc Nephrol*, 11, 1589-99.
- DONOHUE, P., MCMAHON, A. C., WALGAMA, O. V., BERTASO, F., DOCKRELL, M. E., CRAMP, H. A., MULLEN, A. M., SHATTOCK, M. J., HENDRY, B. M. & JAMES, A. F. (2000b) L-type calcium current of isolated rat cardiac myocytes in experimental uraemia. *Nephrol Dial Transplant*, 15, 791-8.
- DRAKE, P. G. & POSNER, B. I. (1998) Insulin receptor-associated protein tyrosine phosphatase(s): role in insulin action. *Mol Cell Biochem*, 182, 79-89.
- DU, J. & MITCH, W. E. (2005) Identification of pathways controlling muscle protein metabolism in uremia and other catabolic conditions. *Curr Opin Nephrol Hypertens*, 14, 378-82.
- DUGANI, C. B. & KLIP, A. (2005) Glucose transporter 4: cycling, compartments and controversies. *EMBO Rep*, 6, 1137-42.
- DUPREZ, D. A. & COHN, J. N. (2007) Arterial stiffness as a risk factor for coronary atherosclerosis. *Curr Atheroscler Rep*, 9, 139-44.
- DWYER, J. T., CUNNIFF, P. J., MARONI, B. J., KOPPLE, J. D., BURROWES, J. D., POWERS, S. N., COCKRAM, D. B., CHUMLEA, W. C., KUSEK, J. W., MAKOFF, R., GOLDSTEIN, D. J. & PARANANDI, L. (1998) The hemodialysis pilot study: nutrition program and participant characteristics at baseline. The HEMO Study Group. *J Ren Nutr*, 8, 11-20.
- EGUEZ, L., LEE, A., CHAVEZ, J. A., MIINEA, C. P., KANE, S., LIENHARD, G. E. & MCGRAW, T. E. (2005) Full intracellular retention of GLUT4 requires AS160 Rab GTPase activating protein. *Cell Metab*, 2, 263-72.
- EL ALAOUI-TALIBI, Z., GUENDOOUZ, A., MORAVEC, M. & MORAVEC, J. (1997) Control of oxidative metabolism in volume-overloaded rat hearts: effect of propionyl-L-carnitine. *Am J Physiol*, 272, H1615-24.

- EVANS, R. K., SCHWARTZ, D. D. & GLADDEN, L. B. (2003) Effect of myocardial volume overload and heart failure on lactate transport into isolated cardiac myocytes. *J Appl Physiol*, 94, 1169-76.
- FABIATO, A. & FABIATO, F. (1978) Effects of pH on the myofilaments and the sarcoplasmic reticulum of skinned cells from cardiac and skeletal muscles. *J Physiol*, 276, 233-55.
- FACCHIN, L., VESCOVO, G., LEVEDIANOS, G., ZANNINI, L., NORDIO, M., LORENZI, S., CATURELLI, G. & AMBROSIO, G. B. (1995) Left ventricular morphology and diastolic function in uraemia: echocardiographic evidence of a specific cardiomyopathy. *Br Heart J*, 74, 174-9.
- FARESE, R. V., SAJAN, M. P. & STANDAERT, M. L. (2005) Atypical protein kinase C in insulin action and insulin resistance. *Biochem Soc Trans*, 33, 350-3.
- FERRANNINI, E., SANTORO, D., BONADONNA, R., NATALI, A., PARODI, O. & CAMICI, P. G. (1993) Metabolic and hemodynamic effects of insulin on human hearts. *Am J Physiol*, 264, E308-15.
- FINCK, B. N. & KELLY, D. P. (2002) Peroxisome proliferator-activated receptor alpha (PPARalpha) signaling in the gene regulatory control of energy metabolism in the normal and diseased heart. *J Mol Cell Cardiol*, 34, 1249-57.
- FINCK, B. N., LEHMAN, J. J., BARGER, P. M. & KELLY, D. P. (2002) Regulatory networks controlling mitochondrial energy production in the developing, hypertrophied, and diabetic heart. *Cold Spring Harb Symp Quant Biol*, 67, 371-82.
- FLISER, D., PACINI, G., ENGELLEITER, R., KAUTZKY-WILLER, A., PRAGER, R., FRANEK, E. & RITZ, E. (1998) Insulin resistance and hyperinsulinemia are already present in patients with incipient renal disease. *Kidney Int*, 53, 1343-7.
- FOWLER, M. R., NAZ, J. R., GRAHAM, M. D., ORCHARD, C. H. & HARRISON, S. M. (2007) Age and hypertrophy alter the contribution of sarcoplasmic reticulum and Na⁺/Ca²⁺ exchange to Ca²⁺ removal in rat left ventricular myocytes. *J Mol Cell Cardiol*, 42, 582-9.
- FOZZARD, H. A. & HAUCK, D. A. (1991) The Sodium Channels. IN FOZZARD, H. A., HABER, E., JENNINGS, R. B., KATZ, A. M. & MORGAN, H. E. (Eds.) *The Heart and Cardiovascular System*. 2 ed., Raven.

- FRASER, H., LOPASCHUK, G. D. & CLANACHAN, A. S. (1998) Assessment of glycogen turnover in aerobic, ischemic, and reperfused working rat hearts. *Am J Physiol*, 275, H1533-41.
- FREESTONE, N., RIBARIC, S. & MASON, W. (1996) The effect of insulin-like growth factor-1 on adult cardiac contractility. *Mol Cell Biochem*, 164, 223-229.
- FROHLICH, E. D. (2001) Fibrosis and ischemia: the real risks in hypertensive heart disease. *Am J Hypertens*, 14, 194S-199S.
- GADIAN, D. G. (2004) *NMR and its applications to living systems*, Oxford Science Publications.
- GALVAN, A. Q., GALETTA, F., NATALI, A., MUSCELLI, E., SIRONI, A. M., CINI, G., CAMASTRA, S. & FERRANNINI, E. (2000) Insulin resistance and hyperinsulinemia: No independent relation to left ventricular mass in humans. *Circulation*, 102, 2233-8.
- GAMCSIK, M. P., FORDER, J. R. & MILLIS, K. K. (1996) A Versatile Oxygenator and Perfusion System for Magnetic Resonance Studies. *Biotechnology and Bioengineering*, 49, 348-354.
- GARVEY, W. T., MAIANU, L., ZHU, J. H., BRECHTEL-HOOK, G., WALLACE, P. & BARON, A. D. (1998) Evidence for defects in the trafficking and translocation of GLUT4 glucose transporters in skeletal muscle as a cause of human insulin resistance. *J Clin Invest*, 101, 2377-86.
- GAW, A. (2004) *Clinical biochemistry : an illustrated colour text*, Churchill Livingstone.
- GERDES, A. M., ONODERA, T., WANG, X. & MCCUNE, S. A. (1996) Myocyte remodeling during the progression to failure in rats with hypertension. *Hypertension*, 28, 609-14.
- GERSTEN, D. (1996) Gel Preparation. IN GERSTEN, D. (Ed.) *Gel Electrophoresis Proteins Essential Techniques*. 1 ed., John Wiley and Sons.
- GLASS, D. J. (2003) Molecular mechanisms modulating muscle mass. *Trends Mol Med*, 9, 344-50.
- GLATZ, J. F. & VAN DER VUSSE, G. J. (1996) Cellular fatty acid binding proteins: their function and physiological significance. *Prog Lipid Res*, 35, 243-282.
- GOULD, G. W. & HOLMAN, G. D. (1993) The glucose transporter family: structure, function and tissue-specific expression. *Biochem J*, 295 (Pt 2), 329-41.

- GREIBER, S., ENGLAND, B. K., PRICE, S. R., MEDFORD, R. M., EBB, R. G. & MITCH, W. E. (1994) Na pump defects in chronic uremia cannot be attributed to changes in Na-K-ATPase mRNA or protein. *Am J Physiol*, 266, F536-42.
- GROSSMAN, W., JONES, D. & MCLAURIN, L. P. (1975) Wall stress and patterns of hypertrophy in the human left ventricle. *J Clin Invest*, 56, 56-64.
- HAFSTAD, A. D., SOLEVAG, G. H., SEVERSON, D. L., LARSEN, T. S. & AASUM, E. (2006) Perfused hearts from Type 2 diabetic (db/db) mice show metabolic responsiveness to insulin. *Am J Physiol Heart Circ Physiol*, 290, H1763-9.
- HARPEL, P. C., ZHANG, X. & BORTH, W. (1996) Homocysteine and hemostasis: pathogenic mechanisms predisposing to thrombosis. *J Nutr*, 126, 1285S-9S.
- HEIN, S., KOSTIN, S., HELING, A., MAENO, Y. & SCHAPER, J. (2000) The role of the cytoskeleton in heart failure. *Cardiovasc Res*, 45, 273-8.
- HEINEKE, J. & MOLKENTIN, J. D. (2006) Regulation of cardiac hypertrophy by intracellular signalling pathways. *Nat Rev Mol Cell Biol*, 7, 589-600.
- HIDVEGI, T., SZATMARI, F., HETYESI, K., BIRO, L. & JERMENDY, G. (2003) Intima-media thickness of the carotid arteries in subjects with hyperinsulinaemia (insulin resistance). *Diabetes Nutr Metab*, 16, 139-44.
- HO, K. K., PINSKY, J. L., KANNEL, W. B. & LEVY, D. (1993) The epidemiology of heart failure: the Framingham Study. *J Am Coll Cardiol*, 22, 6A-13A.
- HODGKINSON, C. P., MANDER, A. & SALE, G. J. (2005) Identification of 80K-H as a protein involved in GLUT4 vesicle trafficking. *Biochem J*, 388, 785-93.
- HOLGADO-MADRUGA, M., EMLET, D. R., MOSCATELLO, D. K., GODWIN, A. K. & WONG, A. J. (1996) A Grb2-associated docking protein in EGF- and insulin-receptor signalling. *Nature*, 379, 560-4.
- HORIO, T., NISHIKIMI, T., YOSHIHARA, F., MATSUO, H., TAKISHITA, S. & KANGAWA, K. (2000) Inhibitory regulation of hypertrophy by endogenous atrial natriuretic peptide in cultured cardiac myocytes. *Hypertension*, 35, 19-24.
- HORL, W. H., STEPINSKI, J. & HEIDLAND, A. (1980) Carbohydrate metabolism and uraemia-mechanisms for glycogenolysis and gluconeogenesis. *Klin Wochenschr*, 58, 1051-64.
- HORTON, E. S., JOHNSON, C. & LEOVITZ, H. E. (1968) Carbohydrate metabolism in uremia. *Ann Intern Med*, 68, 63-74.

- HOW, O. J., AASUM, E., KUNNATHU, S., SEVERSON, D. L., MYHRE, E. S. & LARSEN, T. S. (2005) Influence of substrate supply on cardiac efficiency, as measured by pressure-volume analysis in ex vivo mouse hearts. *Am J Physiol Heart Circ Physiol*, 288, H2979-85.
- HOW, O. J., AASUM, E., SEVERSON, D. L., CHAN, W. Y., ESSOP, M. F. & LARSEN, T. S. (2006) Increased myocardial oxygen consumption reduces cardiac efficiency in diabetic mice. *Diabetes*, 55, 466-73.
- HUROT, J. M., CUCHERAT, M., HAUGH, M. & FOUQUE, D. (2002) Effects of L-carnitine supplementation in maintenance hemodialysis patients: a systematic review. *J Am Soc Nephrol*, 13, 708-14.
- HUSS, J. M. & KELLY, D. P. (2004) Nuclear receptor signaling and cardiac energetics. *Circ Res*, 95, 568-78.
- HWANG, D. Y. & ISMAIL-BEIGI, F. (2001) Stimulation of GLUT-1 glucose transporter expression in response to hyperosmolarity. *Am J Physiol Cell Physiol*, 281, C1365-72.
- IMAMURA, T., HUANG, J., USUI, I., SATOH, H., BEVER, J. & OLEFSKY, J. M. (2003) Insulin-induced GLUT4 translocation involves protein kinase C-lambda-mediated functional coupling between Rab4 and the motor protein kinesin. *Mol Cell Biol*, 23, 4892-900.
- ISHIZAKA, N., ISHIZAKA, Y., TAKAHASHI, E., UNUMA, T., TODA, E., NAGAI, R., TOGO, M., TSUKAMOTO, K., HASHIMOTO, H. & YAMAKADO, M. (2003) Association between insulin resistance and carotid arteriosclerosis in subjects with normal fasting glucose and normal glucose tolerance. *Arterioscler Thromb Vasc Biol*, 23, 295-301.
- JACOBS, D. B., HAYES, G. R., TRUGLIA, J. A. & LOCKWOOD, D. H. (1989) Alterations of glucose transporter systems in insulin-resistant uremic rats. *Am J Physiol*, 257, E193-7.
- JAMES, D. E., STRUBE, M. & MUECKLER, M. (1989) Molecular cloning and characterization of an insulin-regulatable glucose transporter. *Nature*, 338, 83-7.
- JAMIESON, M. J., GONZALES, G. M., JACKSON, T. I., KOERTH, S. M., ROMANO, W. F., TAN, D. X., CASTILLON, F., 3RD, SKINNER, M. H., GROSSMANN, M. & SHEPHERD, A. M. (1997) Evaluation of the IITC tail cuff blood pressure recorder in the rat against intraarterial pressure according to criteria for human devices. *Am J Hypertens*, 10, 209-16.

- JEFFERSON, L. S., LI, J. B. & RANNELS, S. R. (1977) Regulation by insulin of amino acid release and protein turnover in the perfused rat hemicorpus. *J Biol Chem*, 252, 1476-83.
- JEFFREY, M. H. (1990) tcaCALC. <http://www4.utsouthwestern.edu/rogersnmr>.
- JONASSEN, A. K., SACK, M. N., MJOS, O. D. & YELLON, D. M. (2001) Myocardial protection by insulin at reperfusion requires early administration and is mediated via Akt and p70s6 kinase cell-survival signaling. *Circ Res*, 89, 1191-8.
- KATZ, A. (2001) *Physiology of the heart*, Philadelphia, Lippincott Williams and Wilkis.
- KATZ, A. M. (1992) *Physiology of the Heart*. 2nd ed., Raven.
- KAUFFMAN, J. M. & CARO, J. F. (1983) Insulin resistance in uremia. Characterization of insulin action, binding, and processing in isolated hepatocytes from chronic uremic rats. *J Clin Invest*, 71, 698-708.
- KAYSEN, G. A. (2007) Disorders in high-density metabolism with insulin resistance and chronic kidney disease. *J Ren Nutr*, 17, 4-8.
- KELLY, D. P. (2002) Peroxisome proliferator-activated receptor alpha as a genetic determinant of cardiac hypertrophic growth: culprit or innocent bystander? *Circulation*, 105, 1025-7.
- KELLY, D. P. (2003) PPARs of the heart: three is a crowd. *Circ Res*, 92, 482-4.
- KENNEDY, D., OMRAN, E., PERIYASAMY, S. M., NADOOR, J., PRIYADARSHI, A., WILLEY, J. C., MALHOTRA, D., XIE, Z. & SHAPIRO, J. I. (2003) Effect of chronic renal failure on cardiac contractile function, calcium cycling, and gene expression of proteins important for calcium homeostasis in the rat. *J Am Soc Nephrol*, 14, 90-7.
- KERBEY, A. L., RANDLE, P. J., COOPER, R. H., WHITEHOUSE, S., PASK, H. T. & DENTON, R. M. (1976) Regulation of pyruvate dehydrogenase in rat heart. Mechanism of regulation of proportions of dephosphorylated and phosphorylated enzyme by oxidation of fatty acids and ketone bodies and of effects of diabetes: role of coenzyme A, acetyl-coenzyme A and reduced and oxidized nicotinamide-adenine dinucleotide. *Biochem J*, 154, 327-48.
- KITABACHI, A. E. & STENTZ, F. B. (1972) Degradation of insulin and proinsulin by various organ homogenates of rat. *Diabetes Care*, 21, 1091-1101.

- KORANYI, L., JAMES, D., MUECKLER, M. & PERMUTT, M. A. (1990) Glucose transporter levels in spontaneously obese (db/db) insulin-resistant mice. *J Clin Invest*, 85, 962-7.
- KOSS, K. L. & KRANIAS, E. G. (1996) Phospholamban: a prominent regulator of myocardial contractility. *Circ Res*, 79, 1059-63.
- KRAGELUND, C., SNORGAARD, O., KOBER, L., BENGTSSON, B., OTTESEN, M., HOJBERG, S., OLESEN, C., KJAERGAARD, J. J., CARLSEN, J. & TORP-PETERSEN, C. (2004) Hyperinsulinaemia is associated with increased long-term mortality following acute myocardial infarction in non-diabetic patients. *Eur Heart J*, 25, 1891-7.
- KRAUS, L. M., GABER, L., HANDORF, C. R., MARTI, H. P. & KRAUS, A. P., JR. (2001) Carbamylation of glomerular and tubular proteins in patients with kidney failure: a potential mechanism of ongoing renal damage. *Swiss Med Wkly*, 131, 139-4.
- KRAUS, L. M. & KRAUS, A. P., JR. (1991) Tyrosine and N-carbamoyl-tyrosine in end-stage renal disease during continuous ambulatory peritoneal dialysis. *J Lab Clin Med*, 118, 555-62.
- KRAUS, L. M. & KRAUS, A. P., JR. (1998) The search for the uremic toxin: the case for carbamylation of amino acids and proteins. *Wien Klin Wochenschr*, 110, 521-30.
- KRAUS, L. M. & KRAUS, A. P., JR. (2001) Carbamylation of amino acids and proteins in uremia. *Kidney Int Suppl*, 78, S102-7.
- KRAUS, L. M., TRAXINGER, R. & KRAUS, A. P. (2004) Uremia and insulin resistance: N-carbamoyl-asparagine decreases insulin-sensitive glucose uptake in rat adipocytes. *Kidney Int*, 65, 881-7.
- LAEMMLI, U. K. (1970) Cleavage of structural proteins during the assembly of the head of bacteriophage T4. *Nature*, 227, 680-5.
- LARANCE, M., RAMM, G., STOCKLI, J., VAN DAM, E. M., WINATA, S., WASINGER, V., SIMPSON, F., GRAHAM, M., JUNUTULA, J. R., GUILHAUS, M. & JAMES, D. E. (2005) Characterization of the role of the Rab GTPase-activating protein AS160 in insulin-regulated GLUT4 trafficking. *J Biol Chem*, 280, 37803-13.
- LARSEN, T. M., TOUBRO, S. & ASTRUP, A. (2003) PPARgamma agonists in the treatment of type II diabetes: is increased fatness commensurate with long-term efficacy? *Int J Obes Relat Metab Disord*, 27, 147-61.

- LASTRA, G., MANRIQUE, C., MCFARLANE, S. I. & SOWERS, J. R. (2006) Cardiometabolic syndrome and chronic kidney disease. *Curr Diab Rep*, 6, 207-12.
- LATIF, N., BAKER, C. S., DUNN, M. J., ROSE, M. L., BRADY, P. & YACOUB, M. H. (1993) Frequency and specificity of antiheart antibodies in patients with dilated cardiomyopathy detected using SDS-PAGE and western blotting. *J Am Coll Cardiol*, 22, 1378-84.
- LEAHY, J. L. (1993) Increased proinsulin/insulin ratio in pancreas extracts of hyperglycemic rats. *Diabetes* 42, 22-27.
- LEE, R. P., WANG, D., LIN, N. T., CHOU, Y. W. & CHEN, H. I. (2002) A modified technique for tail cuff pressure measurement in unrestrained conscious rats. *J Biomed Sci*, 9, 424-7.
- LEE, S. W., DAI, G., HU, Z., WANG, X., DU, J. & MITCH, W. E. (2004) Regulation of muscle protein degradation: coordinated control of apoptotic and ubiquitin-proteasome systems by phosphatidylinositol 3 kinase. *J Am Soc Nephrol*, 15, 1537-45.
- LEE, S. W., PARK, G. H., LEE, S. W., SONG, J. H., HONG, K. C. & KIM, M. J. (2007) Insulin resistance and muscle wasting in non-diabetic end-stage renal disease patients. *Nephrol Dial Transplant*, 22, 2554-62.
- LEVEY, A. S., ANDREOLI, S. P., DUBOSE, T., PROVENZANO, R. & COLLINS, A. J. (2007) Chronic kidney disease: common, harmful and treatable--World Kidney Day 2007. *Am J Nephrol*, 27, 108-12.
- LEVIN, A. & FOLEY, R. N. (2000) Cardiovascular disease in chronic renal insufficiency. *Am J Kidney Dis*, 36, S24-30.
- LEVIN, A., THOMPSON, C. R., ETHIER, J., CARLISLE, E. J., TOBE, S., MENDELSSOHN, D., BURGESS, E., JINDAL, K., BARRETT, B., SINGER, J. & DJURDJEV, O. (1999) Left ventricular mass index increase in early renal disease: impact of decline in hemoglobin. *Am J Kidney Dis*, 34, 125-34.
- LIAO, R., JAIN, M., CUI, L., D'AGOSTINO, J., AIELLO, F., LUPTAK, I., NGOY, S., MORTENSEN, R. M. & TIAN, R. (2002) Cardiac-specific overexpression of GLUT1 prevents the development of heart failure attributable to pressure overload in mice. *Circulation*, 106, 2125-31.
- LIM, J., GASSON, C. & KAJI, D. M. (1995) Urea inhibits NaK2Cl cotransport in human erythrocytes. *J Clin Invest*, 96, 2126-32.

- LIM, V. S., YARASHESKI, K. E., CROWLEY, J. R., FANGMAN, J. & FLANIGAN, M. (2003) Insulin is protein-anabolic in chronic renal failure patients. *J Am Soc Nephrol*, 14, 2297-304.
- LIPSIC, E., VAN DER MEER, P., HENNING, R. H., SUURMEIJER, A. J., BODDEUS, K. M., VAN VELDHUISEN, D. J., VAN GILST, W. H. & SCHOEMAKER, R. G. (2004) Timing of erythropoietin treatment for cardioprotection in ischemia/reperfusion. *J Cardiovasc Pharmacol*, 44, 473-9.
- LONDON, G. (2001) Pathophysiology of cardiovascular damage in the early renal population. *Nephrol Dial Transplant*, 16 Suppl 2, 3-6.
- LONDON, G. M. (2003) Cardiovascular disease in chronic renal failure: pathophysiologic aspects. *Seminars in Dialysis*, 16, 85-94.
- LONDON, G. M., GUERIN, A. P. & MARCHAIS, S. J. (1999) Pressure-overload cardiomyopathy in end-stage renal disease. *Current Opinion in Nephrology and Hypertension*, 8, 179-186.
- LONDON, G. M. & PARFREY, P. S. (1997) Cardiac disease in chronic uremia: pathogenesis. *Adv Ren Replace Ther*, 4, 194-211.
- LONDON, G. M. G., AP, MARCHAIS, SJ (1999) Hemodynamic overload in end-stage renal disease patients. *Sem Dial*, 12, 77-83.
- LOPASCHUK, G. D., BELKE, D. D., GAMBLE, J., ITOI, T. & SCHONEKESS, B. O. (1994) Regulation of fatty acid oxidation in the mammalian heart in health and disease. *Biochim Biophys Acta*, 1213, 263-76.
- LOPASCHUK, G. D., COLLINS-NAKAI, R. L. & ITOI, T. (1992) Developmental changes in energy substrate use by the heart. *Cardiovasc Res*, 26, 1172-80.
- LUIKEN, J. J., COORT, S. L., WILLEMS, J., COUMANS, W. A., BONEN, A. & GLATZ, J. F. (2004) Dipyridamole alters cardiac substrate preference by inducing translocation of FAT/CD36, but not that of GLUT4. *Mol Pharmacol*, 65, 639-45.
- LUIKEN, J. J., DYCK, D. J., HAN, X. X., TANDON, N. N., ARUMUGAM, Y., GLATZ, J. F. & BONEN, A. (2002) Insulin induces the translocation of the fatty acid transporter FAT/CD36 to the plasma membrane. *Am J Physiol Endocrinol Metab*, 282, E491-5.
- LUIKEN, J. J., SCHAAP, F. G., VAN NIEUWENHOVEN, F. A., VAN DER VUSSE, G. J., BONEN, A. & GLATZ, J. F. (1999a) Cellular fatty acid transport in heart and skeletal muscle as facilitated by proteins. *Lipids*, 34 Suppl, S169-75.

- LUIKEN, J. J., TURCOTTE, L. P. & BONEN, A. (1999b) Protein-mediated palmitate uptake and expression of fatty acid transport proteins in heart giant vesicles. *J Lipid Res*, 40, 1007-16.
- LUIKEN, J. J., VAN NIEUWENHOVEN, F. A., AMERICA, G., VAN DER VUSSE, G. J. & GLATZ, J. F. (1997) Uptake and metabolism of palmitate by isolated cardiac myocytes from adult rats: involvement of sarcolemmal proteins. *J Lipid Res*, 38, 745-58.
- LYDELL, C. P., CHAN, A., WAMBOLT, R. B., SAMBANDAM, N., PARSONS, H., BONDY, G. P., RODRIGUES, B., POPOV, K. M., HARRIS, R. A., BROWNSEY, R. W. & ALLARD, M. F. (2002) Pyruvate dehydrogenase and the regulation of glucose oxidation in hypertrophied rat hearts. *Cardiovasc Res*, 53, 841-51.
- MAK, R. H., CHANG, S. L., DRAKSHARAPU, A. & PAK, Y. K. (2004) Gene expression in uremic left ventricular hypertrophy: effects of hypertension and anemia. *Exp Mol Med*, 36, 251-8.
- MAK, R. H. & DEFRONZO, R. A. (1992) Glucose and insulin metabolism in uremia. *Nephron*, 61, 377-82.
- MALLOY, C. R., SHERRY, A. D. & JEFFREY, F. M. (1990a) Analysis of tricarboxylic acid cycle of the heart using ¹³C isotope isomers. *Am J Physiol*, 259, H987-95.
- MALLOY, C. R., THOMPSON, J. R., JEFFREY, F. M. & SHERRY, A. D. (1990b) Contribution of exogenous substrates to acetyl coenzyme A: measurement by ¹³C NMR under non-steady-state conditions. *Biochemistry*, 29, 6756-61.
- MALOFF, B. L., MCCALED, M. L. & LOCKWOOD, D. H. (1983) Cellular basis of insulin resistance in chronic uremia. *Am J Physiol*, 245, E178-84.
- MANN, J. F., GERSTEIN, H. C., POGUE, J., BOSCH, J. & YUSUF, S. (2001) Renal insufficiency as a predictor of cardiovascular outcomes and the impact of ramipril: the HOPE randomized trial. *Ann Intern Med*, 134, 629-36.
- MARK, P. B., JOHNSTON, N., GROENNING, B. A., FOSTER, J. E., BLYTH, K. G., MARTIN, T. N., STEEDMAN, T., DARGIE, H. J. & JARDINE, A. G. (2006) Redefinition of uremic cardiomyopathy by contrast-enhanced cardiac magnetic resonance imaging. *Kidney Int*, 69, 1839-45.
- MARSHALL, W. (1995) *Clinical Chemistry*, Mosby.
- MARSHALL, W. (2000) The kidneys. *Clinical Chemistry*. Fourth Edition ed., Mosby.

- MARTIN, S., MILLAR, C. A., LYTTLE, C. T., MEERLOO, T., MARSH, B. J., GOULD, G. W. & JAMES, D. E. (2000) Effects of insulin on intracellular GLUT4 vesicles in adipocytes: evidence for a secretory mode of regulation. *J Cell Sci*, 113 Pt 19, 3427-38.
- MARTINI, F. (2001) The Heart. *Fundamentals of Anatomy & Physiology*. 5th ed., Prentice Hall.
- MASSY, Z. A., CHADEFaux-VEKEMANS, B., CHEVALIER, A., BADER, C. A., DRUEKE, T. B., LEGENDRE, C., LACOUR, B., KAMOUN, P. & KREIS, H. (1994) Hyperhomocysteinaemia: a significant risk factor for cardiovascular disease in renal transplant recipients. *Nephrol Dial Transplant*, 9, 1103-8.
- MATSUDA, M. & DEFRONZO, R. A. (1999) Insulin sensitivity indices obtained from oral glucose tolerance testing: comparison with the euglycemic insulin clamp. *Diabetes Care*, 22, 1462-70.
- MATTHEWS, D. R., HOSKER, J. P., RUDENSKI, A. S., NAYLOR, B. A., TREACHER, D. F. & TURNER, R. C. (1985) Homeostasis model assessment: insulin resistance and beta-cell function from fasting plasma glucose and insulin concentrations in man. *Diabetologia*, 28, 412-9.
- MAZUMDER, P. K., O'NEILL, B. T., ROBERTS, M. W., BUCHANAN, J., YUN, U. J., COOKSEY, R. C., BOUDINA, S. & ABEL, E. D. (2004) Impaired cardiac efficiency and increased fatty acid oxidation in insulin-resistant ob/ob mouse hearts. *Diabetes*, 53, 2366-74.
- MAZUMUDER, P. K., O'NEILL, B. T., ROBERTS, M. W., BUCHNAN, J., YUN, U. J., COOKSEY, R. C., BOUDINA SIHEM & ABEL, E. D. (2004) Impaired Cardiac Efficiency and Increased Fatty Acid Oxidation in Insulin-Resistant ob/ob Mouse Hearts. *Diabetes*, 53, 2365-2374.
- MCCALEB, M. L., MALOFF, B. L., NOWAK, S. M. & LOCKWOOD, D. H. (1984a) Sulfonylurea effects on target tissues for insulin. *Diabetes Care*, 7 Suppl 1, 42-6.
- MCCALEB, M. L., MEVORACH, R., FREEMAN, R. B., IZZO, M. S. & LOCKWOOD, D. H. (1984b) Induction of insulin resistance in normal adipose tissue by uremic human serum. *Kidney Int*, 25, 416-21.
- MCMAHON, A., NAQVI, R., HURST, M., RAINE, A. E. G. & MACLEOD, K. (2006) Diastolic dysfunction and abnormality of the Na/Ca exchanger in single uraemic cardiac myocytes. *Kidney International*, 69, 846-851.

- MCMAHON, A. C., GREENWALD, S. E., DODD, S. M., HURST, M. J. & RAINE, A. E. (2002) Prolonged calcium transients and myocardial remodelling in early experimental uraemia. *Nephrol Dial Transplant*, 17, 759-64.
- MCMAHON, A. C., VESCOVO, G., DALLA LIBERA, L., WYNNE, D. G., FLUCK, R. J., HARDING, S. E. & RAINE, A. E. (1996) Contractile dysfunction of isolated ventricular myocytes in experimental uraemia. *Exp Nephrol*, 4, 144-50.
- MEDINA, R. A., SOUTHWORTH, R., FULLER, W. & GARLICK, P. B. (2002) Lactate-induced translocation of GLUT1 and GLUT4 is not mediated by the phosphatidyl-inositol-3-kinase pathway in the rat heart. *Basic Res Cardiol*, 97, 168-76.
- MEERSON, F. Z. (1971) Mechanism of hypertrophy of the heart and experimental prevention of acute cardiac insufficiency. *Br Heart J*, 33, Suppl:100-8.
- METIVIER, F., MARCHAIS, S. J., GUERIN, A. P., PANNIER, B. & LONDON, G. M. (2000) Pathophysiology of anaemia: focus on the heart and blood vessels. *Nephrol Dial Transplant*, 15 Suppl 3, 14-8.
- MIDDLETON, R. J., PARFREY, P. S. & FOLEY, R. N. (2001) Left ventricular hypertrophy in the renal patient. *J Am Soc Nephrol*, 12, 1079-84.
- MIINEA, C. P., SANO, H., KANE, S., SANO, E., FUKUDA, M., PERANEN, J., LANE, W. S. & LIENHARD, G. E. (2005) AS160, the Akt substrate regulating GLUT4 translocation, has a functional Rab GTPase-activating protein domain. *Biochem J*, 391, 87-93.
- MONTESSUIT, C. & THORBURN, A. (1999) Transcriptional activation of the glucose transporter GLUT1 in ventricular cardiac myocytes by hypertrophic agonists. *J Biol Chem*, 274, 9006-12.
- MONTI, J. P., BRUNET, P. J., BERLAND, Y. F., VANUXEM, D. C., VANUXEM, P. A. & CREVAT, A. D. (1995) Opposite effects of urea on hemoglobin-oxygen affinity in anemia of chronic renal failure. *Kidney Int*, 48, 827-31.
- MORGAN-HUGHES, J. A., DARVENIZA, P., KAHN, S. N., LANDON, D. N., SHERRATT, R. M., LAND, J. M. & CLARK, J. B. (1977) A mitochondrial myopathy characterized by a deficiency in reducible cytochrome b. *Brain*, 100, 617-40.
- MORGAN, H. E. & BAKER, K. M. (1991) Cardiac hypertrophy. Mechanical, neural, and endocrine dependence. *Circulation*, 83, 13-25.

- MYERS, V. & BAILEY, C. (1916) The Lewis and Benedict method for the estimation of blood sugar, with some observations obtained in disease. *J Biol Chem*, 24, 147.
- NEELY, J. R., LIEBERMEISTER, H., BATTERSBY, E. J. & MORGAN, H. E. (1967) Effect of pressure development on oxygen consumption by isolated rat heart. *Am. J. Physiol.*, 212, 804-814.
- NEUBAUER, F. (1910) Uber hyperglukamie bei Hockdrucknephritis und Glucosurie beim Diabetes mellitus. *Biochem Z.*, 25, 285-291.
- NISHIMURA, M., MURASE, M., HASHIMOTO, T., KOBAYASHI, H., YAMAZAKI, S., IMAI, R., OKINO, K., FUJITA, H., INOUE, N., TAKAHASHI, H. & ONO, T. (2006) Insulin resistance and impaired myocardial fatty acid metabolism in dialysis patients with normal coronary arteries. *Kidney Int*, 69, 553-9.
- NIWA, A., TANIGUCHI, K., ITO, H., NAKAGAWA, S., TAKEUCHI, J., SASAOKA, T. & KANAYAMA, M. (1985) Echocardiographic and Holter findings in 321 uremic patients on maintenance hemodialysis. *Jpn Heart J*, 26, 403-11.
- OGINO, H., SMOLENSKI, R. T., ZYCH, M., SEYMOUR, A. M. & YACOUB, M. H. (1996) Influence of preconditioning on rat heart subjected to prolonged cardioplegic arrest. *Ann Thorac Surg*, 62, 469-74.
- OIMOMI, M., HATANAKA, H., YOSHIMURA, Y., YOKONO, K., BABA, S. & TAKETOMI, Y. (1987) Carbamylation of insulin and its biological activity. *Nephron*, 46, 63-6.
- OKADA, T., LIEW, C. W., HU, J., HINAULT, C., MICHAEL, M. D., KRTZFELDT, J., YIN, C., HOLZENBERGER, M., STOFFEL, M. & KULKARNI, R. N. (2007) Insulin receptors in beta-cells are critical for islet compensatory growth response to insulin resistance. *Proc Natl Acad Sci U S A*, 104, 8977-82.
- OMATA, W., SHIBATA, H., LI, L., TAKATA, K. & KOJIMA, I. (2000) Actin filaments play a critical role in insulin-induced exocytotic recruitment but not in endocytosis of GLUT4 in isolated rat adipocytes. *Biochem J*, 346 Pt 2, 321-8.
- OPIE, L. H. (1984) *The Heart: Physiology, Metabolism, Pharmacology and Therapy*, Grune & Stratton.
- PAP, M. & COOPER, G. M. (1998) Role of glycogen synthase kinase-3 in the phosphatidylinositol 3-Kinase/Akt cell survival pathway. *J Biol Chem*, 273, 19929-32.

- PARFREY, P. S. & FOLEY, R. N. (1999) The clinical epidemiology of cardiac disease in chronic renal failure. *J Am Soc Nephrol*, 10, 1606-15.
- PARFREY, P. S., FOLEY, R. N., HARNETT, J. D., KENT, G. M., MURRAY, D. C. & BARRE, P. E. (1996) Outcome and risk factors for left ventricular disorders in chronic uraemia. *Nephrol Dial Transplant*, 11, 1277-85.
- PATERNOSTRO, G., CAMICI, P. G., LAMMERSTMA, A. A., MARINHO, N., BALIGA, R. R., KOONER, J. S., RADDA, G. K. & FERRANNINI, E. (1996) Cardiac and skeletal muscle insulin resistance in patients with coronary heart disease. A study with positron emission tomography. *J Clin Invest*, 98, 2094-9.
- PATERNOSTRO, G., CLARKE, K., HEATH, J., SEYMOUR, A.-M. L. & RADDA, G. K. (1995a) Decreased GLUT-4 mRNA content and insulin-sensitive deoxyglucose uptake show insulin resistance in the hypertensive rat heart. *Cardiovascular Reserach*, 30, 205-211.
- PATERNOSTRO, G., CLARKE, K., HEATH, J., SEYMOUR, A. M. & RADDA, G. K. (1995b) Decreased GLUT-4 mRNA content and insulin-sensitive deoxyglucose uptake show insulin resistance in the hypertensive rat heart. *Cardiovasc Res*, 30, 205-11.
- PATERNOSTRO, G., PAGANO, D., GNECCHI-RUSCONE, T., BONSER, R. & CAMICI, P. (1999a) Insulin resistance in patients with cardiac hypertrophy. *Cardiovascular Reserach*, 42, 246-253.
- PATERNOSTRO, G., PAGANO, D., GNECCHI-RUSCONE, T., BONSER, R. S. & CAMICI, P. G. (1999b) Insulin resistance in patients with cardiac hypertrophy. *Cardiovasc Res*, 42, 246-53.
- PAVLOVIC, D., FULLER, W. & SHATTOCK, M. J. (2007) The intracellular region of FXYP1 is sufficient to regulate cardiac Na/K ATPase. *Faseb J*, 21, 1539-46.
- PENPARGKUL, S. & SCHEUER, J. (1974) Regulation of glycogen metabolism in acute uremic hearts. *Metabolism*, 23, 631-44.
- PERIYASAMY, S. M., CHEN, J., COONEY, D., CARTER, P., OMRAN, E., TIAN, J., PRIYADARSHI, S., BAGROV, A., FEDOROVA, O., MALHOTRA, D., XIE, Z. & SHAPIRO, J. I. (2001) Effects of uremic serum on isolated cardiac myocyte calcium cycling and contractile function. *Kidney Int*, 60, 2367-76.
- PESSIN, J. E. & BELL, G. I. (1992) Mammalian facilitative glucose transporter family: structure and molecular regulation. *Annu Rev Physiol*, 54, 911-30.

- PESSIN, J. E., THURMOND, D. C., ELMENDORF, J. S., COKER, K. J. & OKADA, S. (1999) Molecular basis of insulin-stimulated GLUT4 vesicle trafficking. Location! Location! Location! *J Biol Chem*, 274, 2593-6.
- PRABHAKAR, S. S., ZEBALLOS, G. A., MONTOYA-ZAVALA, M. & LEONARD, C. (1997) Urea inhibits inducible nitric oxide synthase in macrophage cell line. *Am J Physiol*, 273, C1882-8.
- PUDDU, P., PUDDU, G. M., CRAVERO, E., DE PASCALIS, S. & MUSCARI, A. (2007) The putative role of mitochondrial dysfunction in hypertension. *Clin Exp Hypertens*, 29, 427-34.
- RAINE, A. E. G., SEYMOUR, A.-M. L., ROBERTS, A. F. C., RADDA, G. K. & LEDINGHAM, J. G. G. (1993) Impairment of Cardiac Function and Energetics in Experimental Renal Failure. *Journal of Clinical Investigation*, 92, 2934-2940.
- RANDLE, P. J. (1986) Fuel selection in animals. *Biochem Soc Trans*, 14, 799-806.
- RANDLE, P. J., NEWSHOLME, E. A. & GARLAND, P. B. (1964) Regulation of glucose uptake by muscle. 8. Effects of fatty acids, ketone bodies and pyruvate, and of alloxan-diabetes and starvation, on the uptake and metabolic fate of glucose in rat heart and diaphragm muscles. *Biochem J*, 93, 652-65.
- RAZEGHI, P., YOUNG, M. E., ALCORN, J. L., MORAVEC, C. S., FRAZIER, O. H. & TAEGTMEYER, H. (2001) Metabolic gene expression in fetal and failing human heart. *Circulation*, 104, 2923-31.
- REDDY, V., BHANDARI, S. & SEYMOUR, A. M. (2007) Myocardial function, energy provision, and carnitine deficiency in experimental uremia. *J Am Soc Nephrol*, 18, 84-92.
- REMONDINO, A., ROSENBLATT-VELIN, N., MONTESSUIT, C., TARDY, I., PAPAGEORGIOU, I., DORSAZ, P. A., JORGE-COSTA, M. & LERCH, R. (2000) Altered expression of proteins of metabolic regulation during remodeling of the left ventricle after myocardial infarction. *J Mol Cell Cardiol*, 32, 2025-34.
- RHODES, J., UDELSON, J., MARX, G., SCHMID, C., KONSTAM, M., HIJAZI, Z., BOVA, S. & FULTON, D. (1993) A new noninvasive method for the estimation of peak dP/dt. *Circulation*, 88, 2693-2699.
- RICHARDS, A. M. (1996) The renin-angiotensin-aldosterone system and the cardiac natriuretic peptides. *Heart*, 76, 36-44.
- RIGATTO, C. P., PS (2001) Uraemic Cardiomyopathy: an Overload Cardiomyopathy. *Journal of Clinical and Basic Cardiology*, 4, 93-95.

- RITZ, E. (2003) Renal dysfunction: a novel indicator and potential promoter of cardiovascular risk. *Clinical Medicine*, 3, 357-360.
- ROCKMAN, H. A., ROSS, R. S., HARRIS, A. N., KNOWLTON, K. U., STEINHELPER, M. E., FIELD, L. J., ROSS, J., JR. & CHIEN, K. R. (1991) Segregation of atrial-specific and inducible expression of an atrial natriuretic factor transgene in an in vivo murine model of cardiac hypertrophy. *Proc Natl Acad Sci U S A*, 88, 8277-81.
- ROCKMAN, H. A., WACHHORST, S. P., MAO, L. & ROSS, J., JR. (1994) ANG II receptor blockade prevents ventricular hypertrophy and ANF gene expression with pressure overload in mice. *Am J Physiol*, 266, H2468-75.
- RODERICK, P. & FEEST, T. (2005) The epidemiology of renal disease. IN DAVIDSON, A., GRUMFELD, J.-P., CAMERON, S., PONTICELLI, C., RITZ, E., WINEARLS, C. & YPERSELE, C. (Eds.) *Oxford Textbook of Clinical Nephrology*. Oxford, Oxford University Press.
- ROMMEL, C., BODINE, S. C., CLARKE, B. A., ROSSMAN, R., NUNEZ, L., STITT, T. N., YANCOPOULOS, G. D. & GLASS, D. J. (2001) Mediation of IGF-1-induced skeletal myotube hypertrophy by PI(3)K/Akt/mTOR and PI(3)K/Akt/GSK3 pathways. *Nat Cell Biol*, 3, 1009-13.
- ROSENBLATT-VELIN, N., LERCH, R., PAPAGEORGIOU, I. & MONTESSUIT, C. (2004) Insulin resistance in adult cardiomyocytes undergoing dedifferentiation: role of GLUT4 expression and translocation. *Faseb J*, 18, 872-4.
- ROSS, B. (1972) Heart and skeletal muscle. IN ROSS, B. (Ed.) *Perfusion book*.
- ROSTAND, S. G., BRUNZELL, J. D., CANNON, R. O., 3RD & VICTOR, R. G. (1991) Cardiovascular complications in renal failure. *J Am Soc Nephrol*, 2, 1053-62.
- ROSTAND, S. G., KIRK, K. A. & RUTSKY, E. A. (1986) The epidemiology of coronary artery disease in patients on maintenance hemodialysis: implications for management. *Contrib Nephrol*, 52, 34-41.
- RUBENSTEIN, A. H., MAKO, M. E. & HORWITZ, D. L. (1975) Insulin and the kidney. *Nephron*, 15, 306-26.
- RUSSELL, R. R., 3RD, MRUS, J. M., MOMMESSIN, J. I. & TAEGTMEYER, H. (1992) Compartmentation of hexokinase in rat heart. A critical factor for tracer kinetic analysis of myocardial glucose metabolism. *J Clin Invest*, 90, 1972-7.

- SACHECK, J. M., OHTSUKA, A., MCLARY, S. C. & GOLDBERG, A. L. (2004) IGF-I stimulates muscle growth by suppressing protein breakdown and expression of atrophy-related ubiquitin ligases, atrogin-1 and MuRF1. *Am J Physiol Endocrinol Metab*, 287, E591-601.
- SALTIEL, A. R. & PESSIN, J. E. (2002) Insulin signaling pathways in time and space. *Trends Cell Biol*, 12, 65-71.
- SAMBANDAM, N., LOPASCHUK, G. D., BROWNSEY, R. W. & ALLARD, M. F. (2002) Energy metabolism in the hypertrophied heart. *Heart Fail Rev*, 7, 161-73.
- SAMBRANO, G. R., FRASER, I., HAN, H., NI, Y., O'CONNELL, T., YAN, Z. & STULL, J. T. (2002) Navigating the signalling network in mouse cardiac myocytes. *Nature*, 420, 712-4.
- SAMPLE, J., CLELAND, J. G. & SEYMOUR, A. (2006) Metabolic remodeling in the aging heart. *J Mol Cell Cardiol*, 40, 56-63.
- SANDE, J. B., SJAASTAD, I., HOEN, I. B., BOKENES, J., TONNESSEN, T., HOLT, E., LUNDE, P. K. & CHRISTENSEN, G. (2002) Reduced level of serine(16) phosphorylated phospholamban in the failing rat myocardium: a major contributor to reduced SERCA2 activity. *Cardiovasc Res*, 53, 382-91.
- SANO, H., KANE, S., SANO, E., MIINEA, C. P., ASARA, J. M., LANE, W. S., GARNER, C. W. & LIENHARD, G. E. (2003) Insulin-stimulated phosphorylation of a Rab GTPase-activating protein regulates GLUT4 translocation. *J Biol Chem*, 278, 14599-602.
- SANTALUCIA, T., CAMPS, M., CASTELLO, A., MUNOZ, P., NUEL, A., TESTAR, X., PALACIN, M. & ZORZANO, A. (1992) Developmental regulation of GLUT-1 (erythroid/Hep G2) and GLUT-4 (muscle/fat) glucose transporter expression in rat heart, skeletal muscle, and brown adipose tissue. *Endocrinology*, 130, 837-46.
- SCHLANT, R. C., SONNENBLICK, E. H. & KATZ, A. M. (1998) Normal Physiology of the Cardiovascular System. IN ALEXANDER, R. W. S., R.C. FUSTER, V. (Ed.) *Hurst's The Heart*. 9th ed., McGraw-Hill.
- SCHREIBER, B. & LEWIS, V. (2001) Management of carnitine deficiency in ESRD patients undergoing dialysis: challenges and considerations. *Dialysis and Transplantation*, 30.

- SCWARTZ, G. G. & WEINER, M. W. (1992) Magnetic resonance spectroscopy: Basic principles and the potential applications in the study of the cardiovascular system. IN SCHAEFER, S. & BALABAN, R. (Eds.) *Cardiovascular Magnetic Resonance Spectroscopy*. Boston, Kluwer Academic Publishers.
- SEYMOUR, A.-M. L. (2003a) Imaging Cardiac Metabolism in Heart Failure: The potential of NMR Spectroscopy in the Era of Metabolism Revisited. *Heart, Lung and Circulation*, 25-30.
- SEYMOUR, A.-M. L. & CHATHAM, J. C. (1997) The effects of hypertrophy and diabetes on cardiac pyruvate dehydrogenase activity. *Journal of Molecular Cell Cardiology*, 29, 2771-2778.
- SEYMOUR, A. M. (2003b) Mitochondrial function-A limiting factor in heart failure? , Boston Kluwer academic publishers.
- SEYMOUR, A. M., ELДАР, H. & RADDА, G. K. (1990) Hyperthyroidism results in increased glycolytic capacity in the rat heart. A ³¹P-NMR study. *Biochim Biophys Acta*, 1055, 107-16.
- SHARMA, P., PATCHELL, V. B., GAO, Y., EVANS, J. S. & LEVINE, B. A. (2001) Cytoplasmic interactions between phospholamban residues 1-20 and the calcium-activated ATPase of the sarcoplasmic reticulum. *Biochem J*, 355, 699-706.
- SHEN, Y., PEAKE, P. W. & KELLY, J. J. (2005) Should we quantify insulin resistance in patients with renal disease? *Nephrology (Carlton)*, 10, 599-605.
- SHETTY, M., ISMAIL-BEIGI, N., LOEB, J. N. & ISMAIL-BEIGI, F. (1993a) Induction of GLUT1 mRNA in response to inhibition of oxidative phosphorylation. *Am J Physiol*, 265, C1224-9.
- SHETTY, M., LOEB, J. N., VIKSTROM, K. & ISMAIL-BEIGI, F. (1993b) Rapid activation of GLUT-1 glucose transporter following inhibition of oxidative phosphorylation in clone 9 cells. *J Biol Chem*, 268, 17225-32.
- SHINOHARA, K., SHOJI, T., EMOTO, M., TAHARA, H., KOYAMA, H., ISHIMURA, E., MIKI, T., TABATA, T. & NISHIZAWA, Y. (2002) Insulin resistance as an independent predictor of cardiovascular mortality in patients with end-stage renal disease. *J Am Soc Nephrol*, 13, 1894-900.
- SHULMAN, G. I. (1999) Cellular mechanisms of insulin resistance in humans. *Am J Cardiol*, 84, 3J-10J.

- SIMMERMAN, H. K., COLLINS, J. H., THEIBERT, J. L., WEGENER, A. D. & JONES, L. R. (1986) Sequence analysis of phospholamban. Identification of phosphorylation sites and two major structural domains. *J Biol Chem*, 261, 13333-41.
- SIMMERMAN, H. K. & JONES, L. R. (1998) Phospholamban: protein structure, mechanism of action, and role in cardiac function. *Physiol Rev*, 78, 921-47.
- SLOT, J. W., GEUZE, H. J., GIGENGACK, S., JAMES, D. E. & LIENHARD, G. E. (1991) Translocation of the glucose transporter GLUT4 in cardiac myocytes of the rat. *Proc Natl Acad Sci U S A*, 88, 7815-9.
- SMOLENSKI, R. T., SUITERS, A. & YACOUB, M. H. (1992) Adenine nucleotide catabolism and adenosine formation in isolated human cardiomyocytes. *J Mol Cell Cardiol*, 24, 91-6.
- SNAITH, C., LEE-IRVING, J., GREEN, Y., RAINE, A., RADDA, G. & SEYMOUR, A.-M. L. (1990) Calcium transport into the sarcoplasmic reticulum of uraemic rat hearts. *JMCC*, 22, s23.
- SOHN, H. J., STOKES, G. S. & JOHNSTON, H. (1992) An Na, K ATPase inhibitor from ultrafiltrate obtained by hemodialysis of patients with uremia. *J Lab Clin Med*, 120, 264-71.
- SOWERS, J. R. (2004) Insulin resistance and hypertension. *Am J Physiol Heart Circ Physiol*, 286, H1597-602.
- SOWERS, J. R. & FROHLICH, E. D. (2004) Insulin and insulin resistance: impact on blood pressure and cardiovascular disease. *Med Clin North Am*, 88, 63-82.
- STANLEY, W. C. & CHANDLER, M. P. (2002) Energy Metabolism in The Normal and Failing Heart: Potential for Therapeutic Interventions. *Heart Failure Reviews*, 7, 115-130.
- STANLEY, W. C., LOPASCHUK, G. D. & MCCORMACK, J. G. (1997) Regulation of energy substrate metabolism in the diabetic heart. *Cardiovasc Res*, 34, 25-33.
- STANLEY, W. C., RECCHIA, F. A. & LOPASCHUK, G. D. (2005) Myocardial Substrate Metabolism in the Normal and Failing Heart. *Physiol Rev*, 85, 1093-1129.
- STEFANOVIC, V., NESIC, V. & STOJIMIROVIC, B. (2003) Treatment of insulin resistance in uremia. *Int J Artif Organs*, 26, 100-4.

- STEWART, G. A., GANSEVOORT, R. T., MARK, P. B., ROONEY, E., MCDONAGH, T. A., DARGIE, H. J., STUART, R., RODGER, C. & JARDINE, A. G. (2005) Electrocardiographic abnormalities and uremic cardiomyopathy. *Kidney Int*, 67, 217-26.
- STOKES, G. S., NORRIS, L. A., MARWOOD, J. F., JOHNSTON, H. & CATERSON, R. J. (1990) Effect of dialysis on circulating Na,K ATPase inhibitor in uremic patients. *Nephron*, 54, 127-33.
- SUGA, H. (1990) Ventricular energetics. *Physiol Rev*, 70, 247-77.
- SUGDEN, M. C., LANGDOWN, M. L., HARRIS, R. A. & HOLNESS, M. J. (2000) Expression and regulation of pyruvate dehydrogenase kinase isoforms in the developing rat heart and in adulthood: role of thyroid hormone status and lipid supply. *Biochem J*, 352 Pt 3, 731-8.
- TAEGTMEYER, H. (1994) Energy metabolism of the heart: from basic concepts to clinical applications. *Curr Probl Cardiol*, 19, 59-113.
- TAEGTMEYER, H. (1999) Fuels for the heart. IN WILLERSON, T. J. & COHN, J. N. (Eds.) *Cardiovascular Medicine*. 2 ed., Churchill Livingstone.
- TAEGTMEYER, H. (2000) Genetics of energetics: transcriptional responses in cardiac metabolism. *Ann Biomed Eng*, 28, 871-6.
- TAEGTMEYER, H., WILSON, C. R., RAZEGHI, P. & SHARMA, S. (2005) Metabolic energetics and genetics in the heart. *Ann N Y Acad Sci*, 1047, 208-18.
- TEN HOVE, M. & NEUBAUER, S. (2007) MR spectroscopy in heart failure--clinical and experimental findings. *Heart Fail Rev*, 12, 48-57.
- TERRITO, P. R., MOOTHA, V. K., FRENCH, S. A. & BALABAN, R. S. (2000) Ca(2+) activation of heart mitochondrial oxidative phosphorylation: role of the F(0)/F(1)-ATPase. *Am J Physiol Cell Physiol*, 278, C423-35.
- THIEMERMANN, C. (2004) Ligands of the peroxisome proliferator-activated receptor-gamma and heart failure. *Br J Pharmacol*, 142, 1049-51.
- TIAN, R. (2003) Transcriptional regulation of energy substrate metabolism in normal and hypertrophied heart. *Curr Hypertens Rep*, 5, 454-8.
- TORNIG, J., AMANN, K., RITZ, E., NICHOLS, C., ZEIER, M. & MALL, G. (1996) Arteriolar wall thickening, capillary rarefaction and interstitial fibrosis in the heart of rats with renal failure: the effects of ramipril, nifedipine and moxonidine. *J Am Soc Nephrol*, 7, 667-75.

- TORNIG, J., GROSS, M. L., SIMONAVICIENE, A., MALL, G., RITZ, E. & AMANN, K. (1999) Hypertrophy of intramyocardial arteriolar smooth muscle cells in experimental renal failure. *J Am Soc Nephrol*, 10, 77-83.
- TSAI, C., PERRELLA, M., YOSHIKUMI, M., HSIEN, C., HABE, E., SCHLAGEL, R. & LEE, M. (1992) Promotion of vascular smooth muscle cell growth by homocysteine: A link to atherosclerosis. *Proc Natl Acad Sci U S A*, 91, 10193-10197.
- VAN BILSEN, M., SMEETS, P. J., GILDE, A. J. & VAN DER VUSSE, G. J. (2004) Metabolic remodelling of the failing heart: the cardiac burn-out syndrome? *Cardiovasc Res*, 61, 218-26.
- VAN DER VUSSE, G. J., VAN BILSEN, M. & GLATZ, J. F. (2000) Cardiac fatty acid uptake and transport in health and disease. *Cardiovasc Res*, 45, 279-93.
- VANHOLDER, R., ARGILES, A., BAURMEISTER, U., BRUNET, P., CLARK, W., COHEN, G., DE DEYN, P. P., DEPPISCH, R., DESCAMPS-LATSCHA, B., HENLE, T., JORRES, A., MASSY, Z. A., RODRIGUEZ, M., STEGMAYR, B., STENVINKEL, P. & WRATTEN, M. L. (2001) Uremic toxicity: present state of the art. *Int J Artif Organs*, 24, 695-725.
- VANHOLDER, R. & DE SMET, R. (1999) Pathophysiologic effects of uremic retention solutes. *J Am Soc Nephrol*, 10, 1815-23.
- VELLIQUETTE, R. A., KOLETSKY, R. J. & ERNSBERGER, P. (2002) Plasma glucagon and free fatty acid responses to a glucose load in the obese spontaneous hypertensive rat (SHROB) model of metabolic syndrome X. *Exp Biol Med (Maywood)*, 227, 164-70.
- VERHEY, K. J., YEH, J. I. & BIRNBAUM, M. J. (1995) Distinct signals in the GLUT4 glucose transporter for internalization and for targeting to an insulin-responsive compartment. *J Cell Biol*, 130, 1071-9.
- VERMA, A., ANAVEKAR, N., MERIS, A., THUNE, J. J., ARNOLD, M., GHALI, J., VELAZQUEZ, E., MCMURRAY, J., PFEFFER, M. & SOLOMON, S. (2007) The Relationship Between Renal Function and Cardiac Structure, Function, and Prognosis After Myocardial Infarction. *J Am Coll Cardiol*, 50, 1238-1245.
- VIK-MO, H. & MJOS, O. D. (1981) Influence of free fatty acids on myocardial oxygen consumption and ischemic injury. *Am J Cardiol*, 48, 361-5.

- VOLPE, M., TRITTO, C., DE LUCA, N., MELE, A. F., LEMBO, G., RUBATTU, S., ROMANO, M., DE CAMPORA, P., ENEA, I., RICCIARDELLI, B. & ET AL. (1991) Failure of atrial natriuretic factor to increase with saline load in patients with dilated cardiomyopathy and mild heart failure. *J Clin Invest*, 88, 1481-9.
- VOZZI, C., DUPONT, E., COPPEN, S. R., YEH, H. I. & SEVERS, N. J. (1999) Chamber-related differences in connexin expression in the human heart. *J Mol Cell Cardiol*, 31, 991-1003.
- WALAAS, O. & WALAAS, E. (1950) Effect of epinephrine on rat diaphragm. *J Biol Chem*, 187, 769-776.
- WALLBERG-HENRIKSSON, H. & ZIERATH, J. R. (2001) GLUT4: a key player regulating glucose homeostasis? Insights from transgenic and knockout mice (review). *Mol Membr Biol*, 18, 205-11.
- WALLER, B. F. & SCHLANT, R. C. (1998) Anatomy of the heart. IN ALEXANDER, R. W. S., R.C. VALENTIN, F (Ed.) *Hurst's The Heart*. 9th ed., McGraw-Hill.
- WATANABE, K., FUJII, H., TAKAHASHI, T., KODAMA, M., AIZAWA, Y., OHTA, Y., ONO, T., HASEGAWA, G., NAITO, M., NAKAJIMA, T., KAMIJO, Y., GONZALEZ, F. J. & AOYAMA, T. (2000) Constitutive regulation of cardiac fatty acid metabolism through peroxisome proliferator-activated receptor alpha associated with age-dependent cardiac toxicity. *J Biol Chem*, 275, 22293-9.
- WEINBERG, E. O. T., C.D. LORELL, B.H. (1995) Pretranslational regulation of glucose transporter isoform expression in hearts with pressure-overload left ventricular hypertrophy. *Circulation*, 92, I-385.
- WEISENSEE, D., LOW-FRIEDRICH, I., RIEHLE, M., BEREITER-HAHN, J. & SCHOEPPE, W. (1993) In vitro approach to 'uremic cardiomyopathy'. *Nephron*, 65, 392-400.
- WEISENSEE, D., SCHNAARS, Y., SCHOEPPE, W., BEREITER-HAHN, J. & LOW-FRIEDRICH, I. (1997) Potential uremic toxins modulate energy metabolism of cardiac myocytes in vitro. *Exp Nephrol*, 5, 194-200.
- WELSH, G. I., HERS, I., BERWICK, D. C., DELL, G., WHERLOCK, M., BIRKIN, R., LENEY, S. & TAVARE, J. M. (2005) Role of protein kinase B in insulin-regulated glucose uptake. *Biochem Soc Trans*, 33, 346-9.
- WELSH, G. I., WILSON, C. & PROUD, C. G. (1996) GSK3: a SHAGGY frog story. *Trends Cell Biol*, 6, 274-9.

- WHITE, M. F. (1998) The IRS-signalling system: a network of docking proteins that mediate insulin action. *Mol Cell Biochem*, 182, 3-11.
- WIDBERG, C. H., BRYANT, N. J., GIROTTI, M., REA, S. & JAMES, D. E. (2003) Tomosyn interacts with the t-SNAREs syntaxin4 and SNAP23 and plays a role in insulin-stimulated GLUT4 translocation. *J Biol Chem*, 278, 35093-101.
- WILKINS, B. J., DAI, Y. S., BUENO, O. F., PARSONS, S. A., XU, J., PLANK, D. M., JONES, F., KIMBALL, T. R. & MOLKENTIN, J. D. (2004) Calcineurin/NFAT coupling participates in pathological, but not physiological, cardiac hypertrophy. *Circ Res*, 94, 110-8.
- WING, A. J., BRUNNER, F. P., BRYNGER, H., JACOBS, C., KRAMER, P., SELWOOD, N. H. & GRETZ, N. (1984) Cardiovascular-related causes of death and the fate of patients with renovascular disease. *Contrib Nephrol*, 41, 306-11.
- WISNESKI, J. A., GERTZ, E. W., NEESE, R. & MAYR, M. (1987) Myocardial metabolism of free fatty acids: studies with ¹⁴C-labelled substrates in humans. *J clin Invest*, 79, 359-366.
- WOLD, L. E., DUTTA, K., MASON, M. M., REN, J., CALA, S. E., SCHWANKE, M. L. & DAVIDOFF, A. J. (2005) Impaired SERCA function contributes to cardiomyocyte dysfunction in insulin resistant rats. *J Mol Cell Cardiol*, 39, 297-307.
- WWW.KIDNEYRESEARCHUK.ORG (2008) Kidney Disease in UK Today.
- XIE, Z., KOMETIANI, P., LIU, J., LI, J., SHAPIRO, J. I. & ASKARI, A. (1999) Intracellular reactive oxygen species mediate the linkage of Na⁺/K⁺-ATPase to hypertrophy and its marker genes in cardiac myocytes. *J Biol Chem*, 274, 19323-8.
- YAMAMOTO, K., OHKI, R., LEE, R. T., IKEDA, U. & SHIMADA, K. (2001) Peroxisome proliferator-activated receptor gamma activators inhibit cardiac hypertrophy in cardiac myocytes. *Circulation*, 104, 1670-5.
- YANASE, M., TAKATSU, F., TAGAWA, T., KATO, T., ARAI, K., KOYASU, M., HORIBE, H., NOMOTO, S., TAKEMOTO, K., SHIMIZU, S. & WATARAI, M. (2004) Insulin resistance and fasting hyperinsulinemia are risk factors for new cardiovascular events in patients with prior coronary artery disease and normal glucose tolerance. *Circ J*, 68, 47-52.

- YANG, J., GILLINGHAM, A. K., HODEL, A., KOUMANOV, F., WOODWARD, B. & HOLMAN, G. D. (2002) Insulin-stimulated cytosol alkalinization facilitates optimal activation of glucose transport in cardiomyocytes. *Am J Physiol Endocrinol Metab*, 283, E1299-307.
- YIN, F. C., SPURGEON, H. A., RAKUSAN, K., WEISFELDT, M. L. & LAKATTA, E. G. (1982) Use of tibial length to quantify cardiac hypertrophy: application in the aging rat. *Am J Physiol*, 243, H941-7.
- YOUNG, L. H., RENFU, Y., RUSSELL, R., HU, X., CAPLAN, M., REN, J., SHULMAN, G. I. & SINUSAS, A. J. (1997) Low-flow ischemia leads to translocation of canine heart GLUT-4 and GLUT-1 glucose transporters to the sarcolemma in vivo. *Circulation*, 95, 415-22.
- YOUNG, M. E., GUTHRIE, P. H., RAZEGHI, P., LEIGHTON, B., ABBASI, S., PATIL, S., YOUKER, K. A. & TAEGTMEYER, H. (2002a) Impaired long-chain fatty acid oxidation and contractile dysfunction in the obese Zucker rat heart. *Diabetes*, 51, 2587-95.
- YOUNG, M. E., MCNULTY, P. & TAEGTMEYER, H. (2002b) Adaptation and maladaptation of the heart in diabetes: Part II: potential mechanisms. *Circulation*, 105, 1861-70.
- YOUNG, M. E., PATIL, S., YING, J., DEPRE, C., AHUJA, H. S., SHIPLEY, G. L., STEPKOWSKI, S. M., DAVIES, P. J. & TAEGTMEYER, H. (2001) Uncoupling protein 3 transcription is regulated by peroxisome proliferator-activated receptor (alpha) in the adult rodent heart. *Faseb J*, 15, 833-45.
- YU, X., WHITE, L. T., DOUMEN, C., DAMICO, L. A., LANOUE, K. F., ALPERT, N. M. & LEWANDOWSKI, E. D. (1995) Kinetic analysis of dynamic ¹³C NMR spectra: metabolic flux, regulation, and compartmentation in hearts. *Biophys J*, 69, 2090-102.
- ZERIAL, M. & MCBRIDE, H. (2001) Rab proteins as membrane organizers. *Nat Rev Mol Cell Biol*, 2, 107-17.
- ZHAI, J., SCHMIDT, A. G., HOIT, B. D., KIMURA, Y., MACLENNAN, D. H. & KRANIAS, E. G. (2000) Cardiac-specific overexpression of a superinhibitory pentameric phospholamban mutant enhances inhibition of cardiac function in vivo. *J Biol Chem*, 275, 10538-44.
- ZHOU, Y. Y., WANG, S. Q., ZHU, W. Z., CHRUSCINSKI, A., KOBILKA, B. K., ZIMAN, B., WANG, S., LAKATTA, E. G., CHENG, H. & XIAO, R. P. (2000) Culture and adenoviral infection of adult mouse cardiac myocytes: methods for cellular genetic physiology. *Am J Physiol Heart Circ Physiol*, 279, H429-36.

ZISMAN, A., PERONI, O. D., ABEL, E. D., MICHAEL, M. D., MAUVAIS-JARVIS, F., LOWELL, B. B., WOJTASZEWSKI, J. F., HIRSHMAN, M. F., VIRKAMAKI, A., GOODYEAR, L. J., KAHN, C. R. & KAHN, B. B. (2000) Targeted disruption of the glucose transporter 4 selectively in muscle causes insulin resistance and glucose intolerance. *Nat Med*, 6, 924-8.

ZOCCALI, C., MALLAMACI, F., BENEDETTO, F. A., TRIPEPI, G., PARLONGO, S., CATALIOTTI, A., CUTRUPI, S., GIACONE, G., BELLANUOVA, I., COTTINI, E. & MALATINO, L. S. (2001) Cardiac natriuretic peptides are related to left ventricular mass and function and predict mortality in dialysis patients. *J Am Soc Nephrol*, 12, 1508-15.